CRACKED SEMI-INFINITE CYLINDER AND

FINITE CYLINDER PROBLEMS

A THESIS SUBMITTED TO
THE GRADUATE SCHOOL OF NATURAL AND APPLIED SCIENCES
OF
MIDDLE EAST TECHNICAL UNIVERSITY

BY

METE ONUR KAMAN

IN PARTIAL FULFILLMENT OF THE REQUIREMENTS
FOR
THE DEGREE OF DOCTOR OF PHILOSOPHY
IN
ENGINEERING SCIENCES

MAY 2006

Approval of the Graduate School of Natural and Applied Sciences

_____
Prof.Dr. Canan Özgen
Director

I certify that this thesis satisfies all the requirements as a thesis for the degree of Doctor of Philosophy.

_____
Prof.Dr. Turgut Tokdemir
Head of Department

This is to certify that we have read this thesis and that in our opinion it is fully adequate, in scope and quality, as a thesis for the degree of Doctor of Philosophy.

_____
Prof.Dr. M. Ruşen Geçit
Supervisor

Examining Committee Members

Prof.Dr. Turgut Tokdemir	(METU, ES)	_____
Prof.Dr. M. Ruşen Geçit	(METU, ES)	_____
Prof.Dr. Aydın Turgut	(Fırat Univ., ME)	_____
Assoc.Prof.Dr. Ahmet N. Eraslan	(METU, ES)	_____
Assist.Prof.Dr. Serkan Dağ	(METU, ME)	_____

I hereby declare that all information in this document has been obtained and presented in accordance with academic rules and ethical conduct. I also declare that, as required by these rules and conduct, I have fully cited and referenced all material and results that are not original to this work.

Name, Last name : Mete Onur Kaman

Signature   :

ABSTRACT

CRACKED SEMI-INFINITE CYLINDER AND
FINITE CYLINDER PROBLEMS

Kaman, Mete Onur

Ph.D., Department of Engineering Sciences

Supervisor: Prof. Dr. M. Ruşen Geçit

May 2006, 208 pages

This work considers a cracked semi-infinite cylinder and a finite cylinder. Material of the cylinder is linearly elastic and isotropic. One end of the cylinder is bonded to a fixed support while the other end is subject to axial tension. Solution for this problem can be obtained from the solution for an infinite cylinder having a penny-shaped rigid inclusion at $z = 0$ and two penny-shaped cracks at $z = \pm L$. General expressions for this problem are obtained by solving Navier equations using Fourier and Hankel transforms. When the radius of the inclusion approaches the radius of the cylinder, the end at $z = 0$ becomes fixed and when the radius of the cracks approaches the radius of the cylinder, the ends at $z = \pm L$ become cut and subject to uniformly distributed tensile load. Formulation of the problem is reduced to a system of three singular integral equations. By using Gauss-Lobatto and Gauss-Jacobi integration formulas, these three singular integral equations are converted to a system of linear algebraic equations which is solved numerically.

Keywords: Axisymmetric, Finite cylinder, Penny-shaped crack, Rigid inclusion, Stress intensity factor.

ÖZ

ÇATLAK İÇEREN YARI SONSUZ SİLİNDİR VE
SONLU SİLİNDİR PROBLEMLERİ

Kaman, Mete Onur

Doktora, Mühendislik Bilimleri Bölümü

Tez Yöneticisi: Prof. Dr. M. Ruşen Geçit

Mayıs 2006, 208 sayfa

Bu çalışma, çatlak içeren yarı sonsuz silindir ve sonlu uzunlukta silindir problemlerini incelemektedir. Silindir malzemesi lineer elastik ve izotroptur. Silindirin bir ucu sabit mesnetlenmiş olup diğer ucu eksenel çekme yükü etkisindedir. Problemin çözümü, $z = 0$ düzleminde disk şeklinde bir rijit enklozyon ve $z = \pm L$ düzlemlerinde disk şeklinde çatlaklar bulunan sonsuz silindir probleminin çözümünden elde edilmektedir. Bu problemin genel ifadeleri, Navier denklemlerinin Fourier ve Hankel dönüşümleri kullanılarak çözülmesinden elde edilmektedir. Enklozyon yarıçapı silindir yarıçapına ulaştığında silindirin $z = 0$ düzlemindeki ucu sabitlenmiş olur. Çatlak yarıçapı silindir yarıçapına ulaştığında ise silindir $z = \pm L$ düzlemlerinde kopar ve burada oluşan uçlar düzgün yayılı çekme yükü etkisinde kalır. Problemin formülasyonu üç tekil integral denkleme dönüştürülür. Bu üç tekil integral denklem Gauss-Lobatto ve Gauss-Jacobi integrasyon formülleri kullanılarak bir lineer cebrik denklem takımına çevrilir ve sayısal olarak çözülür.

Anahtar Kelimeler: Eksenel simetri, Sonlu uzunlukta silindir, Disk şeklinde çatlak, Rijit enklozyon, Gerilme şiddeti katsayısı.

To My Grandmother, Fevziye Özkan

ACKNOWLEDGMENTS

TABLE OF CONTENTS

LIST OF TABLES

TABLES

LIST OF FIGURES

FIGURES

xiii

NOMENCLATURE

a	Radius of penny-shaped cracks
A	Radius of cylinder
b	Radius of penny-shaped inclusion
B_i, F_i, G_i, H_i	Bounded functions
c_i	Arbitrary integration constants
C_i	Weighting constants of the Gauss-Lobatto polynomials
d_i, g_i, h_i	Coefficient functions
E_1, E_2	Functions used as abbreviations
$f(r), g(r)$	Crack surface displacement derivatives
$f^*(t), g^*(t)$	Hölder-continuous functions on cracks
$f^{**}(r), h_i^{**}(r)$	Bounded functions
$F(\xi), G(\xi)$	Hankel transforms of $f(r)$ and $g(r)$
$\overline{F}(\phi), \overline{G}(\phi)$	Normalized Hölder-continuous functions on cracks
$\overline{\overline{F}}(\phi), \overline{\overline{G}}(\phi)$	Normalized bounded functions on cracks
$h(r)$	Shear stress jump on rigid inclusion
$h^*(t)$	Hölder-continuous function on inclusion
$H(\xi)$	Hankel transform of $h(r)$
$\overline{H}(\eta)$	Normalized Hölder-continuous function on inclusion
$\overline{\overline{H}}(\eta)$	Normalized bounded function on inclusion
I_0, I_1	Modified Bessel functions of the 1st kind of order zero and one
J_0, J_1	Bessel functions of the 1st kind of order zero and one
k_{1a}, k_{2a}	Mode I and II stress intensity factors at the edge of crack

k_{1A}, k_{2A}	Mode I and II stress intensity factors at the edge of rigid support
k_{1b}, k_{2b}	Mode I and II stress intensity factors at the edge of inclusion
$\bar{k}_{1a}, \bar{k}_{2a}$	Normalized Mode I and II stress intensity factors at the edge of crack
$\bar{k}_{1A}, \bar{k}_{2A}$	Normalized Mode I and II stress intensity factors at the edge of rigid support
$\bar{k}_{1b}, \bar{k}_{2b}$	Normalized Mode I and II stress intensity factors at the edge of inclusion
K, E	Complete elliptic integrals of the 1st and the 2nd kinds
K_0, K_1	Modified Bessel functions of the 2nd kind of order zero and one
K_{ij}	Integrands of the kernels N_{ij}
$K_{ij\infty}, K_{ij\infty 0}$	Dominant parts of K_{ij} as $\alpha \to \infty$ and as $\alpha \to 0$
L	Distance between cracks and inclusion
$m(r,t), m^*(r,t)$	Kernels
m_i, M_i, R_i, S_i	Kernels
N_{ij}	Kernels of the integral equations
N_{ij_b}, N_{ij_s}	Bounded and singular parts of N_{ij} as $\alpha \to \infty$
$N_{ij_{s0}}$	Singular parts of N_{ij} as $\alpha \to 0$
p_0	Intensity of the axial tensile load
$P_n^{(\alpha,\beta)}$	Jacobi polynomials
q_i, r_i, s_i, y_i, z_i	Coefficients
r, θ, z	Cylindrical coordinates
t	Integration variable
$T(1,\phi_i)$	Interpolation kernel
u, w	Displacement components in r- and z-directions
U, W	Hankel transforms of u, w

$U_c(r,\alpha)$	Fourier cosine transform of $u(r,z)$
$\bar{U}$	Strain energy
$\bar{w}$	Normalized strain energy release rate
W_i	Weighting constants of the Jacobi polynomials
$W_s(r,\alpha)$	Fourier sine transform of $w(r,z)$
α	Fourier transform variable
β	Power of singularity at the edge of crack
γ	Power of singularity at the edge of inclusion
Γ	Gamma function
Δ	4th order linear ordinary differential operator
Δ_i	2nd order linear ordinary differential operators
η, ε	Normalized variables on inclusion
θ	Probable crack propagation angle
κ	$3 - 4\nu$
μ	Shear modulus of elasticity
ν	Poisson's ratio
ξ	Hankel transform variable
σ, τ	Normal and shearing stresses
σ_{zb}, σ_{zs}	Bounded and singular parts of σ_z
	at the edges of cracks and inclusion
ϕ, ψ	Normalized variables on cracks

CHAPTER I

INTRODUCTION

Many machine elements used in various engineering fields have discontinuities in the form of holes, notches, cracks or inclusions which are very important factors influencing stress distributions in the structures. Stresses around these discontinuities may reach very large values in a small region and this phenomenon is called stress concentration. Furthermore, stresses become infinite at the corners of elements or edges of cracks and inclusions. In such cases, stress concentration can not be defined as a strength parameter and it is necessary to consider the stress distributions from fracture mechanics point of view. Fracture toughness, which is a widely accepted fracture parameter, can be easily calculated in terms of the stress intensity factors. Mechanical systems can be designed by using the fracture mechanics parameters.

Stress intensity factor depends on both the geometric properties and the loading conditions of the body. These loading conditions are defined as of three types: Mode I loading, where the principal load is applied normal to the crack plane, tends to open the crack. Mode II corresponds to in plane shear loading and tends to slide one crack face with respect to the other. Mode III refers to out of plane shear loading.

Cylinders, like screws, shafts, etc., are the most widely used machine elements with axisymmetric geometries which have particular importance in fracture mechanics due to possible singularities. For cracked semi-infinite or infinite cylinder configurations subjected to external forces, it is possible to derive closed form expressions for stresses in the body, assuming isotropic linear elastic material behavior. If a polar coordinate system with the origin at the crack tip is defined, it

is known that the stress field in any linear elastic cracked body is proportional to $1/\sqrt{r}$. As $r \to 0$, the stresses approach infinity. Thus, the stress near the crack tip varies with singularity, regardless of the configuration of the cracked body. In general, these types of problems are examined by using numerical and analytical methods based on partial differential equations. For linear elastic materials, individual components of stress, strain and displacement are additive (superposition). In many instances of analytical solutions, the principle of superposition allows stress intensity solutions for complex configurations to be built from simple cases for which the solutions are well established.

In this context, although infinite and semi-infinite cylinder problems with no crack have been already studied in literature, cracked infinite cylinder having rigid penny-shaped inclusion, cracked semi-infinite and finite cylinder problems have not been solved by the method used in this study.

1.1 Literature Review

Collins (1962) considered some axially symmetric stress distributions in an infinite elastic solid and in a thick plate containing penny-shaped cracks. It was shown that, by use of a representation for the displacement in an infinite elastic solid containing a single crack, representations for the displacements in an infinite solid containing two or more cracks and in a thick plate containing a single crack can be constructed and used to reduce the problems of determining the stresses in these solids to the solutions of Fredholm integral equations of the second kind. Various stress distributions investigated include those due to the opening of a crack in an infinite solid by a point force acting at an interior point of the solid and the opening of cracks in an infinite solid and a thick plate under the action of constant pressure over the cracks.

Sneddon and Welch (1963) made an analysis of the distribution of the stress in a long circular cylinder of elastic material when it is deformed by the application of

pressure to the inner surfaces of a penny-shaped crack situated symmetrically at the center of the cylinder. It was assumed that the cylinder surface is free from stress. The equations of the classical theory of elasticity were solved in terms of an unknown function which was then shown to be the solution of a Fredholm integral equation of the second kind previously derived by Collins (1962). The solutions of this equation for constant pressure and various crack radii, obtained using computer, have been discussed and quantities of physical interest have been calculated. Calculations have been repeated for the case of a variable pressure following a parabolic law and these results are also reported.

Two axially symmetric mixed boundary value problems in elastic dissimilar layered medium have been considered by Arın and Erdoğan (1971). It has been assumed that an elastic layer is bonded to two semi-infinite half spaces along its plane surfaces, and contains a penny-shaped crack parallel to the interfaces. In the first problem the two half spaces have been assumed to have the same elastic properties and the crack is located in the mid-plane of the layer. In the second problem, they considered the case of three different materials and arbitrary crack location in the layer. The numerical examples were given for a constant pressure on the crack surface. Stress intensity factors were evaluated and were plotted as functions of the layer thickness-to-crack radius ratio or the relative distance of the crack from one interface.

Benthem and Minderhoud (1972) solved the problem of the solid cylinder compressed axially between rough rigid stamps. Then, Gupta (1974) considered a semi-infinite cylinder problem with fixed short end. Normal loads far away from the fixed end have been prescribed. An exact formulation of the problem in terms of a singular integral equation has been provided by using an integral transform technique. Stress along the rigid end and stress intensity factors have been computed numerically and presented graphically.

Using transform methods, axisymmetric end-problem for a semi-infinite elastic circular cylinder has been reduced to a system of singular integral equations by Agarwal (1978). The kernels of the integral equations were found to contain Cauchy as well as generalized Cauchy-type singularities. The dominant part of the equations was separated and analyzed to determine the index of the singularity for differing boundary conditions at the end. An approximate method was used to obtain a system of simultaneous algebraic equations from the system of singular integral equations. As an application, axisymmetric solution for joined dissimilar elastic semi-infinite cylinders under uniform tension has been solved.

Erdöl and Erdoğan (1978) studied an elastostatic axisymmetric problem for a long thick-walled cylinder containing a ring-shaped internal or edge crack. Using transform technique the problem has been formulated in terms of an integral equation which has a simple Cauchy kernel for the internal crack and a generalized Cauchy kernel for the edge crack as the dominant part.

Nied and Erdoğan (1983) analyzed the elasticity problem for a long hollow cylinder containing an axisymmetric circumferential crack subjected to general nonaxisymmetric external loads. The problem has been formulated in terms of a system of singular integral equations with the Fourier coefficients of the derivative of the crack surface displacement as density functions. Stress intensity factors and the crack opening displacement have been calculated for a cylinder under uniform tension, bending by end couples and self-equilibrating residual stresses.

Isida et al. (1985) made an analysis of an infinite solid containing two parallel elliptical cracks located in staggered positions. The analysis has been based on the body force method, in which symmetric and axisymmetric type body forces are distributed over the crack surfaces and their densities have been determined from the boundary conditions. Numerical calculations have been performed for a wide range of parameters, and the effects of the shapes and the relative locations of the cracks on the stress intensity factors have been examined.

Geçit and Turgut (1988) considered the elastostatic plane problem of a finite strip. One end of the strip is perfectly bonded to a rigid support while the other is under the action of a uniform tensile load. Solution for the finite strip has been obtained by considering an infinite strip containing a transverse rigid inclusion at the middle and two symmetrically located transverse cracks. In the limiting case when the rigid inclusion and the cracks approach the sides of the infinite strip, the region between one crack and the rigid inclusion becomes equivalent to the finite strip. Formulation of the problem has been reduced to a system of three singular integral equations using Fourier transforms. Numerical results for stresses and stress intensity factors have been given in graphical form.

The method used by Collins (1963), Fu and Keer (1969) to solve co-planar penny-shaped cracks has been generalized to investigate interaction of arbitrarily located penny-shaped cracks by Graham and Lan (1994a). Solution of Kassir and Sih (1975) for the problem of an isolated crack in an infinite solid has been applied together with the superposition principle to reduce the problem to a system of Fredholm integral equations of the second kind. These integral equations have then been solved iteratively when the cracks are far apart. Some asymptotic solutions for the stress intensity factors have been presented and comparisons have been made whenever possible. Numerical solutions reveal some interesting phenomena. Then, Graham and Lan (1994b) examined the interaction of arbitrarily located penny-shaped cracks in a semi-infinite elastic solid, with the aid of the formulation of Muki (1961) for general three-dimensional asymmetric problems and the superposition principle.

Xiao et al. (1996) investigated the stress intensity factors of two penny-shaped cracks with different sizes in a three-dimensional elastic solid under uniaxial tension. The two parallel cracks are symmetrically located in the isotropic solid. A closed-form analytical elastic solution for the stress intensity factors on the boundaries of the cracks has been obtained when the center distance between the two cracks is much larger than the crack sizes. A numerical method has been

employed to extract the solution for the case of small center distance. It has been found that, due to the interaction between the two cracks, Mode I and II stress intensity factors exist at the same time even if the applied stress is pure tension. Numerical examples have been given for different configurations and it has been clearly shown that the stress intensity factors are strongly determined by the distance between the centers of the two cracks.

Leung and Su (1998) extended the two-level finite element method (2LFEM) for the accurate analysis of axisymmetric cracks, where both the crack geometry and applied loads were symmetrical about the axis of rotation. The complete eigenfunction expansion series for axisymmetric cracks developed by them have been employed as the global interpolation function such that the stress intensity factors are primary unknowns. The coupled coefficients in the series have been solved iteratively.

Chen (2000) evaluated stress intensity factors in a cylinder with a circumferential crack. An indirect method, the computing compliance method, has been developed to study the problem. The finite difference method has been used to solve the boundary value problem. Numerical examples have been given which demonstrate the effect of cylinder length on the stress intensity factor.

Selvadurai (2000) examined the axisymmetric problem pertaining to a penny-shaped crack which is located at the bonded plane of two similar elastic half space regions which exhibit axial variations in the linear elastic shear modulus. The equations of elasticity governing this type of non-homogeneity have been solved by employing a Hankel transform technique. The resulting mixed boundary value problem associated with the penny-shaped crack has been reduced to a Fredholm integral equation of the second kind which has been solved in numerical fashion to generate the crack opening mode stress intensity factor at the tip.

Lee (2001) made an analysis of the stress distribution in a long circular cylinder of elastic material containing a penny-shaped crack when it is deformed by the application of a uniform shearing stress. The crack with its center on the axis of the cylinder lies on a plane perpendicular to that axis, and the cylinder surface is stress-free. By making a suitable representation of the stress function, the problem has been reduced to the solution of a pair of Fredholm integral equations of second kind. These have been solved numerically, and the percentage increase in the stress intensity factor due to the effect of the finite radius of the cylinder has been presented in graphical form for various proximity ratios. Then, Lee (2002) made an analysis of the stress distribution in a long circular cylinder of isotropic elastic material with a circumferential edge crack when it is deformed by the application of a uniform shearing stress. Using same procedure given in Lee (2001), the stress intensity factor for varying circumferential edge crack size has been tabulated.

Meshii and Watanabe (2001) presented the development of a practical method, by using prepared tabulated data, to calculate the Mode I stress intensity factor for an inner surface circumferential crack in a finite length cylinder. The crack surfaces are subjected to an axisymmetric stress with an arbitrary biquadratic radial distribution. The method was derived by applying the authors' weight function for the crack. This work is based on the thin shell theory. Their method is valid over a wide range of mean radius to wall thickness ratio and for relatively short cracks. The difference between the stress intensity factor obtained by their method for the geometry and that from finite element analysis is within 5%.

Selvadurai (2002) examined the axial tensile loading of a rigid circular disc which is bonded to the surface of a half-space weakened by a penny-shaped crack. The integral equations governing the problem have been solved numerically to establish the influence of the extent of cracking on the axial stiffness of the bonded disc and on the stress intensity factors at the crack tip.

Tsang et al. (2003) investigated the stress intensity factors of multiple penny-shaped cracks in an elastic solid cylinder under axial tensile loading. The cracks are located symmetrically and parallel to one another in the isotropic cylinder. The fractal-like finite element method has been employed to study the interaction of multiple cracks and to demonstrate the efficiency of the FFEM for multiple crack problems.

An eigenfunction expansion method has been presented to obtain three-dimensional asymptotic stress fields in the vicinity of the front of a penny-shaped discontinuity, e.g., crack, anticrack (infinitely rigid lamella), etc., subjected to the far-field torsion (Mode III), extension/bending (Mode I) and sliding shear/twisting (Mode II) loadings by Chaudhuri (2003). Five different discontinuity-surface boundary conditions have been considered: penny-shaped crack, penny-shaped anticrack or perfectly bonded thin rigid inclusion, penny-shaped thin transversely rigid inclusion, penny-shaped thin rigid inclusion in part perfectly bonded, the remainder with frictionless slip and penny-shaped thin rigid inclusion alongside penny-shaped crack. The computed stress singularity for a penny-shaped anticrack is the same as that of the corresponding crack. The main difference is, however, that all the stress components at the circular tip of an anticrack depend on Poisson's ratio under Mode I and II.

Vrbik et al. (2004) examined the problem of symmetric indentation of a penny-shaped crack by a smoothly embedded rigid circular disc inclusion in a thick layer. Expressions for the resultant pressure applied to the inclusion and for the stress intensity factor at the boundary of the penny-shaped crack have been obtained. The numerical form of the expressions for the resultant stress fields and the tractions along the inclusion have been also derived. Numerical results for the resultant pressure and stress intensity factor, resultant stress fields and the resultant tractions along the inclusion have been obtained and displayed graphically.

8

1.2 A Short Introduction and Method of Solution of the Problem

This study considers the axisymmetric elasticity problem for a semi-infinite cylinder with a crack and a finite cylinder of radius A and length L. One end of the semi-infinite and finite cylinders is perfectly bonded to a rigid support at $z=0$. The other end of the semi-infinite cylinder at $z=\infty$ and the finite cylinder at $z=L$ is under the action of a tensile axial load of uniform intensity p_0. The material of the cylinder is assumed to be linearly elastic and isotropic and surface of the cylinder is free of stresses. Solution for these semi-infinite and finite cylinder problems is obtained by considering an infinite cylinder containing two concentric penny-shaped cracks of radius a at $z=\pm L$ planes and a concentric penny-shaped inclusion of radius b at $z=0$ plane which is subjected to uniformly distributed axial tensile loads of intensity p_0 at infinity.

In the limiting case, when the rigid inclusion approaches the surface of infinite cylinder, i.e., when $b \to A$, the cylinder is fixed at $z=0$. One half of infinite cylinder becomes identical with the semi-infinite cylinder which contains a penny-shaped crack at $z=L$ plane with the short end being bonded to a rigid support at $z=0$. When the crack approaches the surface of the cracked semi-infinite cylinder, i.e., when $a \to A$, the region between one crack and the rigid support becomes equivalent to a finite cylinder of length L.

Formulation for the infinite cylinder problem is obtained by means of superposition of the following two problems: (I) Uniform solution: an infinite cylinder subjected to uniform tension at $z=\pm\infty$, (II) Perturbation problem; an infinite cylinder containing two concentric penny-shaped cracks of radius a at $z=\pm L$ planes and a concentric penny-shaped rigid inclusion of radius b at $z=0$ plane with no load at infinity. General expressions for the perturbation problem (II) are obtained by adding the expressions for (II-i) an axisymmetric infinite elastic medium having two concentric penny-shaped cracks of radius a at $z=\pm L$

planes, (II-ii) an axisymmetric infinite elastic medium containing a penny-shaped rigid inclusion of radius b at $z = 0$ plane, (II-iii) an axisymmetric infinite elastic medium with no cracks or inclusion. Addition of several solutions is necessary for having sufficient number of unknowns in the general expressions so that all of the boundary conditions of the problem can be satisfied.

In this study axisymmetric problems are investigated for three main geometries: infinite cylinder, semi-infinite cylinder and finite cylinder problems. General solutions for these problems are obtained by using Hankel and Fourier transforms on Navier equations. Then, the boundary conditions at the surface of the infinite cylinder are satisfied. By using the boundary conditions on the cracks and the rigid inclusion, formulation of the infinite problem is reduced to a system of three singular integral equations. In the limiting case when the rigid inclusion approaches the surface of the cylinder (i.e., when $b \to A$), cracked semi-infinite cylinder problem is obtained. When additionally the cracks approach the surface of the cylinder (i.e., when $a \to A$), finite cylinder problem is obtained. By using Gauss-Lobatto and Gauss-Jacobi integration formulas, these singular integral equations are converted to a system of linear algebraic equations which is solved numerically. Mode I and Mode II stress intensity factors at the edges of cracks and inclusion and, normal and shearing stresses along the rigid support are calculated and are given in Table 1 and Figs. 6.1-6.85.

CHAPTER II

INFINITE CYLINDER PROBLEM

2.1. General Equations

An axisymmetric, linearly elastic, isotropic and infinite cylinder of radius A, containing two concentric penny-shaped cracks of radius a symmetrically located at $z = \pm L$ planes and a concentric penny-shaped rigid inclusion of radius b with negligible thickness at the symmetry plane $z = 0$ is considered. Both ends of this infinite cylinder are subjected to axial tensile loads of uniform intensity p_0 at infinity (Fig. 2.1).
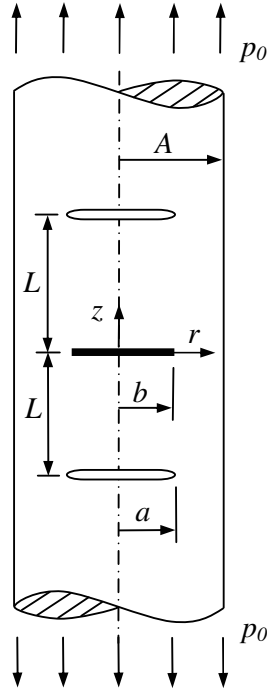
Figure 2.1 Geometry and loading of the infinite cylinder.

For the linearly elastic, isotropic and axisymmetric elasticity problems, Navier equations can be written as, Geçit (1986),

$$(\kappa+1)(\frac{\partial^2 u}{\partial r^2}+\frac{1}{r}\frac{\partial u}{\partial r}-\frac{u}{r^2})+(\kappa-1)\frac{\partial^2 u}{\partial z^2}+2\frac{\partial^2 w}{\partial r\partial z}=0,$$

$$2(\frac{\partial^2 u}{\partial r\partial z}+\frac{1}{r}\frac{\partial u}{\partial z})+(\kappa-1)(\frac{\partial^2 w}{\partial r^2}+\frac{1}{r}\frac{\partial w}{\partial r})+(\kappa+1)\frac{\partial^2 w}{\partial z^2}=0, \qquad (2.1a,b)$$

where u and w are displacements in r- and z-directions in cylindrical coordinate system, $\kappa=3-4\nu$ and ν is the Poisson's ratio. Necessary stress-displacement relations can be listed as follows,

$$\sigma_r=\frac{\mu}{\kappa-1}\left[(\kappa+1)\frac{\partial u}{\partial r}+(3-\kappa)(\frac{u}{r}+\frac{\partial w}{\partial z})\right],$$

$$\sigma_z=\frac{\mu}{\kappa-1}\left[(\kappa+1)\frac{\partial w}{\partial z}+(3-\kappa)(\frac{\partial u}{\partial r}+\frac{u}{r})\right],$$

$$\tau_{rz}=\mu(\frac{\partial u}{\partial z}+\frac{\partial w}{\partial r}), \qquad (2.2a-c)$$

where σ and τ denote normal and shearing stresses, μ is the shear modulus.

2.2 Formulation of the Problem

Solution for the infinite cylinder having a rigid penny-shaped inclusion and two penny-shaped cracks and loaded at infinity is obtained by superposition of the following two problems: (I) an infinite cylinder subjected to uniformly distributed axial tension of intensity p_0 at infinity with no cracks or inclusion, (II) an infinite

cylinder with an inclusion and two cracks for which the loading is the negative of the stresses at the location of the cracks and displacements at the location of the inclusion calculated from the solution of problem (I) (Fig. 2.2).
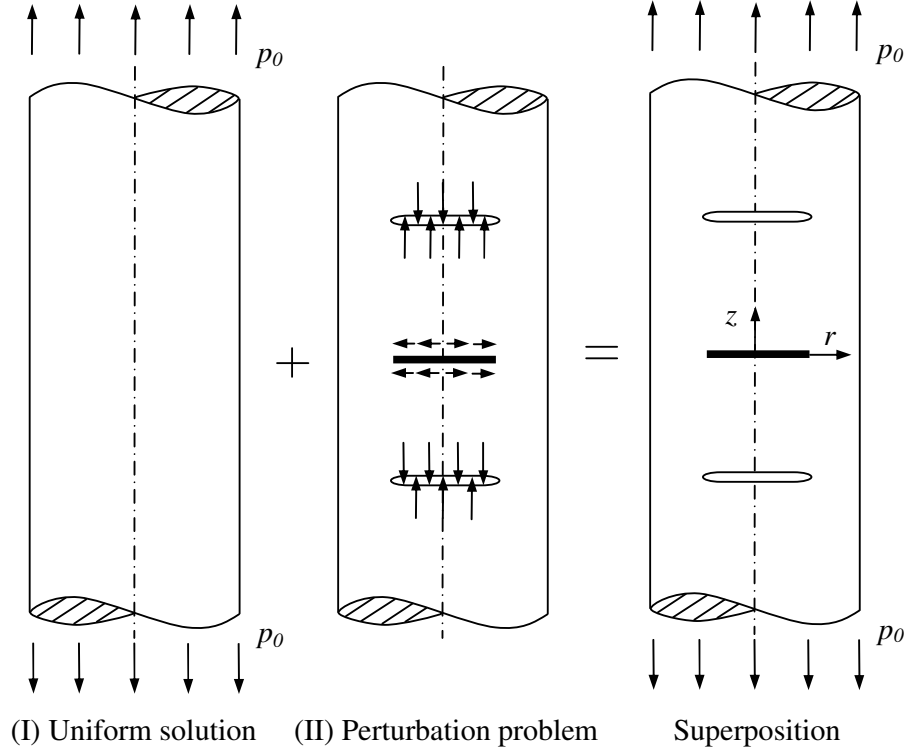
Figure 2.2 Superposition scheme of the infinite cylinder problem.

2.2.1 Perturbation Problem

General expressions of the displacements and stress components for the perturbation problem with no loads at infinity can be obtained by adding the general expressions of (II-i) an infinite cylinder containing two penny-shaped cracks of radius a symmetrically located at $z = \pm L$ planes, (II-ii) an infinite cylinder having a penny-shaped rigid inclusion of radius b at the symmetry plane

$z = 0$ and (II-iii) an infinite cylinder without cracks and inclusion under the action of arbitrary axisymmetric loading (Fig. 2.3). This is necessary in order for the expressions to contain sufficient number of unknowns so that all of the boundary conditions can be satisfied.

(II-i)	(II-ii)	(II-iii)	(II)
Hankel transform in r-direction	Hankel transform in r-direction	Fourier transform in z-direction	Perturbation problem
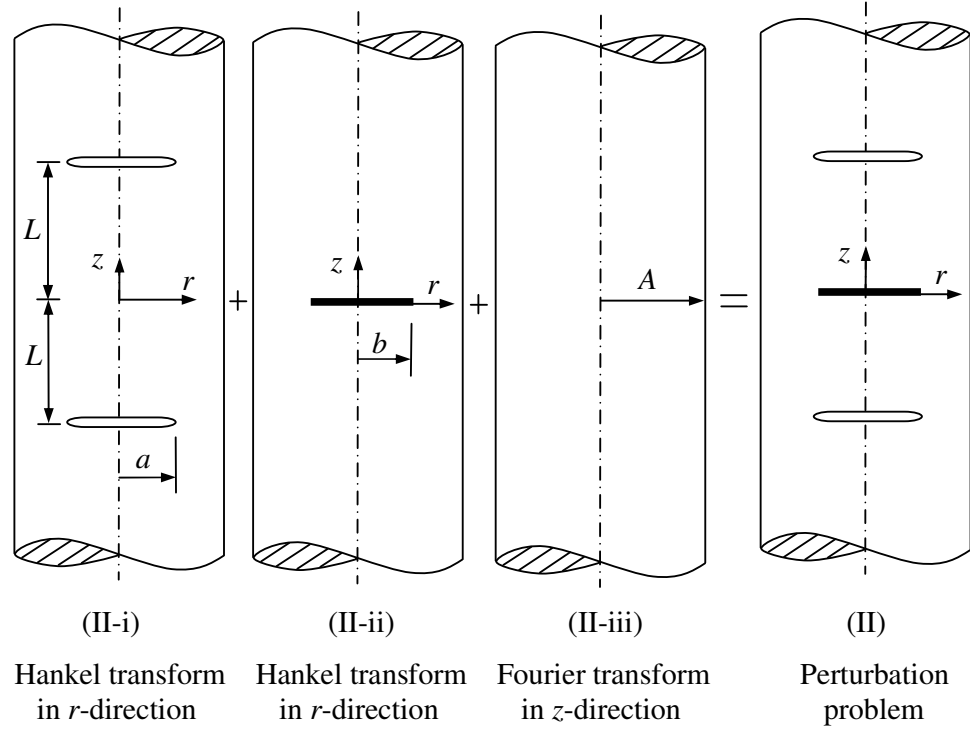
Figure 2.3 Addition of several solutions for the perturbation problem.

General expressions for the infinite cylinder $(0 \leq r < A)$ problems may adequately be obtained from infinite medium $(0 \leq r < \infty)$ solutions with appropriate boundary conditions imposed at $r = A$. Due to symmetry about $z = 0$ plane, it is sufficient to solve the problem in the upper half space $z \geq 0$ only.

2.2.1.1 Infinite Medium Having Two Cracks

Two penny-shaped cracks of radius a are located symmetrically at distances of L from $z = 0$ plane. Considering an infinite medium with Region i-1 $(0 \leq r < \infty, -L \leq z \leq L)$, Region i-2 $(0 \leq r < \infty, L \leq z < \infty)$ and Region i-3 $(0 \leq r < \infty, -\infty < z \leq -L)$, using integral transforms, H_0 Hankel transform, Sneddon (1972), of Eq. (2.1b) and H_1 transform of Eq. (2.1a), in r- direction (Fig. 2.4) and
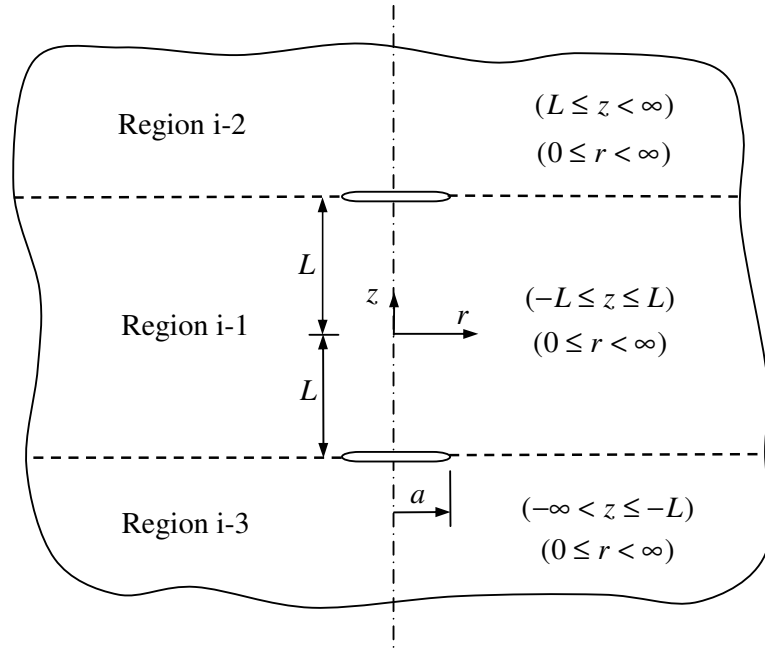
Figure 2.4 Formulation of the cracked infinite medium problem.

combining the resulting equations, one obtains,

$$\frac{d^4 U}{dz^4} - 2\xi^2 \frac{d^2 U}{dz^2} + \xi^4 U = 0 \tag{2.3}$$

where ξ is the Hankel transform variable, $U(\xi, z)$ is H_1 Hankel transform of $u(r, z)$ and $W(\xi, z)$ is H_0 Hankel transform of $w(r, z)$ in r-direction,

$$U(\xi, z) = \int_0^\infty u(r, z) r J_1(\xi r) dr ,$$

$$W(\xi, z) = \int_0^\infty w(r, z) r J_0(\xi r) dr . \qquad \text{(2.4a,b)}$$

Solution of Eq. (2.3) for the Region i-2 $(0 \leq r < \infty, L \leq z < \infty)$ (Fig. 2.4) is

$$U_{i-2}(\xi, z) = (c_1 + c_2 z) e^{-\xi z} + (c_3 + c_4 z) e^{\xi z} , \qquad \text{(2.5)}$$

where c_1, c_2, c_3 and c_4 are arbitrary unknown constants. By back substitution in the transformed ordinary differential equations, one may obtain

$$W_{i-2}(\xi, z) = \left[c_1 + (z + \frac{\kappa}{\xi}) c_2 \right] e^{-\xi z} - \left[c_3 + (z - \frac{\kappa}{\xi}) c_4 \right] e^{\xi z} . \qquad \text{(2.6)}$$

In order to have finite displacements at infinity $(z \to \infty)$, c_3 and c_4 must be zero. Therefore,

$$U_{i-2}(\xi, z) = (c_1 + c_2 z) e^{-\xi z} ,$$

$$W_{i-2}(\xi, z) = \left[c_1 + (z + \frac{\kappa}{\xi}) c_2 \right] e^{-\xi z} . \qquad \text{(2.7a,b)}$$

Taking the inverse transforms of Eqs. (2.7), displacement components are found to be

$$u_{i-2}(r,z) = \int_0^\infty (c_1 + c_2 z) e^{-\xi z} \xi J_1(\xi r) d\xi,$$

$$w_{i-2}(r,z) = \int_0^\infty \left[c_1 + (z + \frac{\kappa}{\xi}) c_2 \right] e^{-\xi z} \xi J_0(\xi r) d\xi, \tag{2.8a,b}$$

where J_0 and J_1 are the Bessel functions of the first kind of order zero and one, respectively. Substituting Eqs. (2.8) in Eqs. (2.2), one obtains the following expressions for the stress components in the Region i-2 $(0 \le r < \infty, L \le z < \infty)$,

$$\sigma_{r_{i-2}}(r,z) = \mu \int_0^\infty - 2(c_1 + c_2 z) e^{-\xi z} \frac{\xi}{r} J_1(\xi r) d\xi$$

$$+ \mu \int_0^\infty [2\xi(c_1 + c_2 z) + (\kappa - 3)c_2] e^{-\xi z} \xi J_0(\xi r) d\xi,$$

$$\sigma_{z_{i-2}}(r,z) = \mu \int_0^\infty [- 2\xi(c_1 + c_2 z) - (\kappa + 1)c_2] e^{-\xi z} \xi J_0(\xi r) d\xi,$$

$$\tau_{rz_{i-2}}(r,z) = \mu \int_0^\infty [- 2\xi(c_1 + c_2 z) - (\kappa - 1)c_2] e^{-\xi z} \xi J_1(\xi r) d\xi. \tag{2.9a-c}$$

Applying a similar procedure for the Region i-1 $(0 \le r < \infty, -L \le z \le L)$, the displacement and stress expressions are obtained in the form,

$$u_{i-1}(r,z) = \int_0^\infty [(c_5 + c_6 z) e^{-\xi z} + (c_5 - c_6 z) e^{\xi z}] \xi J_1(\xi r) d\xi,$$

$$w_{i-1}(r,z) = \int_0^\infty \left\{ \left[c_5 + (\frac{\kappa}{\xi} + z) c_6 \right] e^{-\xi z} - \left[c_5 + (\frac{\kappa}{\xi} - z) c_6 \right] e^{\xi z} \right\} \xi J_0(\xi r) d\xi, \tag{2.10a,b}$$

17

$$\sigma_r \atop i-1 (r,z) = \mu \int_0^\infty \{[2\xi(c_5 + c_6 z) + (\kappa - 3)c_6]e^{-\xi z}$$

$$+ [2\xi(c_5 - c_6 z) + (\kappa - 3)c_6]e^{\xi z}\}\xi J_0(\xi r)d\xi$$

$$- 2\mu \int_0^\infty [(c_5 + c_6 z)e^{-\xi z} + (c_5 - c_6 z)e^{\xi z}]\frac{\xi}{r} J_1(\xi r)d\xi,$$

$$\sigma_z \atop i-1 (r,z) = \mu \int_0^\infty \{[-2\xi(c_5 + c_6 z) - (\kappa + 1)c_6]e^{-\xi z}$$

$$+ [-2\xi(c_5 - c_6 z) - (\kappa + 1)c_6]e^{\xi z}\}\xi J_0(\xi r)d\xi,$$

$$\tau_{rz} \atop i-1 (r,z) = \mu \int_0^\infty \{[-2\xi(c_5 + c_6 z) - (\kappa - 1)c_6]e^{-\xi z}$$

$$+ [2\xi(c_5 - c_6 z) + (\kappa - 1)c_6]e^{\xi z}\}\xi J_1(\xi r)d\xi. \qquad (2.11a\text{-}c)$$

General expressions given in Eqs. (2.8) and (2.9) for Region i-2 $(0 \le r < \infty, L \le z < \infty)$ and Eqs. (2.10) and (2.11) for Region i-1 $(0 \le r < \infty, -L \le z \le L)$ must satisfy the following conditions at $z = L$ plane,

$$\sigma_z \atop i-1 (r,L^-) = \sigma_z \atop i-2 (r,L^+), \qquad\qquad (0 \le r < \infty)$$

$$\tau_{rz} \atop i-1 (r,L^-) = \tau_{rz} \atop i-2 (r,L^+), \qquad\qquad (0 \le r < \infty)$$

$$u_{i-1}(r,L^-) = u_{i-2}(r,L^+), \qquad\qquad (a < r < \infty)$$

$$w_{i-1}(r,L^-) = w_{i-2}(r,L^+). \qquad\qquad (a < r < \infty) \qquad (2.12a\text{-}d)$$

Note here that Eqs. (2.12a,b) are stress type continuity conditions while Eqs. (2.12c,d) are displacement type. In order to have the same type of continuity conditions, say stress type, Eqs. (2.12c,d) may be replaced by

$$\frac{\partial}{\partial r}\left[w_{i-2}(r,L^+)\right]-\frac{\partial}{\partial r}\left[w_{i-1}(r,L^-)\right]= f(r), \qquad (0\le r<\infty)$$

$$\frac{1}{r}\frac{\partial}{\partial r}\left[ru_{i-2}(r,L^+)\right]-\frac{1}{r}\frac{\partial}{\partial r}\left[ru_{i-1}(r,L^-)\right]= g(r), \qquad (0\le r<\infty) \qquad (2.13a,b)$$

where $f(r)$ and $g(r)$ are unknown functions such that $f(r)=0$ and $g(r)=0$ when $(a<r<\infty)$. Now substituting Eqs. (2.8), (2.9), (2.10) and (2.11) in Eqs. (2.12a,b) and (2.13), one obtains the following expressions for the unknown constants,

$$c_1 = -\frac{e^{-\xi L}\left[F(\xi)(1-\kappa+2L\xi)+G(\xi)(1+\kappa-2L\xi)\right]}{2(\kappa+1)\xi}$$
$$+\frac{e^{\xi L}\left[F(\xi)(-1+\kappa+2L\xi)+G(\xi)(1+\kappa+2L\xi)\right]}{2(\kappa+1)\xi},$$

$$c_2 = -\frac{e^{-\xi L}\left[F(\xi)-G(\xi)\right]}{(\kappa+1)}-\frac{e^{\xi L}\left[F(\xi)+G(\xi)\right]}{(\kappa+1)},$$

$$c_5 = \frac{e^{-\xi L}\left[F(\xi)(-1+\kappa-2L\xi)+G(\xi)(-1-\kappa+2L\xi)\right]}{2(\kappa+1)\xi},$$

$$c_6 = \frac{e^{-\xi L}\left[-F(\xi)+G(\xi)\right]}{(\kappa+1)}, \qquad (2.14a\text{-}d)$$

where

19

$$F(\xi) = \int_0^\infty f(r)rJ_1(\xi r)dr\,,$$

$$G(\xi) = \int_0^\infty g(r)rJ_0(\xi r)dr\,. \qquad (2.15a,b)$$

Hence, the displacements and the stresses are expressed in terms of $F(\xi)$ and $G(\xi)$ for Region i-1 $(0 \le r < \infty, -L \le z \le L)$ and Region i-2 $(0 \le r < \infty, L \le z < \infty)$ shown in Fig. 2.4,

$$u_{i-1}(r,z) = \frac{1}{2(\kappa+1)}\int_0^\infty \Big\{ -\big[(1-\kappa+2L\xi+2z\xi)F(\xi)+(1+\kappa-2L\xi-2z\xi)G(\xi)\big]e^{-\xi(L+z)}$$
$$+\big[(-1+\kappa-2L\xi+2z\xi)F(\xi)-(1+\kappa-2L\xi+2z\xi)G(\xi)\big]e^{\xi(-L+z)}\Big\}J_1(\xi r)d\xi\,,$$

$$w_{i-1}(r,z) = \frac{-1}{2(\kappa+1)}\int_0^\infty \Big\{ \big[(1+\kappa+2L\xi+2z\xi)F(\xi)+(1-\kappa-2L\xi-2z\xi)G(\xi)\big]e^{-\xi(L+z)}$$
$$-\big[(1+\kappa+2L\xi-2z\xi)F(\xi)-(-1+\kappa+2L\xi-2z\xi)G(\xi)\big]e^{\xi(-L+z)}\Big\}J_0(\xi r)d\xi\,,$$

$$\sigma_{r_{i-1}}(r,z) = \frac{2\mu}{(\kappa+1)}\int_0^\infty \Big\{ -\big[(-1+L\xi+z\xi)F(\xi)-(-2+L\xi+z\xi)G(\xi)\big]e^{-\xi(L+z)}$$
$$+\big[(1-L\xi+z\xi)F(\xi)+(-2+L\xi-z\xi)G(\xi)\big]e^{\xi(-L+z)}\Big\}\xi J_0(\xi r)d\xi$$
$$+\frac{\mu}{(\kappa+1)}\int_0^\infty \Big\{ \big[(1-\kappa+2L\xi+2z\xi)F(\xi)+(1+\kappa-2L\xi-2z\xi)G(\xi)\big]e^{-\xi(L+z)}$$
$$-\big[(-1+\kappa-2L\xi+2z\xi)F(\xi)-(1+\kappa-2L\xi+2z\xi)G(\xi)\big]e^{\xi(-L+z)}\Big\}\frac{J_1(\xi r)}{r}d\xi\,,$$

$$\sigma_{z_{i-1}}(r,z) = \frac{2\mu}{(\kappa+1)}\int_0^\infty \Big\{ \big[(1+L\xi+z\xi)F(\xi)-(L+z)\xi G(\xi)\big]e^{-\xi(L+z)}$$
$$-\big[(-1-L\xi+z\xi)F(\xi)+(L-z)\xi G(\xi)\big]e^{\xi(-L+z)}\Big\}\xi J_0(\xi r)d\xi\,,$$

20

$$\tau_{rz \atop i-1}(r,z) = \frac{2\mu}{(\kappa+1)}\int_0^\infty \{[(L+z)\xi F(\xi)-(-1+L\xi+z\xi)G(\xi)]e^{-\xi(L+z)}$$

$$+[-(L+z)\xi F(\xi)+(-1+L\xi-z\xi)G(\xi)]e^{\xi(-L+z)}\}\xi J_1(\xi r)d\xi, \qquad (2.16\text{a-e})$$

$$u_{i-2}(r,z) = \frac{-1}{2(\kappa+1)}\int_0^\infty \{[(1-\kappa+2L\xi+2z\xi)F(\xi)+(1+\kappa-2L\xi-2z\xi)G(\xi)]e^{-\xi(L+z)}$$

$$+[(1-\kappa-2L\xi+2z\xi)F(\xi)-(1+\kappa+2L\xi-2z\xi)G(\xi)]e^{\xi(L-z)}\}J_1(\xi r)d\xi,$$

$$w_{i-2}(r,z) = \frac{-1}{2(\kappa+1)}\int_0^\infty \{[(1+\kappa+2L\xi+2z\xi)F(\xi)-(-1+\kappa+2L\xi+2z\xi)G(\xi)]e^{-\xi(L+z)}$$

$$+[(1+\kappa-2L\xi+2z\xi)F(\xi)+(-1+\kappa-2L\xi+2z\xi)G(\xi)]e^{\xi(L-z)}\}J_0(\xi r)d\xi,$$

$$\sigma_{r \atop i-2}(r,z) = -\frac{2\mu}{(\kappa+1)}\int_0^\infty \{[(-1+L\xi+z\xi)F(\xi)+(2-L\xi-z\xi)G(\xi)]e^{-\xi(L+z)}$$

$$+[(-1-L\xi+z\xi)F(\xi)-(2+L\xi-z\xi)G(\xi)]e^{\xi(L-z)}\}\xi J_0(\xi r)d\xi$$

$$+\frac{\mu}{(\kappa+1)}\int_0^\infty \{[(1-\kappa+2L\xi+2z\xi)F(\xi)+(1+\kappa-2L\xi-2z\xi)G(\xi)]e^{-\xi(L+z)}$$

$$+[(1-\kappa-2L\xi+2z\xi)F(\xi)-(1+\kappa+2L\xi-2z\xi)G(\xi)]e^{\xi(L-z)}\}\frac{J_1(\xi r)}{r}d\xi,$$

$$\sigma_{z \atop i-2}(r,z) = \frac{2\mu}{(\kappa+1)}\int_0^\infty \{[(1+L\xi+z\xi)F(\xi)-(L+z)\xi G(\xi)]e^{-\xi(L+z)}$$

$$+[(1-L\xi+z\xi)F(\xi)-(L-z)\xi G(\xi)]e^{\xi(L-z)}\}\xi J_0(\xi r)d\xi,$$

$$\tau_{rz \atop i-2}(r,z) = \frac{2\mu}{(\kappa+1)}\int_0^\infty \{[(L+z)\xi F(\xi)+(1-L\xi-z\xi)G(\xi)]e^{-\xi(L+z)}$$

$$+[-(L-z)\xi F(\xi)-(1+L\xi-z\xi)G(\xi)]e^{\xi(L-z)}\}\xi J_1(\xi r)d\xi. \qquad (2.17\text{a-e})$$

21

2.2.1.2 Infinite Medium Having an Inclusion

Now consider an infinite medium having a penny-shaped rigid inclusion of radius b located at the symmetry plane $(z = 0)$. Considering an infinite medium with Region ii-1 $(0 \leq r < \infty, 0 \leq z < \infty)$ and Region ii-2 $(0 \leq r < \infty, -\infty < z \leq 0)$, using integral transforms, H_0 Hankel transform of Eq. (2.1b) and H_1 transform of Eq. (2.1a) in r-direction (Fig. 2.5), solution of Eq. (2.3) for the Region ii-1 $(0 \leq r < \infty, 0 \leq z < \infty)$ is obtained in the form

$$U_{ii-1}(\xi, z) = (c_9 + c_{10}z)e^{-\xi z} + (c_{11} + c_{12}z)e^{\xi z}, \tag{2.18}$$

where c_9, c_{10}, c_{11} and c_{12} are arbitrary unknown constants. Similarly, one may write

$$W_{ii-1}(\xi, z) = \left[c_9 + (z + \frac{\kappa}{\xi})c_{10} \right] e^{-\xi z} - \left[c_{11} + (z - \frac{k}{\xi})c_{12} \right] e^{\xi z}. \tag{2.19}$$

In order to have finite displacements at infinity $(z \to \infty)$, c_{11} and c_{12} must be zero. Taking the inverse transforms of Eqs. (2.18) and (2.19), displacement components are found to be

$$u_{ii-1}(r, z) = \int_0^\infty (c_9 + c_{10}z)e^{-\xi z} \xi J_1(\xi r)d\xi,$$

$$w_{ii-1}(r, z) = \int_0^\infty \left[c_9 + (z + \frac{\kappa}{\xi})c_{10} \right] e^{-\xi z} \xi J_0(\xi r)d\xi. \tag{2.20a,b}$$

Region ii-1 $(0 \le z < \infty)$
                     $(0 \le r < \infty)$

z r

b
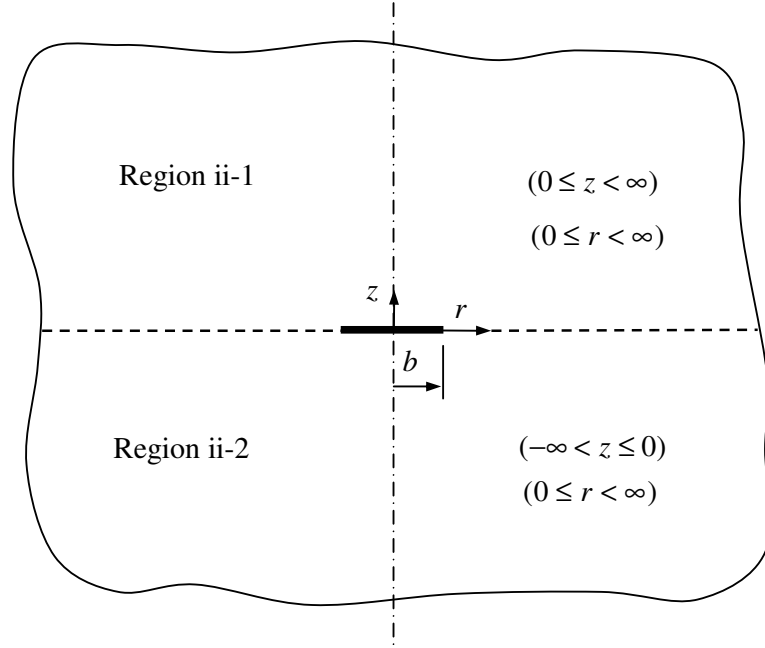
Region ii-2 $(-\infty < z \le 0)$
                     $(0 \le r < \infty)$

Figure 2.5 Infinite medium having an inclusion.

Substituting Eqs. (2.20) in Eqs. (2.2), one obtains the following expressions for the stress components in the Region ii-1 $(0 \le r < \infty, 0 \le z < \infty)$ (Fig. 2.5):

$$\sigma_{r \atop ii-1}(r,z) = \mu \int_0^\infty \left[-2(c_9 + c_{10}z)\right] e^{-\xi z} \xi \frac{J_1(\xi r)}{r} d\xi$$

$$+ \mu \int_0^\infty \left[2\xi(c_9 + c_{10}z) + (\kappa - 3)c_{10}\right] e^{-\xi z} \xi J_0(\xi r) d\xi,$$

$$\sigma_{z \atop ii-1}(r,z) = \mu \int_0^\infty \left[-2\xi(c_9 + c_{10}z) - (\kappa + 1)c_{10}\right] e^{-\xi z} \xi J_0(\xi r) d\xi,$$

$$\tau_{rz \atop ii-1}(r,z) = \mu \int_0^\infty \left[-2\xi(c_9 + c_{10}z) - (\kappa - 1)c_{10}\right] e^{-\xi z} \xi J_1(\xi r) d\xi. \qquad (2.21\text{a-c})$$

23

Expressions for the lower semi infinite space $(0 \le r < \infty, -\infty < z \le 0)$ are obtained similarly in the form,

$$u_{ii-2}(r,z) = \int_0^\infty (c_{15} + c_{16}z)e^{\xi z}\xi J_1(\xi r)d\xi ,$$

$$w_{ii-2}(r,z) = \int_0^\infty \left[-c_{15} - (z - \frac{\kappa}{\xi})c_{16} \right] e^{\xi z}\xi J_0(\xi r)d\xi , \qquad (2.22\text{a,b})$$

$$\sigma_{r_{ii-2}}(r,z) = \mu\int_0^\infty \left[2\xi(c_{15} + c_{16}z) - (\kappa - 3)c_{16} \right] e^{\xi z}\xi J_0(\xi r)d\xi$$

$$- 2\mu\int_0^\infty (c_{15} + c_{16}z)e^{\xi z}\xi \frac{J_1(\xi r)}{r} d\xi ,$$

$$\sigma_{z_{ii-2}}(r,z) = \mu\int_0^\infty \left[-2\xi(c_{15} + c_{16}z) + (\kappa + 1)c_{16} \right] e^{\xi z}\xi J_0(\xi r)d\xi ,$$

$$\tau_{rz_{ii-2}}(r,z) = \mu\int_0^\infty \left[2\xi(c_{15} + c_{16}z) - (\kappa - 1)c_{16} \right] e^{\xi z}\xi J_1(\xi r)d\xi . \qquad (2.23\text{a-c})$$

The expressions in Eqs. (2.20), (2.21) and (2.22), (2.23) are matched on the $z = 0$ plane by means of the following continuity conditions,

$$u_{ii-1}(r,0^+) = u_{ii-2}(r,0^-), \qquad\qquad (0 \le r < \infty)$$

$$w_{ii-1}(r,0^+) = w_{ii-2}(r,0^-), \qquad\qquad (0 \le r < \infty)$$

$$\sigma_{z_{ii-1}}(r,0^+) = \sigma_{z_{ii-2}}(r,0^-), \qquad\qquad (0 \le r < \infty)$$

24

$$\tau_{\underset{ii-1}{rz}}(r,0^+) - \tau_{\underset{ii-2}{rz}}(r,0^-) = h(r), \qquad (0 \le r < \infty) \qquad \text{(2.24a-d)}$$

where $h(r)$ is the jump in the shearing stress τ_{rz} through the rigid inclusion and it is such that $h(r) = 0$ when $b < r < \infty$. The unknown constants can be expressed in terms of $H(\xi)$ as,

$$c_9 = c_{15} - \frac{\kappa H(\xi)}{2(\kappa+1)\mu\xi},$$

$$c_{10} = -c_{16} = \frac{H(\xi)}{2(\kappa+1)\mu}, \qquad \text{(2.25a,b)}$$

where

$$H(\xi) = \int_0^\infty h(r)rJ_1(\xi r)dr . \qquad \text{(2.26)}$$

Since the infinite medium having an inclusion is symmetric about $z = 0$ plane, the axisymmetric problem is considered in the upper half space Region ii-1 $(0 \le r < \infty, 0 \le z < \infty)$ (Fig. 2.5). The displacements and the stresses for this region may be written as,

$$u_{ii-1}(r,z) = \frac{1}{2\mu(\kappa+1)} \int_0^\infty [(-\kappa + z\xi)H(\xi)]e^{-\xi z}J_1(\xi r)d\xi ,$$

$$w_{ii-1}(r,z) = \frac{1}{2\mu(\kappa+1)} \int_0^\infty [z\xi H(\xi)]e^{-\xi z}J_0(\xi r)d\xi ,$$

$$\sigma_{\substack{r\\ii-1}}(r,z) = \frac{1}{(\kappa+1)}\int_0^\infty [(\kappa-z\xi)H(\xi)]e^{-\xi z}\frac{J_1(\xi r)}{r}d\xi$$

$$-\frac{1}{2(\kappa+1)}\int_0^\infty [(3+\kappa-2z\xi)H(\xi)]e^{-\xi z}\xi J_0(\xi r)d\xi,$$

$$\sigma_{\substack{z\\ii-1}}(r,z) = \frac{1}{2(\kappa+1)}\int_0^\infty [(-1+\kappa-2z\xi)H(\xi)]e^{-\xi z}\xi J_0(\xi r)d\xi,$$

$$\tau_{\substack{rz\\ii-1}}(r,z) = \frac{1}{2(\kappa+1)}\int_0^\infty [(1+\kappa-2z\xi)H(\xi)]e^{-\xi z}\xi J_1(\xi r)d\xi. \qquad (2.27a\text{-}e)$$

2.2.1.3 Infinite Medium under the Action of Arbitrary Axisymmetric Loading

In this section, the infinite medium problem without crack and inclusion is considered. For the solution of this problem, taking the Fourier cosine transform, Sneddon (1951), of the first Navier equation, (2.1a), and the Fourier cosine transform of the second Navier equation, (2.1b), in z- direction and combining the resulting equations, one obtains,

$$x^4\frac{d^4U_c}{dx^4}+2x^3\frac{d^3U_c}{dx^3}-(2x^4+3x^2)\frac{d^2U_c}{dx^2}-(2x^3-3x)\frac{dU_c}{dx}+(x^4+2x^2-3)U_c=0$$

$$(2.28)$$

where U_c is the Fourier cosine transform of $u(r,z)$,

$$U_c(r,\alpha) = \int_0^\infty u(r,z)\cos(\alpha z)dz, \qquad (2.29)$$

$x=\alpha r$, α being Fourier transform variable. By taking into consideration that Eq. (2.28) is in the form

26

$$\Delta U_c = 0, \tag{2.30}$$

where Δ is a 4th order linear ordinary differential operator with variable coefficients in x, McLachlan (1934), Eq. (2.30) may be written as

$$\Delta_1(\Delta_2 U_c) + \Delta_3(\Delta_4 U_c) = 0, \tag{2.31}$$

where $\Delta_1, \Delta_2, \Delta_3$ and Δ_4 are second order linear ordinary differential operators with variable coefficients in x:

$$\Delta_1 = x^2 \frac{d^2}{dx^2} - 3x \frac{d}{dx} - x^2 + 3,$$

$$\Delta_2 = x^2 \frac{d^2}{dx^2} + x \frac{d}{dx} - x^2 - 1,$$

$$\Delta_3 = x^2 \frac{d^2}{dx^2} + x \frac{d}{dx} - x^2 - 4,$$

$$\Delta_4 = x \frac{d^2}{dx^2} - \frac{d}{dx} + \frac{1}{x} - x. \tag{2.32a-d}$$

Solution of Eq. (2.31) is

$$U_c(r, \alpha) = -\frac{1}{2} c_{17} I_1(\alpha r) + \frac{1}{2} c_{18} K_1(\alpha r) + c_{19} \alpha r I_0(\alpha r) + c_{20} \alpha r K_0(\alpha r), \tag{2.33}$$

where I_0, K_0, I_1 and K_1 are the modified Bessel functions of the first and second kinds of order zero and one, respectively, and c_{17}, c_{18}, c_{19} and c_{20} are arbitrary constants. Because of symmetry about z-axis, c_{18} and c_{20} must be zero (Fig. 2.6).

Region iii-1 $(0 \leq z < \infty)$

$(0 \leq r < \infty)$

z r

Region iii-2 $(-\infty < z \leq 0)$

$(0 \leq r < \infty)$
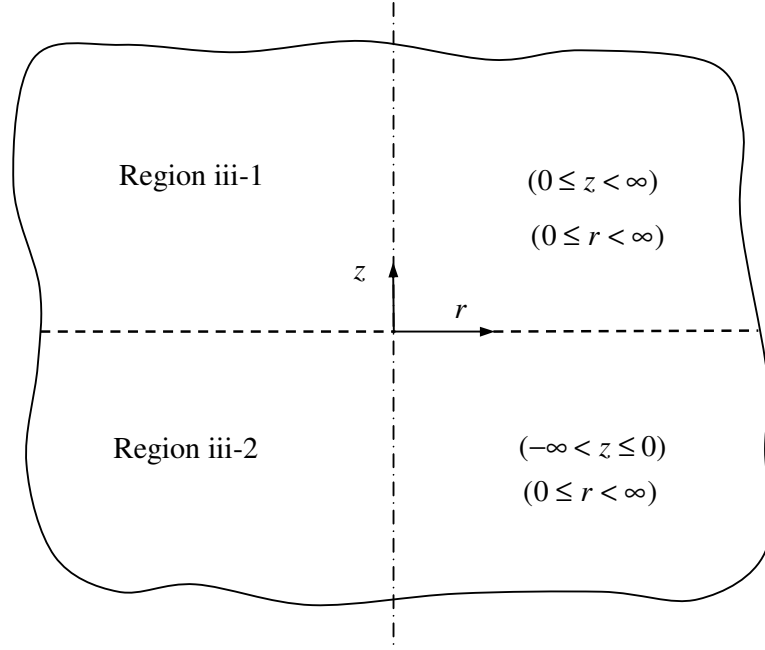
Figure 2.6 Infinite axisymmetric medium with no crack or inclusion.

By similar consideration,

$$W_s(r,\alpha) = \frac{1}{2}c_{17}I_0(\alpha r) - c_{19}\left[(\kappa+1)I_0(\alpha r) + \alpha r I_1(\alpha r)\right] \tag{2.34}$$

is obtained where $W_s(r,\alpha)$ is the Fourier sine transform of $w(r,z)$,

$$W_s(r,\alpha) = \int_0^\infty w(r,z)\sin(\alpha z)dz . \tag{2.35}$$

Taking the inverse transform of Eqs. (2.33) and (2.34), the displacement components are found to be

$$u_{fourier}(r,z) = \frac{2}{\pi}\int_0^\infty \left[-\frac{1}{2}c_{17}I_1(\alpha r) + c_{19}\alpha r I_0(\alpha r) \right]\cos(\alpha z)d\alpha \ ,$$

$$w_{fourier}(r,z) = \frac{2}{\pi}\int_0^\infty \left\{ \frac{1}{2}c_{17}I_0(\alpha r) - c_{19}\left[(\kappa+1)I_0(\alpha r) + \alpha r I_1(\alpha r) \right] \right\}\sin(\alpha z)dz \ . \quad (2.36a,b)$$

Substituting Eqs. (2.36) in Eqs. (2.2), one obtains the following expressions for the stress components

$$\sigma_{r\ fourier}(r,z) = \frac{2\mu}{\pi}\int_0^\infty \left\{ c_{17}\left[\frac{I_1(\alpha r)}{r} - \alpha I_0(\alpha r) \right] \right.$$
$$\left. + c_{19}\left[(\kappa-1)\alpha I_0(\alpha r) + 2\alpha^2 r I_1(\alpha r) \right] \right\}\cos(\alpha z)d\alpha \ ,$$

$$\sigma_{z\ fourier}(r,z) = \frac{2\mu}{\pi}\int_0^\infty \left\{ c_{17}\alpha I_0(\alpha r) - c_{19}\left[(\kappa+5)\alpha I_0(\alpha r) + 2\alpha^2 r I_1(\alpha r) \right] \right\}\cos(\alpha z)d\alpha \ ,$$

$$\tau_{rz\ fourier}(r,z) = \frac{2\mu}{\pi}\int_0^\infty \left\{ c_{17}\alpha I_1(\alpha r) - c_{19}\left[(\kappa+1)\alpha I_1(\alpha r) + 2\alpha^2 r I_0(\alpha r) \right] \right\}\sin(\alpha z)d\alpha \ .$$

$$(2.37a\text{-}c)$$

Now the general expressions for the infinite medium containing two penny-shaped cracks, a penny-shaped inclusion and subjected to arbitrary axisymmetric loads (not at infinity) may be obtained when the individual expressions are added together:

$$u_{perturbation} = u_{cracks} + u_{inclusion} + u_{fourier} \ ,$$

$$w_{perturbation} = w_{cracks} + w_{inclusion} + w_{fourier} \ ,$$

$$\sigma_{r\,perturbation} = \sigma_{r\,cracks} + \sigma_{r\,inclusion} + \sigma_{r\,fourier},$$

$$\sigma_{z\,perturbation} = \sigma_{z\,cracks} + \sigma_{z\,inclusion} + \sigma_{z\,fourier},$$

$$\tau_{rz\,perturbation} = \tau_{rz\,cracks} + \tau_{rz\,inclusion} + \tau_{rz\,fourier}. \tag{2.38a-e}$$

These expressions may give those for the perturbation problem for an infinite cylinder with stress-free surface if they are forced to satisfy the homogeneous boundary conditions

$$\sigma_{r\,perturbation}(A, z) = 0, \qquad (0 \le z < \infty)$$

$$\tau_{rz\,perturbation}(A, z) = 0. \qquad (0 \le z < \infty) \tag{2.39a,b}$$

Eqs. (2.39) with (2.16), (2.17), (2.27), (2.37) and (2.38) give

$$c_{17}\alpha I_1(\alpha A) - c_{19}\left[(\kappa+1)\alpha I_1(\alpha A) + 2A\alpha^2 I_0(\alpha A)\right]$$

$$= \frac{\cos(\alpha L)}{(\kappa+1)} \int_0^\infty \left[\frac{-8\alpha\xi^3}{(\alpha^2+\xi^2)^2}\right] J_1(\xi A) F(\xi) d\xi$$

$$+ \frac{\sin(\alpha L)}{(\kappa+1)} \int_0^\infty \left[\frac{8\alpha^2\xi^2}{(\alpha^2+\xi^2)^2}\right] J_1(\xi A) G(\xi) d\xi$$

$$+ \frac{1}{2\mu(\kappa+1)} \int_0^\infty \left\{\frac{-\alpha\xi\left[(\kappa+1)\alpha^2+(\kappa-3)\xi^2\right]}{(\alpha^2+\xi^2)^2}\right\} J_1(\xi A) H(\xi) d\xi,$$

$$c_{17}\left[\frac{I_1(\alpha A)}{A} - \alpha I_0(\alpha A)\right] + c_{19}\left[(\kappa-1)\alpha I_0(\alpha A) + 2A\alpha^2 I_1(\alpha A)\right]$$

$$= \frac{\cos(\alpha L)}{(\kappa+1)} \int_0^\infty \left\{\frac{2\xi\left[(\kappa+1)\alpha^2+(\kappa-3)\xi^2\right]}{(\alpha^2+\xi^2)^2} \frac{J_1(\xi A)}{A} - \frac{8\alpha^2\xi^2}{(\alpha^2+\xi^2)^2} J_0(\xi A)\right\} F(\xi) d\xi$$

$$+\frac{\sin(\alpha L)}{(\kappa+1)}\int_0^\infty\left\{\frac{-2\alpha\left[(\kappa+1)\alpha^2+(\kappa-3)\xi^2\right]J_1(\xi A)}{(\alpha^2+\xi^2)^2}+\frac{8\alpha^3\xi}{(\alpha^2+\xi^2)^2}J_0(\xi A)\right\}G(\xi)d\xi$$

$$+\frac{1}{2\mu(\kappa+1)}\int_0^\infty\left\{\frac{-2\xi\left[(\kappa+1)\alpha^2+(\kappa-1)\xi^2\right]J_1(\xi A)}{(\alpha^2+\xi^2)^2}\right.$$

$$\left.+\frac{\xi^2\left[(\kappa+5)\alpha^2+(\kappa+1)\xi^2\right]}{(\alpha^2+\xi^2)^2}J_0(\xi A)\right\}H(\xi)d\xi\ . \tag{2.40a,b}$$

following routine manipulations. Solution of Eqs. (2.40) give

$$c_{17}=A\left\{\frac{\left[I_0(\alpha A)(\kappa-1)+2AI_1(\alpha A)\alpha\right]E_1+\left[I_1(\alpha A)+I_1(\alpha A)\kappa+2AI_0(\alpha A)\alpha\right]E_2}{-2A^2I_0^{\ 2}(\alpha A)\alpha^2+I_1^{\ 2}(\alpha A)(1+\kappa+2A^2\alpha^2)}\right\},$$

$$c_{19}=\frac{1}{\alpha}\left\{\frac{\left[-I_1(\alpha A)+AI_0(\alpha A)\alpha\right]E_1+\left[AI_1(\alpha A)\alpha\right]E_2}{-2A^2I_0^{\ 2}(\alpha A)\alpha^2+I_1^{\ 2}(\alpha A)(1+\kappa+2A^2\alpha^2)}\right\}, \tag{2.41a,b}$$

in which, by the aid of integral formulas given in Appendix A one may show that,

$$E_1=\frac{\cos(\alpha L)}{(\kappa+1)}\int_0^a f(t)t\left\{-4\alpha^2\left[tK_1(\alpha A)I_0(\alpha t)-AK_0(\alpha A)I_1(\alpha t)\right]\right\}dt$$

$$+\frac{\sin(\alpha L)}{(\kappa+1)}\int_0^a g(t)t\left\{4\alpha^2\left[AK_0(\alpha A)I_0(\alpha t)-tK_1(\alpha A)I_1(\alpha t)\right]\right\}dt$$

$$+\frac{1}{2\mu(\kappa+1)}\int_0^b h(t)t\left\{2\alpha^2\left[tK_1(\alpha A)I_0(\alpha t)-AK_0(\alpha A)I_1(\alpha t)\right]\right.$$

$$\left.-\alpha(\kappa+1)K_1(\alpha A)I_1(\alpha t)\right\}dt\ ,$$

$$E_2=\frac{\cos(\alpha L)}{(\kappa+1)}\int_0^a f(t)t\left\{-\frac{4\alpha t}{A}K_1(\alpha A)I_0(\alpha t)+4\alpha K_0(\alpha A)I_1(\alpha t)\right.$$

$$\left.-4\alpha^2tK_0(\alpha A)I_0(\alpha t)+\left[\frac{2(\kappa+1)}{A}+4\alpha^2A\right]K_1(\alpha A)I_1(\alpha t)\right\}dt$$

31

$$+ \frac{\sin(\alpha L)}{(\kappa+1)} \int_0^a g(t)t \left\{ -\frac{4\alpha t}{A} K_1(\alpha A) I_1(\alpha t) + 4\alpha K_0(\alpha A) I_0(\alpha t) \right.$$

$$\left. -4\alpha^2 t K_0(\alpha A) I_1(\alpha t) + \left[\frac{2(\kappa+1)}{A} + 4\alpha^2 A \right] K_1(\alpha A) I_0(\alpha t) - \frac{2(\kappa+1)}{A^2 \alpha} \right\} dt$$

$$+ \frac{1}{2\mu(\kappa+1)} \int_0^b h(t)t \left\{ \frac{2\alpha t}{A} K_1(\alpha A) I_0(\alpha t) + 2\alpha^2 t K_0(\alpha A) I_0(\alpha t) \right.$$

$$\left. - \left[\frac{2(\kappa+1)}{A} + 2\alpha^2 A \right] K_1(\alpha A) I_1(\alpha t) - [\alpha(\kappa+1) + 2\alpha] K_0(\alpha A) I_1(\alpha t) \right\} dt .$$

$$(2.42a,b)$$

Then, the general expressions for the perturbation problem of an infinite cylinder with two cracks, an inclusion and a stress-free lateral surface become

$$u_{cyl.per.}(r,z) = \frac{1}{(\kappa+1)} \int_0^a f(t)t \left\langle \frac{1}{2} \int_0^\infty [(-1+\kappa-2L\xi-2z\xi)e^{-\xi(L+z)} + (-1+\kappa-2L\xi \right.$$

$$+ 2z\xi)e^{-\xi(L-z)}] J_1(\xi t) J_1(\xi r) d\xi + \frac{2}{\pi} \int_0^\infty \frac{1}{d_0} \{ -2r\alpha I_0(\alpha r)[-2t\alpha I_0(\alpha t)$$

$$+ I_1(t\alpha)(d_2 + d_1 d_3)] + I_1(r\alpha) \{ -2t\alpha I_0(t\alpha)(1+\kappa+d_2+d_1 d_3)$$

$$+ I_1(t\alpha)[(1+\kappa)d_2 + 2d_1 + d_1 d_3(1+\kappa)] \} \} \cos(\alpha L) \cos(\alpha z) d\alpha \rangle dt$$

$$+ \frac{1}{(\kappa+1)} \int_0^a g(t)t \left\langle \frac{1}{2} \int_0^\infty [(-1-\kappa+2L\xi+2z\xi)e^{-\xi(L+z)} - (1+\kappa-2L\xi \right.$$

$$+ 2z\xi)e^{-\xi(L-z)}] J_0(\xi t) J_1(\xi r) d\xi + \frac{2}{\pi} \int_0^\infty -\frac{1}{A\alpha d_0} \{ 2r\alpha I_0(r\alpha) \{ A\alpha[-2\alpha t I_1(t\alpha)$$

$$+ d_2 I_0(t\alpha)] - I_1(A\alpha)(1+\kappa) + A\alpha d_1 d_3 I_0(t\alpha) \} + I_1(r\alpha) \{ I_1(A\alpha)(1$$

$$+ 2\kappa + \kappa^2) + I_1(t\alpha) 2At\alpha^2(1+\kappa) + 2A\alpha I_0(A\alpha)(1+\kappa) - A\alpha(1+\kappa)d_2 I_0(t\alpha)$$

$$+ 2At\alpha^2 d_2 I_1(t\alpha) + d_1 d_3 2At\alpha^2 I_1(t\alpha)$$

$$- A\alpha d_1 I_0(t\alpha)[2 + (1+\kappa)d_3] \} \} \sin(\alpha L) \cos(\alpha z) d\alpha \rangle dt$$

$$+\frac{1}{\mu(\kappa+1)}\int_0^b h(t)t\left\langle\frac{1}{2}\int_0^\infty(-\kappa+z\xi)e^{-\xi z}J_1(\xi t)J_1(\xi r)d\xi\right.$$

$$+\frac{1}{2\pi}\int_0^\infty\frac{1}{d_0}\{2r\alpha I_0(\alpha r)[-2t\alpha I_0(t\alpha)+I_1(t\alpha)(1+\kappa+d_2+d_1d_3)]$$

$$+I_1(r\alpha)\{2t\alpha I_0(t\alpha)(1+\kappa+d_2+d_1d_3)-I_1(t\alpha)[1+\kappa(2+\kappa+2d_2)+3d_2$$

$$\left.+2d_1d_3(1+\kappa)]\}\}\cos(\alpha z)d\alpha\right\rangle dt,$$

$$w_{cyl.per.}(r,z)=\frac{1}{(\kappa+1)}\int_0^a f(t)t\left\langle\frac{1}{2}\int_0^\infty[(-1-\kappa-2L\xi-2z\xi)e^{-\xi(L+z)}+(1+\kappa+2L\xi\right.$$

$$-2z\xi)e^{-\xi(L-z)}]J_1(\xi t)J_0(\xi r)d\xi\ +\frac{2}{\pi}\int_0^\infty\frac{1}{d_0}\{2r\alpha I_1(r\alpha)[-2t\alpha I_0(t\alpha)$$

$$+I_1(t\alpha)(d_2+d_1d_3)]+I_0(r\alpha)\{2t\alpha I_0(t\alpha)(-1-\kappa+d_2+d_1d_3)$$

$$\left.+I_1(t\alpha)[(1+\kappa)d_2-2d_1+d_1d_3(1+\kappa)]\}\}\cos(\alpha L)\sin(\alpha z)d\alpha\right\rangle dt$$

$$+\frac{1}{(\kappa+1)}\int_0^a g(t)t\left\langle\frac{1}{2}\int_0^\infty[(-1+\kappa+2L\xi+2z\xi)e^{-\xi(L+z)}-(-1+\kappa+2L\xi\right.$$

$$-2z\xi)e^{-\xi(L-z)}]J_0(\xi t)J_0(\xi r)d\xi\ +\frac{2}{\pi}\int_0^\infty\frac{1}{A\alpha d_0}\{A\alpha\{2r\alpha d_2I_0(t\alpha)I_1(r\alpha)$$

$$+I_0(r\alpha)[2(1+\kappa)I_0(A\alpha)+(1+\kappa)d_2I_0(t\alpha)+2t\alpha d_2I_1(t\alpha)]\}$$

$$+2r\alpha I_1(r\alpha)[-2At\alpha^2I_1(t\alpha)-I_1(A\alpha)(1+\kappa)+A\alpha d_1d_3I_0(t\alpha)]$$

$$+I_0(r\alpha)\{-2A(1+\kappa)t\alpha^2I_1(t\alpha)+A\alpha d_1I_0(t\alpha)[-2+(1+\kappa)d_3]$$

$$\left.-I_1(A\alpha)(1+\kappa)^2+2At\alpha^2d_1d_3I_1(t\alpha)\}\}\sin(\alpha L)\sin(\alpha z)d\alpha\right\rangle dt$$

$$+\frac{1}{\mu(\kappa+1)}\int_0^b h(t)t\left\langle\frac{1}{2}\int_0^\infty ze^{-\xi z}\xi J_1(\xi t)J_0(\xi r)d\xi-\frac{1}{2\pi}\int_0^\infty\frac{1}{d_0}\{I_0(\alpha r)[(-1+\kappa^2\right.$$

$$-4A^2\alpha^2)I_1(t\alpha)+2t\alpha I_0(t\alpha)(-1-\kappa+d_2+d_1d_3)]+2r\alpha I_1(r\alpha)[-2t\alpha I_0(t\alpha)$$

$$\left.+I_1(t\alpha)(1+\kappa+d_2+d_1d_3)]\}\sin(\alpha z)d\alpha\right\rangle dt,$$

$$\sigma_{r\,cyl.per.}(r,z) = \frac{\mu}{(\kappa+1)}\int_0^a f(t)t\left\langle 2\int_0^\infty \left[(1-L\xi-z\xi)e^{-\xi(L+z)}+(1-L\xi\right.\right.$$

$$\left.+z\xi)e^{-\xi(L-z)}\right]\xi J_1(\xi t)J_0(\xi r)d\xi + \int_0^\infty\left[(1-\kappa+2L\xi+2z\xi)e^{-\xi(L+z)}+(1-\kappa\right.$$

$$\left.+2L\xi-2z\xi)e^{-\xi(L-z)}\right]J_1(\xi t)\frac{J_1(\xi r)}{r}d\xi - \frac{4}{\pi}\int_0^\infty\frac{1}{rd_0}\{2r\alpha I_0(r\alpha)\{t\alpha I_0(t\alpha)(2$$

$$+d_2+d_1d_3)-I_1(t\alpha)[d_2+d_1(1+d_3)]\}+I_1(r\alpha)\{-2t\alpha I_0(t\alpha)(d_2+d_4$$

$$+d_1d_3)+I_1(t\alpha)[d_2d_4+2d_1+d_1d_3(d_4-r^2\alpha^2)]\}\}\cos(\alpha L)\cos(\alpha z)d\alpha\Big\rangle dt$$

$$+\frac{\mu}{(\kappa+1)}\int_0^a g(t)t\left\langle 2\int_0^\infty\left[(-2+L\xi+z\xi)e^{-\xi(L+z)}+(-2+L\xi\right.\right.$$

$$\left.-z\xi)e^{-\xi(L-z)}\right]\xi J_0(\xi t)J_0(\xi r)d\xi + \int_0^\infty\left[(1+\kappa-2L\xi-2z\xi)e^{-\xi(L+z)}\right.$$

$$\left.+(1+\kappa-2L\xi+2z\xi)e^{-\xi(L-z)}\right]J_0(\xi t)\frac{J_1(\xi r)}{r}d\xi$$

$$-\frac{4}{\pi}\int_0^\infty\frac{1}{Ar\alpha d_0}\{\{I_1(r\alpha)[2I_0(A\alpha)(-1-\kappa)+2d_4d_2I_0(t\alpha)-2t\alpha d_2I_1(t\alpha)]$$

$$+r\alpha I_0(r\alpha)[2I_0(A\alpha)(1+\kappa)-2d_2I_0(t\alpha)+2t\alpha d_2I_1(t\alpha)]\}$$

$$+2r\alpha I_0(r\alpha)[2At\alpha^2I_1(t\alpha)-A\alpha d_1I_0(t\alpha)(1+d_3)I_1(A\alpha)(1+\kappa)+$$

$$+At\alpha^2d_1d_3I_1(t\alpha)]+I_1(r\alpha)[-2At\alpha^2d_4\,I_1(t\alpha)+A\alpha d_1I_0(t\alpha)(2$$

$$+d_3d_4)-I_1(A\alpha)d_4(1+\kappa)+2At\alpha^2d_1d_3I_1(t\alpha)]\}\cos(\alpha z)\sin(\alpha L)d\alpha\Big\rangle dt$$

$$+\frac{1}{(\kappa+1)}\int_0^b h(t)t\left\langle\int_0^\infty(\kappa-z\xi)e^{-\xi z}J_1(\xi t)\frac{J_1(\xi r)}{r}d\xi\right.$$

$$-\frac{1}{2}\int_0^\infty(3+\kappa-2z\xi)e^{-\xi z}\xi J_1(\xi t)J_0(\xi r)d\xi + \frac{1}{\pi}\int_0^\infty\frac{1}{rd_0}\{r\alpha I_0(r\alpha)\{2t\alpha I_0(t\alpha)(2$$

$$+d_2+d_1d_3)-I_1(t\alpha)[4(d_1-A^2\alpha^2)+d_2(3+\kappa)+d_1d_3(3+\kappa)]\}$$

$$+I_1(r\alpha)\{-2t\alpha I_0(t\alpha)(d_1d_3+d_2+d_4)+I_1(t\alpha)[d_1+d_4(1+\kappa)+2d_2(d_4-r^2\alpha^2)$$

$$+2[\kappa^2+(1+A^2\alpha^2)(1+r^2\alpha^2)+\kappa d_3(2+2A^2\alpha^2+r^2\alpha^2)]]\}\}\cos(\alpha z)d\alpha\Big\rangle dt\,,$$

$$\sigma_{z\,cyl.per.}(r,z) = \frac{\mu}{(\kappa+1)}\int\limits_0^a f(t)t\left\langle 2\int\limits_0^\infty \left[(1+L\xi+z\xi)e^{-\xi(L+z)}-(-1-L\xi\right.\right.$$

$$+z\xi)e^{-\xi(L-z)}\Big]\xi J_1(\xi t)J_0(\xi r)d\xi + \frac{8}{\pi}\int\limits_0^\infty \frac{\alpha}{d_0}\{r\alpha I_1(\alpha r)[-2t\alpha I_0(\alpha t)$$

$$+I_1(\alpha t)(d_2+d_1 d_3)]+I_0(r\alpha)\{t\alpha I_0(t\alpha)(-4+d_1 d_3+d_2)+I_1(t\alpha)[2d_2$$

$$+d_1(-1+2d_3)]\}\}\cos(\alpha L)\cos(\alpha z)d\alpha\Big\rangle dt$$

$$+\frac{\mu}{(\kappa+1)}\int\limits_0^a g(t)t\left\langle 2\int\limits_0^\infty \left[-(L+z)e^{-\xi(L+z)}-(L-z)e^{-\xi(L-z)}\right]\xi^2 J_0(\xi t)J_0(\xi r)d\xi\right.$$

$$+\frac{8}{\pi}\int\limits_0^\infty \frac{1}{Ad_0}\{A\alpha\{r\alpha d_2 I_0(t\alpha)I_1(r\alpha)+I_0(r\alpha)[I_0(A\alpha)(1+\kappa)+2d_2 I_0(t\alpha)$$

$$+t\alpha d_2 I_1(t\alpha)]\}+r\alpha I_1(r\alpha)\big[-2At\alpha^2 I_1(t\alpha)-I_1(A\alpha)(1+\kappa)$$

$$+A\alpha d_1 d_3 I_0(t\alpha)\big]+I_0(r\alpha)\big[-4At\alpha^2 I_1(t\alpha)+A\alpha d_1 I_0(t\alpha)(2d_3$$

$$-1)-2(1+\kappa)I_1(A\alpha)+At\alpha^2 d_1 d_3 I_1(t\alpha)\big]\}\cos(\alpha z)\sin(\alpha L)d\alpha\Big\rangle dt$$

$$+\frac{1}{(\kappa+1)}\int\limits_0^b h(t)t\left\langle \frac{1}{2}\int\limits_0^\infty (-1+\kappa-2z\xi)e^{-\xi z}\xi J_1(\xi t)J_0(\xi r)d\xi\right.$$

$$-\frac{1}{\pi}\int\limits_0^\infty \frac{\alpha}{d_0}\{2r\alpha I_1(\alpha r)[-2t\alpha I_0(\alpha t)+I_1(\alpha t)(1+\kappa+d_2+d_1 d_3)]$$

$$+I_0(r\alpha)\{2t\alpha I_0(t\alpha)(-4+d_2+d_1 d_3)+I_1(t\alpha)[2(d_1-4A^2\alpha^2)+d_2(3-\kappa)$$

$$+d_3(1-\kappa^2+d_1-2A^2\kappa\alpha^2)]\}\}\cos(\alpha z)d\alpha\Big\rangle dt\,,$$

$$\tau_{rz\,cyl.per.}(r,z) = \frac{\mu}{(\kappa+1)}\int\limits_0^a f(t)t\left\langle 2\int\limits_0^\infty \left[(L+z)e^{-\xi(L+z)}-(L-z)e^{-\xi(L-z)}\right]\xi^2 J_1(\xi t)J_1(\xi r)d\xi\right.$$

$$+\frac{8}{\pi}\int\limits_0^\infty \frac{\alpha}{d_0}\{I_1(\alpha r)[-d_1 I_1(t\alpha)+t\alpha I_0(t\alpha)(d_2+d_1 d_3)]+r\alpha I_0(r\alpha)[-2t\alpha I_0(t\alpha)$$

$$+I_1(t\alpha)(d_2+d_1 d_3)]\}\cos(\alpha L)\sin(\alpha z)d\alpha\Big\rangle dt$$

$$+\frac{\mu}{(\kappa+1)}\int\limits_0^a g(t)t\left\langle 2\int\limits_0^\infty \left[(1-L\xi-z\xi)e^{-\xi(L+z)}+(-1+L\xi\right.\right.$$

$$
\begin{aligned}
&- z\xi)e^{-\xi(L-z)}\Big]\xi J_0(\xi t)J_1(\xi r)d\xi + \frac{8}{\pi}\int_0^\infty \frac{\alpha}{Ad_0}\{rI_0(r\alpha)\{A\alpha[-2\alpha t I_1(t\alpha)\\
&+ d_2 I_0(t\alpha)] - I_1(A\alpha)(1+\kappa) + A\alpha d_1 d_3 I_0(t\alpha)\} + AI_1(r\alpha)[I_0(A\alpha)(1+\kappa)\\
&+ t\alpha d_2 I_1(t\alpha) - d_1 I_0(t\alpha) + t\alpha d_1 d_3 I_1(t\alpha)]\}\sin(\alpha z)\sin(\alpha L)\Big\rangle dt\\
&+ \frac{1}{(\kappa+1)}\int_0^b h(t)t\Big\langle \frac{1}{2}\int_0^\infty (1+\kappa-2z\xi)e^{-\xi z}\xi J_1(\xi t)J_1(\xi r)d\xi\\
&+ \frac{1}{\pi}\int_0^\infty \frac{\alpha}{d_0}\{-2r\alpha I_0(\alpha r)[-2t\alpha I_0(\alpha t) + I_1(\alpha t)(1+\kappa+d_2+d_1 d_3)]\\
&+ I_1(r\alpha)\{-2t\alpha I_0(t\alpha)(d_1 d_3 + d_2) + I_1(t\alpha)[(1+\kappa)d_2\\
&+ 2d_1 + d_1 d_3(1+\kappa)]\}\}\sin(\alpha z)d\alpha\Big\rangle dt, \quad\quad\quad\quad\quad (2.43\text{a-e})
\end{aligned}
$$

where

$$
d_0 = 2A^2\alpha^2 I_0^2(A\alpha) - (1+\kappa+2A^2\alpha^2)I_1^2(A\alpha),
$$

$$
d_1 = 1+\kappa+2A^2\alpha^2,
$$

$$
d_2 = 2A^2\alpha^2 I_0(A\alpha)K_0(A\alpha),
$$

$$
d_3 = I_1(A\alpha)K_1(A\alpha),
$$

$$
d_4 = 1+\kappa+2r^2\alpha^2, \quad\quad\quad\quad\quad\quad\quad\quad\quad\quad (2.44\text{a-e})
$$

and integrals of Bessel functions are given in terms of the complete elliptic integrals K and E in Appendix B.

2.2.2 Uniform Solution

Consider an infinite cylinder of radius A subjected to uniformly distributed axial tension of intensity p_0 at infinity. In this special case, one may expect that u is independent of z and w is independent of r:

$$u(r,z) = u(r),$$

$$w(r,z) = w(z).$$

(2.45a,b)

For this uniform axial loading, Eqs. (2.1) are uncoupled and become

$$\frac{d^2u}{dr^2} + \frac{1}{r}\frac{du}{dr} - \frac{u}{r^2} = 0,$$

$$\frac{d^2w}{dz^2} = 0.$$

(2.46a,b)

These equations must be solved subjected to the following conditions

$$u(0) = 0,$$

$$w(0) = 0,$$

$$\sigma_r(A,z) = 0,$$

$$\tau_{rz}(A,z) = 0,$$

$$\sigma_z(r,\infty) = p_0$$

(2.47a-e)

for which one can easily obtain the solution in the form

$$u_{uniform}(r) = -\frac{(\kappa-3)p_0}{2\mu(\kappa-7)}r,$$

$$w_{uniform}(z) = -\frac{2p_0}{\mu(\kappa-7)}z,$$

$$\sigma_{r\,uniform}(r,z) = 0,$$

$$\sigma_{z\,uniform}(r,z) = p_0,$$

$$\tau_{rz\,uniform}(r,z) = 0. \qquad\qquad\qquad\qquad (2.48\text{a-e})$$

2.2.3 Superposition

General expressions for the infinite cylinder which contains two penny-shaped cracks at $z = \pm L$, a penny-shaped inclusion at $z = 0$ and subjected to axial tension of uniform intensity p_0 at $z = \pm\infty$ are obtained by the superposition of the uniform solution and the general expressions for the perturbation problem:

$$u = u_{cyl.per.} + u_{uniform},$$

$$w = w_{cyl.per.} + w_{uniform},$$

$$\sigma_r = \sigma_{r\,cyl.per.} + \sigma_{r\,uniform},$$

$$\sigma_z = \sigma_{z\,cyl.per.} + \sigma_{z\,uniform},$$

38

$$\tau_{rz} = \tau_{rz \, cyl.per.} + \tau_{rz \, uniform}.$$

(2.49a-e)

CHAPTER III

INTEGRAL EQUATIONS

3.1. Derivation of Integral Equations

The expressions for the stresses and the displacements, Eqs. (2.43) or (2.49), contain three unknown functions, $f(t)$, $g(t)$ and $h(t)$, which are the crack surface displacement derivatives in z- and r-directions and the jump in the shearing stress through the rigid inclusion, respectively. Since crack surfaces are free of stress and the rigid inclusion is perfectly bonded to the cylinder, the stress and the displacement expressions, Eqs. (2.49), must satisfy the following conditions

$$\sigma_z(r,L) = 0, \qquad\qquad (0 \le r < a)$$

$$\tau_{rz}(r,L) = 0, \qquad\qquad (0 \le r < a) \qquad\qquad\qquad (3.1a,b)$$

on the crack and

$$u(r,0) = 0, \qquad\qquad (0 \le r < b) \qquad\qquad\qquad\qquad (3.1c)$$

on the rigid inclusion. Eqs. (3.1a,b) are stress type boundary conditions while Eq. (3.1c) is displacement type which is satisfied if instead

$$\frac{1}{r}\frac{\partial}{\partial r}\left[ru(r,0)\right] = 0 \qquad\qquad (0 \le r < b) \qquad\qquad\qquad (3.2)$$

is satisfied. Now, Eqs. (3.1a,b) and (3.2) are all stress type conditions. Substituting

Eqs. (2.49d,e) in Eqs. (3.1a,b) and Eq. (2.49a) in Eq. (3.2) gives the following singular integral equations

$$\frac{1}{\pi}\int_0^a \{f(t)[2m(r,t)+tN_{11}(r,t)+tS_1(r,t)]+g(t)[N_{12}(r,t)+S_2(r,t)]t\}dt$$

$$+\frac{1}{\mu\pi}\int_0^b h(t)[N_{13}(r,t)+S_3(r,t)]tdt = -\frac{(\kappa+1)}{2\mu}p_0, \qquad (0\le r<a)$$

$$\frac{1}{\pi}\int_0^a \{f(t)[N_{21}(r,t)+S_4(r,t)]t+g(t)[2m^*(r,t)+tN_{22}(r,t)+tS_5(r,t)]\}dt$$

$$+\frac{1}{\mu\pi}\int_0^b h(t)[N_{23}(r,t)+S_6(r,t)]tdt = 0, \qquad (0\le r<a)$$

$$\frac{1}{\pi}\int_0^a \{f(t)[N_{31}(r,t)+S_7(r,t)]+g(t)[N_{32}(r,t)+S_8(r,t)]\}tdt$$

$$+\frac{1}{\mu\pi}\int_0^b h(t)[-\kappa m(r,t)+t\,N_{33}(r,t)]dt = \frac{(\kappa-3)(\kappa+1)}{(\kappa-7)\mu}p_0, \qquad (0\le r<b) \quad (3.3a\text{-}c)$$

where

$$m(r,t) = \frac{t}{t^2-r^2}\begin{cases}\dfrac{t^2-r^2}{tr}K(\dfrac{t}{r})+\dfrac{r}{t}E(\dfrac{t}{r}), & t<r \\[2mm] E(\dfrac{r}{t}), & t>r\end{cases}, \qquad (3.4)$$

$$m^*(r,t) = \frac{r}{t^2-r^2}\begin{cases}\dfrac{t}{r}E(\dfrac{t}{r}), & t<r \\[2mm] \dfrac{t^2}{r^2}E(\dfrac{r}{t})-\dfrac{t^2-r^2}{r^2}K(\dfrac{r}{t}), & t>r\end{cases}, \qquad (3.5)$$

41

Noting that $f(t)$ and $h(t)$ are odd, $g(t)$ is even, integrals in Eqs. (3.3) may be converted to integrals from $-a$ to a and from $-b$ to b and Eqs. (3.3) may be written in the form

$$\frac{1}{2\pi}\int_{-a}^{a}\left\{f(t)\left[\frac{2}{t-r}+2M_2(r,t)+|t|N_{11}(r,t)+|t|S_1(r,t)\right]\right.$$

$$\left.+g(t)[N_{12}(r,t)+S_2(r,t)]|t|\right\}dt$$

$$+\frac{1}{2\mu\pi}\int_{-b}^{b}h(t)[N_{13}(r,t)+S_3(r,t)]|t|dt=-\frac{(\kappa+1)}{2\mu}p_0,\quad(-a<r<a)$$

$$\frac{1}{2\pi}\int_{-a}^{a}\left\{f(t)[N_{21}(r,t)+S_4(r,t)]|t|\right.$$

$$+g(t)\left[\frac{2}{t-r}+2M_1(r,t)+|t|N_{22}(r,t)+|t|S_5(r,t)\right]\bigg\}dt$$

$$+\frac{1}{2\mu\pi}\int_{-b}^{b}h(t)[N_{23}(r,t)+S_6(r,t)]|t|dt=0,\qquad\qquad(-a<r<a)$$

$$\frac{1}{2\pi}\int_{-a}^{a}\{f(t)[N_{31}(r,t)+S_7(r,t)]+g(t)[N_{32}(r,t)+S_8(r,t)]\}|t|dt$$

$$+\frac{1}{2\mu\pi}\int_{-b}^{b}h(t)\left[-\frac{\kappa}{t-r}-\kappa M_2(r,t)+|t|N_{33}(r,t)\right]dt$$

$$=\frac{(\kappa-3)(\kappa+1)}{(\kappa-7)\mu}p_0,\qquad\qquad(-b<r<b)\qquad\qquad\text{(3.6a-c)}$$

where

$$M_1(r,t)=\frac{m_1(r,t)-1}{t-r},$$

42

$$M_2(r,t) = \frac{m_2(r,t) - 1}{t - r} \tag{3.7a,b}$$

and

$$m_1(r,t) = \begin{cases} \left|\frac{t}{r}\right| E(\left|\frac{t}{r}\right|), & |t| < |r| \\ \frac{t^2}{r^2} E(\left|\frac{r}{t}\right|) - \frac{t^2 - r^2}{r^2} K(\left|\frac{r}{t}\right|), & |t| > |r| \end{cases},$$

$$m_2(r,t) = \begin{cases} \left|\frac{r}{t}\right| E(\left|\frac{t}{r}\right|) + \frac{t^2 - r^2}{|tr|} K(\left|\frac{t}{r}\right|), & |t| < |r| \\ E(\left|\frac{r}{t}\right|), & |t| > |r| \end{cases} \tag{3.8a,b}$$

in which K and E are the complete elliptic integrals of the first and the second kinds, respectively. $S_i(r,t)$ $(i = 1 - 8)$ containing complete elliptic integrals are defined in Appendix C. The kernels $N_{ij}(r,t)$ $(i, j = 1 - 3)$ in Eqs. (3.3) are in the form of improper integrals,

$$N_{ij}(r,t) = \int_0^\infty K_{ij}(r,t,\alpha) d\alpha, \qquad (i, j = 1 - 3) \tag{3.9}$$

where the integrands $K_{ij}(r,t,\alpha)$ $(i, j = 1 - 3)$ are given in Appendix D. The three singular integral equations, Eqs. (3.6), must be solved in such a way that the single-valuedness conditions for the crack

$$\int_{-a}^a f(t) t \, dt = 0,$$

$$\int_{-a}^{a} g(t)t\,dt = 0,$$

(3.10a,b)

and the equilibrium equation for the rigid inclusion

$$\int_{-b}^{b} h(t)t\,dt = 0,$$

(3.11)

are also satisfied. In Eqs. (3.6), the simple Cauchy kernel, Muskhelishvili (1953), $1/(t-r)$ becomes unbounded when $t = r$. In addition to this, there may be unbounded parts in the kernels $N_{ij}(r,t)$ $(i, j = 1-3)$. Therefore, the improper integrals giving $N_{ij}(r,t)$ $(i, j = 1-3)$ must be examined closely and those terms in $K_{ij}(r,t,\alpha)$ $(i, j = 1-3)$ giving rise to probable singular terms in $N_{ij}(r,t)$ $(i, j = 1-3)$ must be separately treated. Unbounded terms may be due to behavior of $K_{ij}(r,t,\alpha)$ $(i, j = 1-3)$ around $\alpha = 0$ and $\alpha \to \infty$.

Asymptotic analysis around $\alpha = 0$ gives

$$\lim_{\alpha \to 0} K_{ij}(r,t,\alpha) = 0 \qquad (i = 1-3, j = 2; i = 2, j = 1,3)$$

(3.12)

except

$$\lim_{\alpha \to 0} K_{11}(r,t,\alpha) = \frac{2t\left[4 + (\kappa - 3)\kappa\right]}{A^2(\kappa - 7)},$$

$$\lim_{\alpha \to 0} K_{13}(r,t,\alpha) = -\frac{t(\kappa - 3)}{A^2},$$

$$\lim_{\alpha \to 0} K_{31}(r,t,\alpha) = -\frac{t(\kappa - 3)}{A^2},$$

$$\lim_{\alpha \to 0} K_{33}(r,t,\alpha) = -\frac{8t}{A^2}, \tag{3.13a-d}$$

which do not contribute to unbounded terms when integrated. When $K_{ij}(r,t,\alpha)$ $(i, j = 1-3)$ are examined as $\alpha \to \infty$, with the notation

$$K_{ij\infty}(r,t,\alpha) = \lim_{\alpha \to \infty} K_{ij}(r,t,\alpha), \qquad (i, j = 1-3) \tag{3.14}$$

it is observed that only $K_{ii}(r,t,\alpha)$ $(i = 1-3)$ contain such terms which may be written in the form

$$K_{11\infty}(r,t,\alpha) = \frac{\cos^2(\alpha L)e^{-\alpha(2A-t-r)}}{\sqrt{tr}} \left[4(-A+r)(A-t)\alpha^2 + (8A - 2r - 6t)\alpha - 4 \right],$$

$$K_{22\infty}(r,t,\alpha) = -\frac{\sin^2(\alpha L)e^{-\alpha(2A-t-r)}}{\sqrt{tr}} \left[4(A-r)(A-t)\alpha^2 + 2(t-r)\alpha \right]$$

$$+ \frac{\sin^2(\alpha L)e^{-\alpha(A-r)}}{\sqrt{tr}} \frac{2(1+\kappa)(A-r)\sqrt{At}}{A^2},$$

$$K_{33\infty}(r,t,\alpha) = \frac{e^{-\alpha(2A-t-r)}}{\sqrt{tr}} \left\{ (-A+r)(A-t)\alpha^2 \right.$$

$$\left. + \left[(A-t) + \frac{\kappa}{2}(r+t-2A) \right]\alpha - \frac{1}{4}(\kappa-1)^2 \right\}. \tag{3.15a-c}$$

Integrating $K_{ii\infty}(r,t,\alpha)$ $(i = 1-3)$, the probable singular parts of the kernels $N_{ii}(r,t)$ $(i = 1-3)$,

$$N_{iis}(r,t) = \int_0^\infty K_{ii\infty}(r,t,\alpha)d\alpha \;, \qquad\qquad (i=1-3) \qquad\qquad (3.16)$$

may be calculated to be

$$N_{11s}(r,t) = \frac{1}{\sqrt{tr}}\left\{\left[-2(A-r)^2\frac{\partial^2}{\partial r^2} + 6(A-r)\frac{\partial}{\partial r} - 1\right]\left[\frac{1}{(t+r-2A)} + \frac{1}{(t-r+2A)}\right]\right.$$

$$\left. + \left[-2(A+r)^2\frac{\partial^2}{\partial r^2} - 6(A+r)\frac{\partial}{\partial r} - 1\right]\left[\frac{1}{(t-r-2A)} + \frac{1}{(t+r+2A)}\right]\right\},$$

$$N_{22s}(r,t) = \frac{1}{\sqrt{tr}}\left\{\left[-2(A-r)^2\frac{\partial^2}{\partial r^2} + 6(A-r)\frac{\partial}{\partial r} - 1\right]\left[\frac{1}{(t+r-2A)} + \frac{1}{(t-r+2A)}\right]\right.$$

$$\left. + \left[-2(A+r)^2\frac{\partial^2}{\partial r^2} - 6(A+r)\frac{\partial}{\partial r} - 1\right]\left[\frac{1}{(t-r-2A)} + \frac{1}{(t+r+2A)}\right]\right\},$$

$$N_{33s}(r,t) = \frac{1}{\sqrt{tr}}\left\{\left[(A-r)^2\frac{\partial^2}{\partial r^2} + 3(A-r)\frac{\partial}{\partial r} + \frac{-3+\kappa^2}{4}\right]\left[\frac{1}{(t+r-2A)} + \frac{1}{(t-r+2A)}\right]\right.$$

$$\left. + \left[-(A+r)^2\frac{\partial^2}{\partial r^2} - 3(A+r)\frac{\partial}{\partial r} + \frac{-3+\kappa^2}{4}\right]\left[\frac{1}{(t-r-2A)} + \frac{1}{(t+r+2A)}\right]\right\}.$$

$$(3.17\text{a-c})$$

Bounded parts of kernels $N_{ii}(r,t)$ $(i=1-3)$ are then calculated from

$$N_{iib}(r,t) = \int_0^\infty [K_{ii}(r,t,\alpha) - K_{ii\infty}(r,t,\alpha)]d\alpha \;, \qquad (i=1-3) \qquad\qquad (3.18)$$

in which the subscript b denotes the bounded parts and

$$N_{ii}(r,t) = N_{ii_b}(r,t) + N_{ii_s}(r,t), \qquad\qquad (i=1-3). \qquad\qquad (3.19)$$

Note that $N_{ii_s}(r,t)$ $(i=1-3)$ are singular if $r,t \to A$.

3.2 Characteristic Equations

The unknown functions $f(t)$, $g(t)$ and $h(t)$ are expected to have integrable singularities at the respective edges of cracks and the inclusion. The singular behavior of these unknown functions can be determined by writing

$$f(t) = \frac{f^*(t)}{(a^2 - t^2)^\beta}, \qquad\qquad (0 < \mathrm{Re}(\beta) < 1)$$

$$g(t) = \frac{g^*(t)}{(a^2 - t^2)^\beta}, \qquad\qquad (0 < \mathrm{Re}(\beta) < 1)$$

$$h(t) = \frac{h^*(t)}{(b^2 - t^2)^\gamma}, \qquad\qquad (0 < \mathrm{Re}(\gamma) < 1) \qquad\qquad (3.20a\text{-}c)$$

where $f^*(t)$, $g^*(t)$ and $h^*(t)$ are Hölder-continuous functions, Muskhelishvili (1953), in the respective intervals $(-a,a)$ and $(-b,b)$. β and γ are unknown constants which can be calculated by examining the integral equations, Eqs. (3.6a,b) near the ends $r = \mp a$ and Eq. (3.6c) near the ends $r = \mp b$.

Equations (3.6), together with Eqs. (3.20) may be written in the form

$$\frac{1}{\pi} \int_{-a}^{a} \frac{f^*(t)}{(a^2 - t^2)^\beta} \left[\frac{2}{t-r} + |t| N_{11s}(r,t) \right] dt = B_1(r), \qquad (-a < r < a)$$

$$\frac{1}{\pi}\int_{-a}^{a}\frac{g^*(t)}{(a^2-t^2)^\beta}\left[\frac{2}{t-r}+|t|N_{22s}(r,t)\right]dt = B_2(r), \qquad (-a<r<a)$$

$$\frac{1}{\pi}\int_{-b}^{b}\frac{h^*(t)}{(b^2-t^2)^\gamma}\left[-\frac{\kappa}{t-r}+|t|N_{33s}(r,t)\right]dt = B_3(r), \qquad (-b<r<b) \qquad \text{(3.21a-c)}$$

where all other and bounded terms are collected in $B_i(r)$ $(i=1-3)$. The integrals on the left-hand-sides of Eqs. (3.21) near $r=\mp a$ and $r=\mp b$ may be calculated with the help of the complex function technique given in Muskhelishvili (1953):

$$\frac{1}{\pi}\int_{-a}^{a}\frac{f^*(t)}{(a^2-t^2)^\beta(t-r)}dt = \frac{f^*(-a)\cot(\pi\beta)}{(2a)^\beta(a+r)^\beta}-\frac{f^*(a)\cot(\pi\beta)}{(2a)^\beta(a-r)^\beta}+F_1(r),$$

$$\frac{1}{\pi}\int_{-a}^{a}\frac{g^*(t)}{(a^2-t^2)^\beta(t-r)}dt = \frac{g^*(-a)\cot(\pi\beta)}{(2a)^\beta(a+r)^\beta}-\frac{g^*(a)\cot(\pi\beta)}{(2a)^\beta(a-r)^\beta}+G_1(r),$$

$$\frac{1}{\pi}\int_{-b}^{b}\frac{h^*(t)}{(b^2-t^2)^\gamma(t-r)}dt = \frac{h^*(-b)\cot(\pi\gamma)}{(2b)^\gamma(b+r)^\gamma}-\frac{h^*(b)\cot(\pi\gamma)}{(2b)^\gamma(b-r)^\gamma}+H_1(r), \qquad \text{(3.22a-c)}$$

$$\frac{1}{\pi}\int_{-A}^{A}\frac{f^*(t)}{(A^2-t^2)^\beta[t-(2A-r)]}dt = -\frac{f^*(A)}{(2A)^\beta(A-r)^\beta\sin(\pi\beta)}+F_2(r),$$

$$\frac{1}{\pi}\int_{-A}^{A}\frac{f^*(t)}{(A^2-t^2)^\beta[t-(2A+r)]}dt = -\frac{f^*(A)}{(2A)^\beta(A+r)^\beta\sin(\pi\beta)}+F_3(r),$$

$$\frac{1}{\pi}\int_{-A}^{A}\frac{f^*(t)}{(A^2-t^2)^\beta[t-(-2A+r)]}dt = \frac{f^*(-A)}{(2A)^\beta(A-r)^\beta\sin(\pi\beta)}+F_4(r),$$

$$\frac{1}{\pi}\int_{-A}^{A}\frac{f^*(t)}{(A^2-t^2)^\beta[t-(-2A-r)]}dt = \frac{f^*(-A)}{(2A)^\beta(A+r)^\beta \sin(\pi\beta)} + F_5(r),$$

$$\frac{1}{\pi}\int_{-A}^{A}\frac{g^*(t)}{(A^2-t^2)^\beta[t-(2A-r)]}dt = -\frac{g^*(A)}{(2A)^\beta(A-r)^\beta \sin(\pi\beta)} + G_2(r),$$

$$\frac{1}{\pi}\int_{-A}^{A}\frac{g^*(t)}{(A^2-t^2)^\beta[t-(2A+r)]}dt = \frac{g^*(A)}{(2A)^\beta(A+r)^\beta \sin(\pi\beta)} + G_3(r),$$

$$\frac{1}{\pi}\int_{-A}^{A}\frac{g^*(t)}{(A^2-t^2)^\beta[t-(-2A+r)]}dt = -\frac{g^*(-A)}{(2A)^\beta(A-r)^\beta \sin(\pi\beta)} + G_4(r),$$

$$\frac{1}{\pi}\int_{-A}^{A}\frac{g^*(t)}{(A^2-t^2)^\beta[t-(-2A-r)]}dt = \frac{g^*(-A)}{(2A)^\beta(A+r)^\beta \sin(\pi\beta)} + G_5(r),$$

$$\frac{1}{\pi}\int_{-A}^{A}\frac{h^*(t)}{(A^2-t^2)^\gamma[t-(2A-r)]}dt = -\frac{h^*(A)}{(2A)^\gamma(A-r)^\gamma \sin(\pi\gamma)} + H_2(r),$$

$$\frac{1}{\pi}\int_{-A}^{A}\frac{h^*(t)}{(A^2-t^2)^\gamma[t-(2A+r)]}dt = -\frac{h^*(A)}{(2A)^\gamma(A+r)^\gamma \sin(\pi\gamma)} + H_3(r),$$

$$\frac{1}{\pi}\int_{-A}^{A}\frac{h^*(t)}{(A^2-t^2)^\gamma[t-(-2A+r)]}dt = \frac{h^*(-A)}{(2A)^\gamma(A-r)^\gamma \sin(\pi\gamma)} + H_4(r),$$

$$\frac{1}{\pi}\int_{-A}^{A}\frac{h^*(t)}{(A^2-t^2)^\gamma[t-(-2A-r)]}dt = \frac{h^*(-A)}{(2A)^\gamma(A+r)^\gamma \sin(\pi\gamma)} + H_5(r), \qquad \text{(3.23a-l)}$$

where $F_i(r)$, $G_i(r)$ and $H_i(r)$ $(i=1-5)$ are all bounded everywhere except at the end points $\pm a$, $\pm b$ and $\pm A$.

Now substituting Eq. (3.22a) in Eq. (3.21a) or Eq. (3.22b) in Eq. (3.21b), multiplying the resulting equation by $(a-r)^\beta$, and then considering the limiting case $r \to a$, for an internal crack $(a < A)$, one can obtain the following characteristic equation for β:

$$\cot(\pi\beta) = 0, \qquad (a < A). \qquad (3.24)$$

The acceptable numerical value for β is then 1/2. This is the very well known result for an embedded crack tip in a homogeneous medium, Cook and Erdoğan (1972), Gupta (1973), Delale and Erdoğan (1982), Nied and Erdoğan (1983), Geçit (1987), Turgut and Geçit (1988).

Similarly, substituting Eq. (3.22c) in Eq. (3.21c), multiplying the resulting equation by $(b-r)^\gamma$, and then considering the limiting case $r \to b$, for an internal rigid inclusion $(b < A)$, one can obtain the following characteristic equation for γ:

$$\cot(\pi\gamma) = 0, \qquad (b < A). \qquad (3.25)$$

Here, γ is also equal to 1/2 which is in agreement with previous results, Gupta (1974), Artem and Geçit (2002), Yetmez and Geçit (2005).

When the cracks spread out and the cylinder is completely broken along the cracks $(a = A)$, in addition to Eq. (3.22a), Eq. (3.23a-d) must also be substituted in Eq. (3.21a). Then, multiplying the resulting equation by $(A-r)^\beta$, and considering the limiting case $r \to A$, one can obtain the following characteristic equation for β:

$$\cos(\pi\beta) = 2\beta(\beta - 2) + 1, \qquad (a = A) \qquad (3.26)$$

for which the acceptable value for β is zero. This shows that the stresses at the apex of a 90° wedge with free sides are bounded. This result is in agreement with previous observations, Williams (1952), Geçit (1984), Geçit and Turgut (1988).

When the inclusion spreads out and the midplane $(z = 0)$ of the cylinder is completely fixed $(b = A)$, in addition to Eq. (3.22c), Eqs. (3.23i-l) are also substituted in Eq. (3.21c). Then, the resulting equation is multiplied by $(A - r)^{\gamma}$ and the limiting case $r \rightarrow A$ is considered. This procedure gives the following characteristic equation for γ at the edge of a through rigid inclusion $(b = A)$:

$$2\kappa\cos(\pi\gamma) = \kappa^{2} + 1 - 4(\gamma - 1)^{2} . \qquad (b = A) \qquad (3.27)$$

This equation is in agreement with previous results for the stress singularity at the apex of a 90° wedge with one side being fixed and the other being free, Williams (1952), Gupta (1975), Geçit and Turgut (1988).

CHAPTER IV

SOLUTION OF INTEGRAL EQUATIONS

In this chapter, procedures used for the solution of singular integral equations, Eqs. (3.6), subject to conditions Eqs. (3.10) and (3.11) are given for infinite cylinder, semi-infinite cylinder and finite cylinder problems separately.

First of all, the integral equations will be expressed in terms of non-dimensional quantities. Defining non-dimensional variables ϕ and ψ on the crack by

$$t = a\phi, \qquad (-a < t < a, -1 < \phi < 1)$$

$$r = a\psi, \qquad (-a < r < a, -1 < \psi < 1) \qquad \text{(4.1a,b)}$$

and η and ε on the inclusion by

$$t = b\eta, \qquad (-b < t < b, -1 < \eta < 1)$$

$$r = b\varepsilon, \qquad (-b < r < b, -1 < \varepsilon < 1) \qquad \text{(4.2a,b)}$$

system of singular integral equations, Eqs. (3.6), Eqs. (3.10) and Eq. (3.11), takes the following form

$$-\frac{\mu}{\kappa\pi}\int_{-1}^{1}\left\{ f(a\phi)\left[\frac{2}{\phi-\psi} + 2aM_2(a\psi, a\phi) + a^2|\phi|N_{11}(a\psi, a\phi) + a^2|\phi|S_1(a\psi, a\phi)\right]\right.$$

$$\left. + g(a\phi)[N_{12}(a\psi, a\phi) + S_2(a\psi, a\phi)]a^2|\phi|\right\}d\phi$$

$$-\frac{1}{\pi}\int_{-1}^{1}h(b\eta)\left[N_{13}(a\psi,b\eta)+S_{3}(a\psi,b\eta)\right]\frac{b^{2}|\eta|}{\kappa}d\eta=\frac{(\kappa+1)}{\kappa}p_{0},\quad(-1<\psi<1)$$

$$-\frac{\mu}{\kappa\pi}\int_{-1}^{1}\left\{f(a\phi)\left[N_{21}(a\psi,a\phi)+S_{4}(a\psi,a\phi)\right]a^{2}|\phi|\right.$$

$$+g(a\phi)\left[\frac{2}{\phi-\psi}+2aM_{1}(a\psi,a\phi)+a^{2}|\phi|N_{22}(a\psi,a\phi)+a^{2}|\phi|S_{5}(a\psi,a\phi)\right]\right\}d\phi$$

$$-\frac{1}{\pi}\int_{-1}^{1}h(b\eta)\left[N_{23}(a\psi,b\eta)+S_{6}(a\psi,b\eta)\right]\frac{b^{2}|\eta|}{\kappa}d\eta=0,\qquad(-1<\psi<1)$$

$$-\frac{\mu}{\kappa\pi}\int_{-1}^{1}\left\{f(a\phi)\left[N_{31}(b\varepsilon,a\phi)+S_{7}(b\varepsilon,a\phi)\right]\right.$$

$$+g(a\phi)\left[N_{32}(b\varepsilon,a\phi)+S_{8}(b\varepsilon,a\phi)\right]\right\}a^{2}|\phi|d\phi$$

$$+\frac{1}{\pi}\int_{-1}^{1}h(b\eta)\left[\frac{1}{\eta-\varepsilon}+bM_{2}(b\varepsilon,b\eta)-\frac{b^{2}|\eta|}{\kappa}N_{33}(b\varepsilon,b\eta)\right]d\eta$$

$$=\frac{2(\kappa-3)(\kappa+1)}{(7-\kappa)\kappa}p_{0},\qquad\qquad(-1<\varepsilon<1)\quad(4.3\text{a-c})$$

$$\int_{-1}^{1}f(a\phi)\phi\,d\phi=0,$$

$$\int_{-1}^{1}g(a\phi)\phi\,d\phi=0,$$

$$\int_{-1}^{1}h(b\eta)\eta\,d\eta=0.\qquad\qquad(4.4\text{a-c})$$

Imposing the singular behavior of the unknown functions along with the lines of Eqs. (3.20),

$$f(a\phi) = \frac{\overline{F}(\phi)}{(1-\phi^2)^\beta},$$

$$g(a\phi) = \frac{\overline{G}(\phi)}{(1-\phi^2)^\beta},$$

$$h(b\eta) = \frac{\overline{H}(\eta)}{(1-\eta^2)^\gamma} \tag{4.5a-c}$$

in which $\overline{F}(\phi)$, $\overline{G}(\phi)$ and $\overline{H}(\eta)$ are Hölder-continuous functions in (-1,1), Eqs. (4.3) and (4.4) may be rewritten in the form

$$\frac{1}{\pi}\int_{-1}^{1}\left\{\frac{\overline{\overline{F}}(\phi)}{(1-\phi^2)^\beta}\left[\frac{1}{\phi-\psi}+\overline{M}_2(\psi,\phi)+|\phi|\overline{N}_{11}(\psi,\phi)+|\phi|\overline{S}_1(\psi,\phi)\right]\right.$$

$$\left.+\frac{\overline{\overline{G}}(\phi)}{(1-\phi^2)^\beta}\left[\overline{N}_{12}(\psi,\phi)+\overline{S}_2(\psi,\phi)\right]|\phi|\right\}d\phi$$

$$+\frac{1}{\pi}\int_{-1}^{1}\frac{\overline{\overline{H}}(\eta)}{(1-\eta^2)^\gamma}\left[\overline{N}_{13}(\psi,\eta)+\overline{S}_3(\psi,\eta)\right]|\eta|d\eta = \frac{(\kappa+1)}{\kappa}, \quad (-1<\psi<1)$$

$$\frac{1}{\pi}\int_{-1}^{1}\left\{\frac{\overline{\overline{F}}(\phi)}{(1-\phi^2)^\beta}\left[\overline{N}_{21}(\psi,\phi)+\overline{S}_4(\psi,\phi)\right]|\phi|\right.$$

$$\left.+\frac{\overline{\overline{G}}(\phi)}{(1-\phi^2)^\beta}\left[\frac{1}{\phi-\psi}+\overline{M}_1(\psi,\phi)+|\phi|\overline{N}_{22}(\psi,\phi)+|\phi|\overline{S}_5(\psi,\phi)\right]\right\}d\phi$$

$$+\frac{1}{\pi}\int_{-1}^{1}\frac{\overline{\overline{H}}(\eta)}{(1-\eta^2)^\gamma}\left[\overline{N}_{23}(\psi,\eta)+\overline{S}_6(\psi,\eta)\right]|\eta|d\eta = 0, \quad (-1<\psi<1)$$

$$\frac{1}{\pi}\int_{-1}^{1}\left\{\frac{\overline{\overline{F}}(\phi)}{(1-\phi^2)^\beta}\left[\overline{N}_{31}(\varepsilon,\phi)+\overline{S}_7(\varepsilon,\phi)\right]+\frac{\overline{\overline{G}}(\phi)}{(1-\phi^2)^\beta}\left[\overline{N}_{32}(\varepsilon,\phi)+\overline{S}_8(\varepsilon,\phi)\right]\right\}|\phi|d\phi$$

$$+\frac{1}{\pi}\int_{-1}^{1}\frac{\overline{\overline{H}}(\eta)}{(1-\eta^2)^\gamma}\left[\frac{1}{\eta-\varepsilon}+\overline{M}_2(\varepsilon,\eta)+|\eta|\overline{N}_{33}(\varepsilon,\eta)\right]d\eta$$

$$=\frac{2(\kappa-3)(\kappa+1)}{(7-\kappa)\kappa},\qquad\qquad (-1<\varepsilon<1)\qquad (4.6\text{a-c})$$

and

$$\int_{-1}^{1}\frac{\overline{\overline{F}}(\phi)}{(1-\phi^2)^\beta}\phi\,d\phi=0\,,$$

$$\int_{-1}^{1}\frac{\overline{\overline{G}}(\phi)}{(1-\phi^2)^\beta}\phi\,d\phi=0\,,$$

$$\int_{-1}^{1}\frac{\overline{\overline{H}}(\eta)}{(1-\eta^2)^\gamma}\eta\,d\eta=0\,,\qquad\qquad\qquad (4.7\text{a-c})$$

where

$$\overline{\overline{F}}(\phi)=-\frac{2\mu}{\kappa\,p_0}\overline{F}(\phi)\,,$$

$$\overline{\overline{G}}(\phi)=-\frac{2\mu}{\kappa\,p_0}\overline{G}(\phi)\,,$$

$$\overline{\overline{H}}(\eta)=\frac{\overline{H}(\eta)}{p_0}\,,$$

$$\overline{M}_i(\psi,\phi)=a\,M_i(a\psi,a\phi)\,,\qquad\qquad (i=1,2)$$

$$\overline{M}_2(\varepsilon,\eta)=bM_2(b\varepsilon,b\eta),$$

$$\overline{N}_{ij}(\psi,\phi)=a^2N_{ij}(a\psi,a\phi)/2, \qquad\qquad (i,j=1,2)$$

$$\overline{N}_{i3}(\psi,\eta)=-b^2N_{i3}(a\psi,b\eta)/\kappa, \qquad\qquad (i=1,2)$$

$$\overline{N}_{3j}(\varepsilon,\phi)=a^2N_{3j}(b\varepsilon,a\phi)/2, \qquad\qquad (j=1,2)$$

$$\overline{N}_{33}(\varepsilon,\eta)=-b^2N_{33}(b\varepsilon,b\eta)/\kappa,$$

$$\overline{S}_i(\psi,\phi)=a^2S_i(a\psi,a\phi)/2, \qquad\qquad (i=1,2,4,5)$$

$$\overline{S}_i(\psi,\eta)=-b^2S_i(a\psi,b\eta)/\kappa, \qquad\qquad (i=3,6)$$

$$\overline{S}_i(\varepsilon,\phi)=a^2S_i(b\varepsilon,a\phi)/2, \qquad\qquad (i=7,8) \qquad\qquad (4.8a\text{-}l)$$

4.1 Infinite Cylinder Problem

4.1.1 Infinite Cylinder Having Two Cracks and an Inclusion

For general solution, it is assumed that there are concentric penny-shaped cracks of radius a at $z=\pm L$ and a concentric penny-shaped rigid inclusion of radius b at $z=0$ in the infinite cylinder of radius A. Both ends of this infinite cylinder are subjected to axial tensile loads of uniform intensity p_0 at infinity (Fig. 2.1). In this case, the powers of singularity β and γ are determined from Eqs. (3.24) and (3.25):

$\beta = 1/2$,

$\gamma = 1/2$. $\hspace{8cm}$ (4.9a,b)

In this case, the integrals in Eqs. (4.6) and (4.7) may be calculated by the use of the Gauss-Lobatto integration formula, Krenk (1978), Artem and Geçit (2002). Then, Eqs. (4.6) and (4.7) become

$$\sum_{i=1}^{n} C_i \left\{ \overline{\overline{F}}(\phi_i) \left[\frac{1}{\phi_i - \psi_j} + \overline{M}_2(\psi_j, \phi_i) + |\phi_i| \overline{N}_{11}(\psi_j, \phi_i) + |\phi_i| \overline{S}_1(\psi_j, \phi_i) \right] \right.$$

$$+ \overline{\overline{G}}(\phi_i) \left[\overline{N}_{12}(\psi_j, \phi_i) + \overline{S}_2(\psi_j, \phi_i) \right] |\phi_i|$$

$$\left. + \overline{\overline{H}}(\eta_i) \left[\overline{N}_{13}(\psi_j, \eta_i) + \overline{S}_3(\psi_j, \eta_i) \right] |\eta_i| \right\} = \frac{(\kappa+1)}{\kappa}, \quad (j = 1,...,n-1)$$

$$\sum_{i=1}^{n} C_i \left\{ \overline{\overline{F}}(\phi_i) \left[\overline{N}_{21}(\psi_j, \phi_i) + \overline{S}_4(\psi_j, \phi_i) \right] |\phi_i| \right.$$

$$+ \overline{\overline{G}}(\phi_i) \left[\frac{1}{\phi_i - \psi_j} + \overline{M}_1(\psi_j, \phi_i) + |\phi_i| \overline{N}_{22}(\psi_j, \phi_i) + |\phi_i| \overline{S}_5(\psi_j, \phi_i) \right]$$

$$\left. + \overline{\overline{H}}(\eta_i) \left[\overline{N}_{23}(\psi_j, \eta_i) + \overline{S}_6(\psi_j, \eta_i) \right] |\eta_i| \right\} = 0, \qquad (j = 1,...,n-1)$$

$$\sum_{i=1}^{n} C_i \left\{ \overline{\overline{F}}(\phi_i) \left[\overline{N}_{31}(\varepsilon_j, \phi_i) + \overline{S}_7(\varepsilon_j, \phi_i) \right] |\phi_i| + \overline{\overline{G}}(\phi_i) \left[\overline{N}_{32}(\varepsilon_j, \phi_i) + \overline{S}_8(\varepsilon_j, \phi_i) \right] |\phi_i| \right.$$

$$\left. + \overline{\overline{H}}(\eta_i) \left[\frac{1}{\eta_i - \varepsilon_j} + \overline{M}_2(\varepsilon_j, \eta_i) + |\eta_i| \overline{N}_{33}(\varepsilon_j, \eta_i) \right] \right\}$$

$$= \frac{2(\kappa-3)(\kappa+1)}{(7-\kappa)\kappa}, \hspace{3cm} (j = 1,...,n-1) \hspace{2cm} \text{(4.10a-c)}$$

$$\sum_{i=1}^{n} C_i \overline{\overline{F}}(\phi_i) \phi_i = 0,$$

$$\sum_{i=1}^{n} C_i \overline{\overline{G}}(\phi_i)\phi_i = 0,$$

$$\sum_{i=1}^{n} C_i \overline{\overline{H}}(\eta_i)\eta_i = 0, \qquad\qquad\qquad\qquad\qquad \text{(4.11a-c)}$$

where the roots ϕ_i, η_i and ψ_j, ε_j are given by

$$\phi_i = \eta_i = \cos\left[\frac{(i-1)\pi}{n-1}\right], \qquad\qquad\qquad (i=1,...,n)$$

$$\psi_j = \varepsilon_j = \cos\left[\frac{(2j-1)\pi}{2(n-1)}\right], \qquad\qquad (j=1,...,n-1) \qquad\qquad \text{(4.12a,b)}$$

C_i are the weighting constants of the Lobatto polynomials

$$C_1 = C_n = \frac{1}{2(n-1)}, \qquad C_i = \frac{1}{(n-1)}, \qquad (i=2,...,n-1) \qquad\qquad \text{(4.13)}$$

Equations (4.10) and (4.11) constitute a system of $3n \times 3n$ linear algebraic equations. Note that the unknown functions $\overline{\overline{F}}(\phi)$, $\overline{\overline{H}}(\eta)$ are even, and $\overline{\overline{G}}(\phi)$ is odd. In addition, the roots and weighting constants of the Lobatto polynomials are symmetric. Therefore, the $(3n-3) \times 3n$ system of algebraic equations, Eqs. (4.10), may be reduced to the following $(3n/2) \times (3n/2)$ system

$$\sum_{i=1}^{n/2} C_i \left\{ \overline{\overline{F}}(\phi_i)\left[m_4(\psi_j,\phi_i) + \phi_i \overline{N}_{11}(\psi_j,\phi_i) + \phi_i \overline{S}_1(\psi_j,\phi_i) \right] \right.$$

$$\left. + \overline{\overline{G}}(\phi_i)\left[\overline{N}_{12}(\psi_j,\phi_i) + \overline{S}_2(\psi_j,\phi_i) \right]\phi_i + \overline{\overline{H}}(\eta_i)\left[\overline{N}_{13}(\psi_j,\eta_i) + \overline{S}_3(\psi_j,\eta_i) \right]\eta_i \right\}$$

$$= \frac{(\kappa+1)}{2\kappa}, \qquad\qquad\qquad\qquad (j=1,...,n/2)$$

58

$$\sum_{i=1}^{n/2} C_i \left\{ \overline{\overline{F}}(\phi_i) \left[\overline{N}_{21}(\psi_j, \phi_i) + \overline{S}_4(\psi_j, \phi_i) \right] \phi_i \right.$$

$$+ \overline{\overline{G}}(\phi_i) \left[m_3(\psi_j, \phi_i) + \phi_i \overline{N}_{22}(\psi_j, \phi_i) + \phi_i \overline{S}_5(\psi_j, \phi_i) \right]$$

$$\left. + \overline{\overline{H}}(\eta_i) \left[\overline{N}_{23}(\xi_j, \eta_i) + \overline{S}_6(\xi_j, \eta_i) \right] \eta_i \right\} = 0, \qquad (j = 1,...,n/2)$$

$$\sum_{i=1}^{n/2} C_i \left\{ \overline{\overline{F}}(\phi_i) \left[\overline{N}_{31}(\varepsilon_j, \phi_i) + \overline{S}_7(\varepsilon_j, \phi_i) \right] \phi_i + \overline{\overline{G}}(\phi_i) \left[\overline{N}_{32}(\varepsilon_j, \phi_i) + \overline{S}_8(\varepsilon_j, \phi_i) \right] \phi_i \right.$$

$$\left. + \overline{\overline{H}}(\eta_i) \left[m_4(\varepsilon_j, \eta_i) + \eta_i \overline{N}_{33}(\varepsilon_j, \eta_i) \right] \right\} = \frac{(\kappa - 3)(\kappa + 1)}{(7 - \kappa)\kappa}, \qquad (j = 1,...,n/2) \qquad (4.14\text{a-c})$$

where

$$m_3(\psi_j, \phi_i) = \begin{cases} \dfrac{\phi_i}{2(\phi_i^2 - \psi_j^2)} E(\dfrac{\phi_i}{\psi_j}) & \phi_i < \psi_j \\[3mm] \dfrac{\phi_i^2}{2\psi_j(\phi_i^2 - \psi_j^2)} E(\dfrac{\psi_j}{\phi_i}) - \dfrac{1}{2\psi_j} K(\dfrac{\psi_j}{\phi_i}) & \phi_i > \psi_j \end{cases},$$

$$m_4(\varepsilon_j, \eta_i) = \begin{cases} \dfrac{1}{2\varepsilon_j} K(\dfrac{\eta_i}{\varepsilon_j}) + \dfrac{\varepsilon_j}{2(\eta_i^2 - \varepsilon_j^2)} E(\dfrac{\eta_i}{\varepsilon_j}) & \eta_i < \varepsilon_j \\[3mm] \dfrac{\eta_i}{2(\eta_i^2 - \varepsilon_j^2)} E(\dfrac{\varepsilon_j}{\eta_i}) & \eta_i > \varepsilon_j \end{cases}. \qquad (4.15\text{a-b})$$

Note here that Eqs. (4.11a,c) are automatically satisfied since $\overline{\overline{F}}(\phi)$ and $\overline{\overline{H}}(\eta)$ are even functions. The system of equations, Eqs.(4.14), contains $3n/2$ equations for $3n/2$ unknowns, $\overline{\overline{F}}(\phi_i)$, $\overline{\overline{G}}(\phi_i)$ and $\overline{\overline{H}}(\eta_i)$ $(i = 1,...,n/2)$. However, if n is chosen to be an even integer, it can be shown that Eq. (4.14b) corresponding to $\psi_{n/2} = 0$ is satisfied automatically since

$$\tau_{rz}(0, L) = 0. \qquad (4.16)$$

59

The missing equation, Eq. (4.14b) for $j = n/2$, is complemented by Eq. (4.11b) which can be converted to

$$\sum_{i=1}^{n/2} C_i \phi_i \overline{\overline{G}}(\phi_i) = 0 .$$ (4.17)

It must be noted here that calculation of the coefficients for $j = n/2$ which corresponds to $r = 0$ in Eqs. (4.14a,c) requires special attention. For this purpose, the kernels $N_{ij}(r,t)$ $(i, j = 1-3)$ must be calculated separately for $r = 0$. Let

$$K_{ij\infty 0}(t,\alpha) = \lim_{\alpha \to \infty} K_{ij}(0,t,\alpha) ,$$

$$N_{ij_{s0}}(t) = \int_0^\infty K_{ij\infty 0}(t,\alpha) d\alpha ,$$

$$N_{ij}(0,t) = N_{ij_{s0}}(t) + \int_0^\infty \left[K_{ij}(0,t,\alpha) - K_{ij\infty 0}(t,\alpha) \right] d\alpha , \qquad (i = 1,3; j = 1-3) \quad (4.18\text{a-c})$$

where $K_{ij\infty 0}(t,\alpha)$ and $N_{ij_{s0}}(t)$ $(i = 1,3; j = 1-3)$ are given in Appendix E and F, respectively.

Then, noting also that

$$E(0) = \frac{\pi}{2} ,$$ (4.19)

Eqs. (4.14a,c) for $j = n/2$ may be replaced by

60

$$\sum_{i=1}^{n/2} C_i \left\{ \overline{\overline{F}}(\phi_i) \left[\frac{\pi}{2\phi_i} + \phi_i \overline{N}_{11}(0,\phi_i) + \phi_i \overline{S}_1(0,\phi_i) \right] + \overline{\overline{G}}(\phi_i) \left[\overline{N}_{12}(0,\phi_i) + \overline{S}_2(0,\phi_i) \right] \phi_i \right.$$

$$\left. + \overline{\overline{H}}(\eta_i) \left[\overline{N}_{13}(0,\eta_i) + \overline{S}_3(0,\eta_i) \right] \eta_i \right\} = \frac{(\kappa+1)}{2\kappa} ,$$

$$\sum_{i=1}^{n/2} C_i \left\{ \overline{\overline{F}}(\phi_i) \left[\overline{N}_{31}(0,\phi_i) + \overline{S}_7(0,\phi_i) \right] \phi_i + \overline{\overline{G}}(\phi_i) \left[\overline{N}_{32}(0,\phi_i) + \overline{S}_8(0,\phi_i) \right] \phi_i \right.$$

$$\left. + \overline{\overline{H}}(\eta_i) \left[\frac{\pi}{2\eta_i} + \eta_i \overline{N}_{33}(0,\eta_i) \right] \right\} = \frac{(\kappa-3)(\kappa+1)}{(7-\kappa)\kappa} . \tag{4.20a,b}$$

Infinite integrals for kernels, $N_{ij}(r,t)$ $(i,j=1-3)$, are calculated numerically by using the Laguerre integration formula, Abramowitz and Stegun (1965) .

4.1.2 Infinite Cylinder Having an Inclusion

Consider an infinite circular cylinder of radius A containing a penny-shaped concentric rigid inclusion of radius b at $z=0$. The cylinder is under the action of axial tensile loads of uniform intensity p_0 at $z=\pm\infty$ (Fig. 4.1). If there is no crack in the cylinder, the unknown functions $f(t)$ and $g(t)$ defined on the cracks must be dismissed. Then, the integral equations, Eqs. (4.14a,b), resulting from the conditions on the cracks, Eqs. (3.1a,b), will be unnecessary. Remaining integral equation, Eq. (4.14c), will reduce to

$$\sum_{i=1}^{n/2} C_i \overline{\overline{H}}(\eta_i) \left[m_4(\varepsilon_j,\eta_i) + \eta_i \overline{N}_{33}(\varepsilon_j,\eta_i) \right] = \frac{(\kappa-3)(\kappa+1)}{(7-\kappa)\kappa} , \quad (j=1,...,n/2-1) \tag{4.21}$$

which must be complemented by

$$\sum_{i=1}^{n/2} C_i \overline{\overline{H}}(\eta_i) \left[\frac{\pi}{2\eta_i} + \eta_i \overline{N}_{33}(0,\eta_i) \right] = \frac{(\kappa-3)(\kappa+1)}{(7-\kappa)\kappa} \tag{4.22}$$

61

as the $(n/2)$th equation of the system written separately due to difficulty in calculating the kernels at $r = 0$.
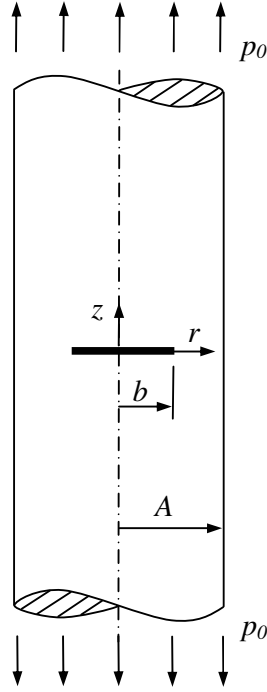

Figure 4.1 Geometry of an infinite cylinder with a penny-shaped inclusion.

4.1.3 Infinite Cylinder Having Two Cracks

Now consider an infinite circular cylinder of radius A containing two penny-shaped concentric cracks of radius a symmetrically located at $z = \pm L$ planes. Both ends of this cracked infinite cylinder are subjected to axial tensile loads of uniform intensity p_0 (Fig. 4.2). In this case, the unknown function $h(t)$ defined on the rigid inclusion must be dismissed.
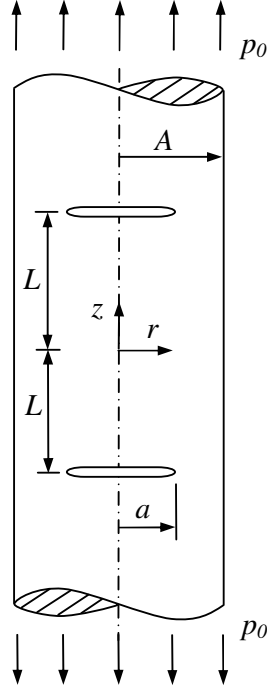
Figure 4.2 Geometry of an infinite cylinder with two penny-shaped cracks.

The integral equation, Eq. (4.14c), resulting from the condition on the rigid inclusion, Eq. (3.1c), must also be eliminated. In this case, Eqs. (4.14a,b) will reduce to

$$
\sum_{i=1}^{n/2} C_i \Big\{ \overline{\overline{F}}(\phi_i) \big[m_4(\psi_j,\phi_i) + \phi_i \overline{N}_{11}(\psi_j,\phi_i) + \phi_i \overline{S}_1(\psi_j,\phi_i) \big]
$$

$$
+ \overline{\overline{G}}(\phi_i) \big[\overline{N}_{12}(\psi_j,\phi_i) + \overline{S}_2(\psi_j,\phi_i) \big] \phi_i \Big\} = \frac{(\kappa+1)}{2\kappa}, \qquad (j=1,...,n/2-1)
$$

$$
\sum_{i=1}^{n/2} C_i \Big\{ \overline{\overline{F}}(\phi_i) \big[\overline{N}_{21}(\psi_j,\phi_i) + \overline{S}_4(\psi_j,\phi_i) \big] \phi_i
$$

$$
+ \overline{\overline{G}}(\phi_i) \big[m_3(\psi_j,\phi_i) + \phi_i \overline{N}_{22}(\psi_j,\phi_i) + \phi_i \overline{S}_5(\psi_j,\phi_i) \big] \Big\} = 0, \quad (j=1,...,n/2) \qquad (4.23a,b)
$$

with

$$\sum_{i=1}^{n/2} C_i \left\{ \overline{\overline{F}}(\phi_i) \left[\frac{\pi}{2\phi_i} + \phi_i \overline{N}_{11}(0,\phi_i) + \phi_i \overline{S}_1(0,\phi_i) \right] \right.$$

$$\left. + \overline{\overline{G}}(\phi_i) \left[\overline{N}_{12}(0,\phi_i) + \overline{S}_2(0,\phi_i) \right] \phi_i \right\} = \frac{(\kappa+1)}{2\kappa} \tag{4.24}$$

being the complementing equation written separately due to delicate nature of the kernels at $r = 0$.

4.2 Semi-Infinite Cylinder Problem

When the rigid inclusion at $z = 0$ spreads out and its radius b approaches A, the radius of the cylinder, the cylinder is fixed completely at $z = 0$. In this case, one half of the infinite cylinder, for example, the upper half, may be regarded as a semi-infinite cylinder with the short end being bonded to a rigid support at $z = 0$.

4.2.1 Semi-Infinite Cylinder Having a Crack

Consider the cracked semi-infinite cylinder problem shown in Fig. 4.3. The semi-infinite cylinder containing a concentric penny-shaped crack of radius a at $z = L$ is fixed at $z = 0$ and tensioned at $z = \infty$ by a uniformly distributed axial load of intensity p_0. In this case, Eq. (3.20c) must be replaced by

$$h(t) = \frac{h^*(t)}{(A^2 - t^2)^\gamma}, \qquad (0 < \mathrm{Re}(\gamma) < 1) \tag{4.25}$$

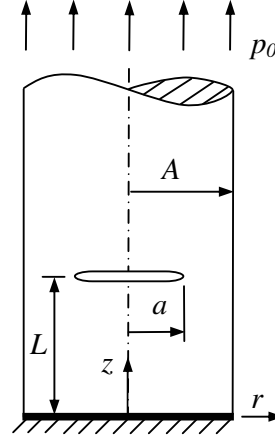such that γ is to be calculated from the characteristic equation, Eq. (3.27).

Figure 4.3 Semi-infinite cylinder having a penny-shaped crack.

Similarly, Eqs. (4.2) defining non-dimensional variables η, ε on the rigid inclusion must be replaced by

$$t = A\eta, \qquad\qquad (-A < t < A, \; -1 < \eta < 1)$$

$$r = A\varepsilon. \qquad\qquad (-A < t < A, \; -1 < \varepsilon < 1) \qquad\qquad (4.26a,b)$$

The integrals containing $\overline{\overline{H}}(\eta)$ in Eq. (4.6) and (4.7) must be calculated by the use of the Gauss-Jacobi integration formula, Erdoğan et al. (1973), Gupta (1974), Geçit (1986), Yetmez and Geçit (2005), so that Eqs. (4.14) are replaced by

$$\sum_{i=1}^{n/2} C_i \left\{ \overline{\overline{F}}(\phi_i) \left[m_4(\psi_j, \phi_i) + \phi_i \overline{N}_{11}(\psi_j, \phi_i) + \phi_i \overline{S}_1(\psi_j, \phi_i) \right] \right.$$

$$\left. + \overline{\overline{G}}(\phi_i) \left[\overline{N}_{12}(\psi_j, \phi_i) + \overline{S}_2(\psi_j, \phi_i) \right] \phi_i \right\}$$

$$+ \frac{1}{\pi} \sum_{i=1}^{n/2} W_i \overline{\overline{H}}(\eta_i) \left[\overline{N}_{13}(\psi_j, \eta_i) + \overline{S}_3(\psi_j, \eta_i) \right] \eta_i = \frac{(\kappa+1)}{2\kappa}, \quad (j = 1, \ldots, n/2)$$

65

$$\sum_{i=1}^{n/2} C_i \left\{ \overline{\overline{F}}(\phi_i) \left[\overline{N}_{21}(\psi_j, \phi_i) + \overline{S}_4(\psi_j, \phi_i) \right] \phi_i \right.$$

$$+ \overline{\overline{G}}(\phi_i) \left[m_3(\psi_j, \phi_i) + \phi_i \overline{N}_{22}(\psi_j, \phi_i) + \phi_i \overline{S}_5(\psi_j, \phi_i) \right] \right\}$$

$$+ \frac{1}{\pi} \sum_{i=1}^{n/2} W_i \overline{\overline{H}}(\eta_i) \left[\overline{N}_{23}(\psi_j, \eta_i) + \overline{S}_6(\psi_j, \eta_i) \right] \eta_i = 0, \qquad (j = 1, ..., n/2)$$

$$\sum_{i=1}^{n/2} C_i \left\{ \overline{\overline{F}}(\phi_i) \left[\overline{N}_{31}(\varepsilon_j, \phi_i) + \overline{S}_7(\varepsilon_j, \phi_i) \right] + \overline{\overline{G}}(\phi_i) \left[\overline{N}_{32}(\varepsilon_j, \phi_i) + \overline{S}_8(\varepsilon_j, \phi_i) \right] \right\} \phi_i$$

$$+ \frac{1}{\pi} \sum_{i=1}^{n/2} W_i \overline{\overline{H}}(\eta_i) \left[m_4(\varepsilon_j, \eta_i) + \eta_i \overline{N}_{33}(\varepsilon_j, \eta_i) \right]$$

$$= \frac{(\kappa - 3)(\kappa + 1)}{(7 - \kappa)\kappa}, \qquad\qquad (j = 1, ..., n/2) \qquad\qquad (4.27\text{a-c})$$

where

$$\overline{\overline{F}}(\phi) = -\frac{2\mu}{\kappa p_0} f(a\phi)(1 - \phi^2)^{1/2},$$

$$\overline{\overline{G}}(\phi) = -\frac{2\mu}{\kappa p_0} g(a\phi)(1 - \phi^2)^{1/2},$$

$$\overline{\overline{H}}(\eta) = \frac{1}{p_0} h(A\eta)(1 - \eta^2)^{\gamma}, \qquad\qquad (4.28\text{a-c})$$

and C_i, ϕ_i, ψ_j $(i, j = 1, ..., n/2)$ are Lobatto weights and integration points, which are still given by Eqs. (4.12) and (4.13). However, W_i, η_i and ε_j $(i, j = 1, ..., n/2)$, are the weights and the roots of the Jacobi polynomials:

$$P_n^{(-\gamma,-\gamma)}(\eta_i) = 0, \qquad\qquad\qquad\qquad (i,...,n)$$

$$P_{n-1}^{(1-\gamma,1-\gamma)}(\varepsilon_j) = 0, \qquad\qquad\qquad\qquad (j,...,n-1)$$

$$W_i = -\frac{2(n-\gamma+1)}{(n+1)!}\frac{[\Gamma(n-\gamma+1)]^2}{\Gamma(n-2\gamma+1)}\frac{(n-2\gamma+1)^{-1}2^{-2\gamma}}{P_n^{(-\gamma,-\gamma)}(\eta_i)P_{n+1}^{(-\gamma,-\gamma)}(\eta_i)}. \quad (i,...,n) \qquad (4.29\text{a-c})$$

Note again that calculation of kernels of Eqs. (4.27a,c) for $j = n/2$ corresponding to $r = 0$ requires special attention. Therefore, these equations are written separately in the form

$$\sum_{i=1}^{n/2}C_i\left\{\overline{\overline{F}}(\phi_i)\left[\frac{\pi}{2\phi_i}+\phi_i\overline{N}_{11}(0,\phi_i)+\phi_i\overline{S}_1(0,\phi_i)\right]+\overline{\overline{G}}(\phi_i)\left[\overline{N}_{12}(0,\phi_i)+\overline{S}_2(0,\phi_i)\right]\phi_i\right\}$$

$$+\frac{1}{\pi}\sum_{i=1}^{n/2}W_i\overline{\overline{H}}(\eta_i)\left[\overline{N}_{13}(0,\eta_i)+\overline{S}_3(0,\eta_i)\right]\eta_i = \frac{(\kappa+1)}{2\kappa},$$

$$\sum_{i=1}^{n/2}C_i\left\{\overline{\overline{F}}(\phi_i)\left[\overline{N}_{31}(0,\phi_i)+\overline{S}_7(0,\phi_i)\right]+\overline{\overline{G}}(\phi_i)\left[\overline{N}_{32}(0,\phi_i)+\overline{S}_8(0,\phi_i)\right]\right\}\phi_i$$

$$+\frac{1}{\pi}\sum_{i=1}^{n/2}W_i\overline{\overline{H}}(\eta_i)\left[\frac{\pi}{2\eta_i}+\eta_i\overline{N}_{33}(0,\eta_i)\right] = \frac{(\kappa-3)(\kappa+1)}{(7-\kappa)\kappa}. \qquad (4.30\text{a,b})$$

4.2.2 Semi-Infinite Cylinder without Crack

Consider the semi-infinite cylinder problem shown in Fig. 4.4. The short end at $z = 0$ is fixed and the far end at $z = \infty$ is tensioned by an axial load of uniform intensity p_0. Solution of this problem has been given by Gupta (1974).
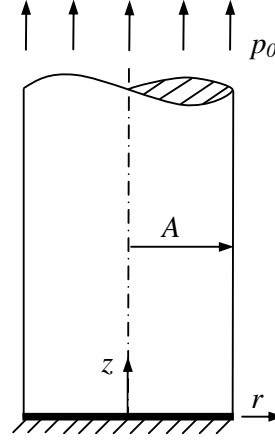
Figure 4.4 Semi infinite cylinder problem.

In this case, the unknown functions $f(t)$ and $g(t)$ related to the crack and Eqs. (4.27a,b) and (4.30a) must be eliminated. Then, Eqs. (4.27c) and (4.30b) reduce to

$$\frac{1}{\pi}\sum_{i=1}^{n/2} W_i \overline{\overline{H}}(\eta_i)\left[m_4(\varepsilon_j,\eta_i)+\eta_i \overline{N}_{33}(\varepsilon_j,\eta_i)\right]$$

$$=\frac{(\kappa-3)(\kappa+1)}{(7-\kappa)\kappa}, \qquad\qquad (j=1,...,n/2-1) \qquad\qquad (4.31)$$

and

$$\frac{1}{\pi}\sum_{i=1}^{n/2} W_i \overline{\overline{H}}(\eta_i)\left[\frac{\pi}{2\eta_i}+\eta_i \overline{N}_{33}(0,\eta_i)\right]=\frac{(\kappa-3)(\kappa+1)}{(7-\kappa)\kappa}. \qquad\qquad (4.32)$$

4.3 Finite Cylinder Problem

When the crack in the semi-infinite cylinder problem given in Section 4.2.1 approaches the edge of the cylinder $(a \to A)$, the cylinder is broken at $z = L$

completely. The portion between $z = 0$ and $z = L$ turns out to be a finite cylinder with the end at $z = 0$ being fixed and the other end at $z = L$ being subjected to axial tension of uniform intensity p_0 (Fig. 4.5).
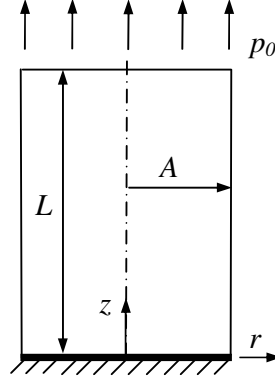
Figure 4.5 Finite cylinder bonded to a rigid support.

In this case, $\beta = 0$ as given by Eq. (3.26). This means that the unknown functions $f(r)$ and $g(r)$ are bounded at $r = \pm A$. The boundary condition, Eq. (3.1a) must be replaced by

$$\sigma_z(r, L) = p_0. \qquad (0 \le r < a) \tag{4.33}$$

Then, Eqs. (4.27) can be put into the following form

$$\sum_{i=1}^{n/2} W_i \left\{ \overline{\overline{F}}(\phi_i) \left[m_4(\psi_j, \phi_i) + \phi_i \overline{N}_{11}(\psi_j, \phi_i) + \phi_i \overline{S}_1(\psi_j, \phi_i) \right] \right.$$

$$\left. + \overline{\overline{G}}(\phi_i) \left[\overline{N}_{12}(\psi_j, \phi_i) + \overline{S}_2(\psi_j, \phi_i) \right] \phi_i + \overline{\overline{H}}(\eta_i) \left[\overline{N}_{13}(\psi_j, \eta_i) + \overline{S}_3(\psi_j, \eta_i) \right] \eta_i \right\}$$

$$= 0, \qquad\qquad (j = 1, ..., n/2 - 1)$$

69

$$\sum_{i=1}^{n/2} W_i \left\{ \overline{\overline{F}}(\phi_i) \left[\overline{N}_{21}(\psi_j, \phi_i) + \overline{S}_4(\psi_j, \phi_i) \right] \phi_i \right.$$

$$+ \overline{\overline{G}}(\phi_i) \left[m_3(\psi_j, \phi_i) + \phi_i \overline{N}_{22}(\psi_j, \phi_i) + \phi_i \overline{S}_5(\psi_j, \phi_i) \right]$$

$$+ \overline{\overline{H}}(\eta_i) \left[\overline{N}_{23}(\psi_j, \eta_i) + \overline{S}_6(\psi_j, \eta_i) \right] \eta_i \bigg\} = 0, \qquad (j = 1, \dots, n/2 - 1)$$

$$\sum_{i=1}^{n/2} W_i \left\{ \overline{\overline{F}}(\phi_i) \left[\overline{N}_{31}(\varepsilon_j, \phi_i) + \overline{S}_7(\varepsilon_j, \phi_i) \right] \phi_i + \overline{\overline{G}}(\phi_i) \left[\overline{N}_{32}(\varepsilon_j, \phi_i) + \overline{S}_8(\varepsilon_j, \phi_i) \right] \phi_i \right.$$

$$+ \overline{\overline{H}}(\eta_i) \left[m_4(\varepsilon_j, \eta_i) + \eta_i \overline{N}_{33}(\varepsilon_j, \eta_i) \right] \bigg\}$$

$$= \frac{(\kappa - 3)(\kappa + 1)}{(7 - \kappa)\kappa} \pi, \qquad\qquad (j = 1, \dots, n/2 - 1) \qquad (4.34\text{a-c})$$

where $\psi_j = \varepsilon_j$ $(j = 1, \dots, n/2 - 1)$ and $\phi_i = \eta_i$, W_i $(i = 1, \dots, n/2)$ are the roots and the weighting constants of Jacobi polynomials which are given by Eqs.(4.29). In writing Eqs. (4.34), following notation is used:

$$\overline{\overline{F}}(\phi) = -\frac{2\mu}{\kappa p_0} f(A\phi)(1 - \phi^2)^\gamma,$$

$$\overline{\overline{G}}(\phi) = -\frac{2\mu}{\kappa p_0} g(A\phi)(1 - \phi^2)^\gamma,$$

$$\overline{\overline{H}}(\eta) = \frac{1}{p_0} h(A\eta)(1 - \eta^2)^\gamma, \qquad\qquad (4.35\text{a-c})$$

for convenience. γ is calculated from Eq. (3.27). It can be shown that Eqs. (4.34a,b) corresponding to $j = n/2$ (or $r = 0$) are satisfied automatically. Eq.

(4.34c) must be written separately for $j = n/2$ due to difficulty in calculating the kernels for $r = 0$ in the form

$$\sum_{i=1}^{n/2} W_i \left\{ \overline{\overline{F}}(\phi_i) \left[\overline{N}_{31}(0,\phi_i) + \overline{S}_7(0,\phi_i) \right] \phi_i + \overline{\overline{G}}(\phi_i) \left[\overline{N}_{32}(0,\phi_i) + \overline{S}_8(0,\phi_i) \right] \phi_i \right.$$

$$\left. + \overline{\overline{H}}(\eta_i) \left[\frac{\pi}{2\eta_i} + \eta_i \overline{N}_{33}(0,\eta_i) \right] \right\} = \frac{(\kappa-3)(\kappa+1)}{(7-\kappa)\kappa} \pi . \tag{4.36}$$

Now the system in Eqs. (4.34) and (4.36) contain $3n/2 - 2$ equations for $3n/2$ unknowns. Remember that $f(r)$ and $g(r)$ are bounded at $r = \pm A$. But Eqs. (4.35a,b) give infinite values for $f(A)$ and $g(A)$ unless $\overline{\overline{F}}(\phi)$ and $\overline{\overline{G}}(\phi)$ are zero at ± 1. In order to make the functions $f(r)$ and $g(r)$ bounded at the end points $r = \pm A$, $\overline{\overline{F}}(\phi)$ and $\overline{\overline{G}}(\phi)$ must be zero at ± 1:

$$\overline{\overline{F}}(\pm 1) = 0 ,$$

$$\overline{\overline{G}}(\pm 1) = 0 . \tag{4.37a,b}$$

Note that $\phi_i = \eta_i$ $(i = 1,...,n/2)$ will never be equal to 1. Therefore, $\overline{\overline{F}}(1)$ and $\overline{\overline{G}}(1)$ must be expressed in terms of $\overline{\overline{F}}(\phi_i)$, $\overline{\overline{G}}(\phi_i)$ $(i = 1,...,n/2)$ first. Following the procedure described by Geçit (1986), one may write

$$\overline{\overline{F}}(1) = 2 \sum_{i=1}^{n/2} W_i T(1,\phi_i) \overline{\overline{F}}(\phi_i) ,$$

$$\overline{\overline{G}}(1) = 2 \sum_{i=1}^{n/2} W_i T(1,\phi_i) \overline{\overline{G}}(\phi_i) , \tag{4.38a,b}$$

71

where

$$T(1,\phi_i) = \sum_{m=0}^{n-1} \frac{1}{h_m} P_m^{(-\gamma,-\gamma)}(1) P_m^{(-\gamma,-\gamma)}(\phi_i), \qquad (i=1,...,n)$$

$$h_m = \frac{2^{1-2\gamma}}{(2m-2\gamma+1)} \frac{[\Gamma(m-\gamma+1)]^2}{m!\Gamma(m-2\gamma+1)}, \qquad (m=1,...,n-1) \qquad (4.39\text{a,b})$$

Γ being the Gamma function. Hence, Eqs. (4.38) can be written in the form

$$\sum_{i=1}^{n/2} W_i T(1,\phi_i)\overline{\overline{F}}(\phi_i) = 0,$$

$$\sum_{i=1}^{n/2} W_i T(1,\phi_i)\overline{\overline{G}}(\phi_i) = 0. \qquad (4.40\text{a,b})$$

Now the system of equations, Eqs. (4.34), (4.36), and (4.40), is complete; $3n/2$ equations for $3n/2$ unknowns, $\overline{\overline{F}}(\phi_i)$, $\overline{\overline{G}}(\phi_i)$, $\overline{\overline{H}}(\eta_i)$, $(i=1,...,n/2)$.

CHAPTER V

STRESSES AND STRESS INTENSITY FACTORS

5.1 Normal Stress at the Rigid Support

For the semi-infinite and finite cylinder problems, significant stresses may develop at the rigid support. The expression for the normal stress $\sigma_z(r,0)$ may be written from Eqs. (2.43d), (2.48d), (2.49d) by the procedure used in deriving the singular integral equations, Eqs. (3.6), in the following form

$$
\begin{aligned}
\sigma_z(r,0) = & \frac{\mu}{(\kappa+1)}\frac{1}{\pi}\int_{-a}^{a}\left\{f(t)\left[N_{41}(r,t)+\pi R_1(r,t)\right]\right. \\
& \left. + g(t)\left[N_{42}(r,t)+\pi R_2(r,t)\right]\right\}|t|\,dt \\
& + \frac{1}{2(\kappa+1)}\frac{1}{\pi}\int_{-A}^{A}h(t)\left[\frac{(\kappa-1)}{t-r}+(\kappa-1)M_2(r,t)+|t|N_{43}(r,t)\right]dt \\
& + p_0, \qquad\qquad (-A<r<A) \qquad\qquad\qquad (5.1)
\end{aligned}
$$

for the semi-infinite cylinder where

$$
R_1(r,t) = \frac{2L}{r_1 r_2}\left\{\frac{L^2}{r_1^2}\left[2E(r_3)-K(r_3)\right]-\frac{r_2-2L^2}{r_2}E(r_3)\right\},
$$

$$
\begin{aligned}
R_2(r,t) = & -\frac{1}{tr_1}\left\{\frac{(t^2-r^2-L^2)}{r_2}E(r_3)+K(r_3)+\frac{L^2\left[(t-r)(5t-r)+L^2\right]}{r_2^2}E(r_3)\right. \\
& \left. + \frac{L^2(t^2-r^2-L^2)}{r_1^2 r_2}\left[2E(r_3)-K(r_3)\right]\right\}, \qquad\qquad (5.2a,b)
\end{aligned}
$$

in which

$$r_1 = \sqrt{(t+r)^2 + L^2} \, ,$$

$$r_2 = (t-r)^2 + L^2 \, ,$$

$$r_3 = \frac{2\sqrt{tr}}{r_1} \, . \qquad\qquad\qquad\qquad\qquad (5.3\text{a-c})$$

Integrands of the kernels

$$N_{4j}(r,t) = \int\limits_0^\infty K_{4j}(r,t,\alpha)d\alpha \, , \qquad\qquad (j=1-3) \qquad\qquad (5.4)$$

their dominant parts as $\alpha \to \infty$, $K_{4j\infty}(r,t,\alpha)$, $(j=1-3)$ and the singular terms $N_{4j_s}(r,t)$, $(j=1-3)$ are given in Appendix G. Equation (5.1) may be expressed in terms of non-dimensional quantities and the integrals in Eq. (5.1) may be calculated by using Gauss-Jacobi and Gauss-Lobatto integration formulas and

$$\frac{\sigma_z(A\varepsilon_j,0)}{p_0} = \frac{\kappa}{(\kappa+1)} \sum_{i=1}^{n/2} C_i \left\{ \overline{\overline{F}}(\phi_i) \left[\overline{N}_{41}(\varepsilon_j,\phi_i) + \overline{R}_1(\varepsilon_j,\phi_i) \right] \right.$$

$$+ \overline{\overline{G}}(\phi_i) \left[\overline{N}_{42}(\varepsilon_j,\phi_i) + \overline{R}_2(\varepsilon_j,\phi_i) \right] \left. \vphantom{\sum} \right\} \phi_i$$

$$+ \frac{1}{(\kappa+1)} \frac{1}{\pi} \sum_{i=1}^{n/2} W_i \overline{\overline{H}}(\eta_i) \left[(\kappa-1)m_4(\varepsilon_j,\eta_i) + \eta_i \overline{N}_{43}(\varepsilon_j,\eta_i) \right]$$

$$+ 1 \, , \qquad\qquad\qquad (j=1,...,n/2-1) \qquad\qquad (5.5)$$

may be written. Again, due to difficulty in calculation of the kernels for $j = n/2$ (or $r = 0$), the expression for $r = 0$ is written separately in the form

74

$$\frac{\sigma_z(0,0)}{p_0} = \frac{\kappa}{(\kappa+1)} \sum_{i=1}^{n/2} C_i \left\{ \overline{\overline{F}}(\phi_i) \left[\overline{N}_{41}(0,\phi_i) - \overline{R}_1(0,\phi_i) \right] \right.$$

$$\left. + \overline{\overline{G}}(\phi_i) \left[\overline{N}_{42}(0,\phi_i) + \overline{R}_2(0,\phi_i) \right] \right\} \phi_i$$

$$+ \frac{1}{(\kappa+1)} \sum_{i=1}^{n/2} W_i \overline{\overline{H}}(\eta_i) \left[\frac{(\kappa-1)}{2\eta_i} + \frac{\eta_i}{\pi} \overline{N}_{43}(0,\eta_i) \right] + 1, \qquad (5.6)$$

where $\overline{N}_{41}(0,\phi)$, $\overline{N}_{42}(0,\phi)$ and $\overline{N}_{43}(0,\eta)$ are given in Appendix H. For the finite cylinder, all integrals in Eq. (5.1) must be calculated by the Gauss-Jacobi integration formula.

5.2 Stress Intensity Factors

From the viewpoint of fracture, particularly important are the stress intensity factors. Stresses become infinitely large at the edges of the crack and the inclusion. In this case, stress state around those edges can be expressed in terms of the power of stress singularity and the stress intensity factors.

5.2.1 Stress Intensity Factors at the Edge of the Crack

The normal (Mode I) and the shear (Mode II) components of the stress intensity factors, k_{1a} and k_{2a}, at the edge of the crack may be defined as

$$k_{1a} = \lim_{r \to a} [2(r-a)]^{1/2} \sigma_z(r,L),$$

$$k_{2a} = \lim_{r \to a} [2(r-a)]^{1/2} \tau_{rz}(r,L). \qquad (5.7a,b)$$

From Eqs. (2.43d), (2.48d) and (2.49d) one may write

$$\sigma_z(r,L) = \frac{2\mu}{\pi(\kappa+1)} \int_{-a}^{a} \frac{f(t)}{t-r} dt + \sigma_{zb}(r,L), \qquad (a < r < A) \qquad (5.8)$$

where the bounded part $\sigma_{zb}(r,L)$ is given by

$$\sigma_{zb}(r,L) = \frac{2\mu}{\pi(\kappa+1)} \int_{-a}^{a} f(t) \left[M_2(r,t) + |t| N_{11}(r,t) + |t| S_1(r,t) \right] dt. \qquad (5.9)$$

Considering

$$f(t) = \frac{f^*(t)}{\sqrt{a^2 - t^2}} = \begin{cases} \dfrac{\left[f^*(t)/\sqrt{a-t} \right]}{\sqrt{t+a}} & t \to -a \\[4mm] \dfrac{\left[f^*(t)/\sqrt{a+t} \right] e^{\pi i/2}}{\sqrt{t-a}} & t \to a \end{cases} \qquad (5.10)$$

the singular part of normal stress given in Eq.(5.8) can be calculated by the method given in Muskhelishvili (1953). Then, Eq.(5.8) can be written in the following form:

$$\sigma_z(r,L) = \frac{2\mu}{(1+\kappa)} \frac{1}{\sqrt{2a}} \left[\frac{f^*(-a)e^{\pi i/2}}{\sqrt{r+a}\,\sin(\frac{\pi}{2})} - \frac{f^*(a)}{\sqrt{r-a}\,\sin(\frac{\pi}{2})} + f^{**}(r) \right] + \sigma_{zb}(r,L) \quad (5.11)$$

where $f^{**}(r)$ contains bounded terms.

Substitution of Eq. (5.11) in Eq. (5.7a) gives

$$k_{1a} = -\frac{2\mu}{(\kappa+1)} \frac{f^*(a)}{\sqrt{a}}. \qquad (5.12)$$

Comparing Eqs. (4.5a) and (5.10) one can relate $f^*(a\phi)$ and $\overline{F}(\phi)$:

$$f^*(a\phi) = a\overline{F}(\phi) \,. \tag{5.13}$$

Now substituting (5.13) in (5.12), the stress intensity factor can be obtained in the form

$$k_{1a} = -\frac{2\mu}{(\kappa+1)}\sqrt{a}\,\overline{F}(1) \,. \tag{5.14}$$

Using Eq.(4.8a), one can further write

$$k_{1a} = \frac{\kappa}{(\kappa+1)}p_0\sqrt{a}\,\overline{\overline{F}}(1) \tag{5.15}$$

and finally

$$\overline{k}_{1a} = \frac{k_{1a}}{p_0\sqrt{a}} = \frac{\kappa}{(\kappa+1)}\overline{\overline{F}}(1) \tag{5.16}$$

for the normalized Mode I stress intensity factor at the edge of the internal crack. One can similarly write

$$\overline{k}_{2a} = \frac{\kappa}{(\kappa+1)}\overline{\overline{G}}(1) \tag{5.17}$$

for the normalized Mode II stress intensity factor at the edge of the internal crack.

5.2.2 Stress Intensity Factor at the Edge of the Internal Inclusion

Mode II stress intensity factor k_{2b} at the edge of inclusion for infinite cylinder may be defined as

$$k_{2b} = \lim_{r \to b} \left[2(b-r) \right]^{1/2} \tau_{rz}(r,0).$$

(5.18)

Using the boundary condition given in Eq. (2.23d), shearing stress at $r = 0$ can be defined in terms of the unknown function $h(r)$ in the form

$$\tau_{rz}(r,0) = \frac{h(r)}{2} = \frac{h^*(r)}{2(b^2 - r^2)^{1/2}}$$

(5.19)

with the help of Eq. (3.20c). By a similar procedure as the one used in Section 5.2.1, Mode II stress intensity factor at the edge of the internal rigid inclusion can be calculated as

$$k_{2b} = \frac{\sqrt{b}}{2} \overline{H}(1)$$

(5.20)

and the normalized stress intensity factor

$$\bar{k}_{2b} = \frac{k_{2b}}{p_0 \sqrt{b}}$$

(5.21)

can be written as

$$\bar{k}_{2b} = \frac{\overline{\overline{H}}(1)}{2}.$$

(5.22)

5.2.3 Stress Intensity Factors at the Edge of the Rigid Support

When the penny-shaped rigid inclusion approaches the surface of the cylinder, the cylinder becomes fixed at $z = 0$. The stresses along the edge of the rigid support are infinity and can be characterized by the stress intensity factors

$$k_{1A} = \lim_{r \to A} \sqrt{2}(A - r)^{\gamma} \sigma_z(r,0),$$

$$k_{2A} = \lim_{r \to A} \sqrt{2}(A - r)^{\gamma} \tau_{rz}(r,0). \qquad (5.23\text{a,b})$$

One may write

$$\sigma_z(r,0) = \sigma_{zs}(r,0) + \sigma_{zb}(r,0), \qquad (5.24)$$

where subscripts s and b denote the singular and the bounded parts of $\sigma_z(r,0)$. Considering Eq. (5.1), singular part of the stress can be expressed in the form

$$\sigma_{zs}(r,0) = \frac{1}{2\pi(\kappa+1)} \int_{-A}^{A} h(t) \left\{ (\kappa-1)\frac{1}{t-r} + |t|\overline{N}_{43s}(r,t) \right\} dt . \qquad (5.25)$$

The integral containing the simple Cauchy kernel, $1/(t-r)$, can be evaluated by the aid of Eqs. (3.20c) and (3.22c):

$$\frac{1}{\pi} \int_{-A}^{A} \frac{h(t)}{t-r} dt = \frac{h^*(-A)\cot(\pi\gamma)}{(2A)^{\gamma}(A+r)^{\gamma}} - \frac{h^*(A)\cot(\pi\gamma)}{(2A)^{\gamma}(A-r)^{\gamma}} + h_1^{**}(r) \qquad (5.26)$$

in which $h_1^{**}(r)$ contains bounded terms. On the other hand, from Eq. (G.8) one can write

$$N_{43_s}(r,t) = \frac{1}{\sqrt{tr}} \left\{ \left[2(A-r)^2 \frac{\partial^2}{\partial r^2} + (\kappa+7)(A-r)\frac{\partial}{\partial r} \right.\right.$$

$$\left. + \frac{5+3\kappa}{2} \left[\frac{1}{(t+r-2A)} + \frac{1}{(t-r+2A)} \right] \right] + \left[2(A+r)^2 \frac{\partial^2}{\partial r^2} \right.$$

$$\left.\left. - (\kappa+7)(A+r)\frac{\partial}{\partial r} + \frac{5+3\kappa}{2} \left[\frac{1}{(t-r-2A)} + \frac{1}{(t+r+2A)} \right] \right] \right\}. \qquad (5.27)$$

Eqs. (3.23i) and (5.27) give then

$$\frac{1}{\pi} \int_{-A}^{A} h(t)|t| \overline{N}_{43_s}(r,t)dt = - \frac{\left[2\gamma(\gamma+1) - (\kappa+7)\gamma + \frac{1}{2}(5+3\kappa) \right] h^*(A)}{(2A)^\gamma (A-r)^\gamma \sin(\pi\gamma)}$$

$$+ \frac{\left[2\gamma(\gamma+1) - (\kappa+7)\gamma + \frac{1}{2}(5+3\kappa) \right] h^*(-A)}{(2A)^\gamma (A-r)^\gamma \sin(\pi\gamma)}$$

$$- \frac{\left[2\gamma(\gamma+1) - (\kappa+7)\gamma + \frac{1}{2}(5+3\kappa) \right] h^*(A)}{(2A)^\gamma (A+r)^\gamma \sin(\pi\gamma)}$$

$$+ \frac{\left[2\gamma(\gamma+1) - (\kappa+7)\gamma + \frac{1}{2}(5+3\kappa) \right] h^*(-A)}{(2A)^\gamma (A+r)^\gamma \sin(\pi\gamma)} + h_2^{**}(r), \quad (5.28)$$

where $h_2^{**}(r)$ contains bounded terms. Now substituting Eqs. (5.26) and (5.28) in Eq. (5.25), then substituting the resulting expression for $\sigma_{zs}(r,0)$ in Eq. (5.24) or Eq. (5.23) one can write the Mode I stress intensity factor in the form

$$k_{1A} = \frac{\sqrt{2}}{2(\kappa+1)} \left\langle \frac{h^*(A)}{(2A)^\gamma \sin(\pi\gamma)} \left\{ (1-\kappa)[\cos(\pi\gamma)+1] + 2(1+\kappa)(\gamma-1) - 4(\gamma-1)^2 \right\} \right\rangle.$$

$$(5.29)$$

80

The normalized Mode I stress intensity factor $\bar{k}_{1A}$ at the edge of the rigid support can be written as

$$\bar{k}_{1A} = \frac{k_{1A}}{p_0 A^\gamma} = \frac{\overline{\overline{H}}(1)}{2^{\gamma+1/2}(\kappa+1)\sin(\pi\gamma)}\left\{(1-\kappa)[\cos(\pi\gamma)+1] + 2(\kappa+1)(\gamma-1) - 4(\gamma-1)^2\right\}$$

(5.30)

Note that in deriving Eq. (5.30), Eqs. (4.5c) and (4.8c) are used. By a similar procedure, normalized Mode II stress intensity factor $\bar{k}_{2A}$ at the edge of the rigid support can be obtained in the form

$$\bar{k}_{2A} = \frac{k_{2A}}{p_0 A^\gamma} = \frac{\overline{\overline{H}}(1)}{2^{\gamma+1/2}},$$

(5.31)

where γ is obtained from Eq.(3.20).

CHAPTER VI

RESULTS AND CONCLUSIONS

6.1 Numerical Results

The system of linear algebraic equations for the particular problems defined in Chapter 4 is solved and the values of unknown functions $\overline{\overline{F}}(\phi_i)$, $\overline{\overline{G}}(\phi_i)$ and $\overline{\overline{H}}(\eta_i)$ $(i = 1,...,n/2)$ are calculated at discrete collocation points. Then, stress distributions, stress intensity factors at the edges of the crack and the inclusion for infinite cylinder and at the edge of rigid support as $b \rightarrow A$ for semi-infinite and finite cylinders are calculated numerically.

All cylinder problems in the scope of this thesis are described by the geometrical parameters A; radius of the cylinder, a; radius of the cracks, b; radius of the rigid inclusion, L; distance from the inclusion to the cracks. The material of the cylinder is described by μ; modulus of rigidity and ν; Poisson's ratio. The loading is described by p_0; uniform intensity of the axial tension. However, for the sake of generalization of the numerical results, dimensionless geometrical parameters a/A, b/A, L/A normalized by the radius of the cylinder are used. Since the normalized stress distributions and normalized stress intensity factors are used, particular numerical values are not selected for μ and p_0 in the analysis. Poisson's ratio ν is used to describe the material. Some of the calculated results are shown in Table 6.1 and in Figs. 6.1-6.85.

6.1.1 Infinite Cylinder Problem

6.1.1.1 Rigid Inclusion in an Infinite Cylinder

Consider the problem shown in Fig. 4.1. In this case, the system of equations, Eqs. (4.21) and (4.22) must be solved for $\overline{\overline{H}}(\eta)$. Figures 6.1 and 6.2 show the normalized Mode II stress intensity factor $\overline{k}_{2b}$ at the edge of the rigid inclusion defined by Eq. (5.22). As can be seen from these figures, $\overline{k}_{2b}$ is negative and it increases with increasing v, but decreases with increasing b/A ratio. Note that $\overline{k}_{2b}$ is zero when $v = 0$. For this situation, there is no Poisson's effect. Consequently, the constraint due to the rigid inclusion disappears and the shearing stresses induced by the inclusion vanish.

6.1.1.2 Two Parallel Cracks in an Infinite Cylinder

Consider the problem shown in Fig. 4.2. In this case, the system given by Eqs. (4.23) and (4.24) must be solved for $\overline{\overline{F}}(\phi)$ and $\overline{\overline{G}}(\phi)$. Figures 6.3 and 6.4 show the normalized Mode I and Mode II stress intensity factors $\overline{k}_{1a}$ and $\overline{k}_{2a}$ at the edges of two parallel penny-shaped cracks in an infinite solid defined by Eqs. (5.16) and (5.17). These figures are produced for the purpose of comparison with the results given by Isida et al. (1985). Numerical results are obtained by solving the following system

$$\sum_{i=1}^{n/2} C_i \left\{ \overline{\overline{F}}(\phi_i) \left[m_4(\psi_j, \phi_i) + \phi_i \overline{S}_1(\psi_j, \phi_i) \right] + \overline{\overline{G}}(\phi_i) \phi_i \overline{S}_2(\psi_j, \phi_i) \right\}$$

$$= \frac{(\kappa + 1)}{2\kappa}, \qquad\qquad\qquad (j = 1,...,n/2 - 1)$$

$$\sum_{i=1}^{n/2} C_i \left\{ \overline{\overline{F}}(\phi_i) \left[\frac{\pi}{2\phi_i} + \phi_i \overline{S}_1(0, \phi_i) \right] + \overline{\overline{G}}(\phi_i) \phi_i \overline{S}_2(0, \phi_i) \right\} = \frac{(\kappa + 1)}{2\kappa},$$

$$\sum_{i=1}^{n/2} C_i \left\{ \overline{\overline{F}}(\phi_i)\phi_i \overline{S}_4(\psi_j,\phi_i) \ + \overline{\overline{G}}(\phi_i)\left[m_3(\psi_j,\phi_i) + \phi_i \overline{S}_5(\psi_j,\phi_i) \right] \right\}$$

$$= 0, \qquad\qquad\qquad (j=1,...,n/2) \qquad\qquad (6.1)$$

which is obtained from Eqs. (4.23) and (4.24). $\overline{k}_{1a}$ increases, $\overline{k}_{2a}$ decreases with increasing L/a ratio and remain unchanged after $L/a \cong 4$. Results seem to be in very good agreement with those given by Isida et al. (1985). Figure 6.5 shows the normalized Mode I stress intensity factor $\overline{k}_{1a}$ at the edge of a single transverse penny-shaped crack in an infinite cylinder together with the results given in Benthem and Koiter (1973), Leung and Su (1998), Tsang et al. (2003) for comparison. Numerical results for this case are obtained from solution of the system in Eqs. (4.23) and (4.24) by selecting $L/A \rightarrow \infty$, so that the interaction between the two cracks is eliminated. Results seem to agree with the previous ones, the best agreement being with Benthem and Koiter (1973). $\overline{k}_{1a}$ increases with increasing crack radius.

Figures 6.6-6.11 show $\overline{k}_{1a}$ at the edges of two parallel penny-shaped cracks in an infinite cylinder. $\overline{k}_{1a}$ is almost insensitive to ν. In most of the cases, $\overline{k}_{1a}$ increases with increasing a/A and/or L/A ratios. As $L/A \rightarrow \infty$, the infinite cylinder problem with two penny-shaped cracks becomes similar to that of an infinite cylinder with a central crack at $z = 0$ plane.

Figures 6.12-6.17 show $\overline{k}_{2a}$ at the edges of two parallel penny-shaped cracks in an infinite cylinder. In Figs. 6.12 and 6.13, variation of $\overline{k}_{2a}$ is shown for $\nu = 0.3$. From these figures one may conclude that, $\overline{k}_{2a}$ increases with increasing crack radius. $\overline{k}_{2a}$ decreases as the cracks go away from each other.

Figures 6.14 and 6.15 show variations of $\overline{k}_{2a}$ with ν for $a = 0.5A$ and $2L = A$, respectively. These figures show that $\overline{k}_{2a}$ is almost insensitive to changes in ν

84

except for very large crack radii. As can be seen from Figs. 6.16 and 6.17 also, $\overline{k}_{2a}$ is sensitive to changes in geometry, i.e., $2L/A$ and/or a/A ratios.

In Table 1, dimensionless ratio of Mode I stress intensity factor $\overline{k}_{1a}$ for double parallel cracks to $\overline{k}_{1a}$ for single crack for various crack distances and crack radii are compared with finite element method (FEM) results of Tsang et al. (2003) for $\nu = 0.33$. It can be observed that there is a very good agreement between the results of analytical solution obtained in the present study and the solution obtained by Tsang et al. (2003) using finite element method (FEM).

In most fracture analyses, approaches based on energy considerations are used with some variations, Geçit (1988). A crack is claimed to propagate if the rate of release of the stored energy per unit growth of the crack exceeds the rate of change of the surface energy required by the new surfaces. The energy release rate for the crack may be calculated in the form, Erdoğan and Sih (1963), Geçit (1988),

$$\frac{\partial \overline{U}}{\partial a} = \frac{\pi^2 a}{\mu} (k_{1a}^2 + k_{2a}^2) \tag{6.2}$$

where $\overline{U}$ is the strain energy. Figure 6.18 shows the dimensionless energy release rate

$$\overline{w} = \frac{\mu}{\pi^2 a^2 p_0^2} \frac{\partial \overline{U}}{\partial a} \tag{6.3}$$

for one crack when $\nu = 0.3$. Note that $\overline{w}$ is larger for larger L/A ratios, i.e., when interaction between the two cracks is less. $\overline{w}$ increases significantly with increasing a/A ratio.

If the material of the cylinder is brittle, crack propagation may be expected to take place, as suggested by Erdoğan and Sih (1963), in a direction perpendicular to the maximum cleavage stress, which is defined by

$$k_{2a}\left[1-3\cos(\theta)\right]-k_{1a}\sin(\theta)=0,$$

$$3k_{2a}\sin(\theta)-k_{1a}\cos(\theta)<0. \qquad (6.4a,b)$$

Figure 6.19 shows the variation of the probable cleavage angle θ at the edge of the penny-shaped crack at $z=L$ plane when $v=0.3$. As can be seen in this figure, the two cracks propagate away from each other, a tendency that is more pronounced when the cracks are closer to each other.

6.1.1.3 Two Parallel Cracks and a Rigid Inclusion in an Infinite Cylinder

Consider the problem shown in Fig. 2.1. In this case, the system given by Eqs. (4.14), (4.17), and (4.20) must be solved for $\overline{\overline{F}}(\phi)$, $\overline{\overline{G}}(\phi)$ and $\overline{\overline{H}}(\eta)$. Variation of normalized Mode I stress intensity factor $\overline{k}_{1a}$ at the edges of penny-shaped cracks is shown in Figs. 6.20-6.26. Figures 6.20 and 6.21 show variation of $\overline{k}_{1a}$ with a/A. In both figures $b=0.5A$. It seems that $\overline{k}_{1a}$ assumes its minimum value around $a=0.5A$. This effect is most pronounced for larger values of v and smaller values of L/A. Relatively high stresses around the edge of the rigid inclusion are responsible for this behavior. It is obvious that the interaction between the rigid inclusion and the cracks is greater when the cracks are closer to the inclusion. The effect of the inclusion is greater for larger v. Besides the interaction, $\overline{k}_{1a}$ increases as the crack radius increases.

Figures 6.22 and 6.23 show variations of $\overline{k}_{1a}$ with L/A when $a/A=0.5$ and $v=0.3$. $\overline{k}_{1a}$ increases with increasing L/A ratio until $L\cong0.8A$. After $L\cong2A$,

the effects of ν and b/A disappear and $\overline{k}_{1a}$ becomes equal to that in the case of a single crack in an infinite cylinder.

Figures 6.24 and 6.25 show variations of $\overline{k}_{1a}$ with b/A when $a = 0.5A$. As can be seen in Fig. 6.24, $\overline{k}_{1a}$ does not change considerably with b/A for a constant crack radius and constant Poisson's ratio, $\nu = 0.3$. Maximum values of $\overline{k}_{1a}$ are realized at $b \cong 0.8A$ for $a = L = 0.5A$ (Fig. 6.25).

Figure 6.26 shows variation of $\overline{k}_{1a}$ with ν when $a = L = 0.5A$. For practical values of ν, $\overline{k}_{1a}$ increases as ν and/or b/A increase(s) for this combination of crack radius and crack distance.

Figures 6.27-6.33 show variation of normalized Mode II stress intensity factor $\overline{k}_{2a}$ at the edges of the cracks. In Figs. 6.27 and 6.28, variation of $\overline{k}_{2a}$ with a/A when $b = 0.5A$ is given. $\overline{k}_{2a}$ is negative and its magnitude increases as the crack radius a and/or crack distance L increase(s) for $b = 0.5A$ and $\nu = 0.3$. As can be seen in Fig. 6.28, $\overline{k}_{2a}$ starts with positive values and increases with increasing crack radius for $\nu > 0.1$ when $b = L = 0.5A$. With further increase in crack radius, $\overline{k}_{2a}$ decreases, becomes negative and increases in negative direction. It may also be noted that, the effect of ν on $\overline{k}_{2a}$ is negligible for $a/A > \sim 0.6$.

Figure 6.29 and 6.30 show the effect of ν and b/A, respectively, on the variation of $\overline{k}_{2a}$ with L/A when $a = 0.5A$. In Fig. 6.29, $b = 0.5A$ and in Fig. 6.30, $\nu = 0.3$. In general $\overline{k}_{2a}$ decreases in magnitude and tends to zero as L/A increases. For $L/A > 2$, interaction becomes negligible and cracks behave similar to a single symmetric crack in an infinite cylinder so that $\overline{k}_{2a}$ is expected to be zero.

In Figs. 6.31 and 6.32, variation of $\overline{k}_{2a}$ with b/A is shown for a constant crack radius $a = 0.5A$ for several values of L/A and ν, respectively. In Fig. 6.31,

$v = 0.3$ and one can say that the magnitude of $\overline{k}_{2a}$ increases for small values of L/A as well as for $b/A > \sim 0.4$ in general. In Fig. 6.32, $L = 0.5A$ and $\overline{k}_{2a}$ is always negative. Relatively small variation for smaller values of v and considerable variation for larger values of v are observed. Figure 6.33 shows variation of $\overline{k}_{2a}$ with v when $a = b = 0.5A$ for several values of L/A ratio. No remarkable variations are observed for fixed geometrical parameters a/A, b/A and L/A.

Figures 6.34 and 6.35 show the dimensionless strain energy release rate $\overline{w}$ and the probable cleavage angle θ, respectively, for the crack at $z = L$ plane when $v = 0.3$ and $b = 0.5A$. As can be seen in Fig. 6.35, cracks try to escape from the high stress domain around the edge of the rigid inclusion at $z = 0$ plane.

The normalized Mode II stress intensity factor $\overline{k}_{2b}$ at the edge of the rigid inclusion is shown in Figs. 6.36-6.40. Figure 6.36 shows variation of $\overline{k}_{2b}$ with L/A when $a = b = 0.5A$. Note in this figure that $\overline{k}_{2b}$ is always negative, its magnitude is larger for larger v values. It decreases first with increasing L/A ratio, passes through a minimum around $L/A \cong 0.75$ for $v = 0.1$, $L/A \cong 0.45$ for $v = 0.5$, and then increases with further increase in L/A. Finally, it remains constant for $L/A > \sim 2$ as if there is no crack (see Figs. 6.1 and 6.2). In Fig. 6.37, variation of $\overline{k}_{2b}$ with a/A is shown when $b = L = 0.5A$. It is observed that $\overline{k}_{2b}$ changes sign from negative to positive as a/A increases. For very small values of a/A, numerical values given in Fig. 6.2 for $b = 0.5A$ are recovered.

Figures 6.38 and 6.39 show variation of $\overline{k}_{2b}$ with b/A when $a = 0.5A$. In Fig. 6.38, results are shown for $v = 0.3$, while $L = 0.5A$ in Fig. 6.39. As can be seen in these figures, $\overline{k}_{2b}$ increases as b/A increases until $b \cong 0.75A$ and then starts decreasing with further increase in b/A for relatively small values of L/A, $L/A < \sim 1$. For greater values of L/A, $\overline{k}_{2b}$ decreases monotonically as b/A

increases. In Fig. 6.40, variation of $\bar{k}_{2b}$ with ν is shown when $b = L = 0.5A$ for various a/A ratios. $\bar{k}_{2b}$ increases in negative direction as ν increases and/or a/A decreases. $\bar{k}_{2b}$ is positive for $a/A > 0.8$.

6.1.2 Semi-Infinite Cylinder Problem

When the rigid inclusion spreads out and $b \rightarrow A$, it turns out to be a rigid support fixing the infinite cylinder throughout its midplane at $z = 0$. The portion corresponding to $z \geq 0$ becomes a semi-infinite cylinder bonded to a rigid support at its short end $(z = 0)$.

6.1.2.1 Semi-Infinite Cylinder

Consider the problem shown in Fig. 4.4. In this case, Eqs. (4.31) and (4.32) must be solved for $\bar{\bar{H}}(\eta)$. Figures 6.41 and 6.42 show the normal stress $\sigma_z(r,0)$ distribution at the rigid support for $\nu = 0.25$ and 0.5, respectively. In Fig. 6.41; results given by Benthem and Minderhoud (1972) and Gupta (1974), in Fig. 6.42; results given by Gupta (1974) and Agarwal (1978) are also plotted for comparison. In Fig. 6.41, perfect agreement with Benthem and Minderhoud (1972) is observed for $\nu = 0.25$. Results given by Gupta (1974) differ a little from those of the present study and Benthem and Minderhoud (1972) at points close to the edge $(r/A \rightarrow 1)$. In Fig. 6.42, perfect agreement with Agarwal (1978) is observed for $\nu = 0.5$. Results given by Gupta (1974) differ considerably from those of the present study and Agarwal (1978) as $r/A \rightarrow 1$.

Figures 6.43 and 6.44 show the shearing stress $\tau_{rz}(r,0)$ distribution at the rigid support for $\nu = 0.25$ and 0.5, respectively. One can make observations similar to Figs. 6.41 and 6.42: Perfect agreement with Benthem and Minderhoud (1972) and Agarwal (1978), whereas Gupta (1974) differs by some amount from all. Note in Figs. 6.41-6.44 that σ_z and τ_{rz} tend to infinity as $r \rightarrow A$. Therefore, the stress

state at the edge of the rigid support is described by the stress intensity factors defined in Eqs. (5.23).

Figures 6.45 and 6.46 show the normalized Mode I and Mode II stress intensity factors $\bar{k}_{1A}$ and $\bar{k}_{2A}$, respectively, at the edge of the rigid support defined by Eqs. (5.30) and (5.31). $\bar{k}_{1A}$ decreases with increasing ν. In Fig. 6.46, results taken from Gupta (1974) are also shown for comparison. For relatively large values of ν there is ~10% difference. Normalized Mode II stress intensity factor $\bar{k}_{2A}$ is negative and its magnitude increases with increasing ν.

6.1.2.2 Semi-Infinite Cylinder with a Transverse Penny-Shaped Crack

Consider the problem shown in Fig. 4.3. In this case, Eqs. (4.27) and (4.30) must be solved for $\bar{\bar{F}}(\phi)$, $\bar{\bar{G}}(\phi)$ and $\bar{\bar{H}}(\eta)$. Figures 6.47-6.52 show the normal stress $\sigma_z(r,0)$ and the shearing stress $\tau_{rz}(r,0)$ distributions at the rigid support for various combinations of ν, L/A and a/A. When the crack is close to the rigid support, the stress distributions are very complicated and the axial stress $\sigma_z(r,0)$ assumes very small values around the center. This variation is also valid for relatively large crack radii. As L/A increases, stress distributions become smoother. When $L/A \rightarrow \infty$, the effect of the crack disappears and the results for a semi-infinite cylinder without crack (Figs. 6.42 and 6.44) are recovered. Figures 6.49 and 6.52 show the normalized axial and shear stresses, $\sigma_z(r,0)$ and $\tau_{rz}(r,0)$, along the rigid support when $a = 0.5A$ and $L = A$. These stresses tend to $+\infty$ and $-\infty$, respectively as $r/A \rightarrow 1$. Stress distributions become smoother as ν decreases.

Figures 6.53-6.58 show the normalized Mode I and Mode II stress intensity factors, $\bar{k}_{1A}$ and $\bar{k}_{2A}$, at the edge of the rigid support. As can be realized from these figures, both $\bar{k}_{1A}$ and $\bar{k}_{2A}$ decrease with increasing L/A except for

relatively small values of $L/A < \sim 0.25$; $\overline{k}_{1A}$ decreases whereas $\overline{k}_{2A}$ increases with increasing ν. Note that, Figs. 6.53 and 6.56 have the same characteristic distribution since $\nu = 0.3$ is fixed. From Eqs. (5.30) and (5.31), it can be noticed that the ratio

$$\frac{\overline{k}_{2A}}{\overline{k}_{1A}} = \frac{(\kappa+1)\sin(\pi\gamma)}{\left\{(\kappa-1)\left[\cos(\pi\gamma)+1\right]+2(\kappa+1)(\gamma-1)-4(\gamma-1)^2\right\}} \qquad (6.5)$$

has a constant value for a fixed value of ν. Variation of $\overline{k}_{1A}$ and $\overline{k}_{2A}$ is relatively small for small cracks when $\nu = 0.3$. There is extensive variation for large cracks if the crack is close to the rigid support (Figs. 6.53 and 6.56). Figures 6.54 and 6.57 show variations of $\overline{k}_{1A}$ and $\overline{k}_{2A}$ with a/A when $L = A$. It seems that the crack is sufficiently far from the rigid support and the interaction is little and $\overline{k}_{1A}$, $\overline{k}_{2A}$ do not vary much with a/A. When the crack radius a is close to zero, it may be said that there is no crack in semi-infinite cylinder. Values of $\overline{k}_{1A}$ and $\overline{k}_{2A}$ with no crack (Figs. 6.45 and 6.46) are reproduced here for $a = 0$.

Figures 6.55 and 6.58 show variations of $\overline{k}_{1A}$ and $\overline{k}_{2A}$ with L/A when $a = 0.5A$ for several values of ν. $\overline{k}_{1A}$ and $\overline{k}_{2A}$ first increase with increasing L/A, experience maximum values around $L \cong 0.25A$, then decrease and reach stationary values after $L \cong 2A$. These stationary values are again those values with no crack.

Figures 6.59-6.63 show variation of normalized Mode I stress intensity factor $\overline{k}_{1a}$ at the edge of the crack in a semi-infinite cylinder. In Figs. 6.59 and 6.60, variation of $\overline{k}_{1a}$ with a/A is shown when $L = A$ and $\nu = 0.3$, respectively. $\overline{k}_{1a}$ increases significantly for $a/A > 0.9$. Figure 6.61 shows variation of $\overline{k}_{1a}$ with L/A when $a = 0.5A$. Similar to the behavior in Fig. 6.22, $\overline{k}_{1a}$ first increases with increasing L/A, experiences a maximum around $L \cong A$, then decreases and finally becomes

stationary with further increase in L/A ($L/A > \sim 2A$). In Figs. 6.62 and 6.63, variation of $\bar{k}_{1a}$ with ν is given when $L=A$ and $a=0.5A$, respectively. As expected, no significant variation with ν is observed.

Figures 6.64-6.67 show variation of normalized Mode II stress intensity factor $\bar{k}_{2a}$ at the edge of the cracks in a semi-infinite cylinder. In Figs. 6.64 and 6.65, variation of $\bar{k}_{2a}$ with a/A is shown when $L=A$ and $\nu=0.3$, respectively. As can be seen in Fig. 6.65, $\bar{k}_{2a}$ increases with increasing a/A and tends to infinity as $a/A \rightarrow 1$. This effect is more pronounced as the crack gets closer to the rigid support. Figure 6.66 shows variation of $\bar{k}_{2a}$ with L/A when $a=0.5A$. It may be noted that $\bar{k}_{2a}$ decreases with increasing L/A and tends to zero for $L/A > \sim 2$.

Figures 6.68 and 6.69 show the dimensionless strain energy release rate $\bar{w}$ and the probable cleavage angle θ, respectively, for the crack at $z=L$ plane when $\nu=0.3$. As can be seen in Fig. 6.69, crack tends to propagate away from the high stress domain around the edge of the rigid support at $z=0$ plane.

6.1.3 Finite Cylinder Problem

When the crack in the semi-infinite cylinder problem spreads out and $a \rightarrow A$, the cylinder is completely broken at $z=L$ and the portion of the cylinder between $z=0$ and $z=L$ planes becomes a finite cylinder whose one end at $z=0$ is fixed and the other end at $z=L$ is subject to uniformly distributed axial tension of intensity p_0. For this problem, Eqs. (4.34), (4.36) and (4.40) must be solved for $\bar{\bar{F}}(\phi)$, $\bar{\bar{G}}(\phi)$, $\bar{\bar{H}}(\eta)$.

Figures 6.70-6.85 show calculated results of the finite cylinder problem for various aspect ratios, L/A, and material properties represented by ν. Figures 6.70-6.75 show the normalized axial stress $\sigma_z(r,0)/p_0$ along the rigid support for various

aspect ratios, L/A and Poisson's ratio ν. When $\nu = 0$, the effect of the rigid support vanishes. Therefore, axial stress $\sigma_z(r,0)/p_0$ distribution becomes uniform (Fig. 6.73). In Figs. 6.70, 6.71 and 6.72, $\nu = 0.1$, 0.3 and 0.5, respectively. In Figs. 6.73, 6.74 and 6.75, $L = 0.25A$, $0.5A$ and A, respectively. Figures 6.76-6.81 show the normalized shearing stress $\tau_{rz}(r,0)/p_0$ along the rigid support for various aspect ratios, L/A, and ν. Larger shearing stresses develop along the rigid support for larger values of ν and/or larger values of L/A in general. $\sigma_z(r,0)$ and $\tau_{rz}(r,0)$ tend to $\pm\infty$ as $r/A \to 1$. Therefore, the stress state around the rigid support can be represented by the stress intensity factors.

Figures 6.82-6.85 show the normalized Mode I and Mode II stress intensity factors $\overline{k}_{1A}$ and $\overline{k}_{2A}$ around the rigid support. In Figs. 6.82 and 6.83, variations of $\overline{k}_{1A}$ with L/A and ν are shown. $\overline{k}_{1A}$ increases as L/A increases and then becomes stationary for $L > {\sim}1.5A$ for fixed values of ν. As may be seen in Fig. 6.83, $\overline{k}_{1A}$ decreases with increasing ν for a fixed aspect ratio L/A.

Figures 6.84 and 6.85 show variations of $\overline{k}_{2A}$ with L/A and ν, respectively. Having smaller numerical values, $\overline{k}_{2A}$ exhibits similar variation with L/A as $\overline{k}_{1A}$ for fixed values of ν. However, it increases with increasing ν for a fixed aspect ratio L/A.

6.2 Conclusions

This work is on the analysis of a cracked semi-infinite cylinder and a finite cylinder with free lateral surface. One end of the cylinder is bonded to a fixed support while the other end is subject to axial tension. The material of the cylinder is assumed to be linearly elastic and isotropic.

The solution of the finite cylinder problem of length L is obtained from the solution for a semi-infinite cylinder of radius A which contains a concentric

penny-shaped crack of radius a located at $z = L$. When the crack approaches the surface of the cylinder, the problem for the region between the rigid support and the crack becomes identical with the finite cylinder problem. Furthermore, the solution for this semi-infinite cylinder is obtained by considering the axisymmetric infinite cylinder problem. The infinite cylinder of radius A contains two concentric penny-shaped cracks of radius a at $z = \pm L$ planes and a concentric penny-shaped rigid inclusion of radius b at $z = 0$ plane. In the limiting case when the rigid penny-shaped inclusion approaches the surface of the infinite cylinder when $b \to A$, the infinite cylinder problem turns out to be the semi-infinite cylinder problem having a penny-shaped crack at $z = L$ plane.

The formulation of the infinite cylinder problem is obtained by the superposition of solutions for the following two subproblems: (I) Uniform problem; an infinite cylinder subjected to arbitrary symmetric loads with no cracks or inclusion, (II) Perturbation problem; an infinite cylinder containing two concentric penny-shaped cracks of radius a at $z = \pm L$ planes and a concentric penny-shaped rigid inclusion of radius b at $z = 0$ plane with no load at infinity.

General solution for the perturbation problem is obtained by adding the expressions for three sub-problems: (II-i) An axisymmetric infinite elastic medium containing two concentric penny-shaped cracks of radius a at $z = \pm L$ planes, (II-ii) An axisymmetric infinite elastic medium containing a concentric penny-shaped rigid inclusion of radius b at $z = 0$ plane, (II-iii) An axisymmetric infinite elastic medium with no cracks or inclusion.

General expressions for the displacement and stress components for perturbation problem are obtained by solving Navier equations using Fourier and Hankel transform techniques. First, the boundary conditions at the surface of the infinite cylinder are satisfied. Then, by using the mixed boundary conditions on the cracks and the rigid inclusion, formulation of the problem is reduced to a system of three singular integral equations in terms of displacement derivatives on the cracks and shearing stress jump on the rigid inclusion. By using Gauss-Lobatto and Gauss-

Jacobi integration formulas, these three singular integral equations are converted to a system of linear algebraic equations which is solved numerically.

The normalized stress intensity factors $\bar{k}_{1a}$ and $\bar{k}_{2a}$ at the edge of the internal crack, $\bar{k}_{1b}$ and $\bar{k}_{2b}$ at the edge of an internal rigid inclusion, $\bar{k}_{1A}$ and $\bar{k}_{2A}$ at the edge of rigid support, the normalized axial stress $\sigma_z(r,0)/p_0$ and shearing stress $\tau_{rz}(r,0)/p_0$ at the rigid support are presented in graphical form in Figs. 6.1-6.85. From the formulation and the presented figures, following conclusions may be deduced:

1. Singularity at the edge of an internal crack is $1/2$.

2. Singularity at the edge of an internal rigid inclusion is also $1/2$.

3. Stresses at the corner of a 90° wedge with free-free sides are bounded.

4. Stresses at the corner of a 90° wedge with fixed-free sides are unbounded and the singularity power γ is given by

$$2\kappa\cos(\pi\gamma) = \kappa^2 + 1 - 4(\gamma-1)^2 \qquad (3.27)$$

5. Mode II stress intensity factor $\bar{k}_{2b}$ at the edge of an internal rigid inclusion in an infinite cylinder is negative and it increases with increasing ν.

6. Mode I and Mode II stress intensity factors $\bar{k}_{1a}$ and $\bar{k}_{2a}$ at the edges of two parallel penny-shaped cracks in an infinite cylinder are insensitive to ν (except when $a \to A$) but they increase as a/A increases and/or L/A decreases.

7. Stress distributions at the rigid support for the semi-infinite cylinder problem match very well with the results of Benthem and Minderhoud (1972) and Agarwal (1978). Results of Gupta (1974) differ (at the worst by ~10%) from Benthem and Minderhoud (1972), Agarwal (1978) and the present study.

8. There is considerable interaction between the crack and the rigid inclusion when ν is large and the crack is close to the support in the semi-infinite cylinder problem.

9. Mode II stress intensity factor $\bar{k}_{2A}$ is considerably small compared to Mode I stress intensity factor $\bar{k}_{1A}$ around the rigid support in semi-infinite and finite cylinder problems.

6.3 Suggestions for Further Studies

Cylindrical geometry is used frequently in many machine elements such as shafts, bolts, screws and rivets. Results and techniques used in this work can be applied in many engineering problems by considering various applications:

1. Two penny-shaped cracks may be replaced by edge cracks so that the problem of external notch in a semi-infinite cylinder is obtained.

2. Axial tension load may be replaced by torsion.

3. Thermal loads can be added to semi-infinite and finite cylinder problems.

4. By using four penny-shaped cracks, problem can be turned out to be finite cylinder problem containing transverse crack.

5. The material of the cylinder may be assumed to be composite.

The author is willing to study these problems in near future.

Table 6.1 Dimensionless SIF ratios $\dfrac{\overline{k}_{1a \text{ double cracks}}}{k_{1a \text{ single crack}}}$ when a cylinder is subjected to axial uniform loading for $\nu = 0.33$.

$\dfrac{L}{a}$	$\dfrac{a}{A}$					
	0.3		0.6		0.9	
	Tsang (2003) FEM	Present study	Tsang (2003) FEM	Present study	Tsang (2003) FEM	Present study
0.1	0.800	0.795	0.760	0.758	0.800	0.794
0.2	0.870	0.872	0.820	0.816	0.890	0.888
0.3	0.930	0.926	0.870	0.864	0.940	0.939
0.4	0.960	0.958	0.910	0.907	0.970	0.966
0.5	0.980	0.977	0.940	0.942	0.980	0.982
0.6	0.990	0.988	0.970	0.968	0.990	0.991
0.7	0.990	0.994	0.980	0.984	1.000	0.996
0.8	1.000	0.997	0.990	0.993	1.000	0.999
0.9	1.000	0.999	1.000	0.998	1.000	1.000
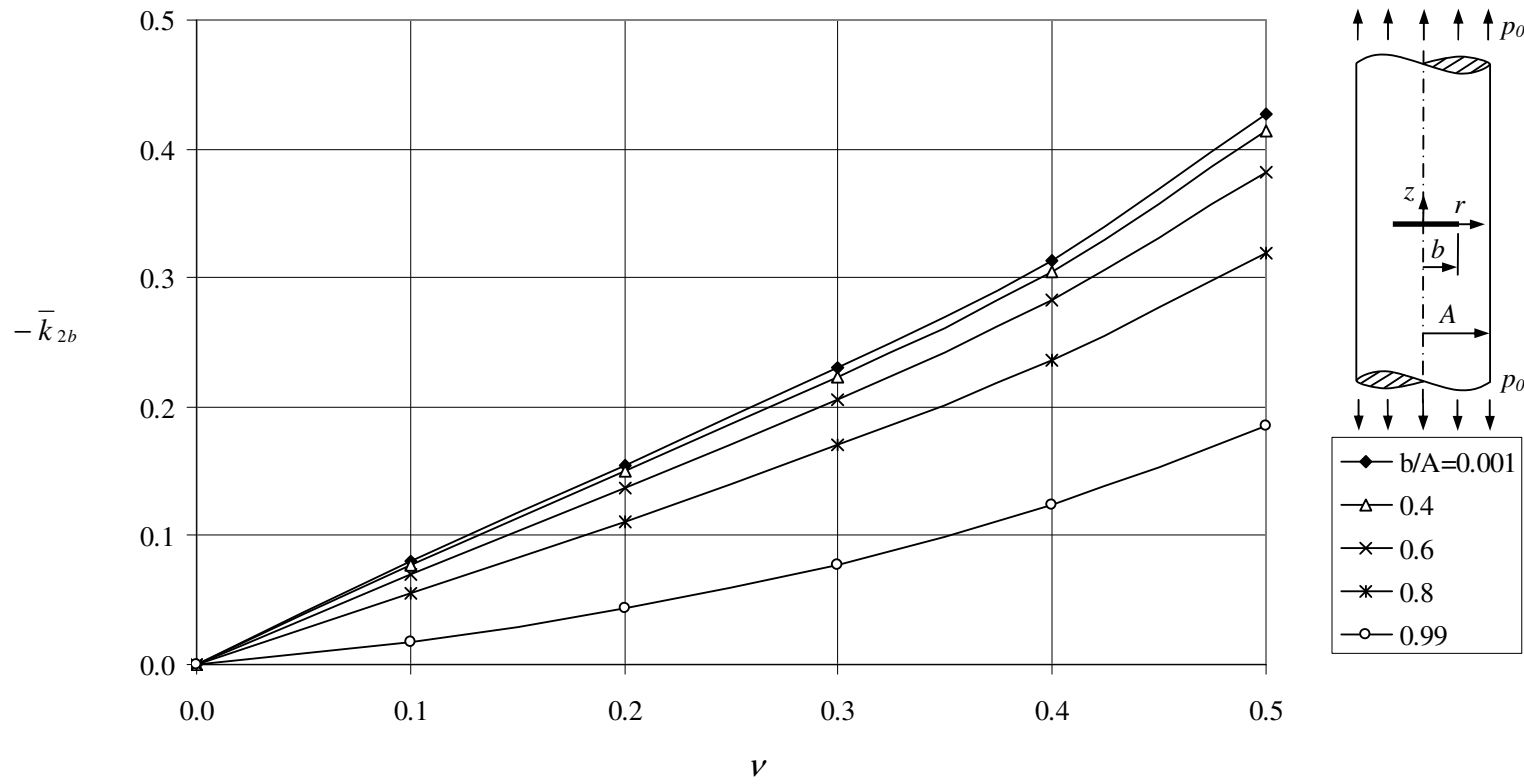
Figure 6.1 Normalized Mode II stress intensity factor $\overline{k}_{2b}$ at the inclusion edge.
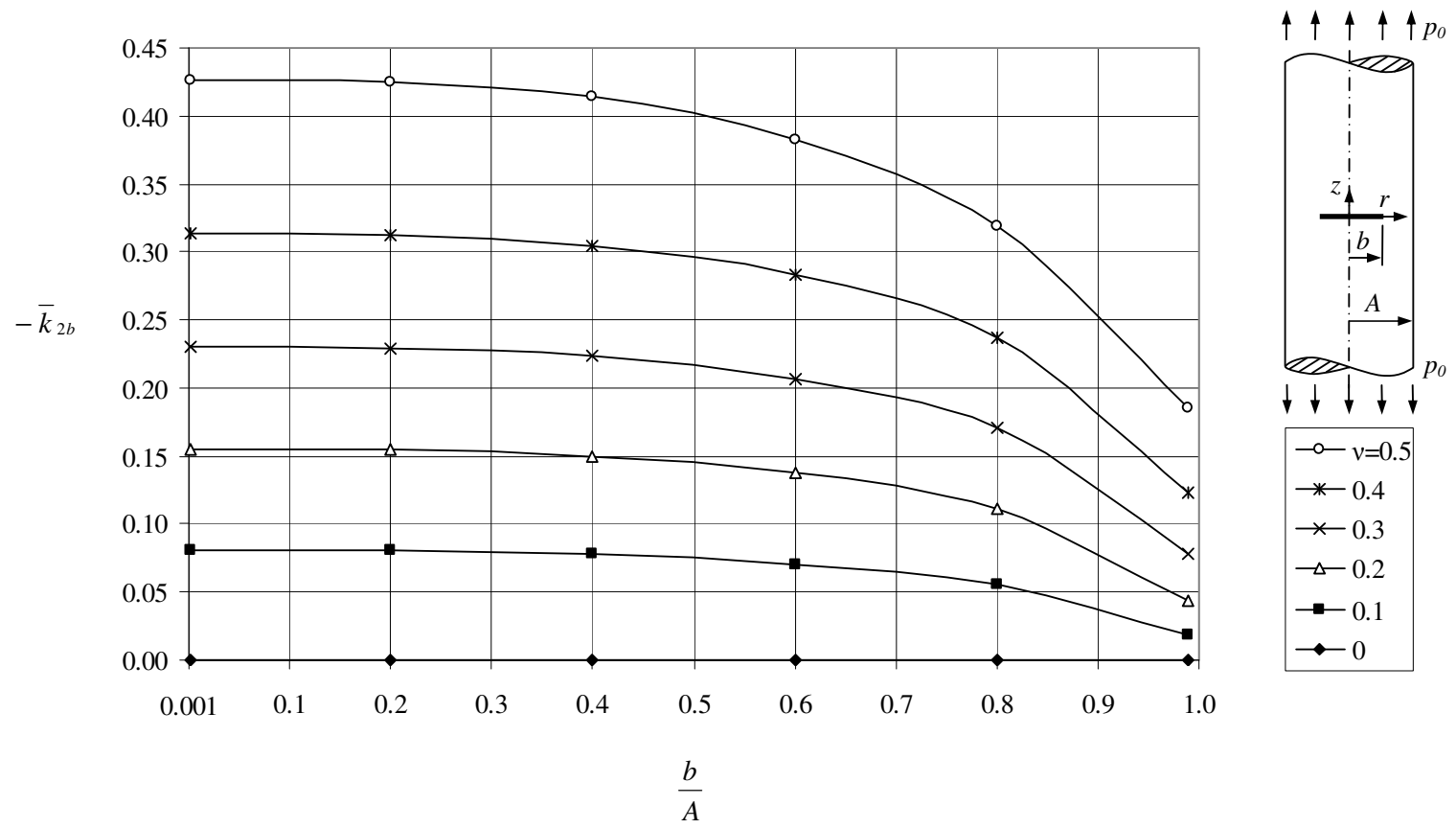
Figure 6.2 Normalized Mode II stress intensity factor $\overline{k}_{2b}$ at the inclusion edge.
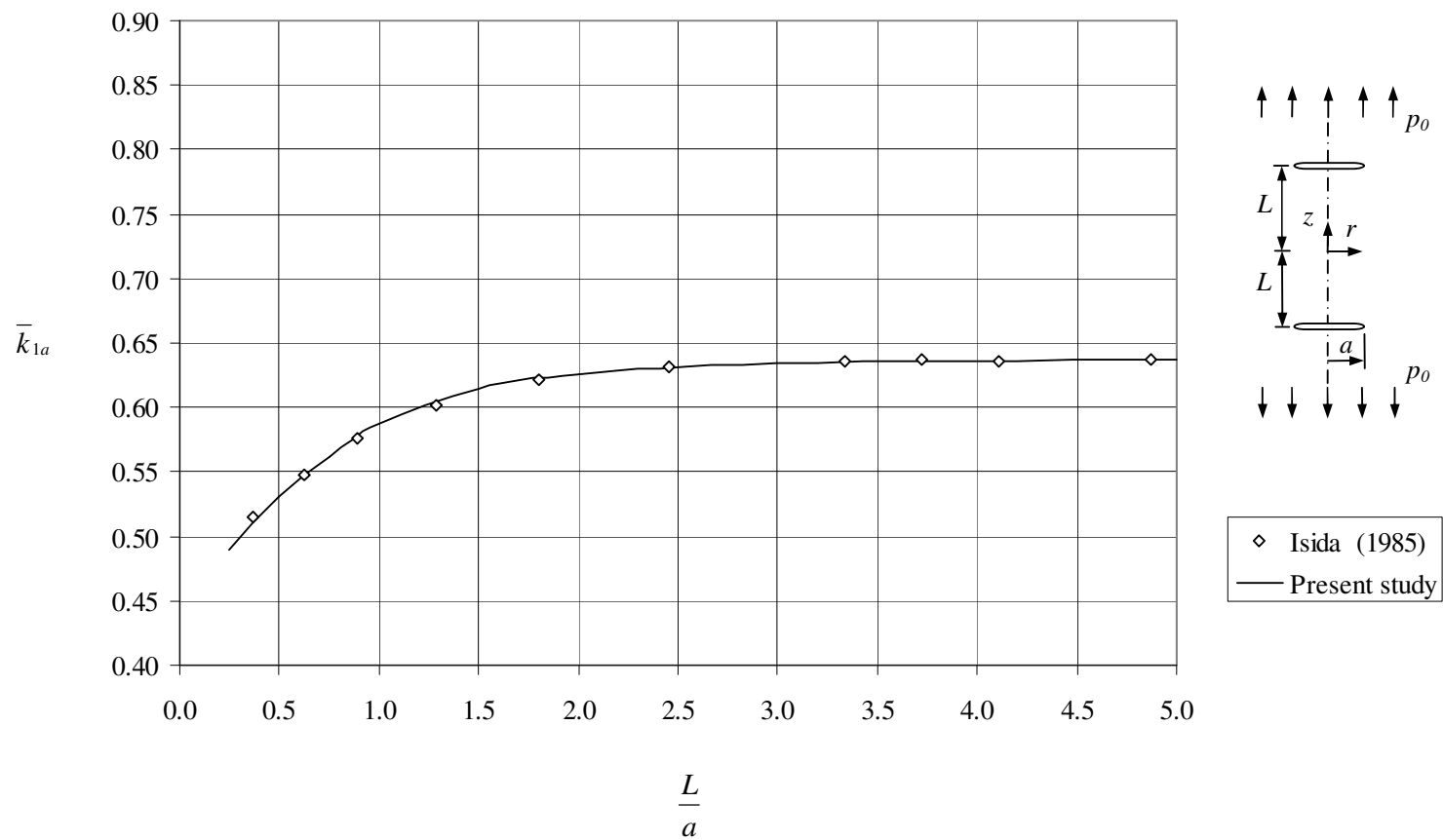
Figure 6.3 Normalized Mode I stress intensity factor $\overline{k}_{1a}$ at the edge of two parallel penny-shaped cracks in an infinite solid.
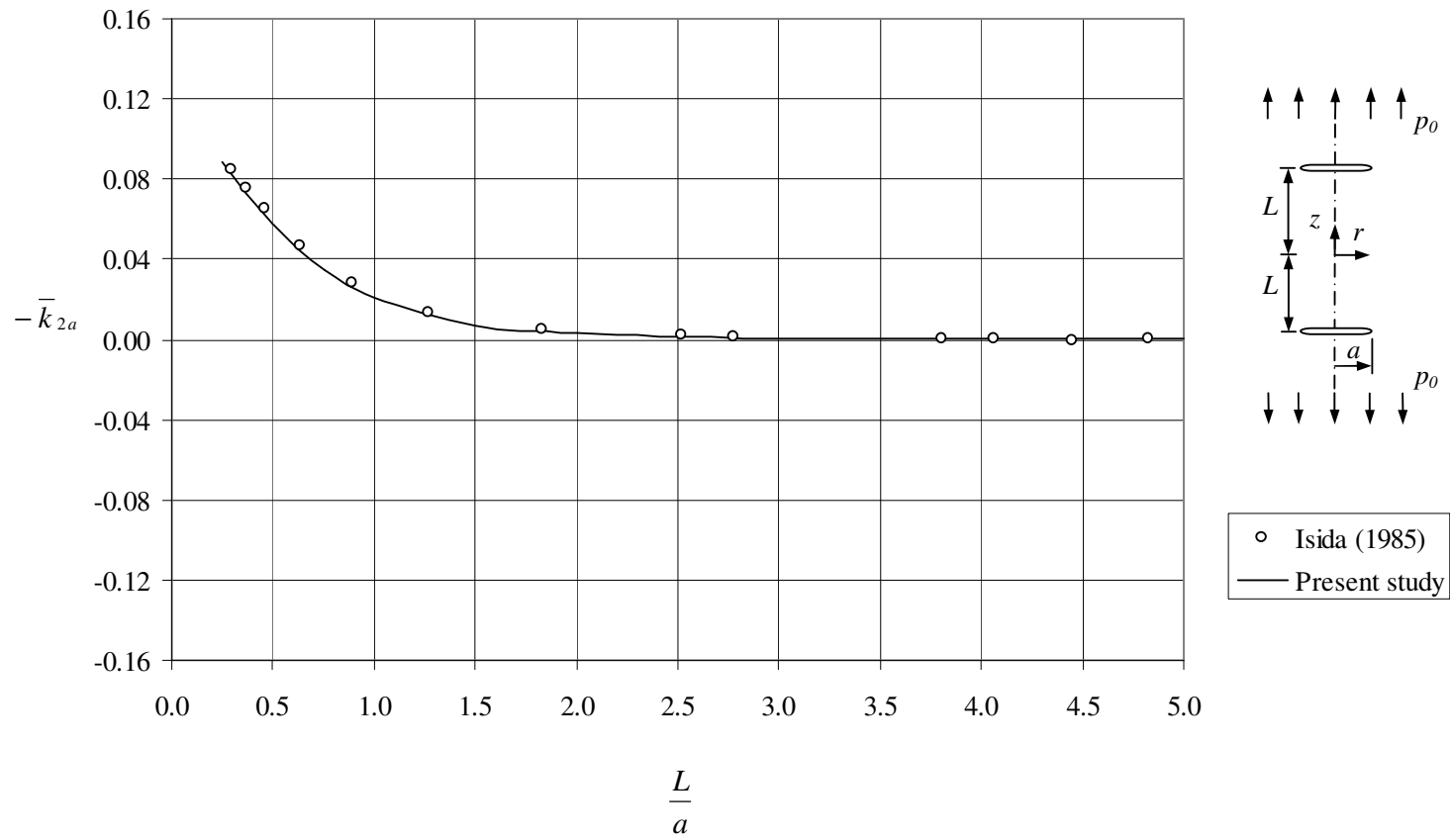
Figure 6.4 Normalized Mode II stress intensity factor $\overline{k}_{2a}$ at the edge of two parallel penny-shaped cracks in an infinite solid.
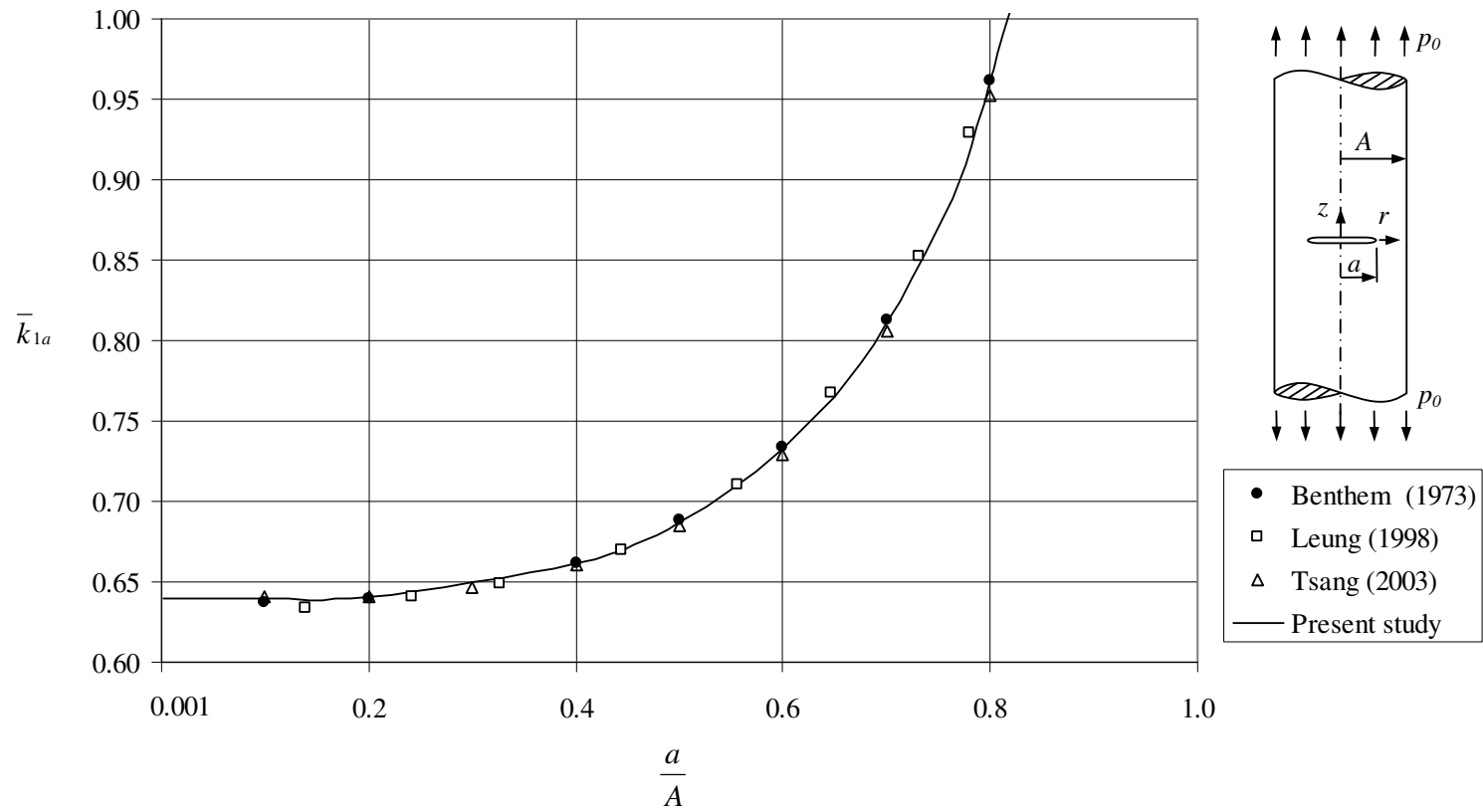
Figure 6.5 Normalized Mode I stress intensity factor $\overline{k}_{1a}$ at the edge of a single crack when $v = 0.3$.
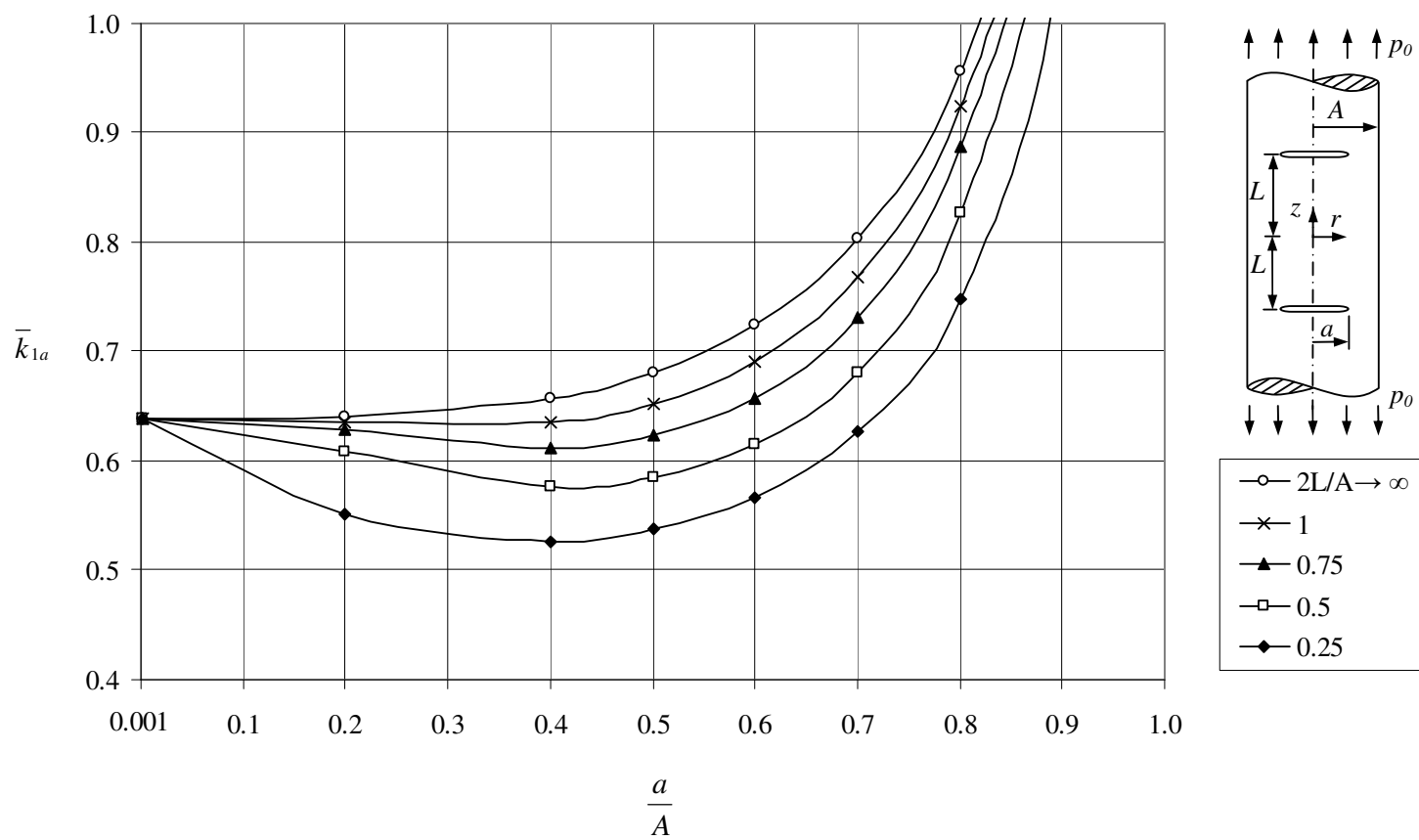
Figure 6.6 Normalized Mode I stress intensity factor $\bar{k}_{1a}$ at the crack edge when $v = 0.3$.
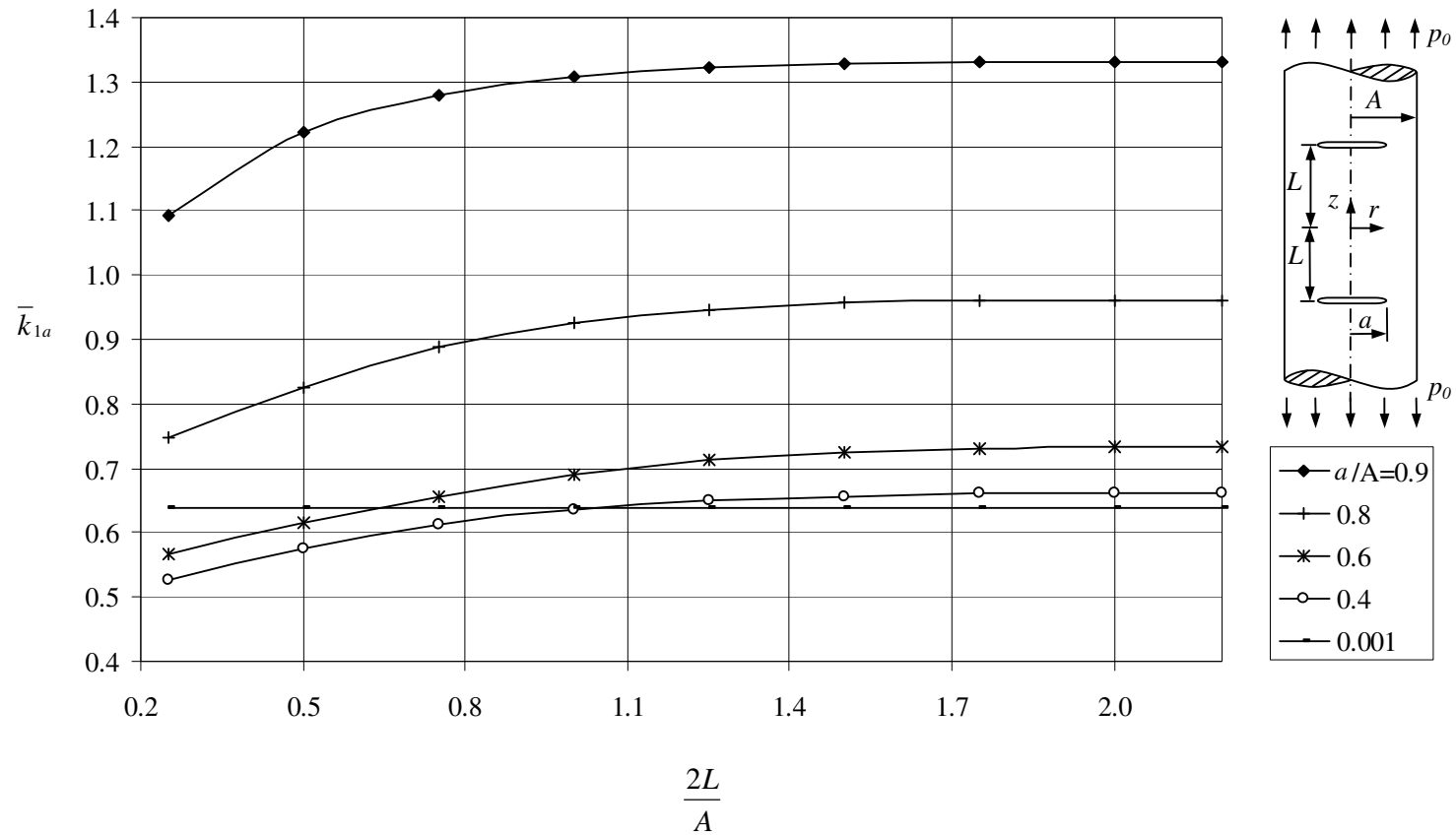
Figure 6.7 Normalized Mode I stress intensity factor $\overline{k}_{1a}$ at the crack edge when $v = 0.3$.
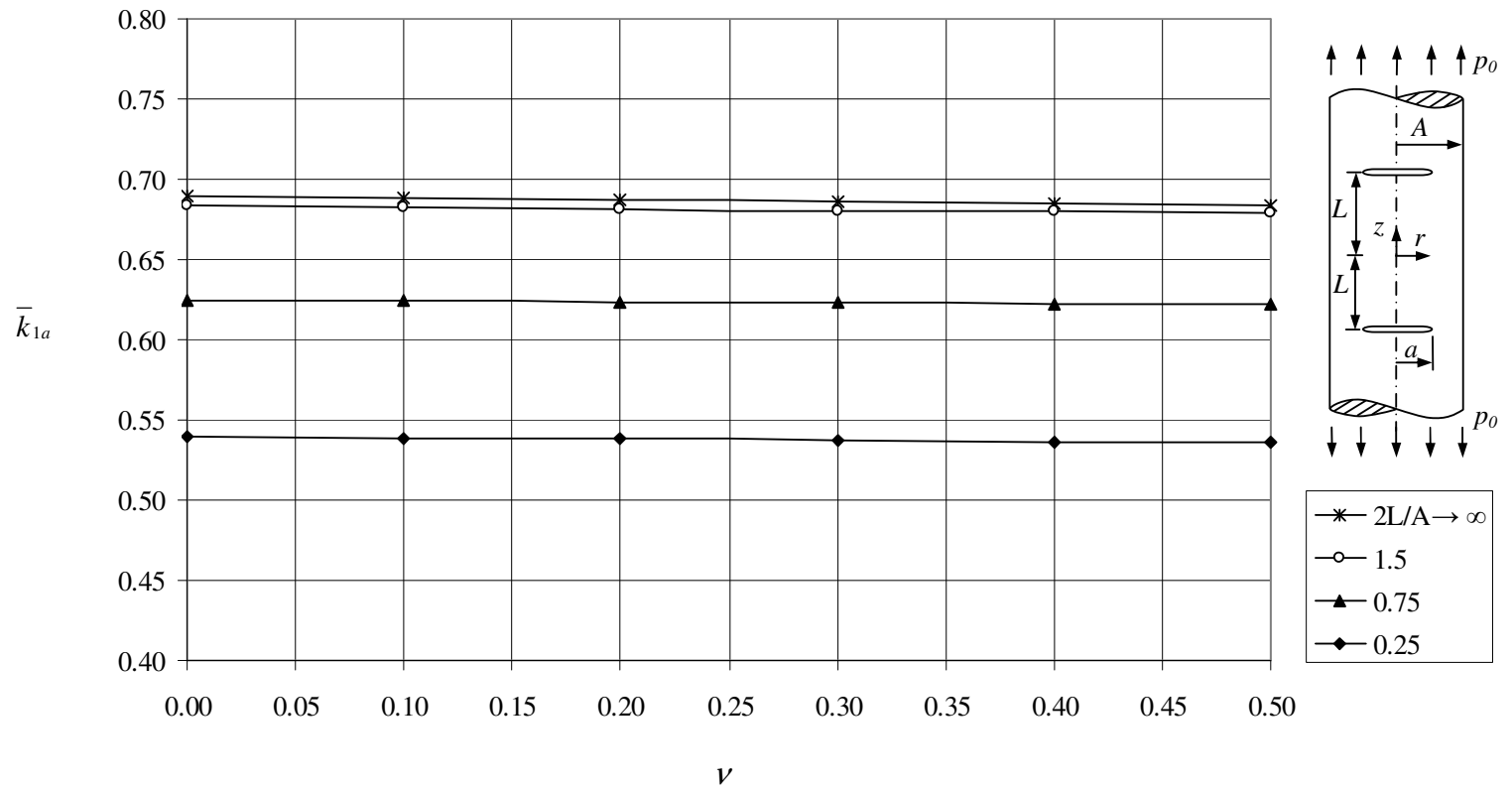
Figure 6.8 Normalized Mode I stress intensity factor $\overline{k}_{1a}$ at the crack edge when $a = 0.5A$.
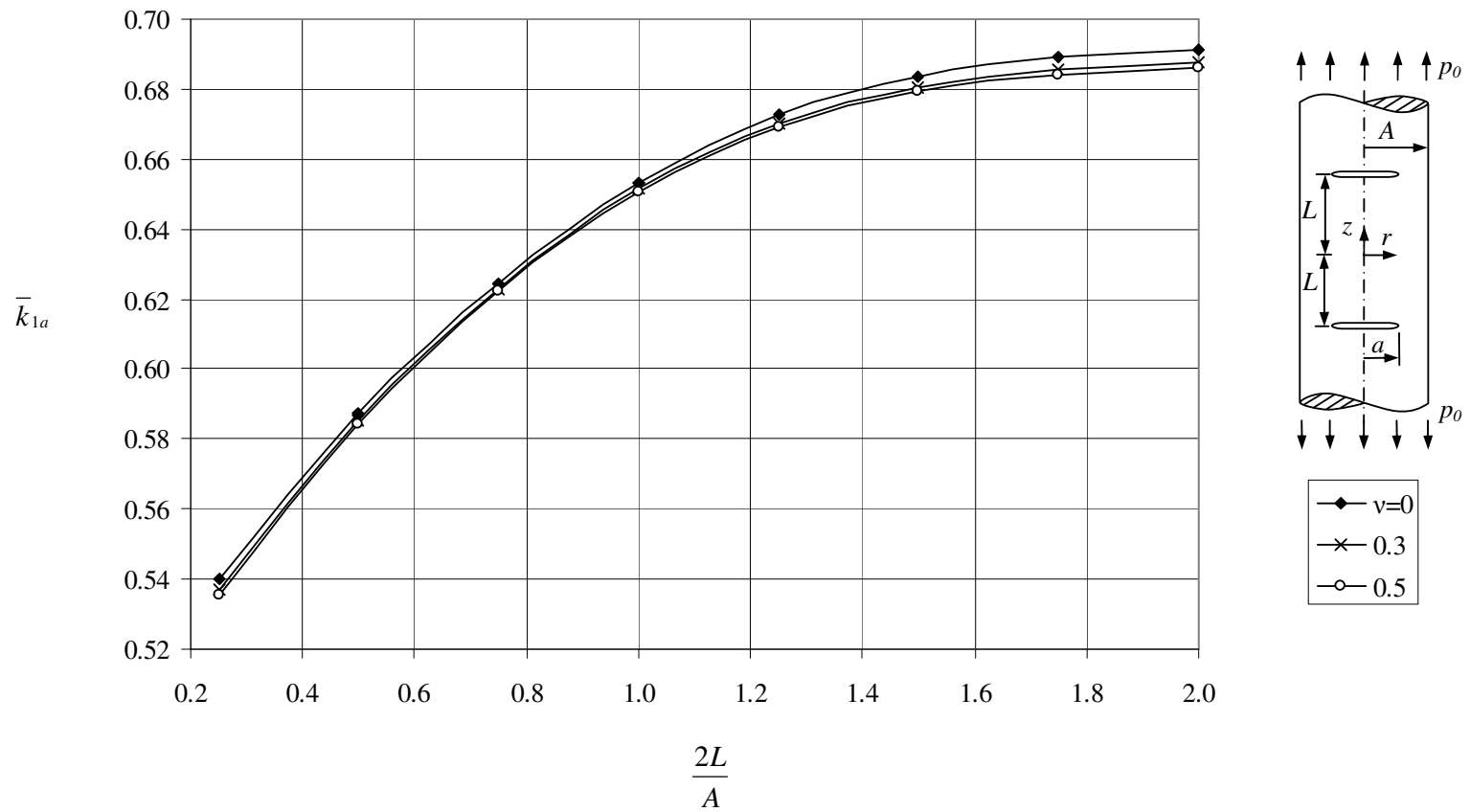
Figure 6.9 Normalized Mode I stress intensity factor $\bar{k}_{1a}$ at the crack edge when $a = 0.5A$.
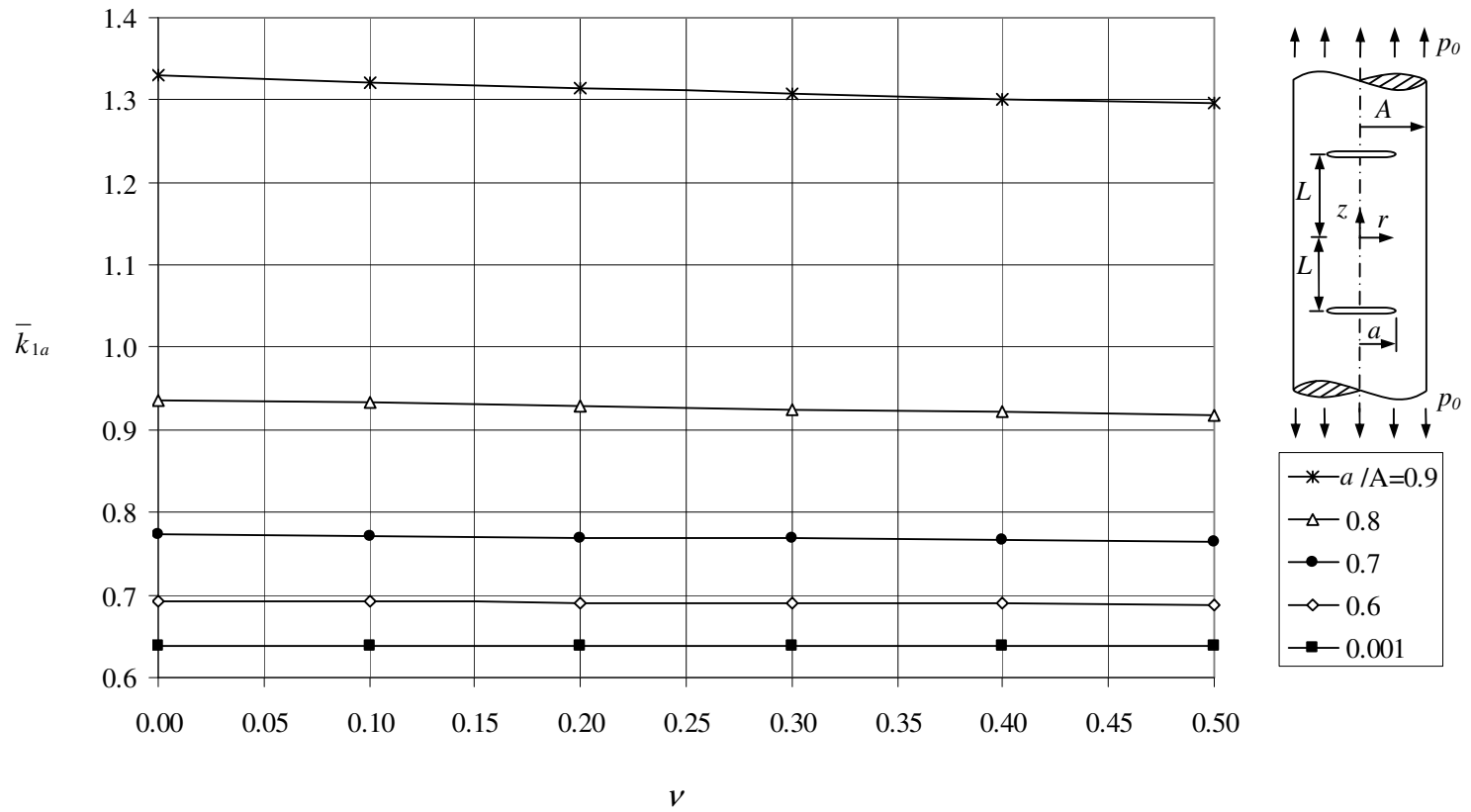
Figure 6.10 Normalized Mode I stress intensity factor $\overline{k}_{1a}$ at the crack edge when $2L = A$.
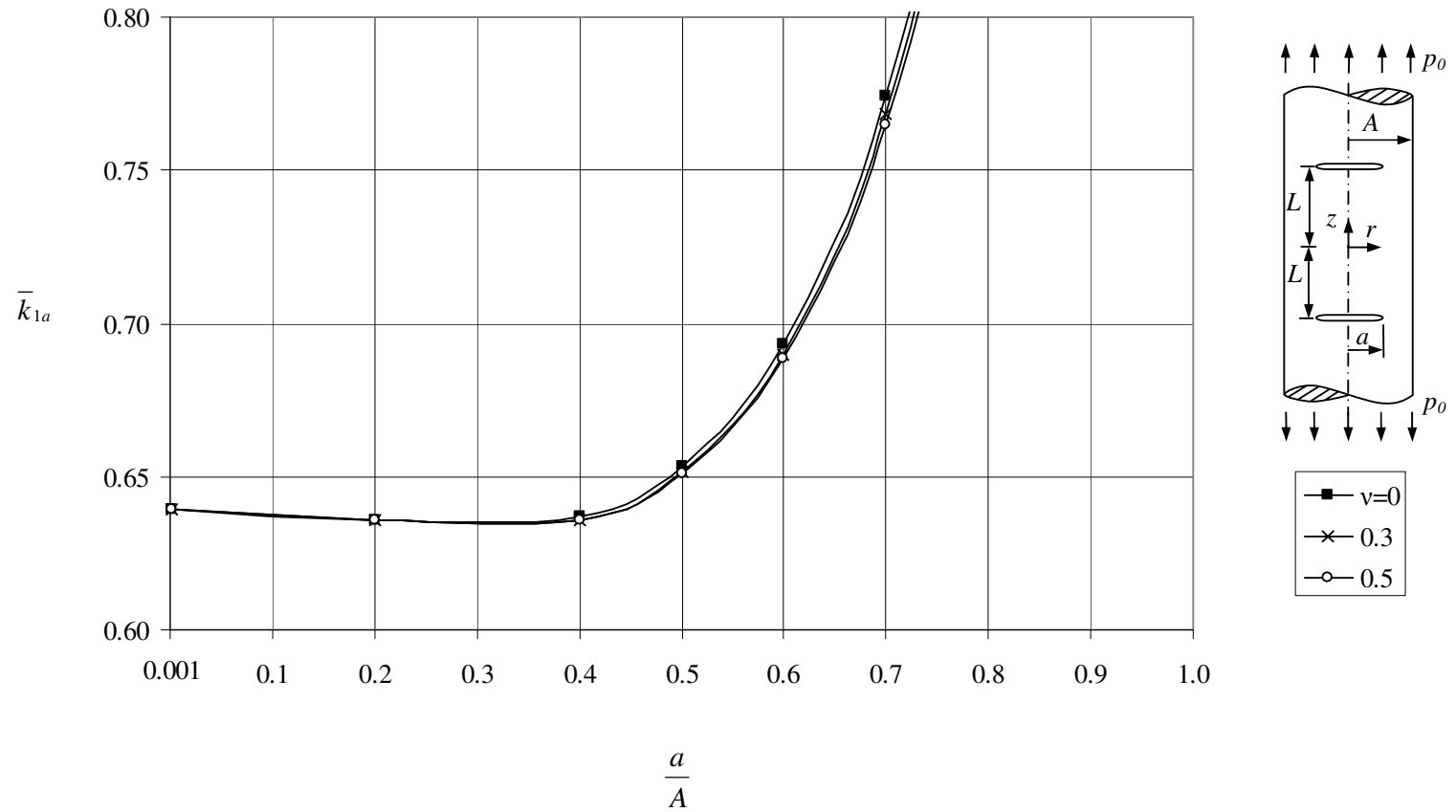
Figure 6.11 Normalized Mode I stress intensity factor $\bar{k}_{1a}$ at the crack edge when $2L = A$.
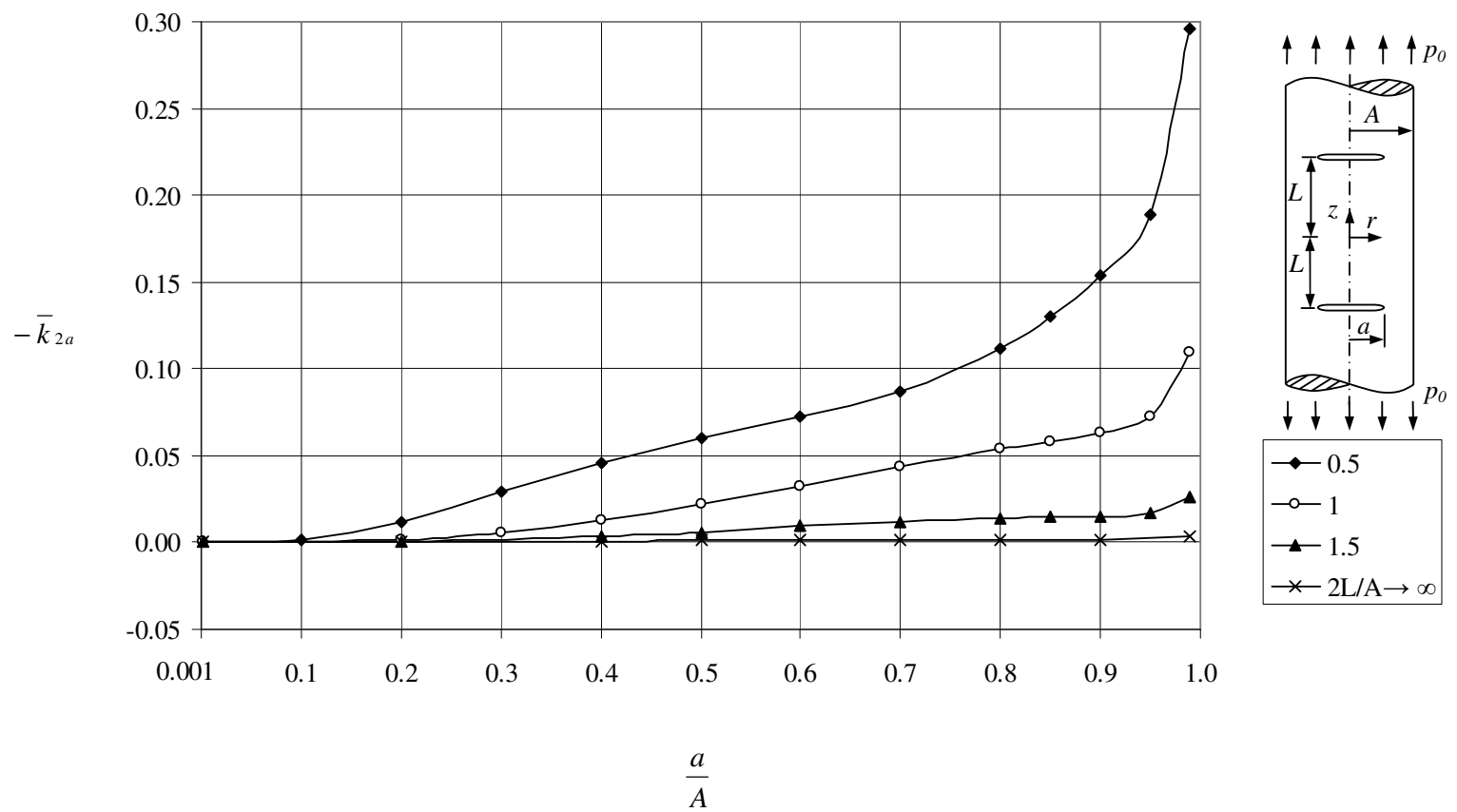
Figure 6.12 Normalized Mode II stress intensity factor $\overline{k}_{2a}$ at the crack edge when $v = 0.3$.
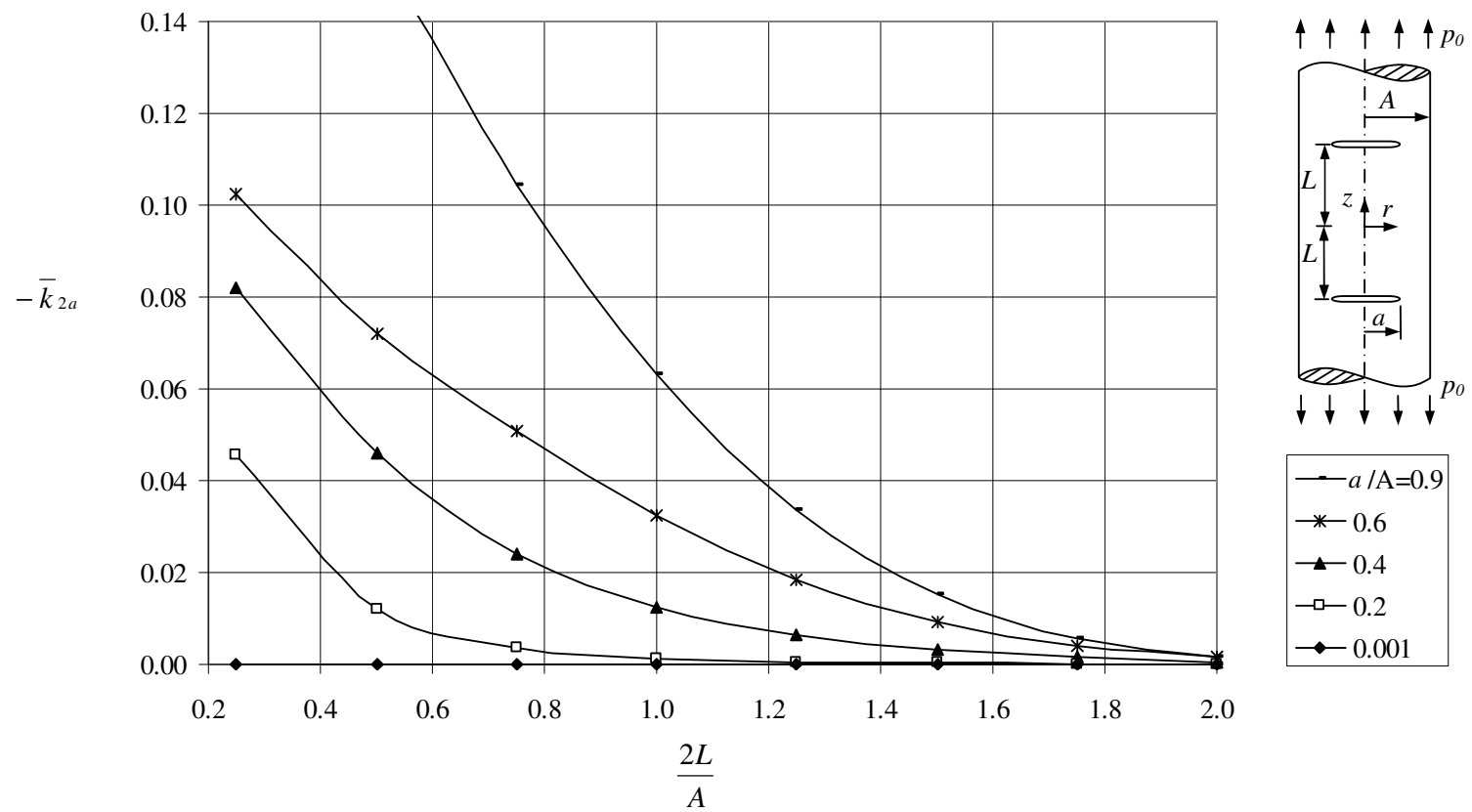
Figure 6.13 Normalized Mode II stress intensity factor $\overline{k}_{2a}$ at the crack edge when $v = 0.3$.
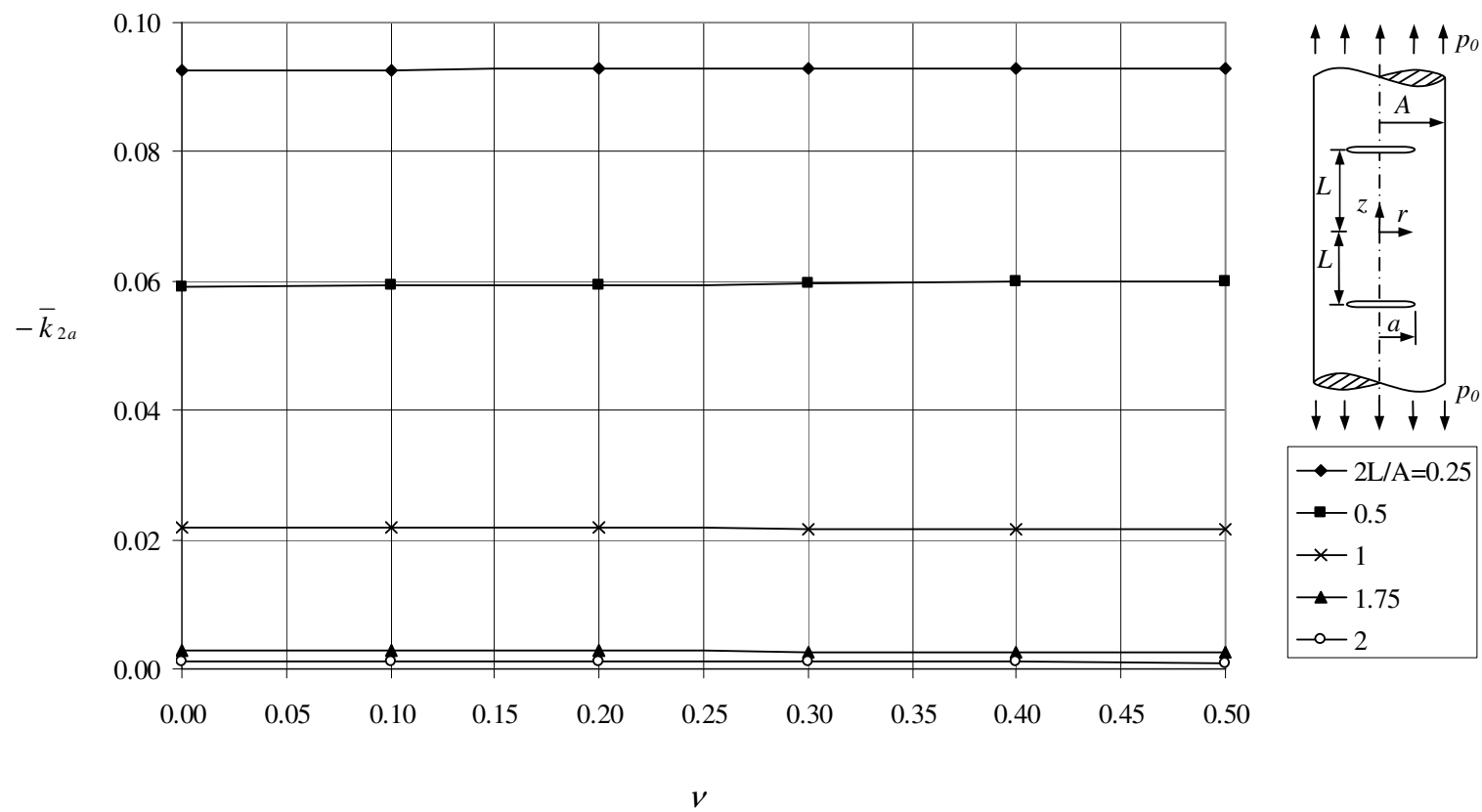
Figure 6.14 Normalized Mode II stress intensity factor $\overline{k}_{2a}$ at the crack edge when $a = 0.5A$.
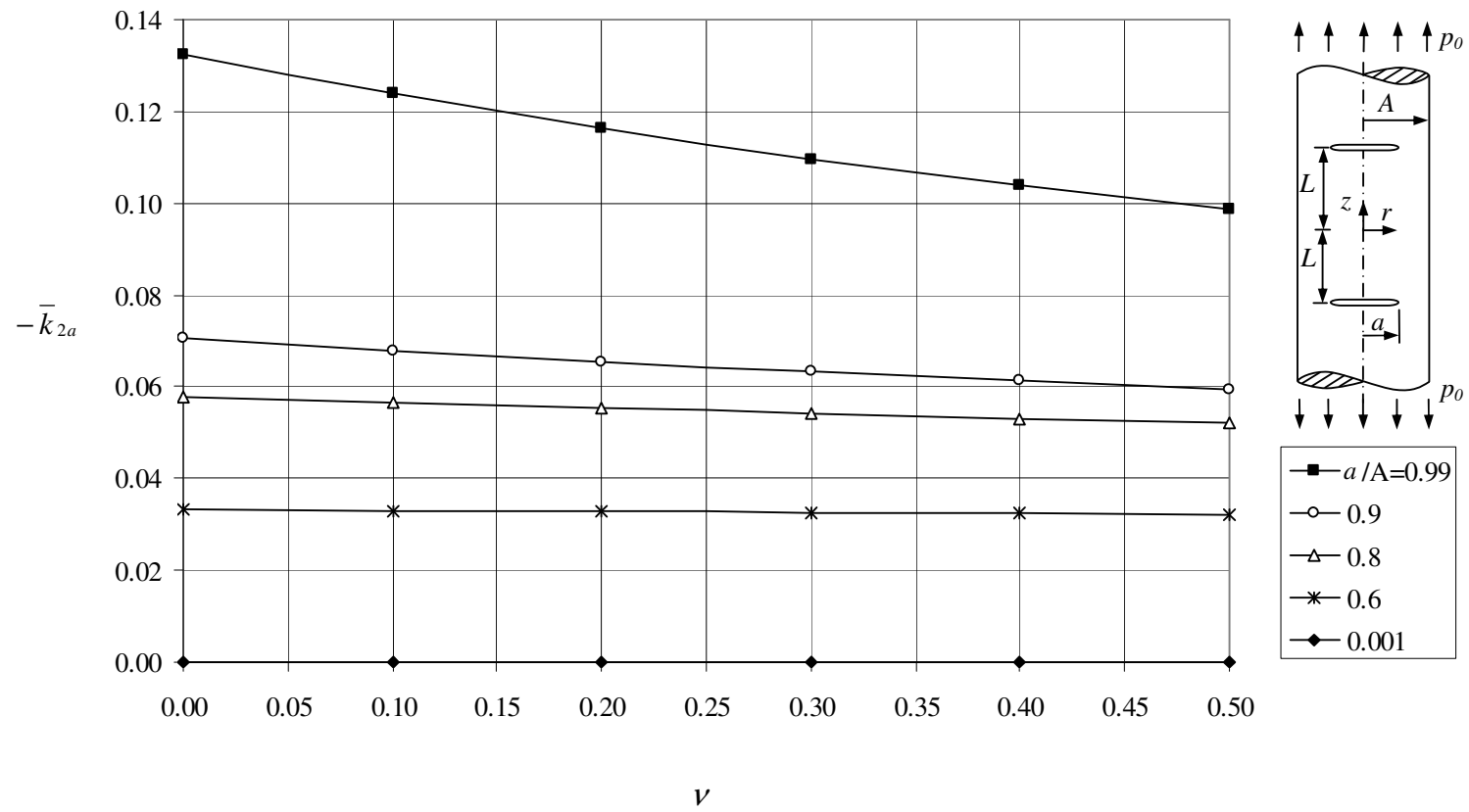
Figure 6.15 Normalized Mode II stress intensity factor $\overline{k}_{2a}$ at the crack edge when $2L = A$.
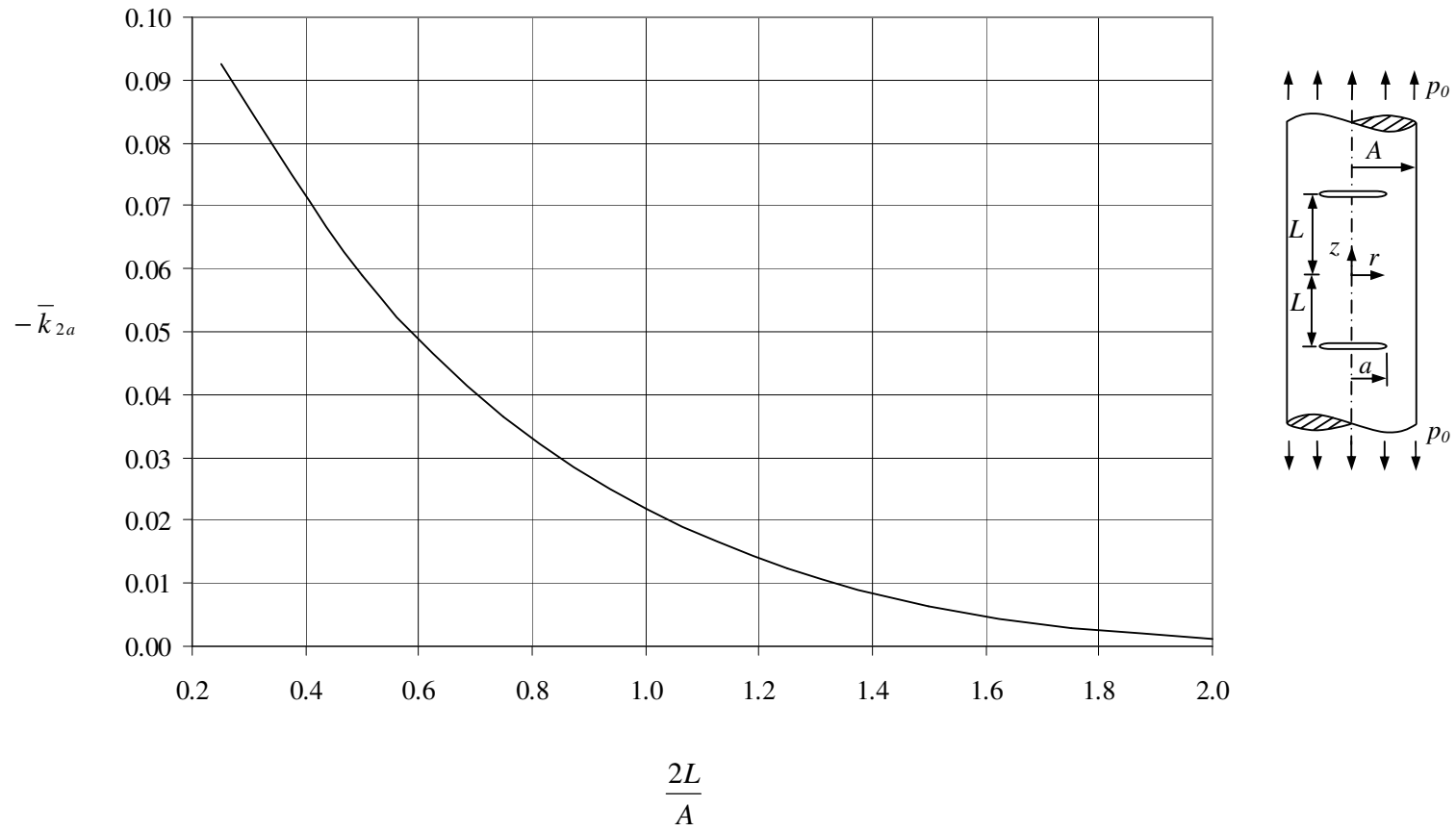
Figure 6.16 Normalized Mode II stress intensity factor $\overline{k}_{2a}$ at the crack edge when $a = 0.5A$, $0 \le \nu \le 0.5$.
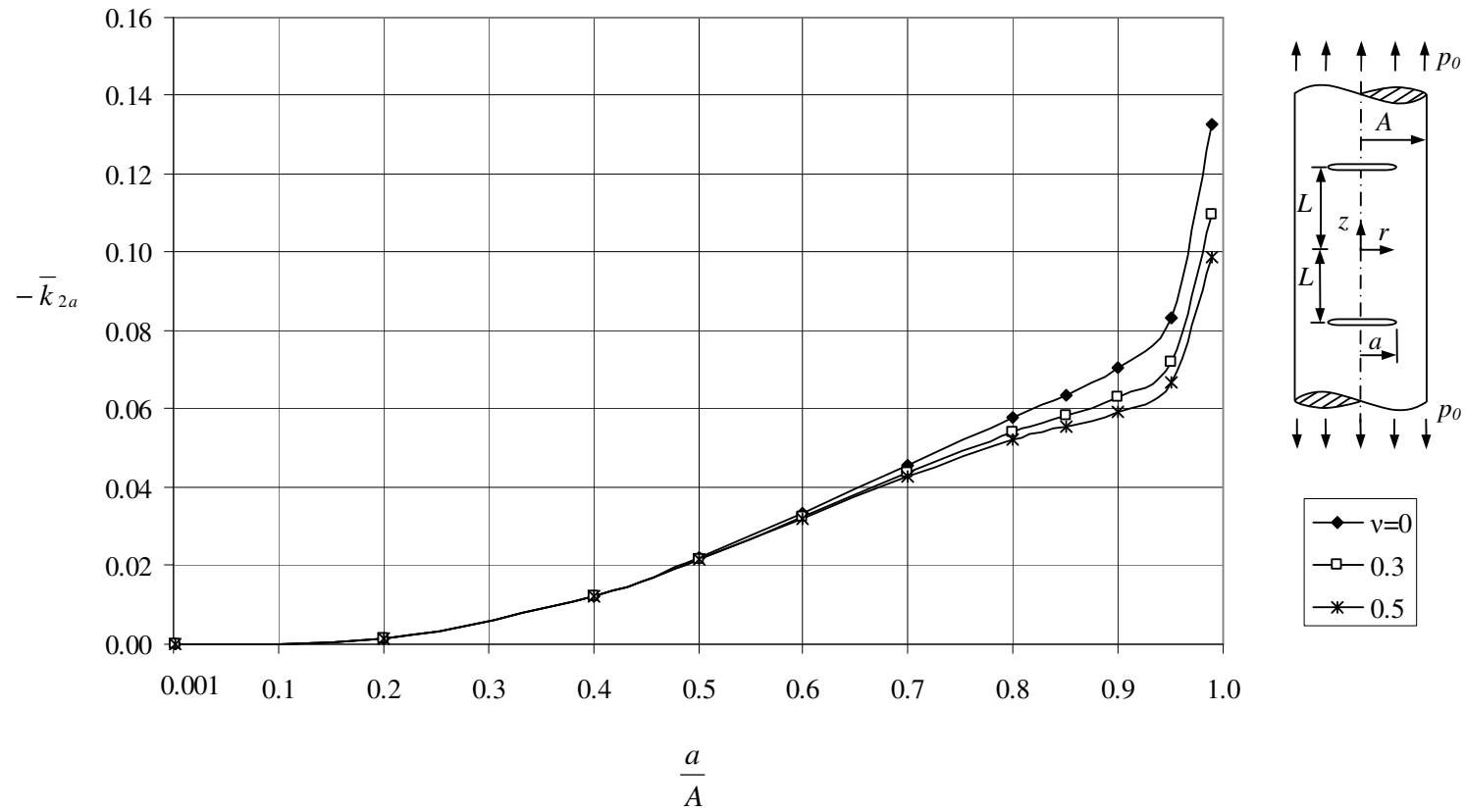
Figure 6.17 Normalized Mode II stress intensity factor $\overline{k}_{2a}$ at the crack edge when $2L = A$.
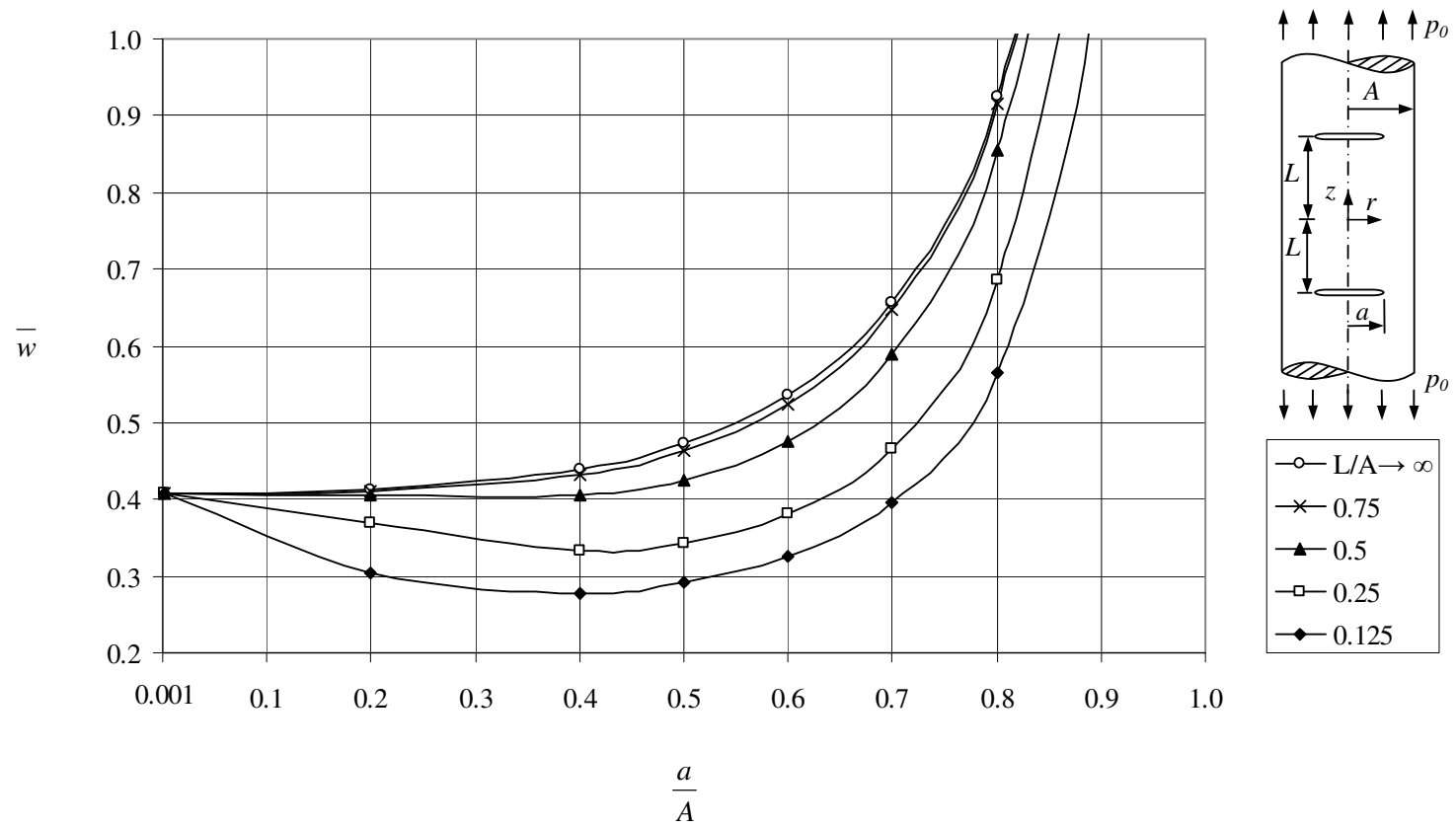
Figure 6.18 Normalized energy release rate $\bar{w}$ when $\nu = 0.3$.
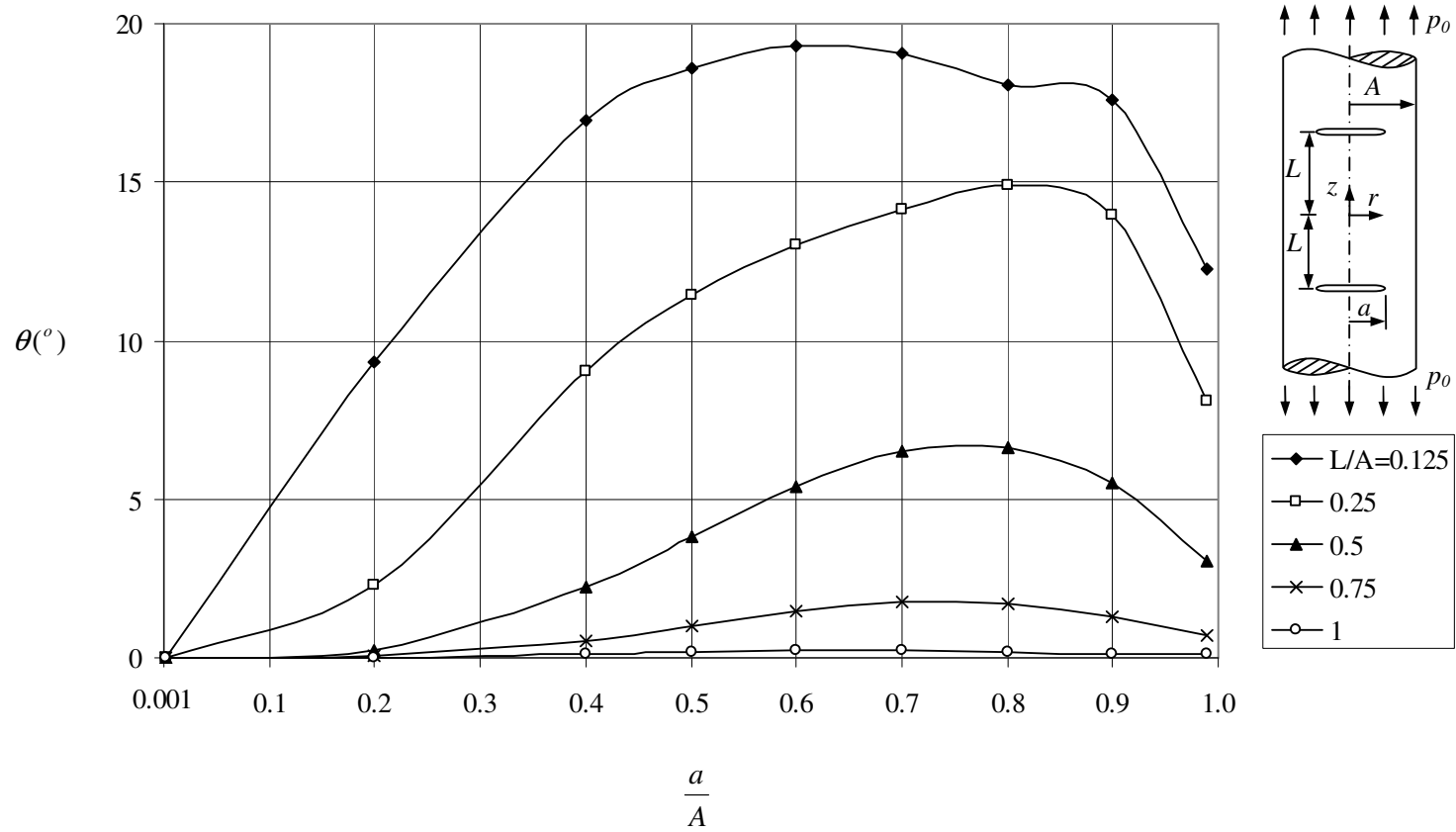
Figure 6.19 Probable crack propagation angle θ when $\nu = 0.3$.
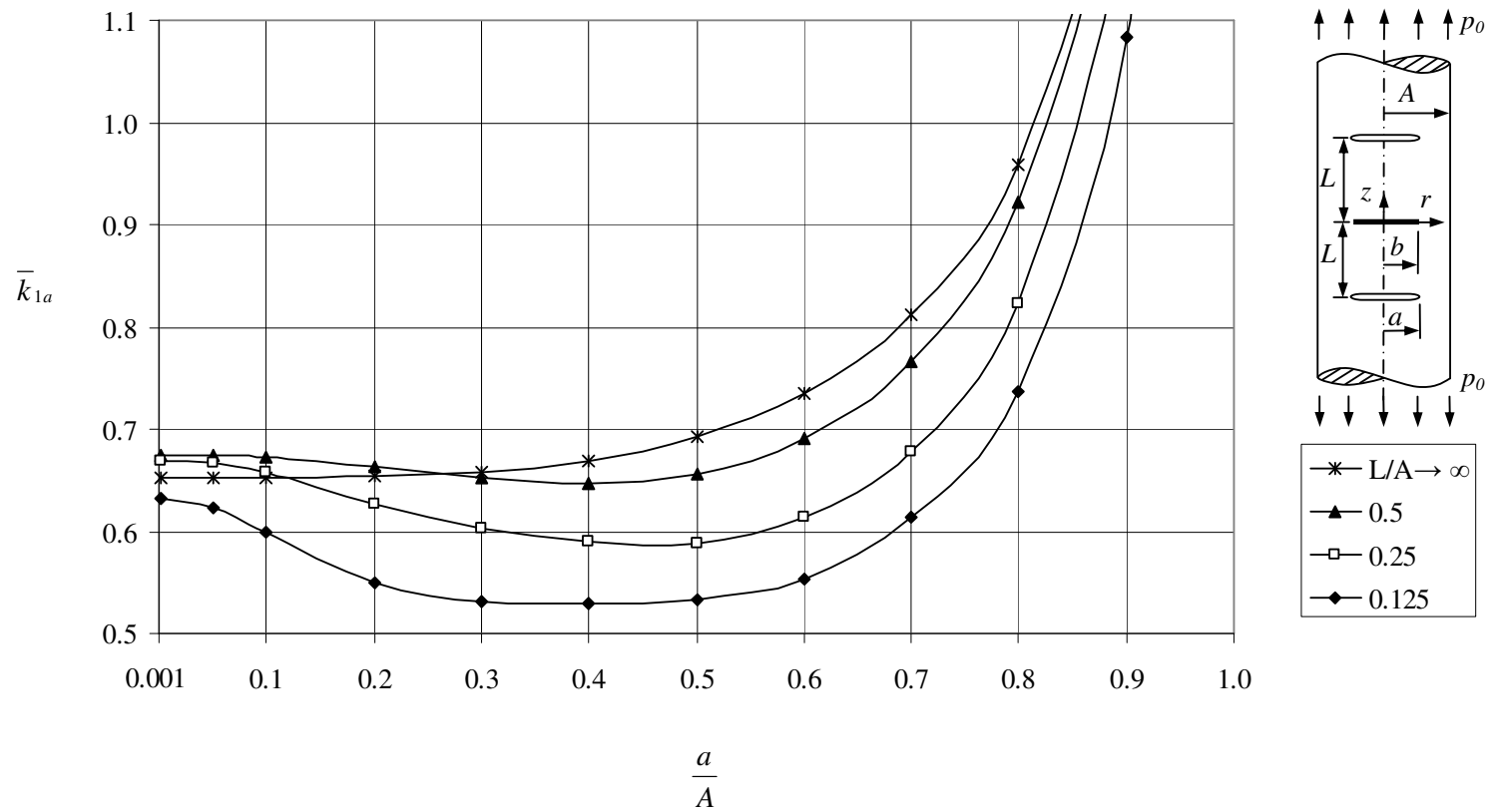
Figure 6.20 Normalized Mode I stress intensity factor $\bar{k}_{1a}$ when $b = 0.5A$, $\nu = 0.3$.
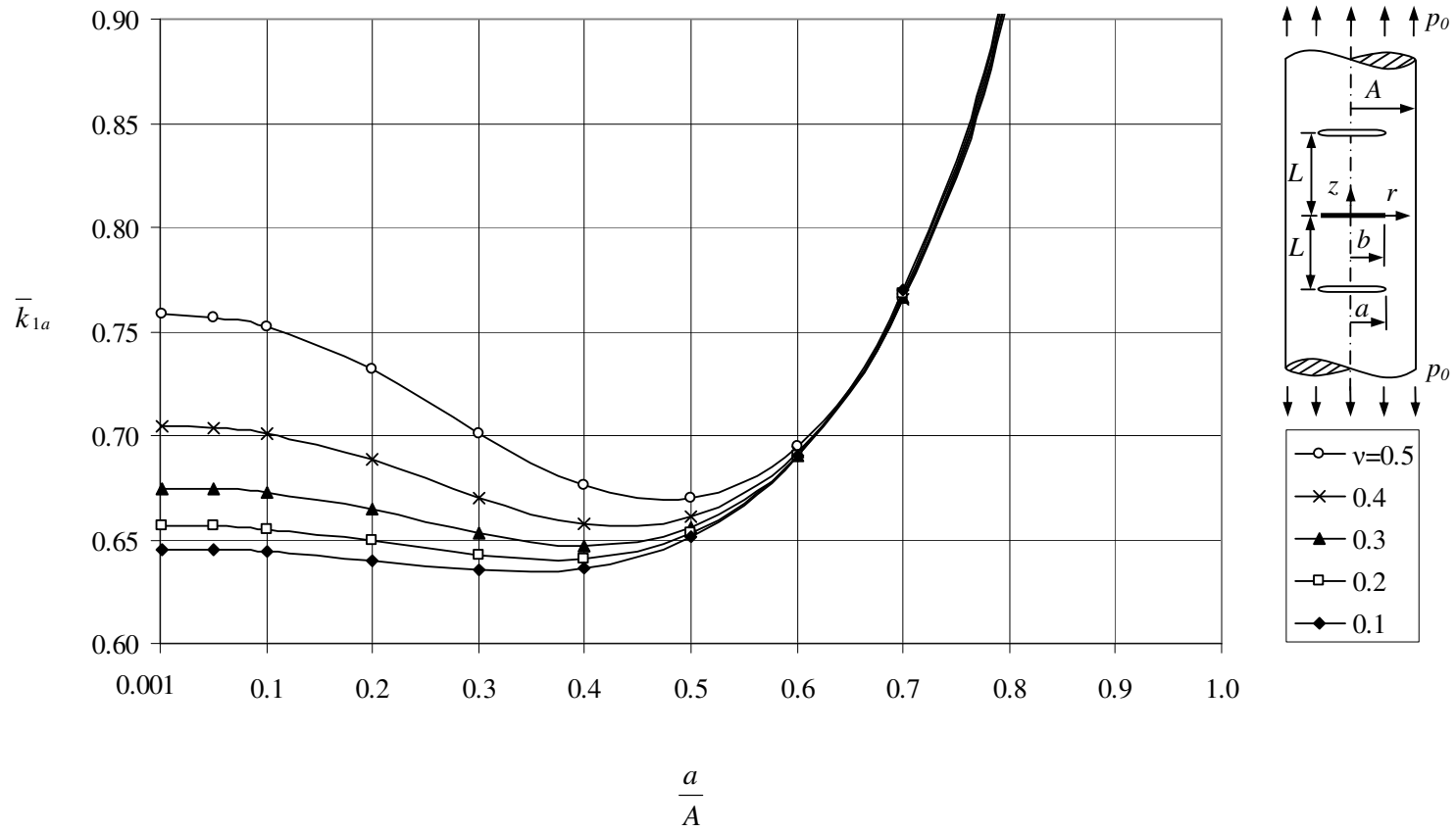
Figure 6.21 Normalized Mode I stress intensity factor $\bar{k}_{1a}$ when $b = L = 0.5A$.
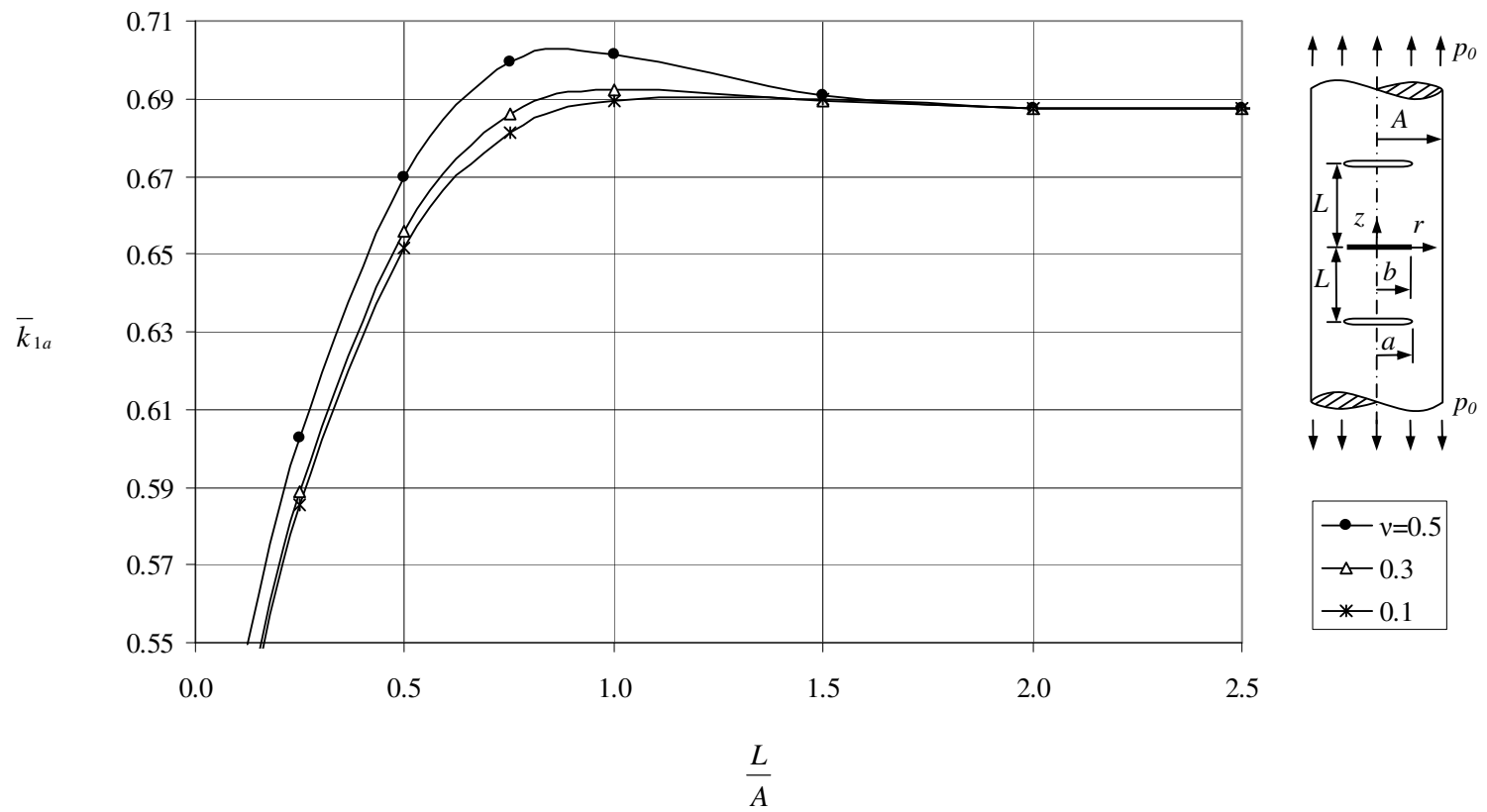
Figure 6.22 Normalized Mode I stress intensity factor $\overline{k}_{1a}$ when $a = b = 0.5A$.
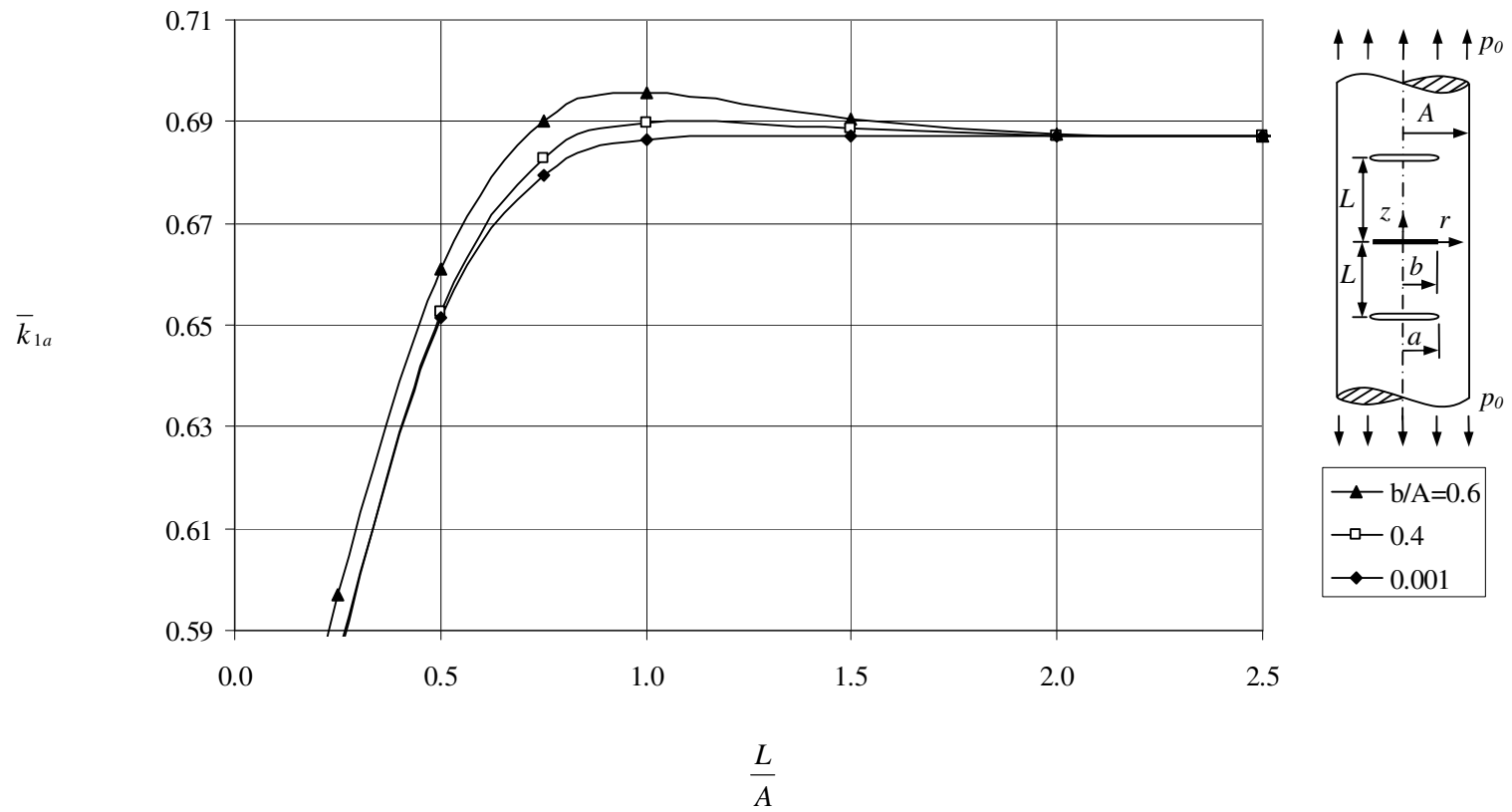
Figure 6.23 Normalized Mode I stress intensity factor $\bar{k}_{1a}$ when $a = 0.5A$, $\nu = 0.3$.
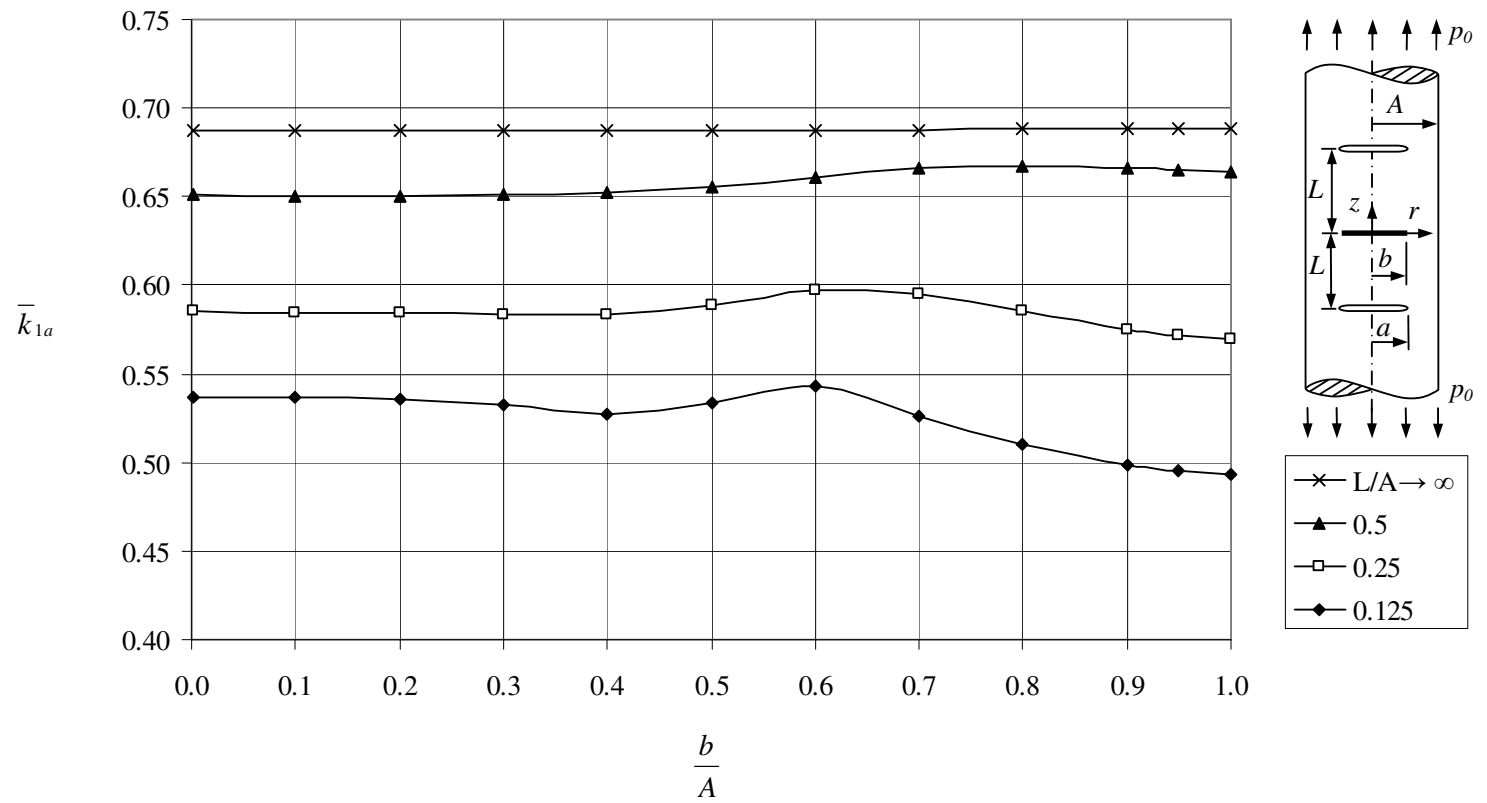
Figure 6.24 Normalized Mode I stress intensity factor $\bar{k}_{1a}$ when $a = 0.5A$, $\nu = 0.3$.
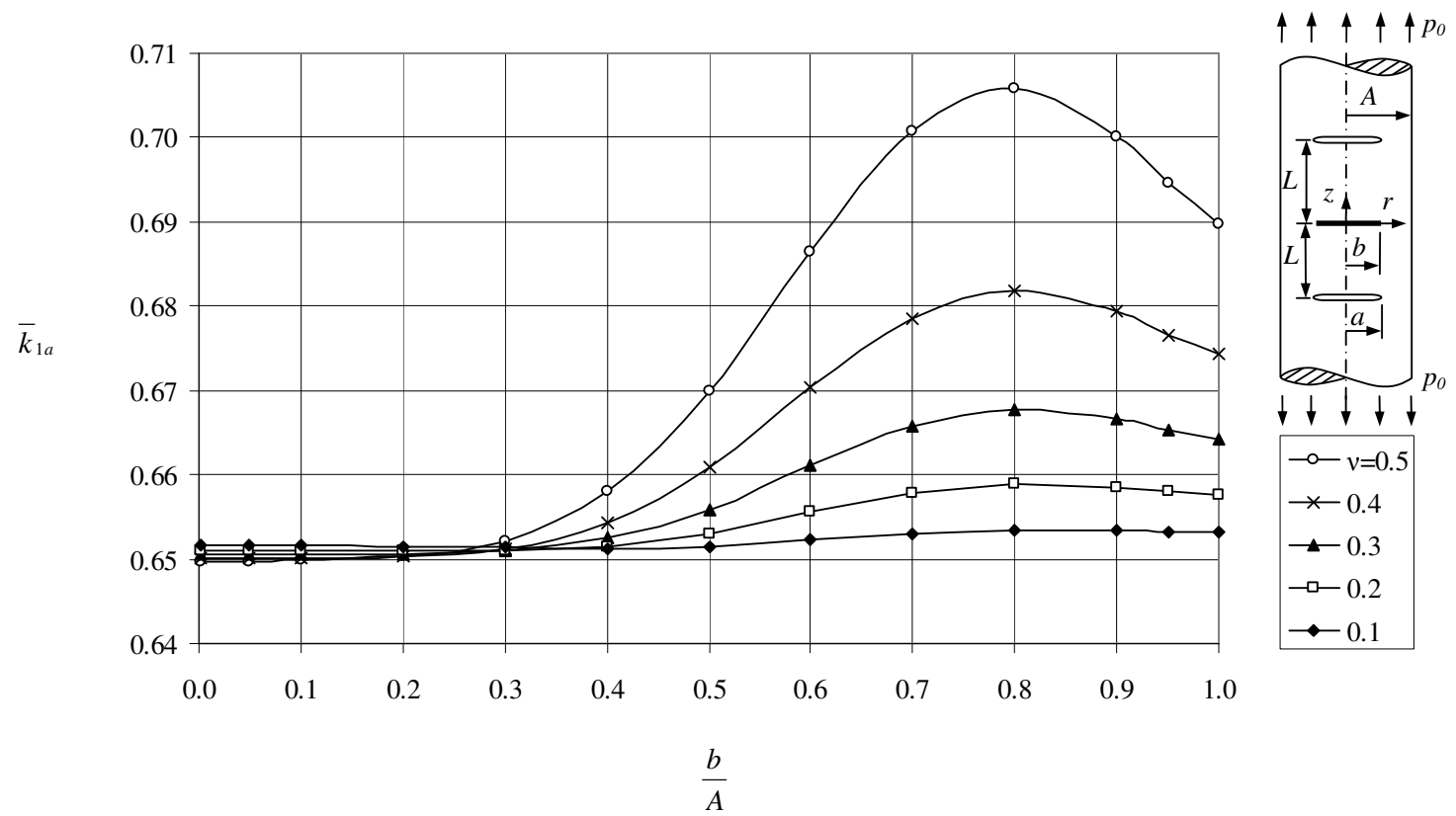
Figure 6.25 Normalized Mode I stress intensity factor $\bar{k}_{1a}$ when $a = L = 0.5A$.
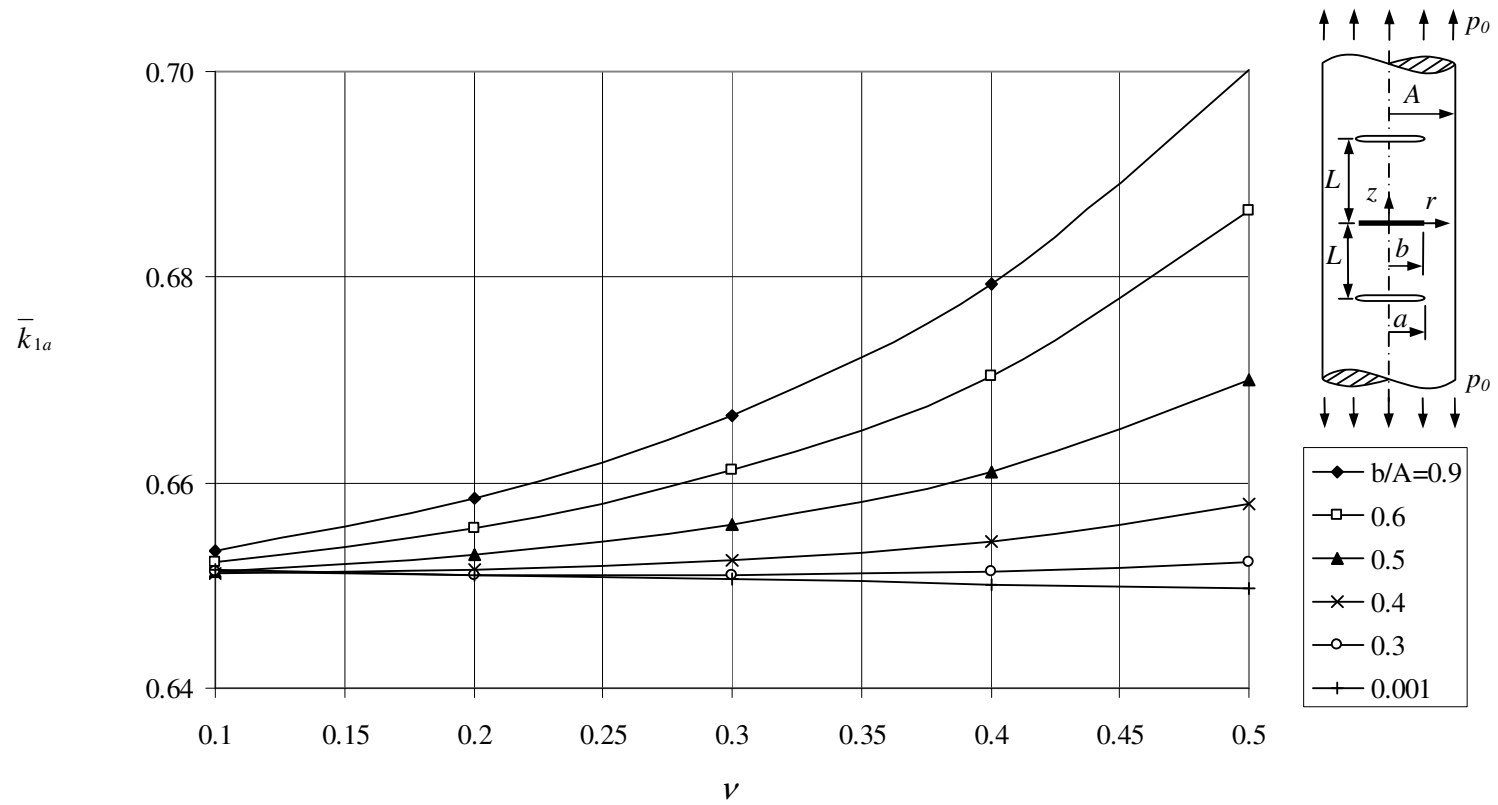
Figure 6.26 Normalized Mode I stress intensity factor $\overline{k}_{1a}$ when $a = L = 0.5A$.
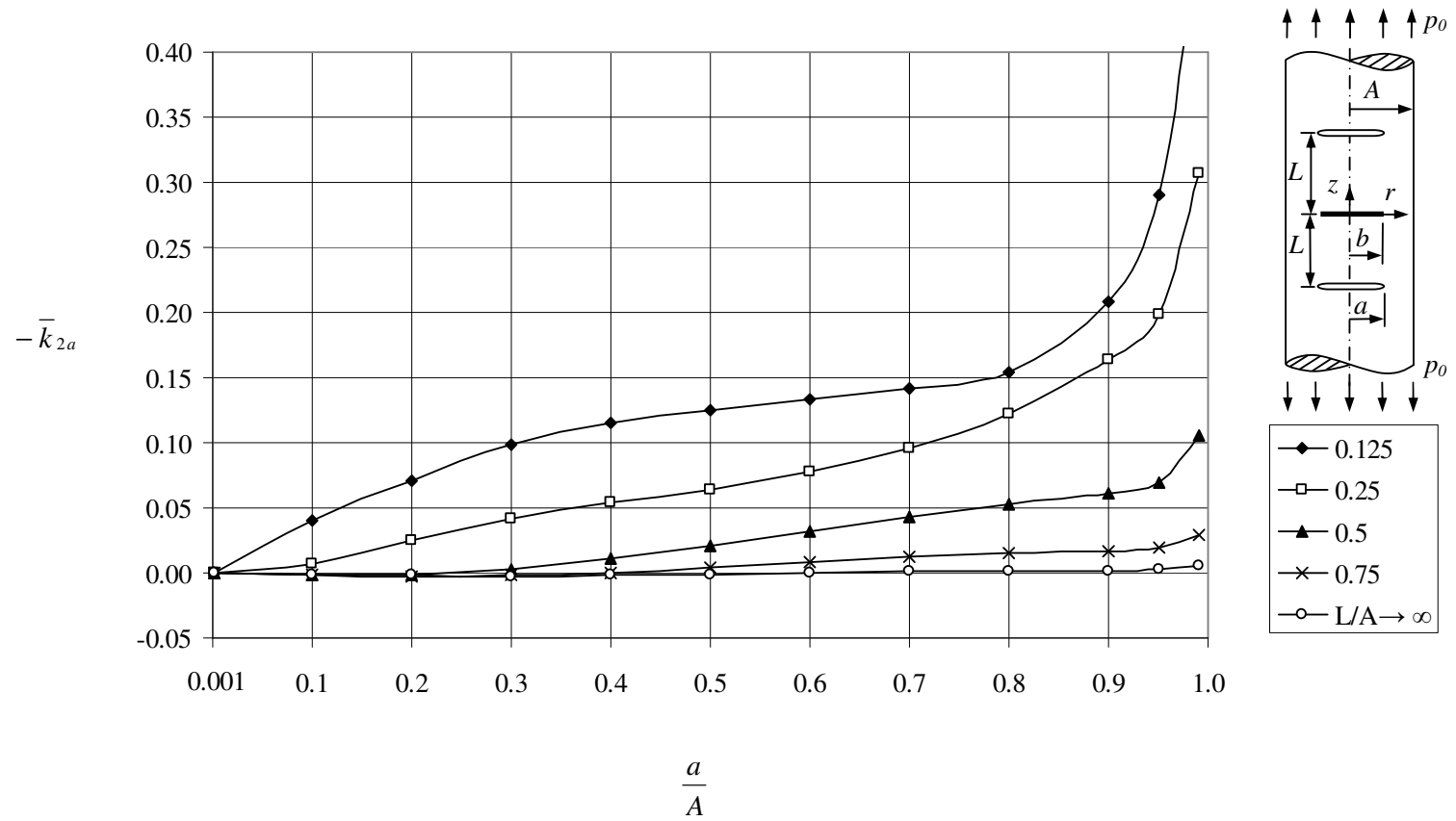
Figure 6.27 Normalized Mode II stress intensity factor $\bar{k}_{2a}$ when $b = 0.5A$, $\nu = 0.3$.
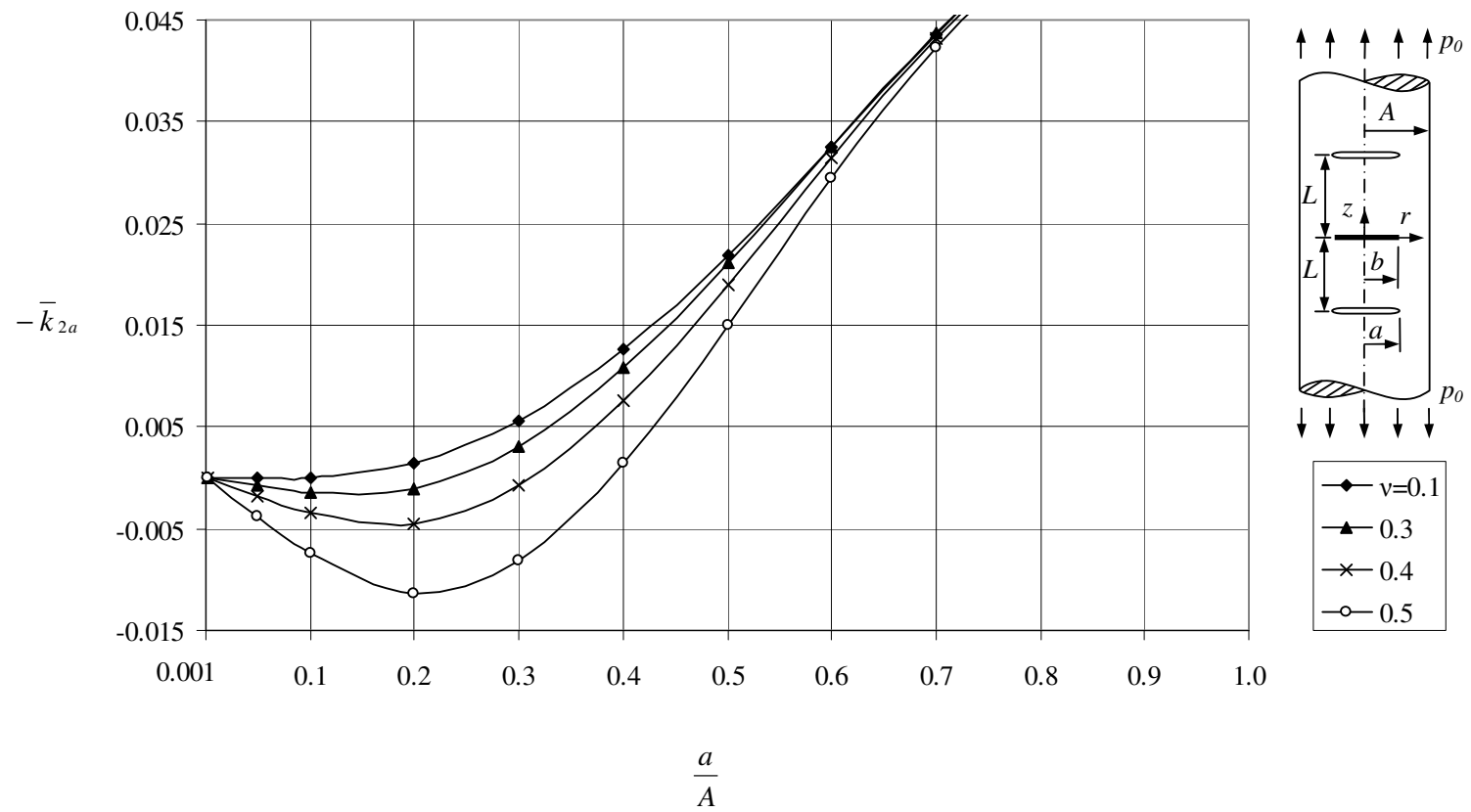
Figure 6.28 Normalized Mode II stress intensity factor $\overline{k}_{2a}$ when $b = L = 0.5A$.
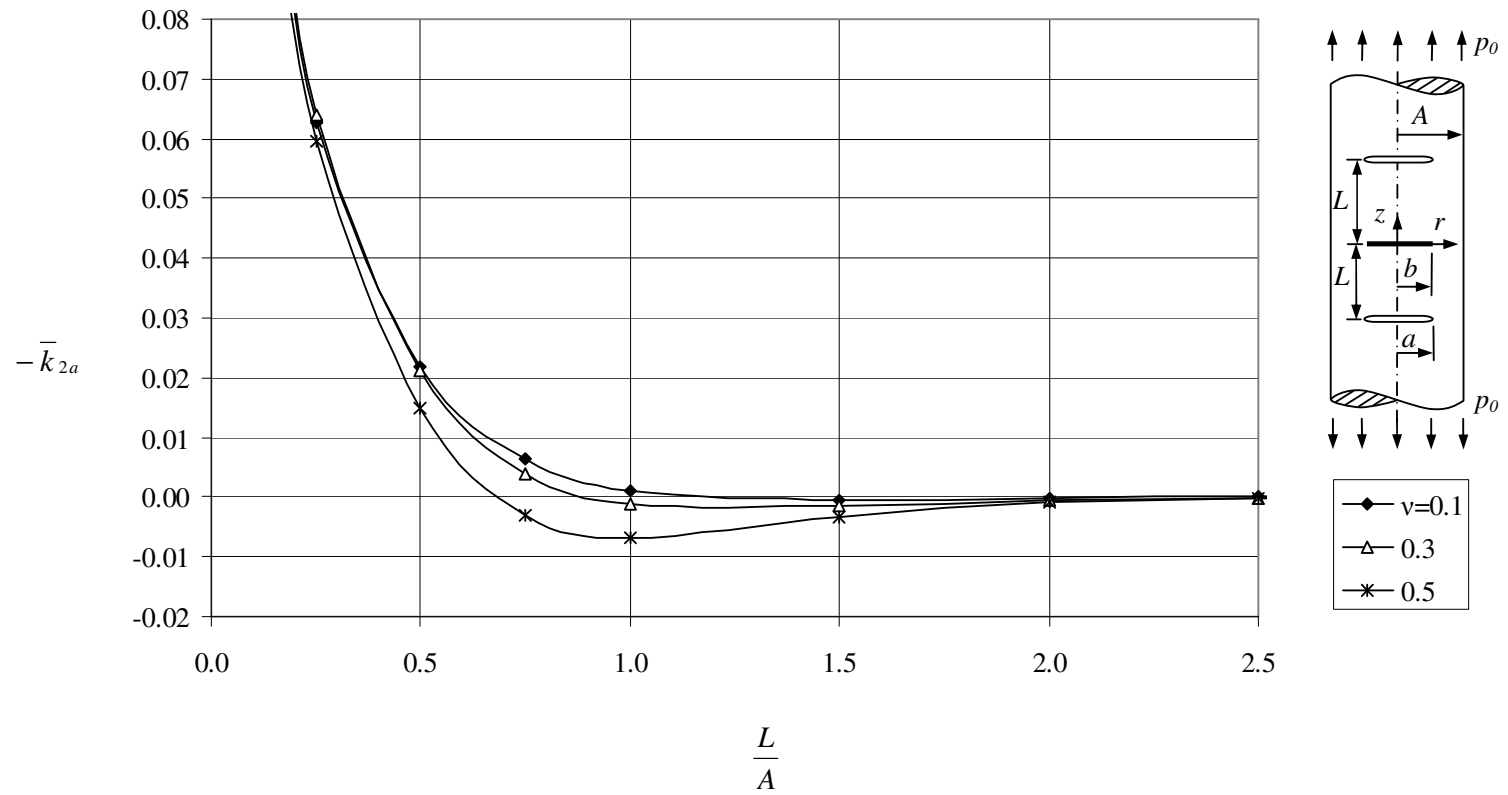
Figure 6.29 Normalized Mode II stress intensity factor $\overline{k}_{2a}$ when $a = b = 0.5A$.
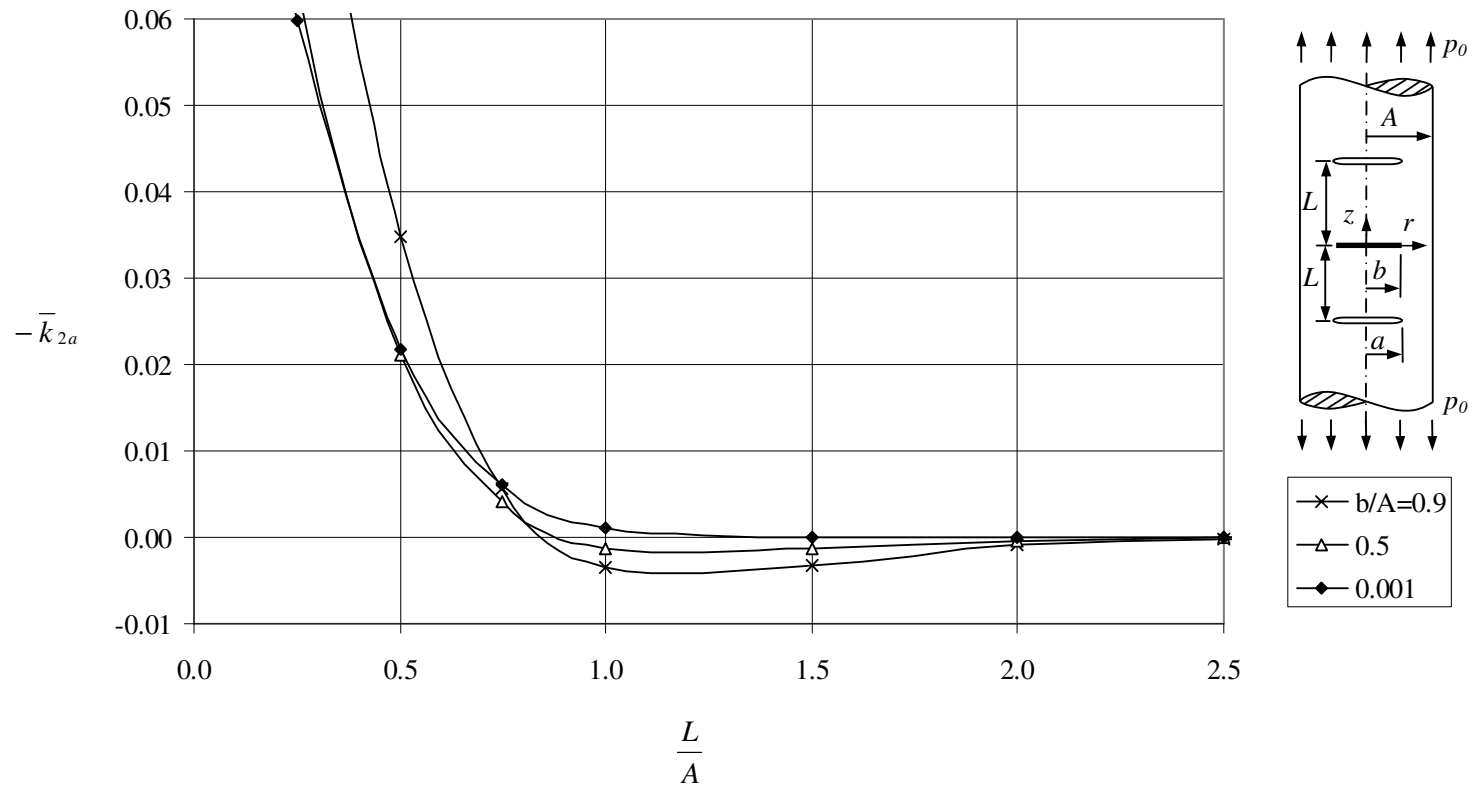
Figure 6.30 Normalized Mode II stress intensity factor $\bar{k}_{2a}$ when $a = 0.5A$, $\nu = 0.3$.
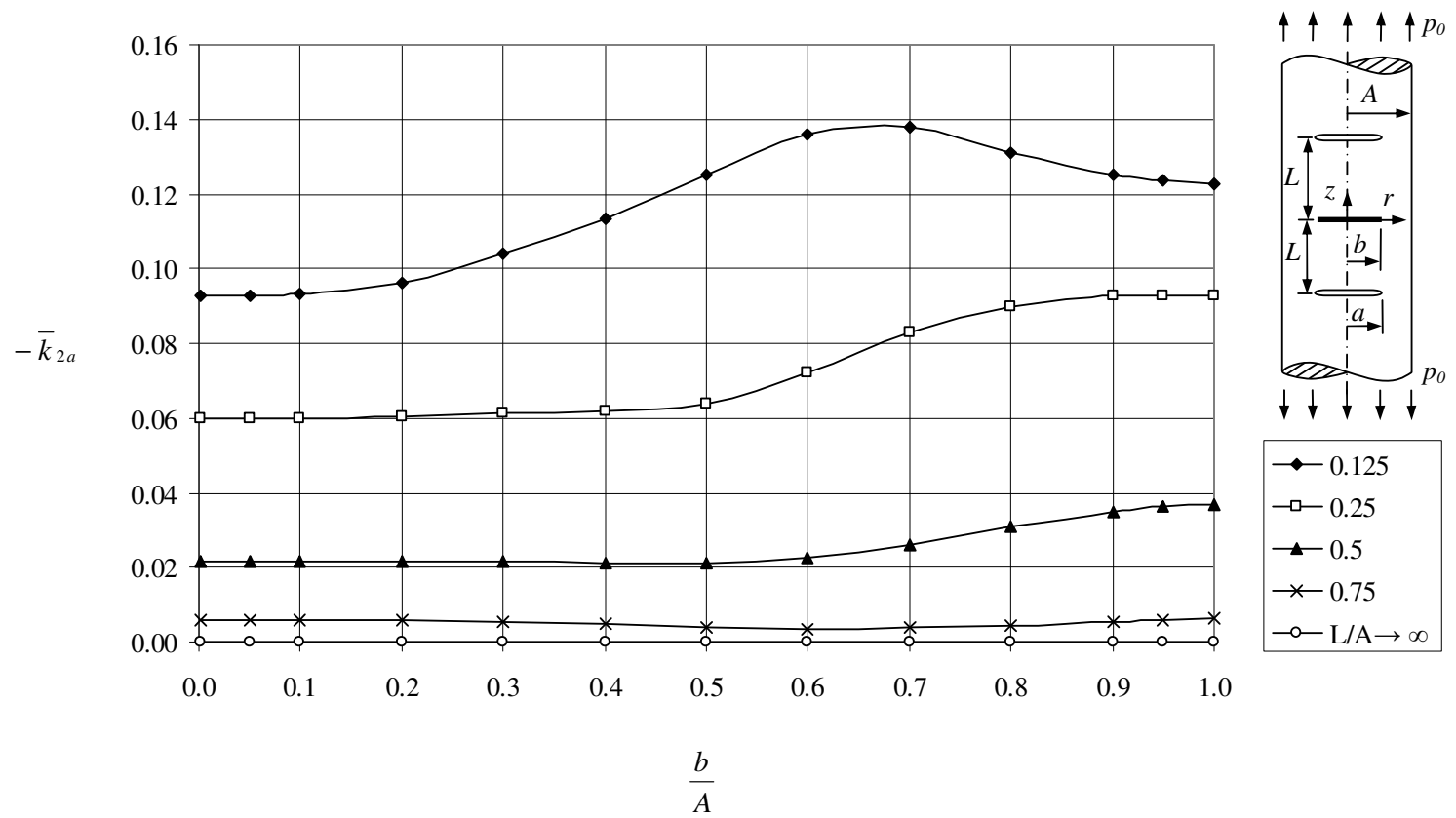
Figure 6.31 Normalized Mode II stress intensity factor $\bar{k}_{2a}$ when $a = 0.5A$, $\nu = 0.3$.
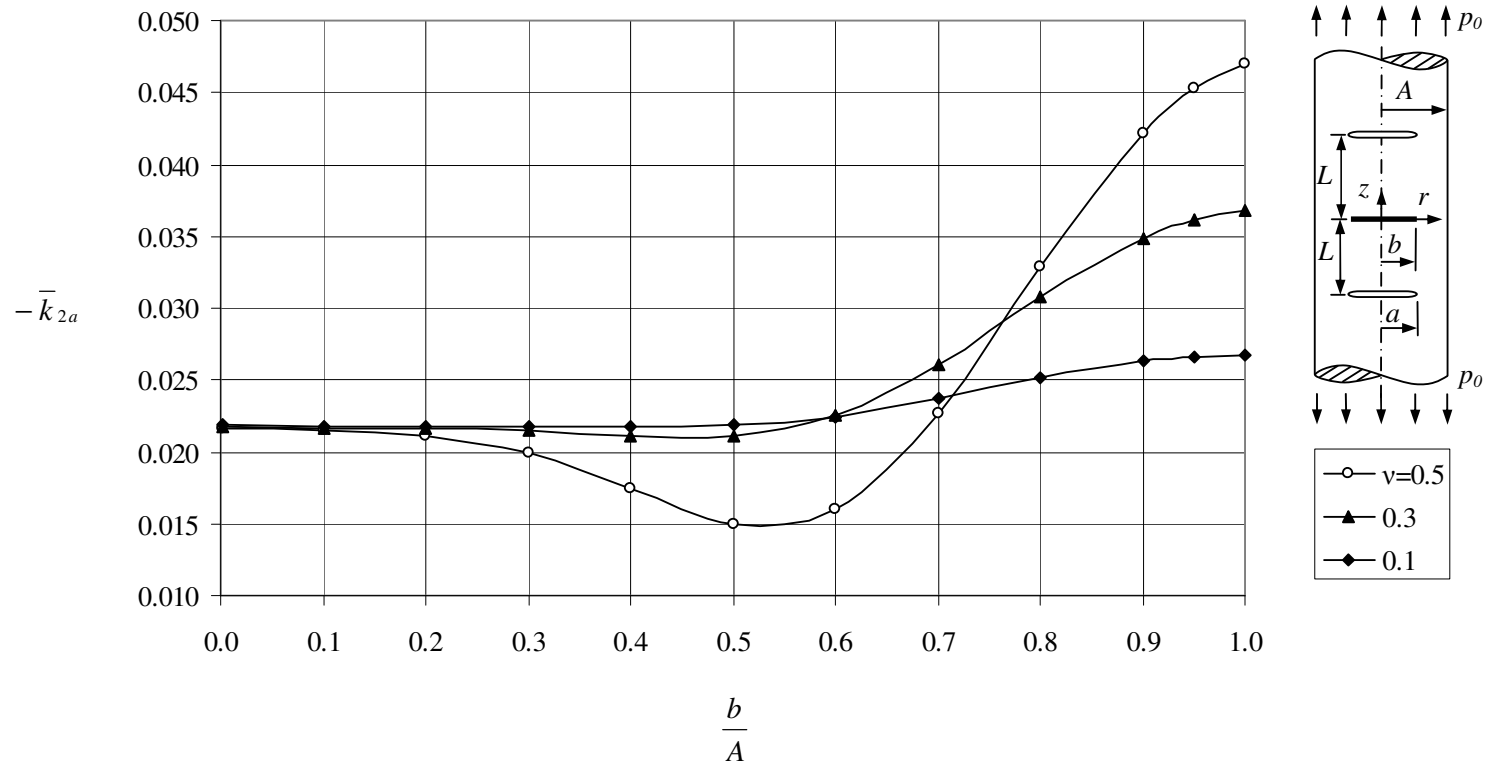
Figure 6.32 Normalized Mode II stress intensity factor $\overline{k}_{2a}$ when $a = L = 0.5A$.
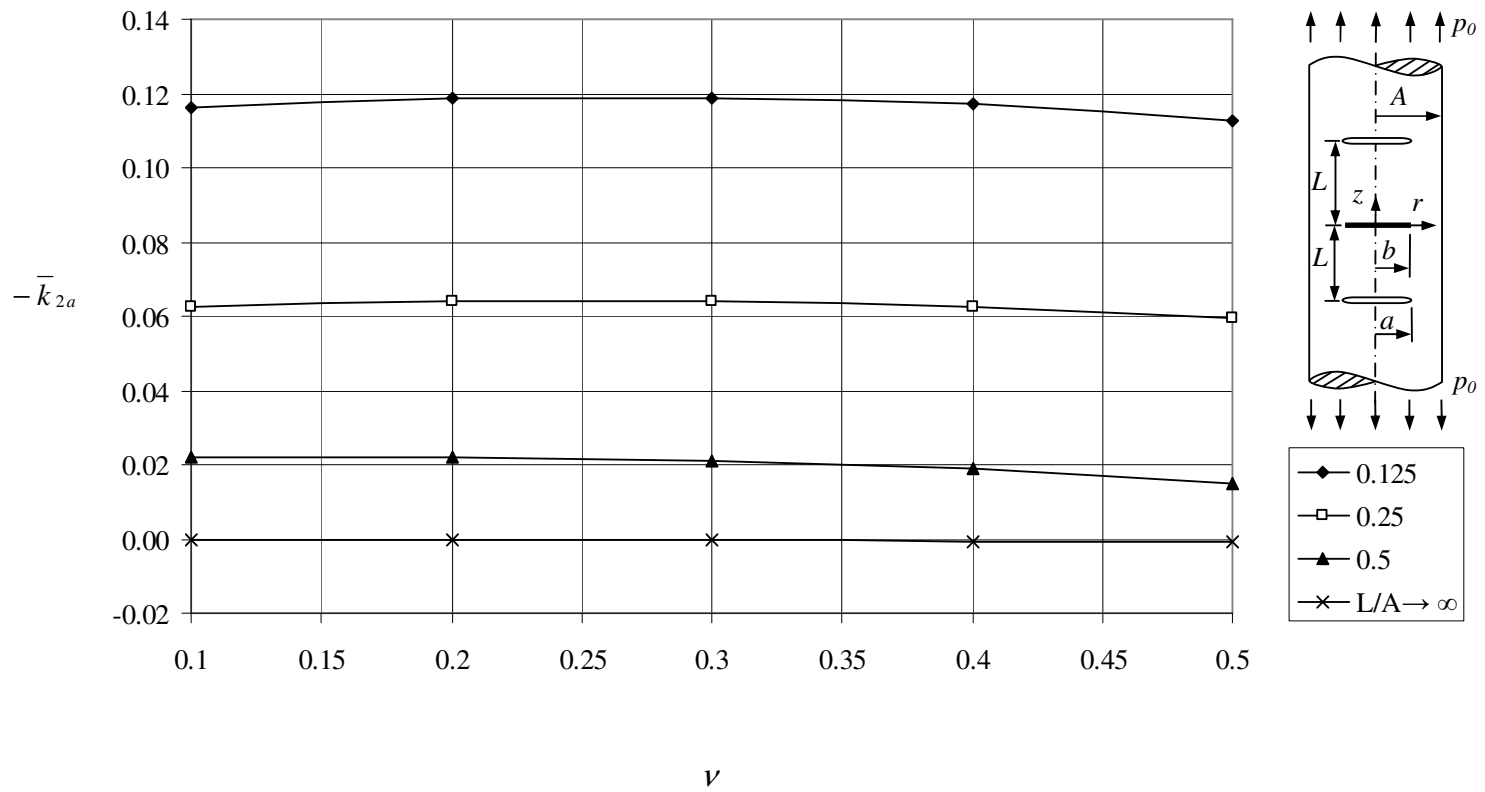
Figure 6.33 Normalized Mode II stress intensity factor $\overline{k}_{2a}$ when $a = b = 0.5A$.
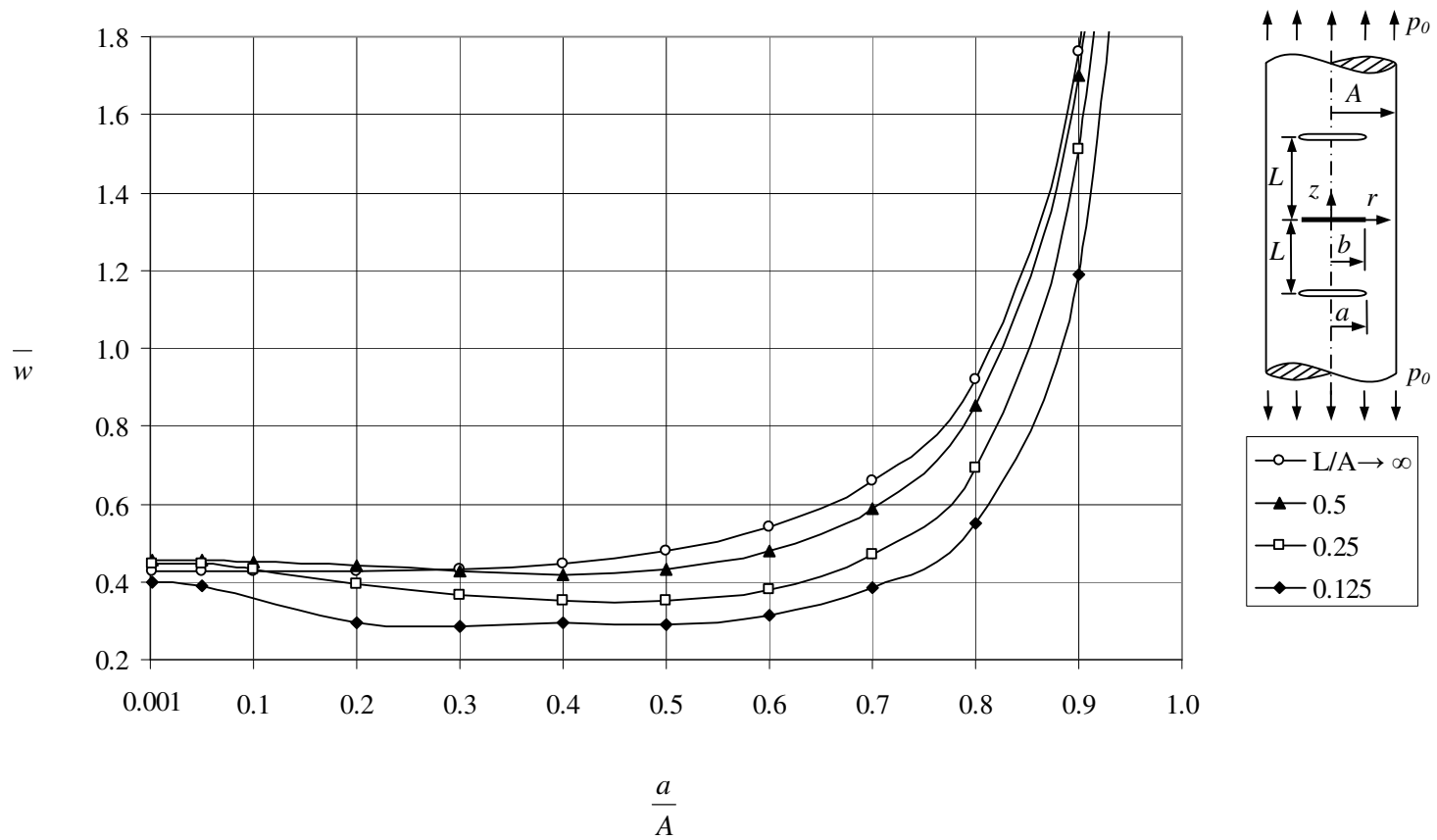
Figure 6.34 Normalized energy release rate $\overline{w}$ when $b = 0.5A$, $\nu = 0.3$.
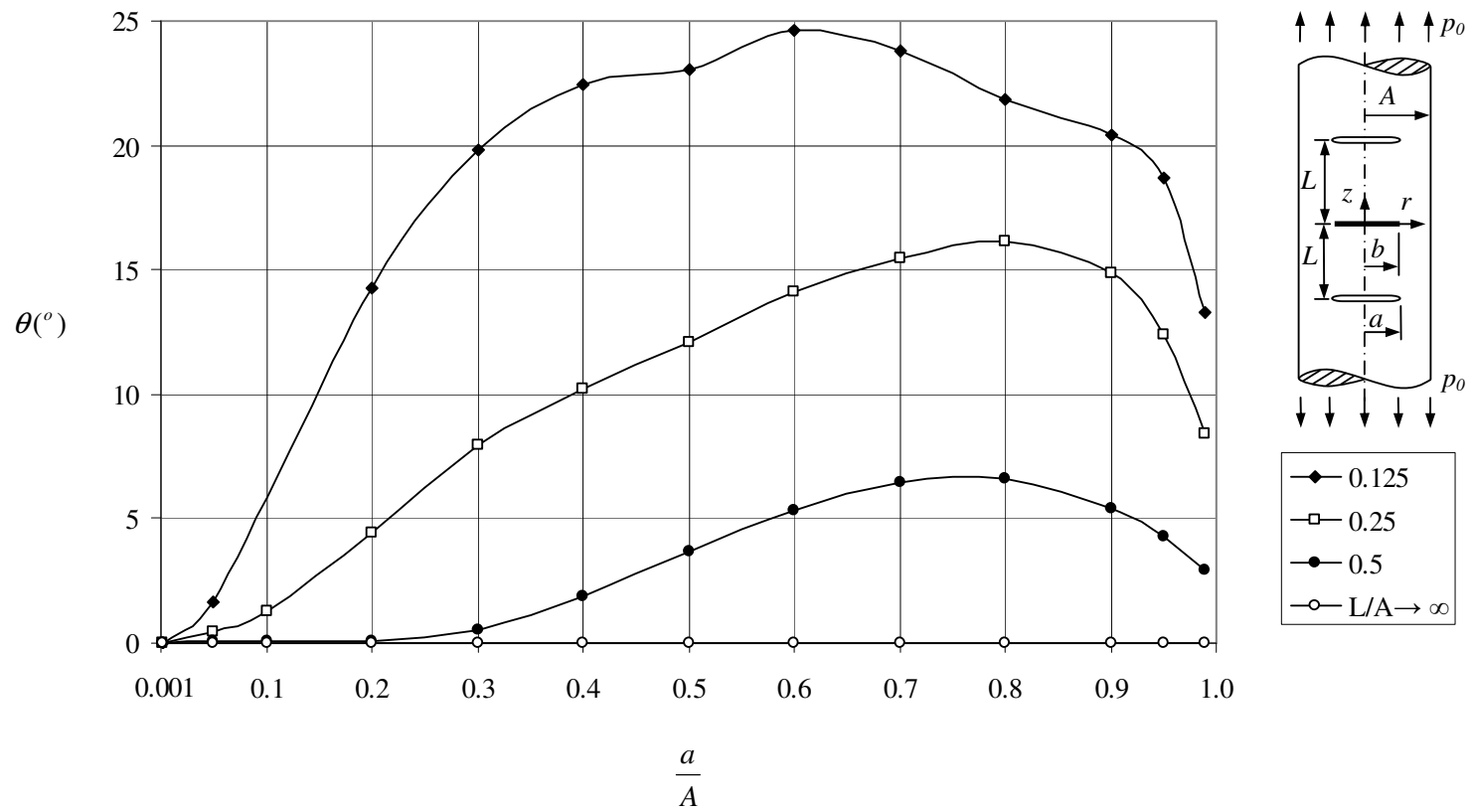
Figure 6.35 Probable crack propagation angle θ when $b = 0.5A$, $\nu = 0.3$.
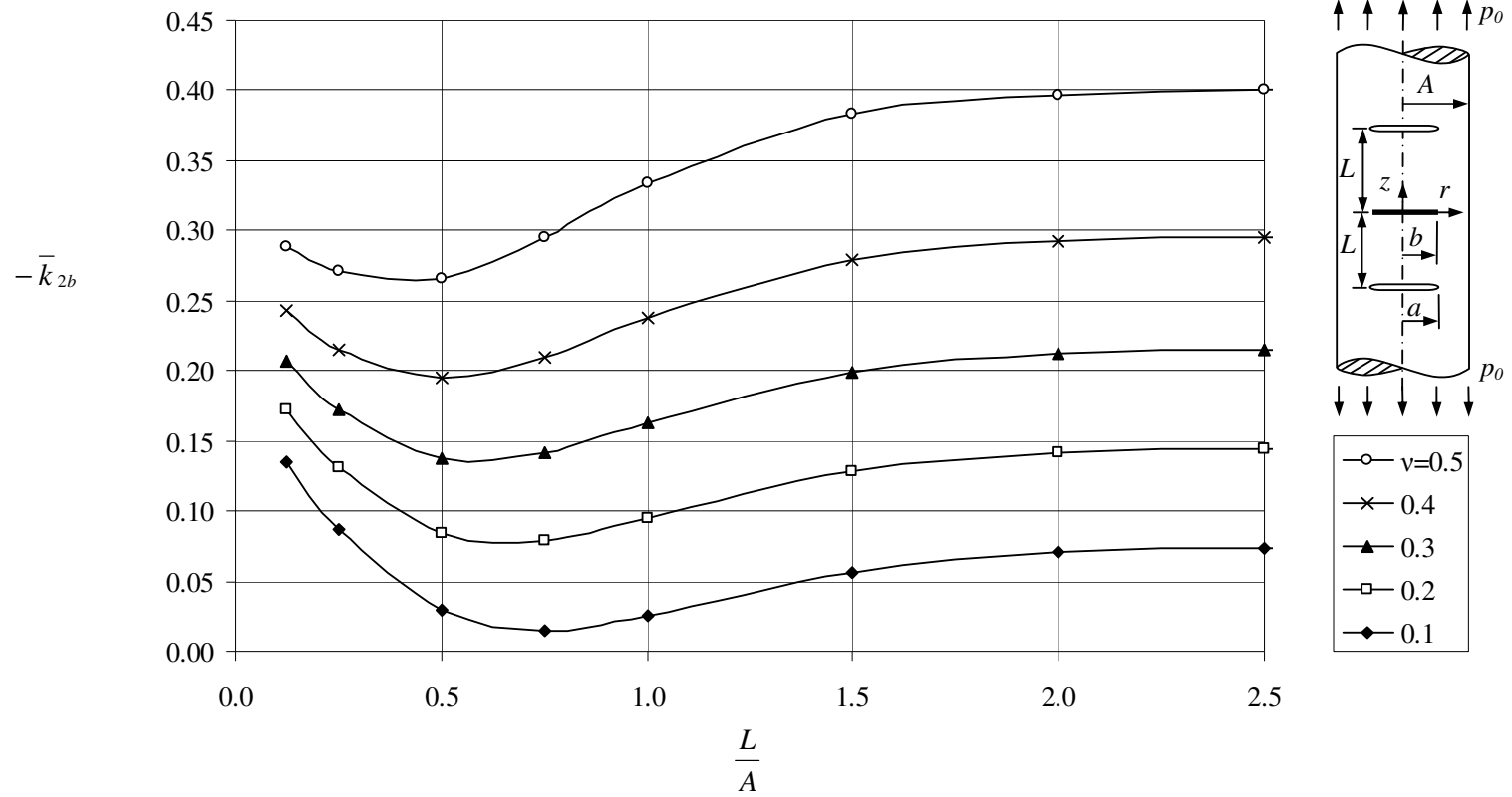
Figure 6.36 Normalized Mode II stress intensity factor $\overline{k}_{2b}$ when $a = b = 0.5A$.
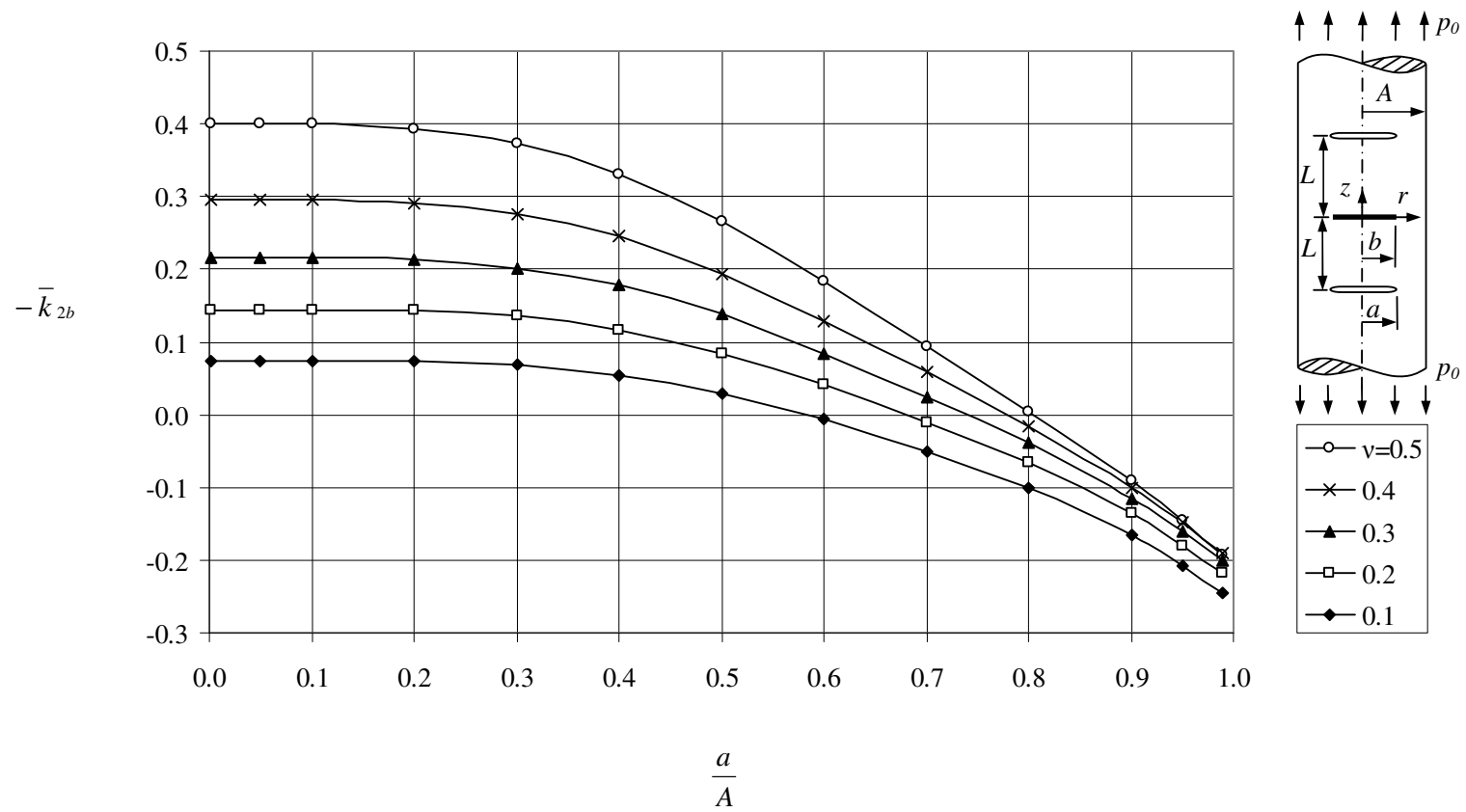
Figure 6.37 Normalized Mode II stress intensity factor $\bar{k}_{2b}$ when $b = L = 0.5A$.
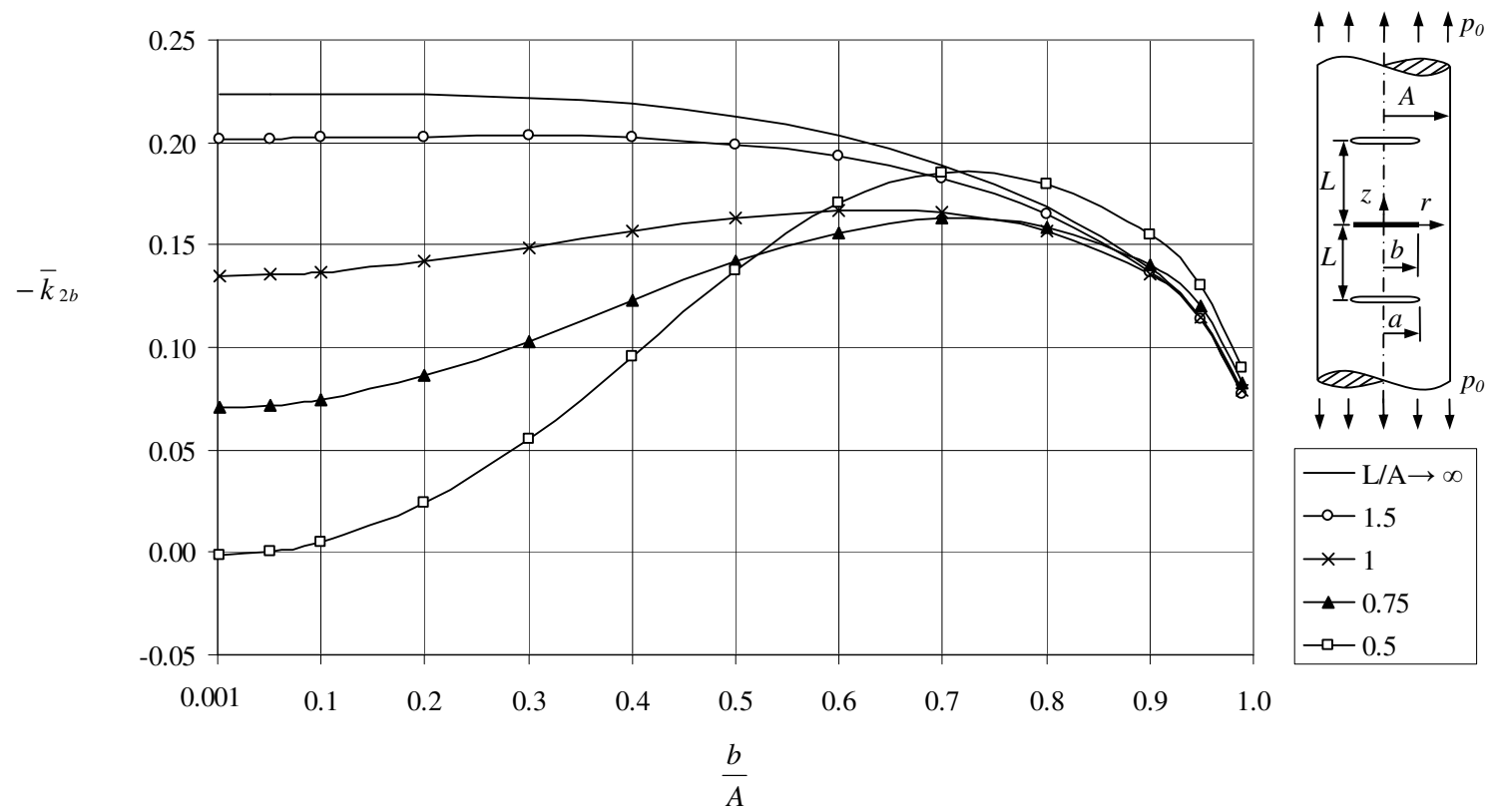
Figure 6.38 Normalized Mode II stress intensity factor $\bar{k}_{2b}$ when $a = 0.5A$, $\nu = 0.3$.
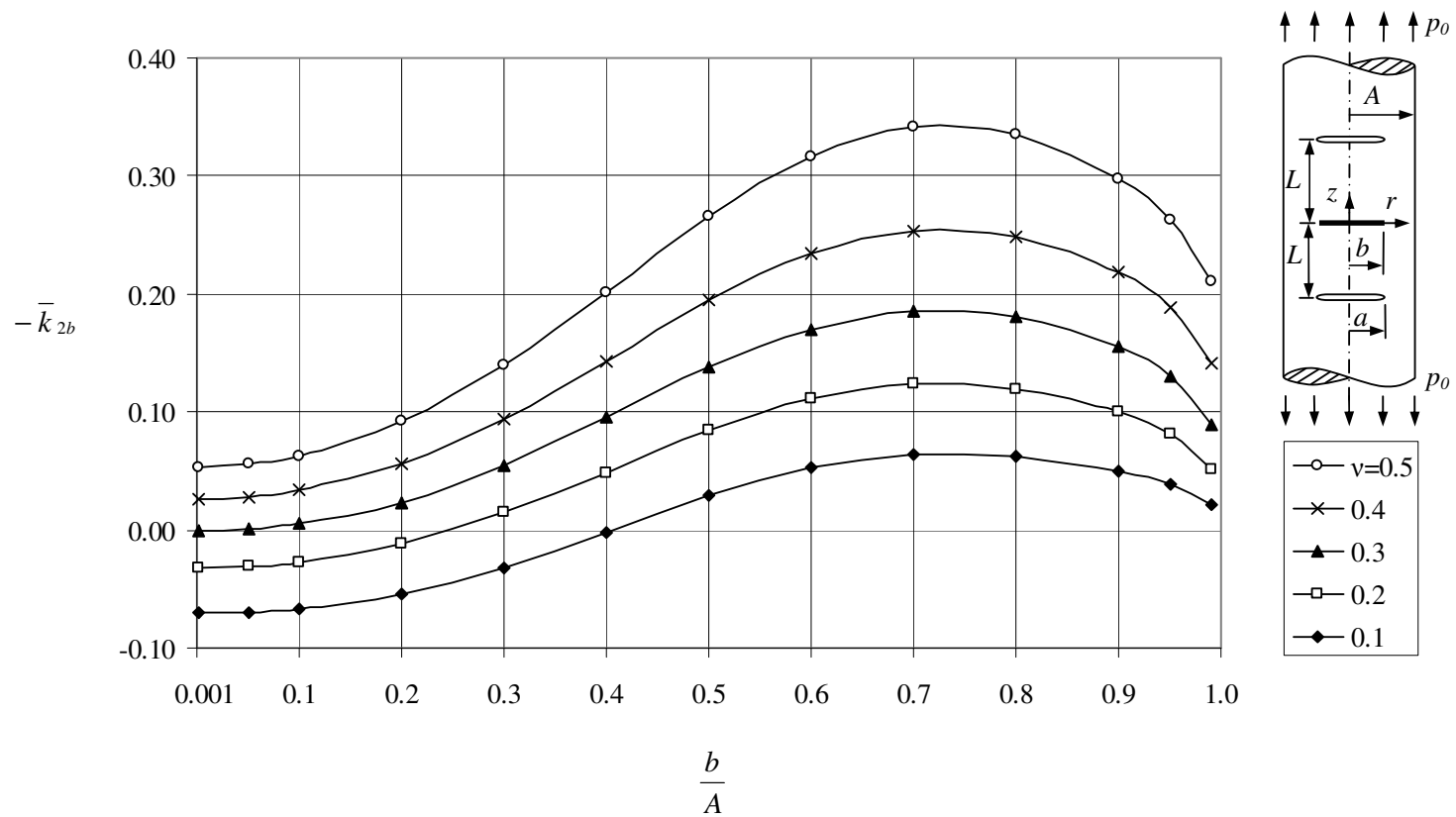
Figure 6.39 Normalized Mode II stress intensity factor $\bar{k}_{2b}$ when $a = L = 0.5A$.
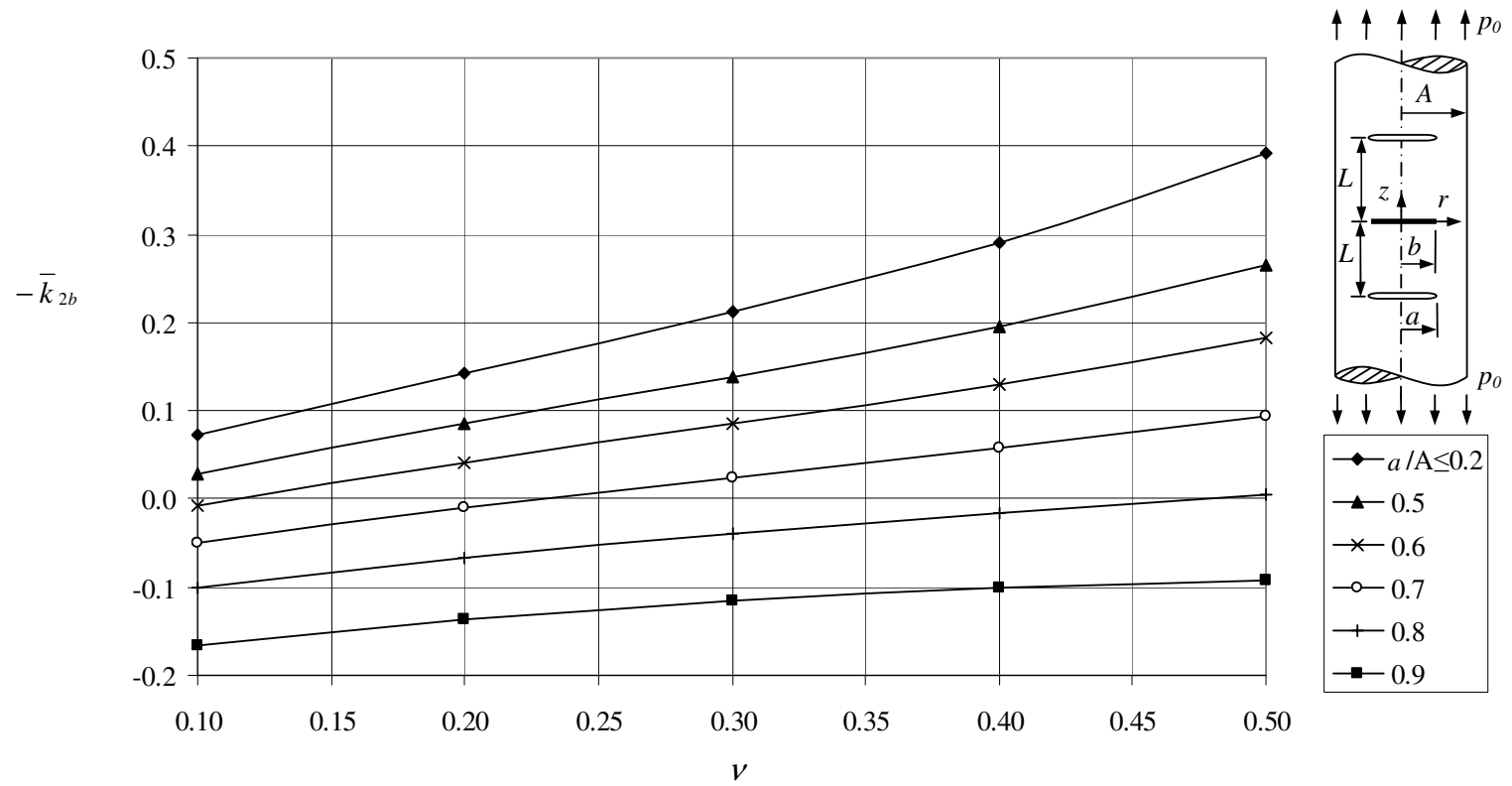
Figure 6.40 Normalized Mode II stress intensity factor $\overline{k}_{2b}$ when $b = L = 0.5A$.
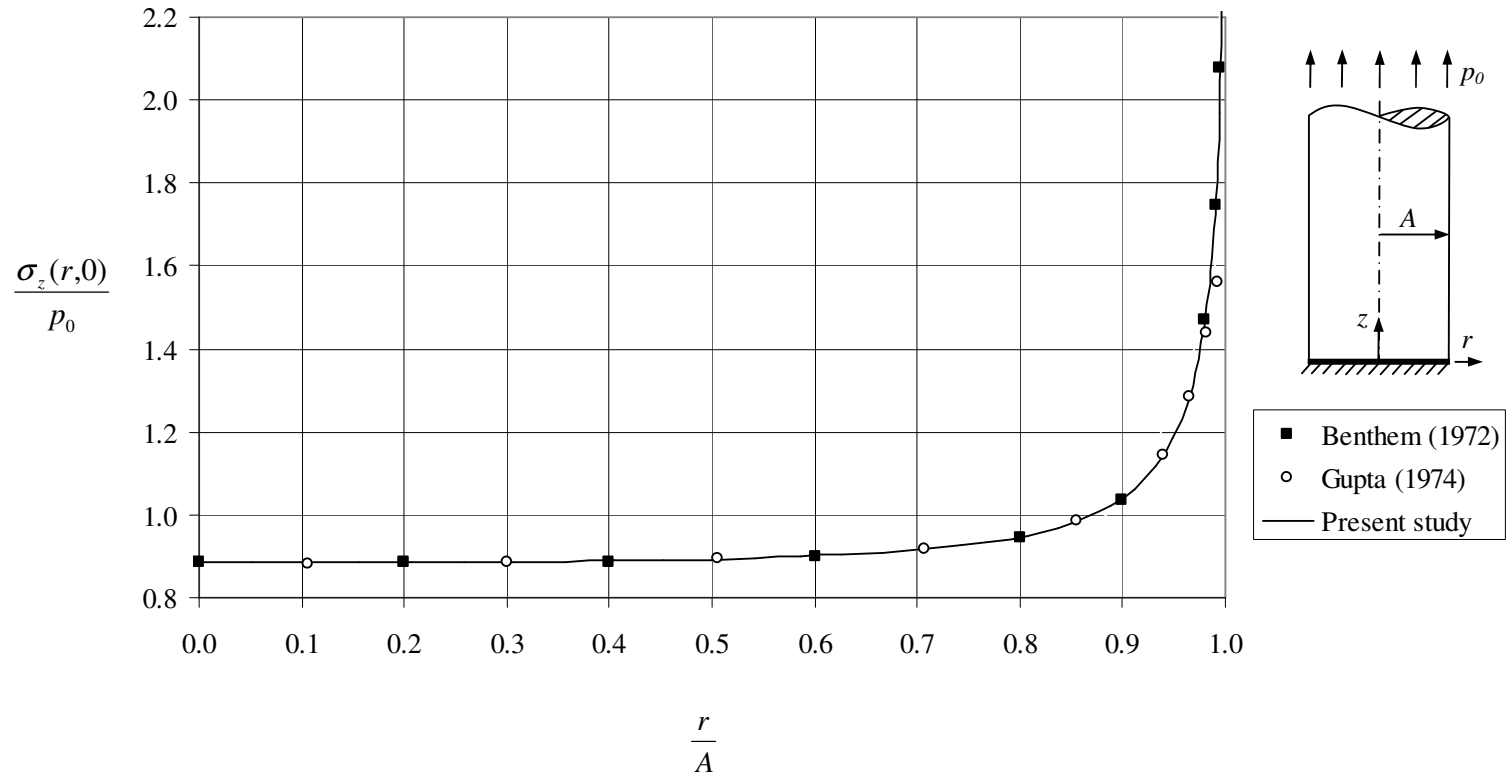
Figure 6.41 Normal stress $\sigma_z(r,0)$ along the rigid support when $\nu = 0.25$.
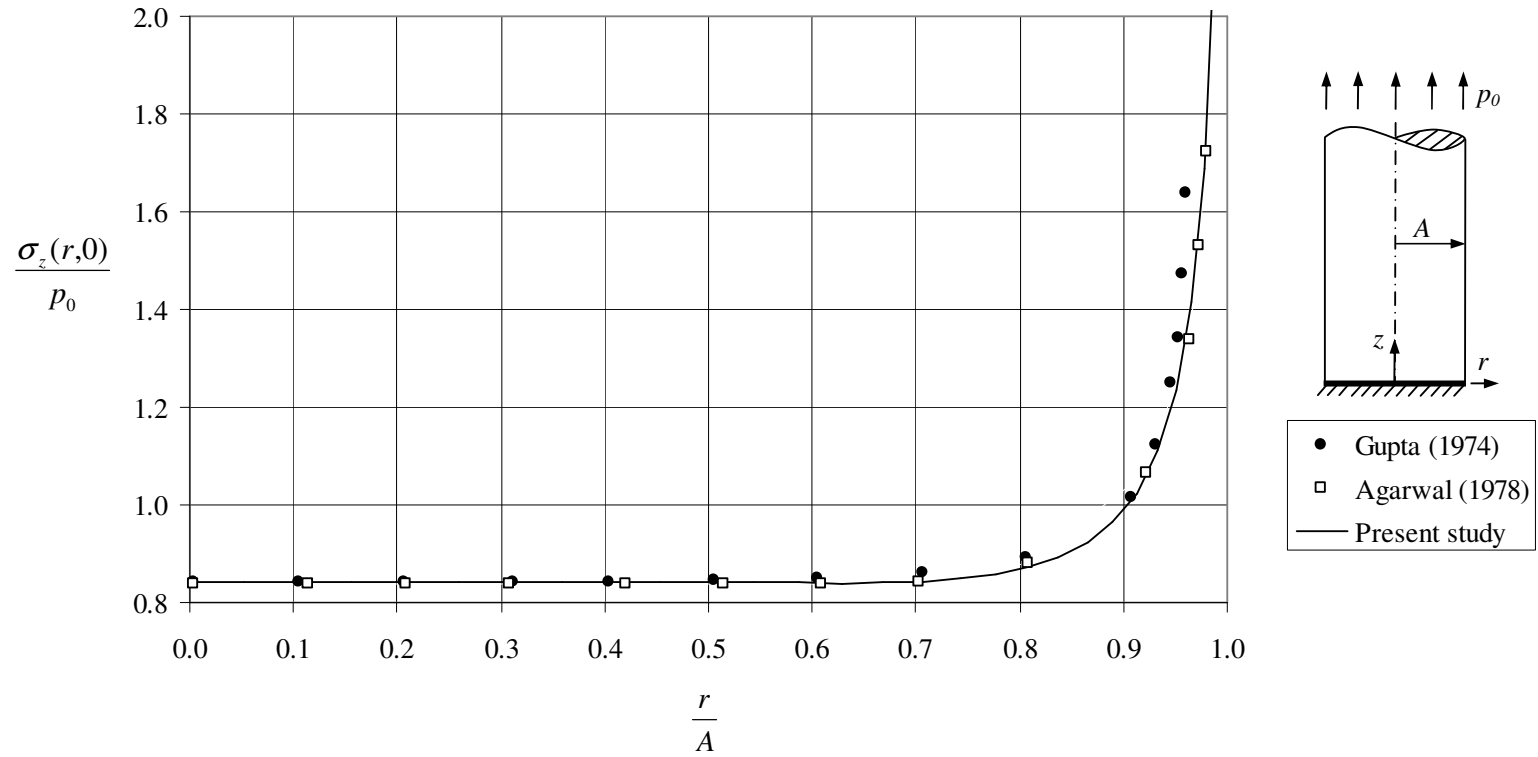
Figure 6.42 Normal stress $\sigma_z(r,0)$ along the rigid support when $\nu = 0.5$.
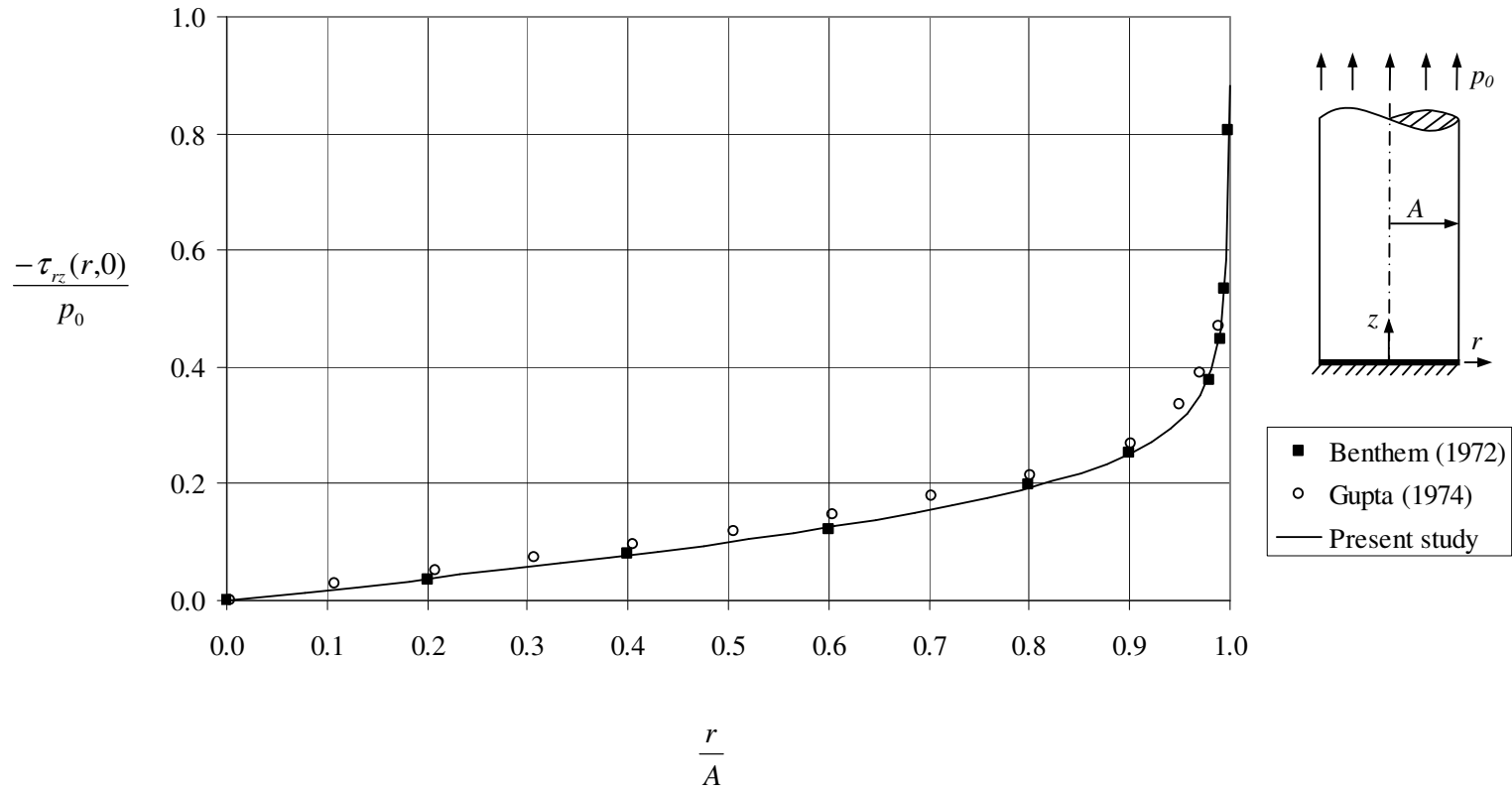
Figure 6.43 Shearing stress $\tau_{rz}(r,0)$ along the rigid support when $\nu = 0.25$.
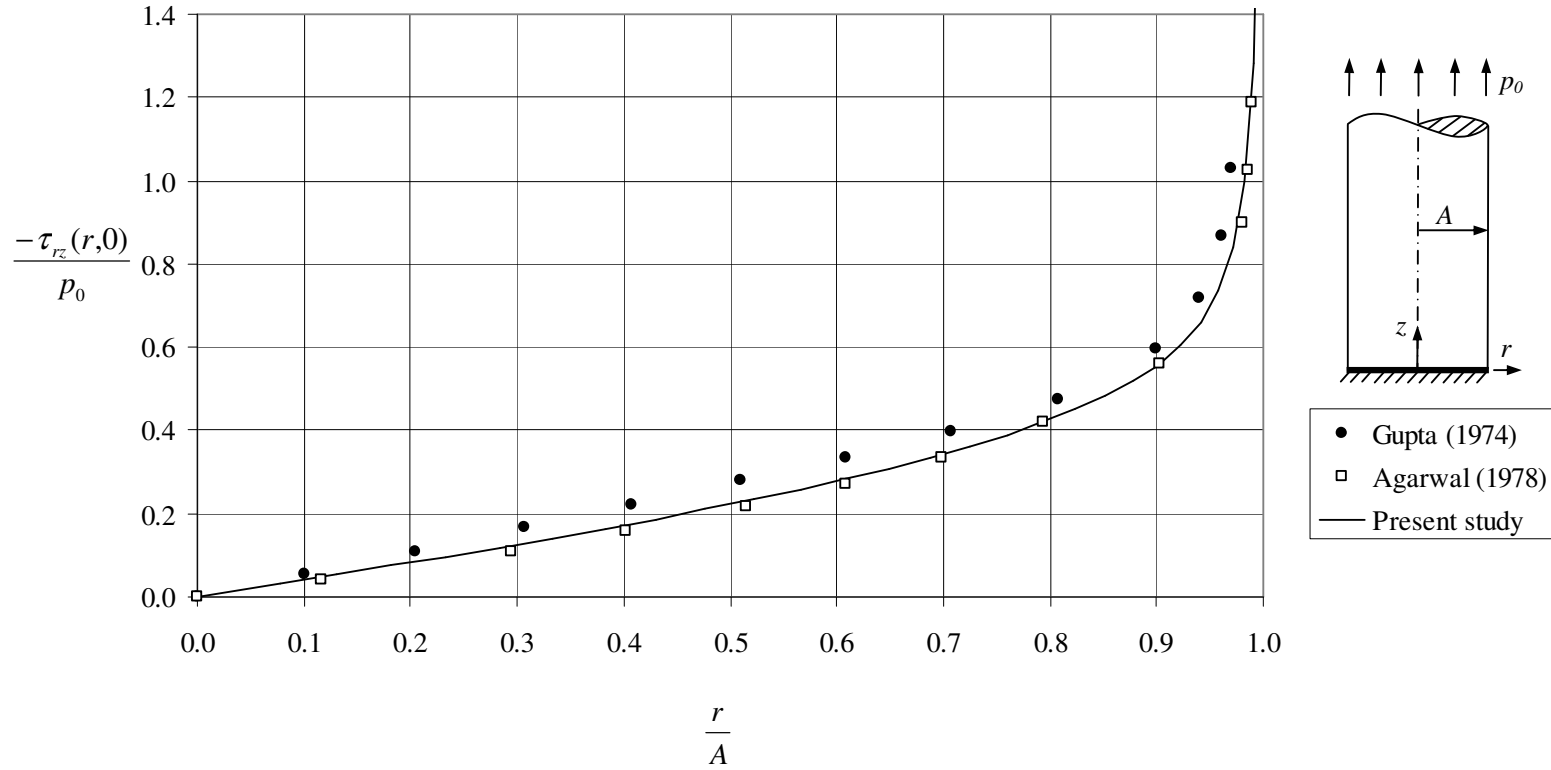
Figure 6.44 Shearing stress $\tau_{rz}(r,0)$ along the rigid support when $\nu = 0.5$.
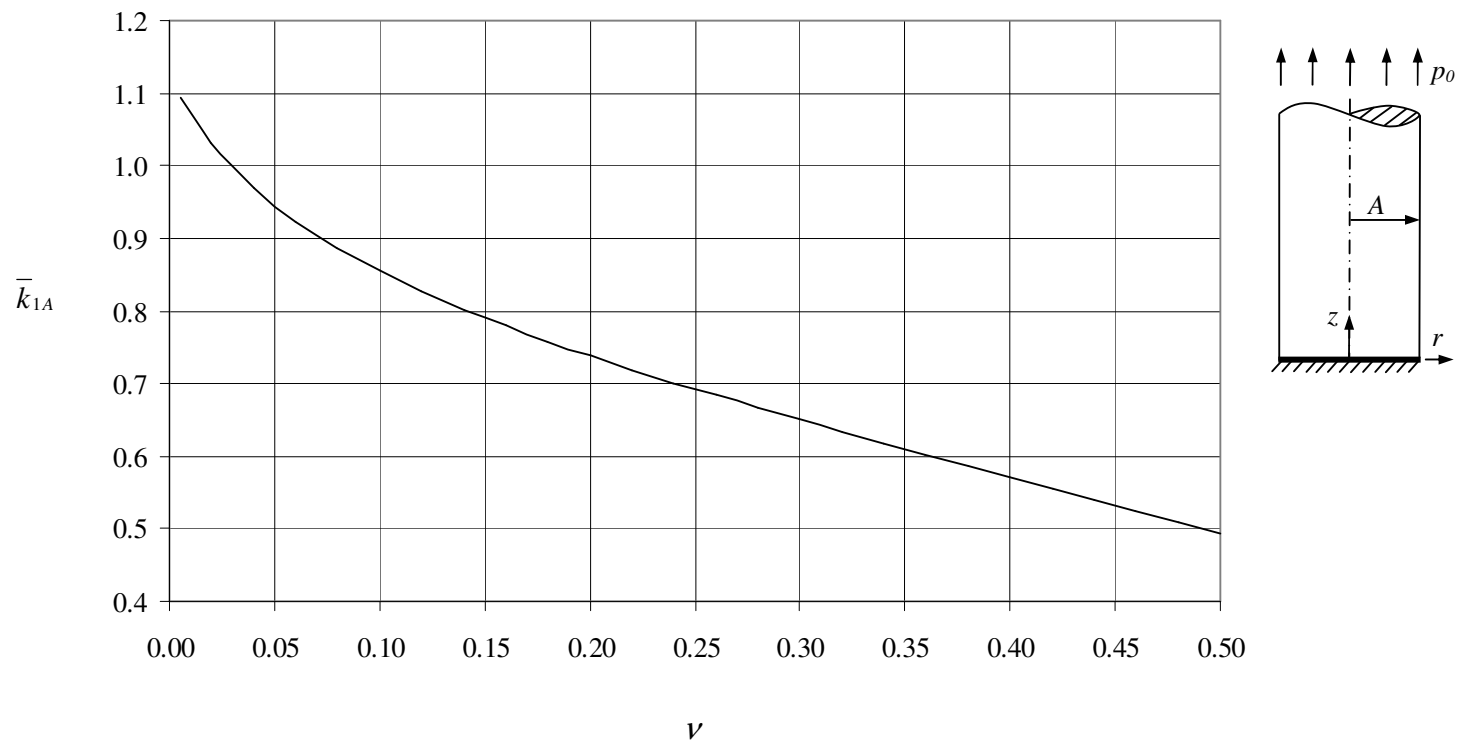
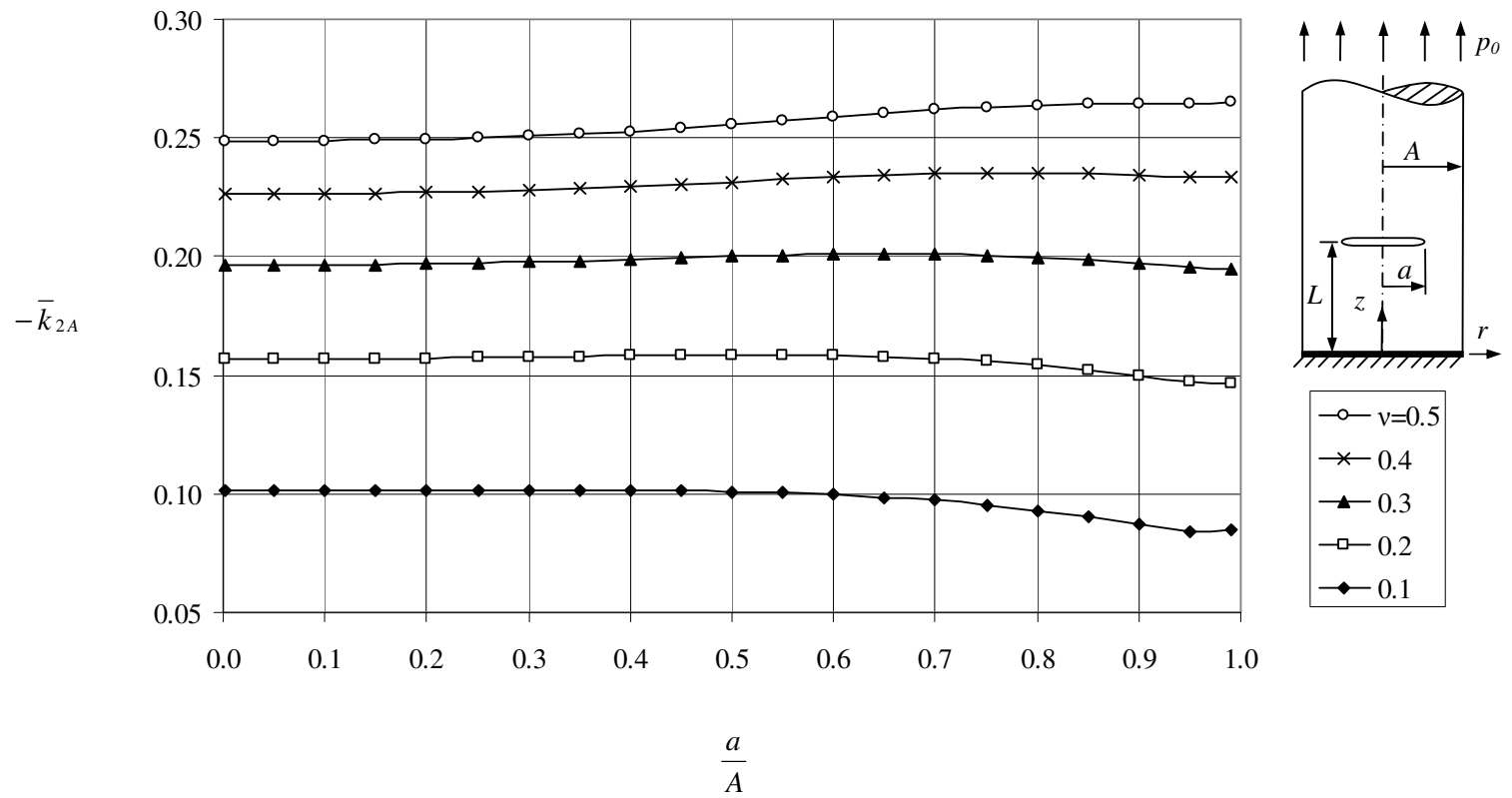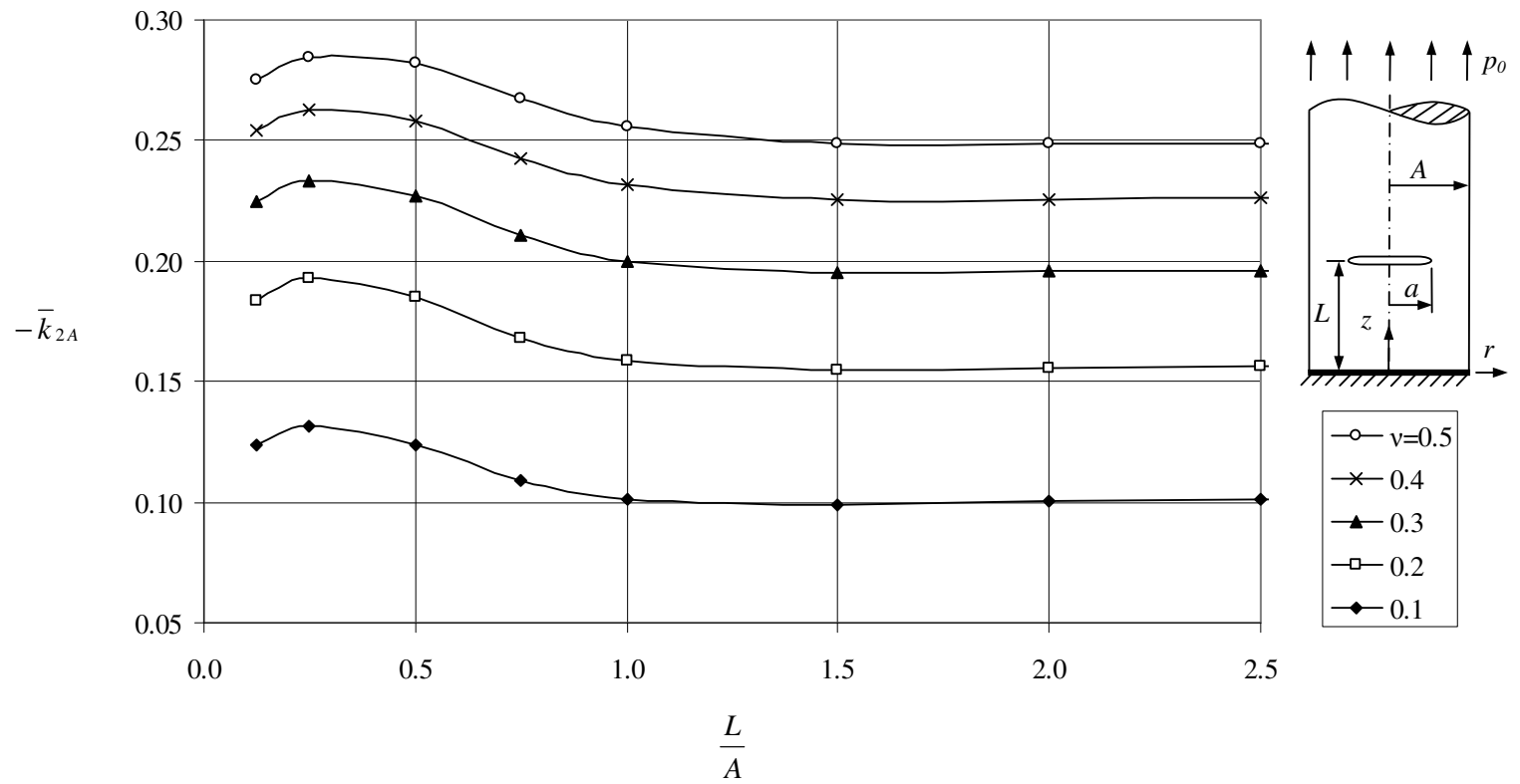Figure 6.45 Normalized Mode I stress intensity factor $\overline{k}_{1A}$ at the edge of rigid support.
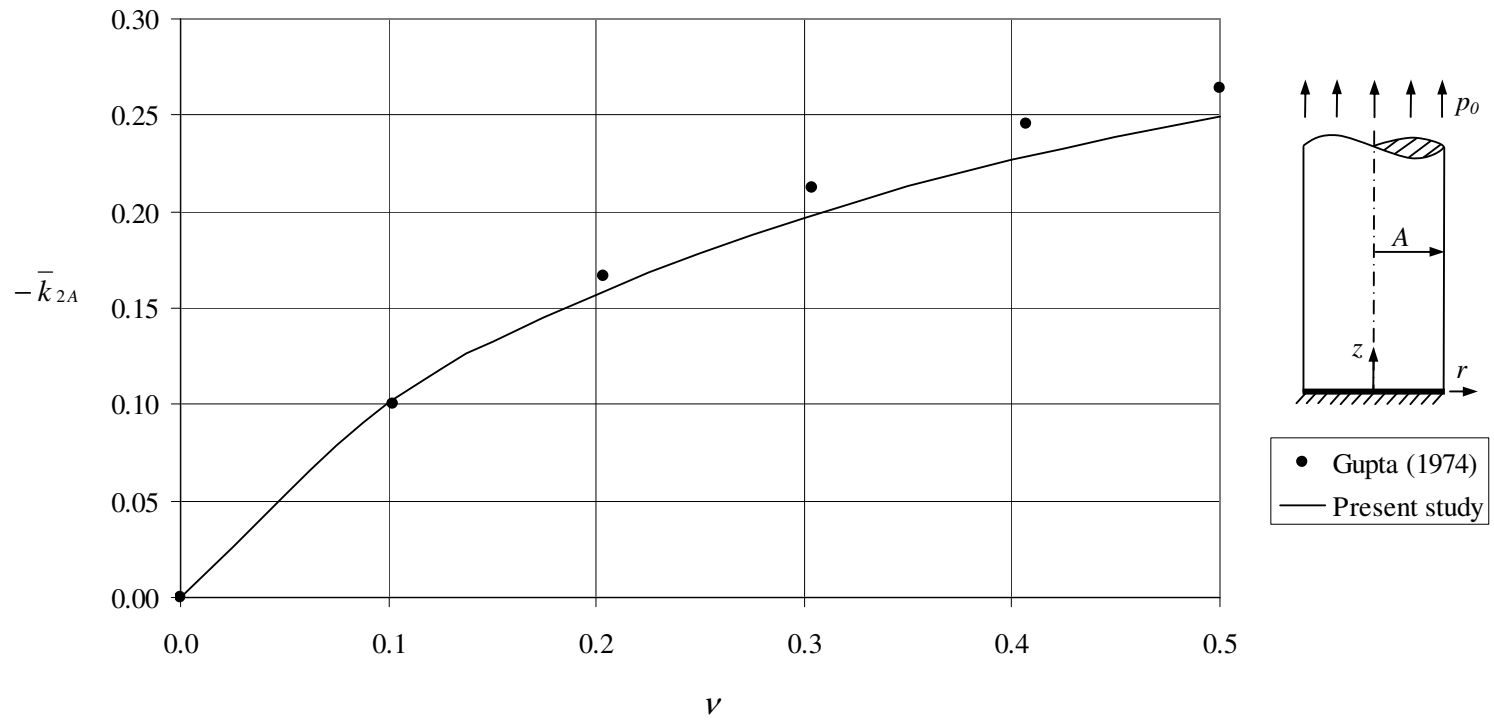
Figure 6.46 Normalized Mode II stress intensity factor $\overline{k}_{2A}$ at the edge of rigid support.
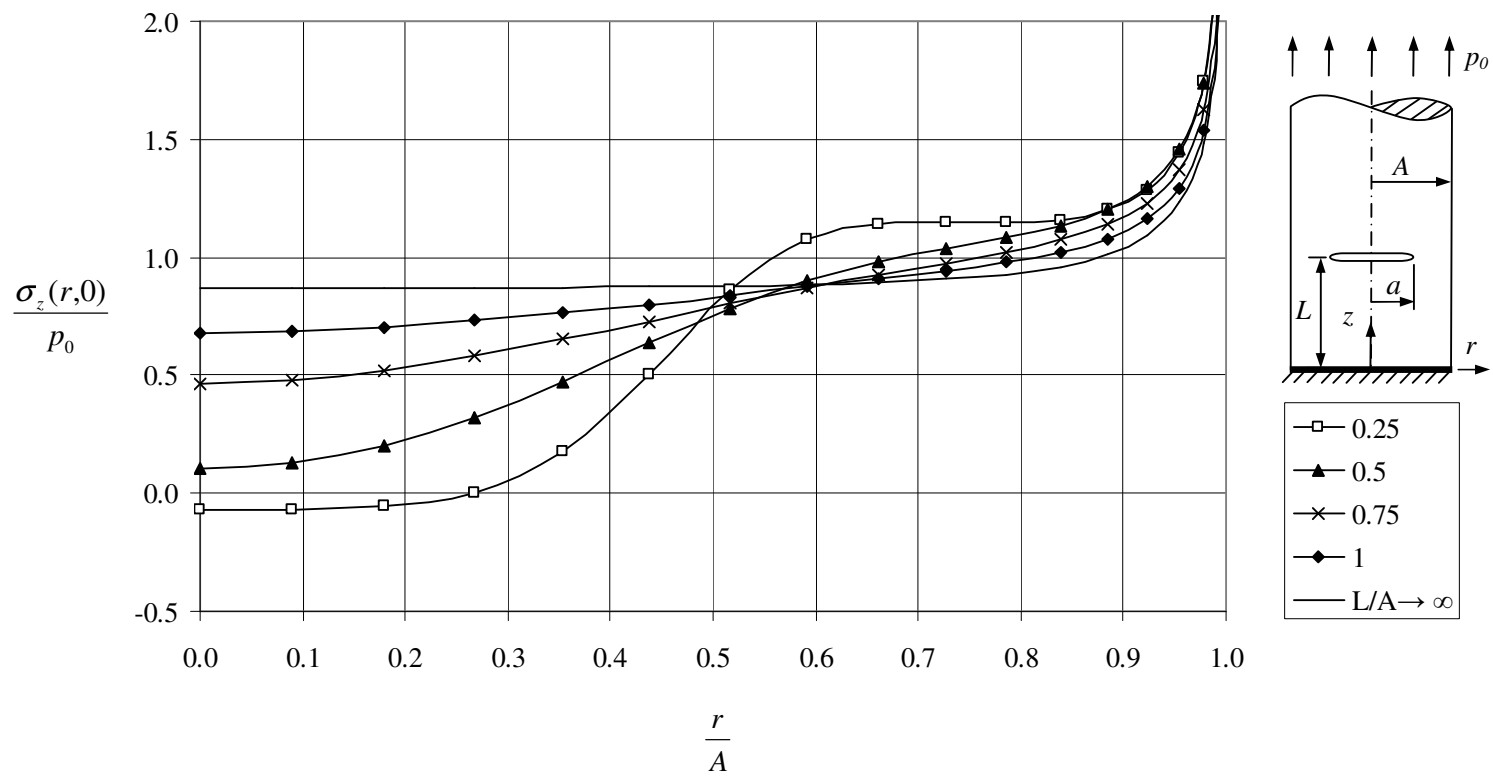
Figure 6.47 Normal stress $\sigma_z(r,0)$ along the rigid support when $a = 0.5A$, $\nu = 0.3$.
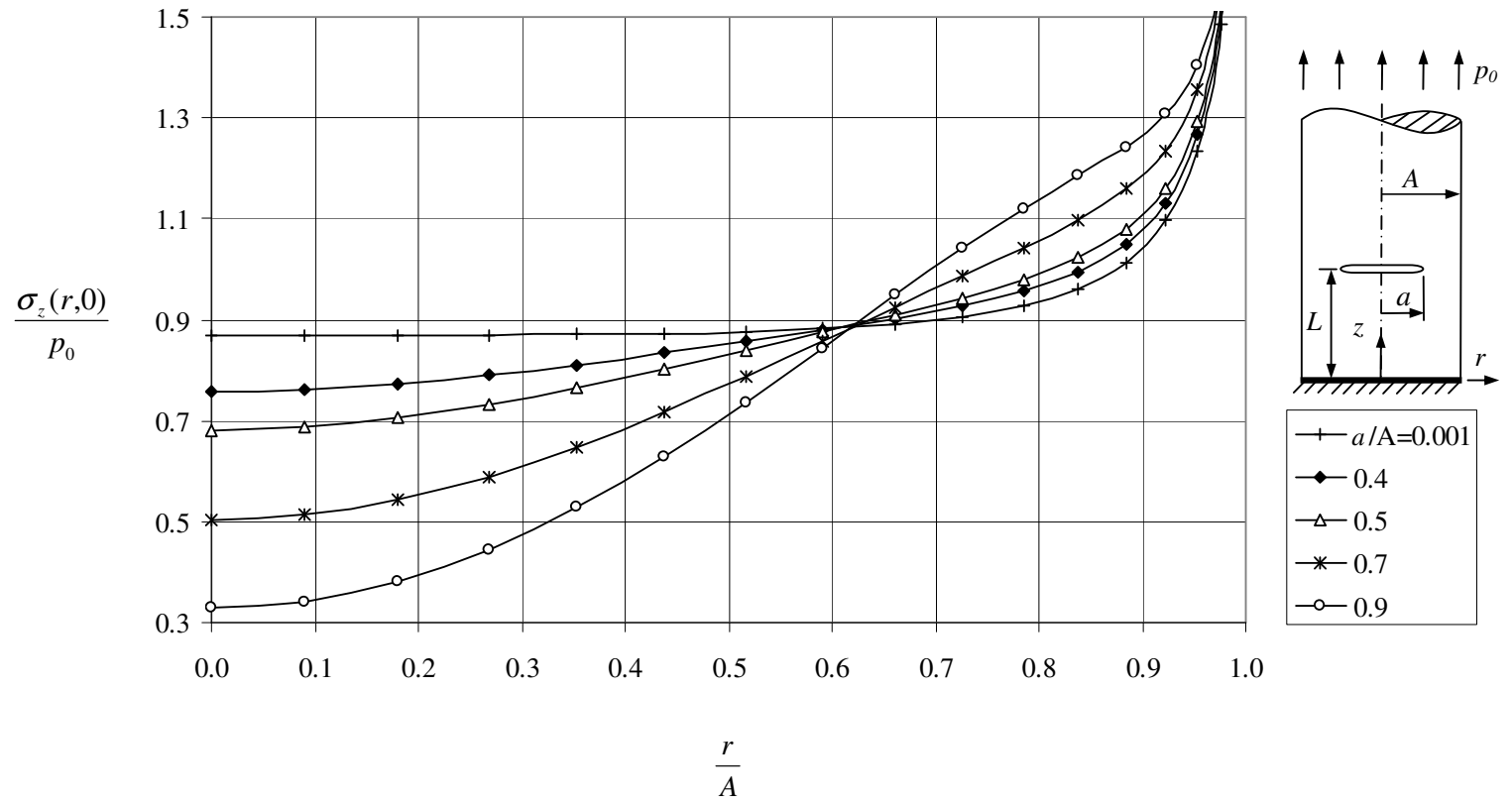
Figure 6.48 Normal stress $\sigma_z(r,0)$ along the rigid support when $L = A$, $v = 0.3$.
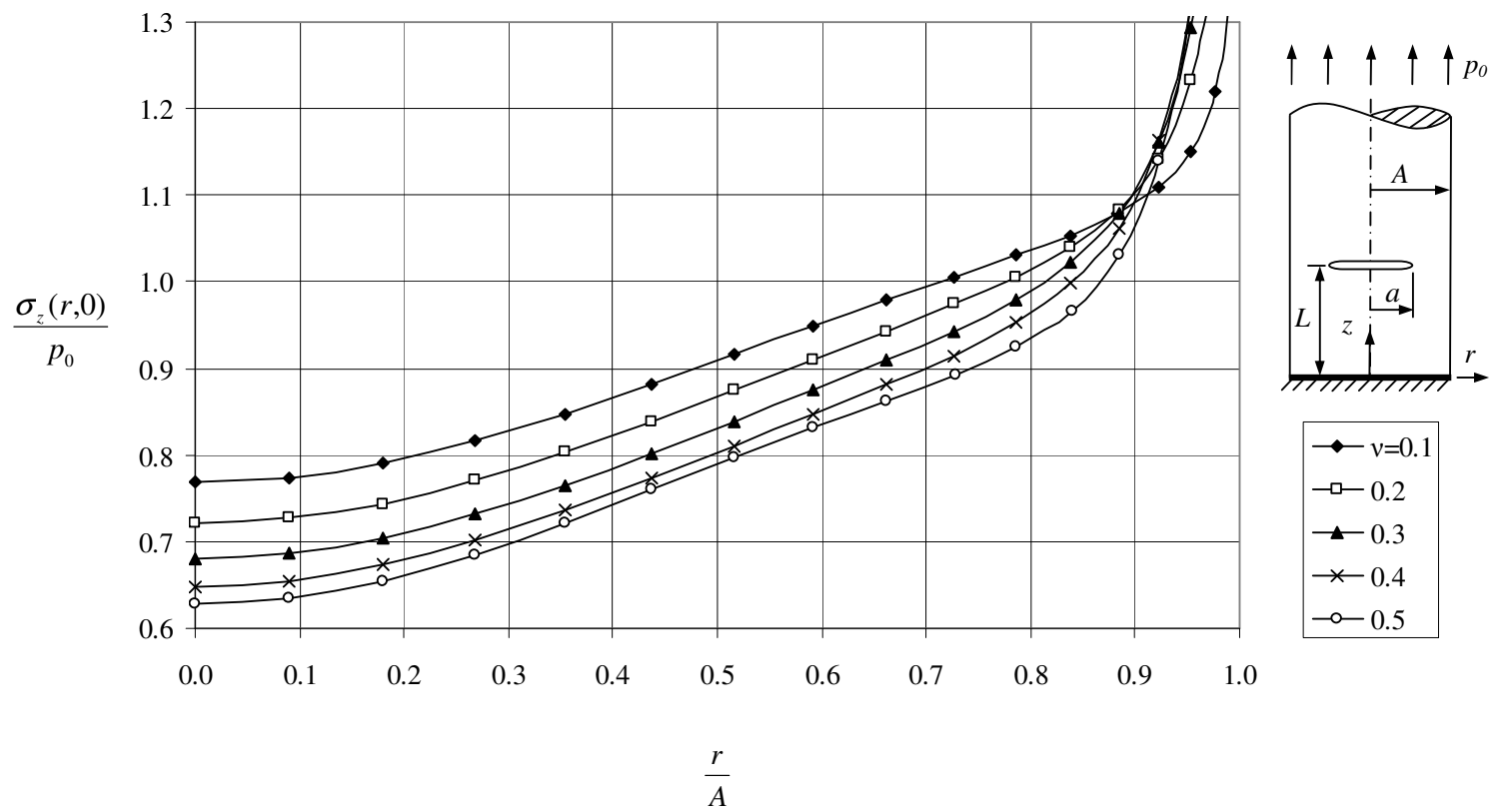
Figure 6.49 Normal stress $\sigma_z(r,0)$ along the rigid support when $a = 0.5A$, $L = A$.
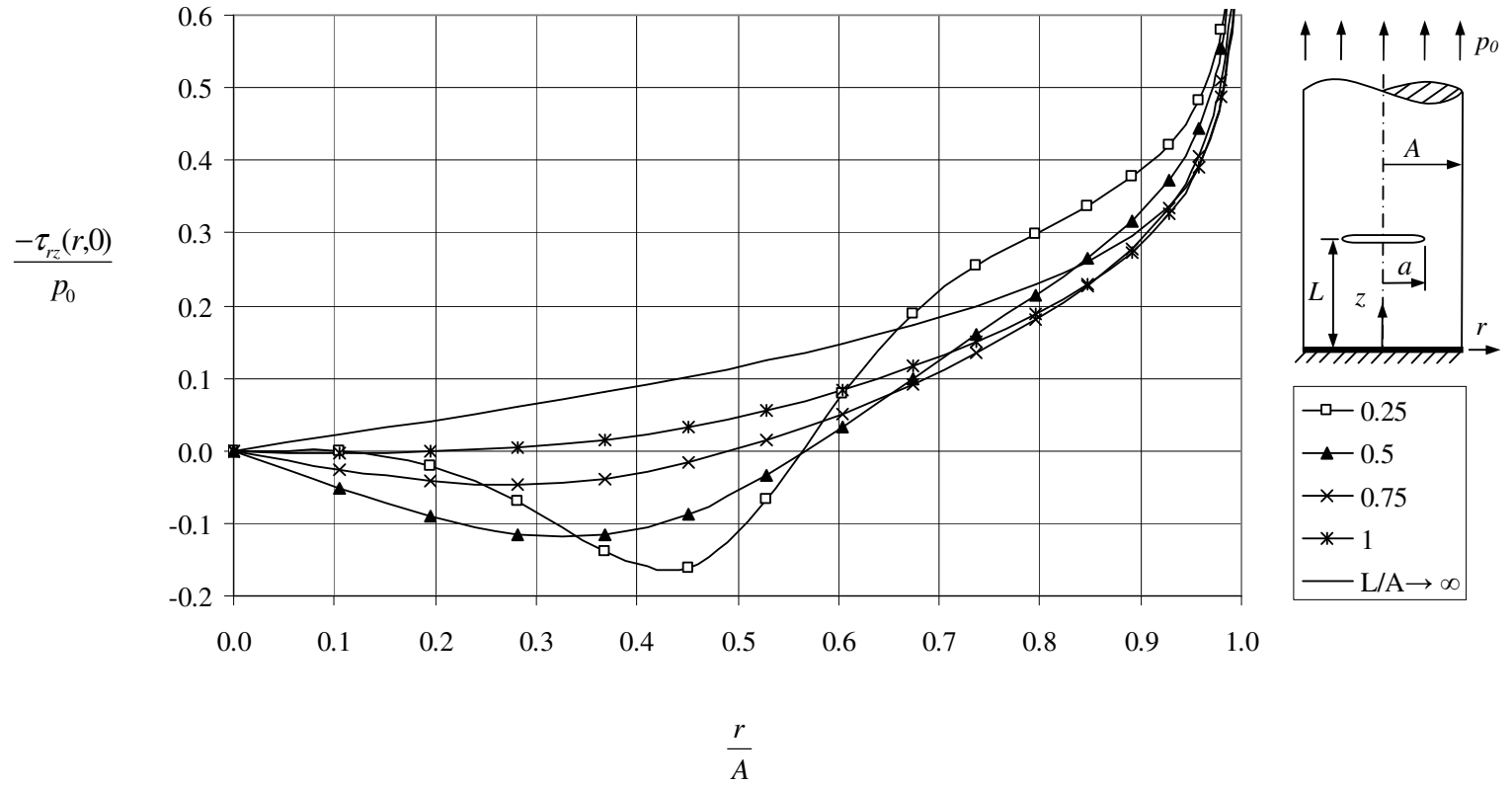
Figure 6.50 Shearing stress $\tau_{rz}(r,0)$ along the rigid support when $a = 0.5A$, $\nu = 0.3$.
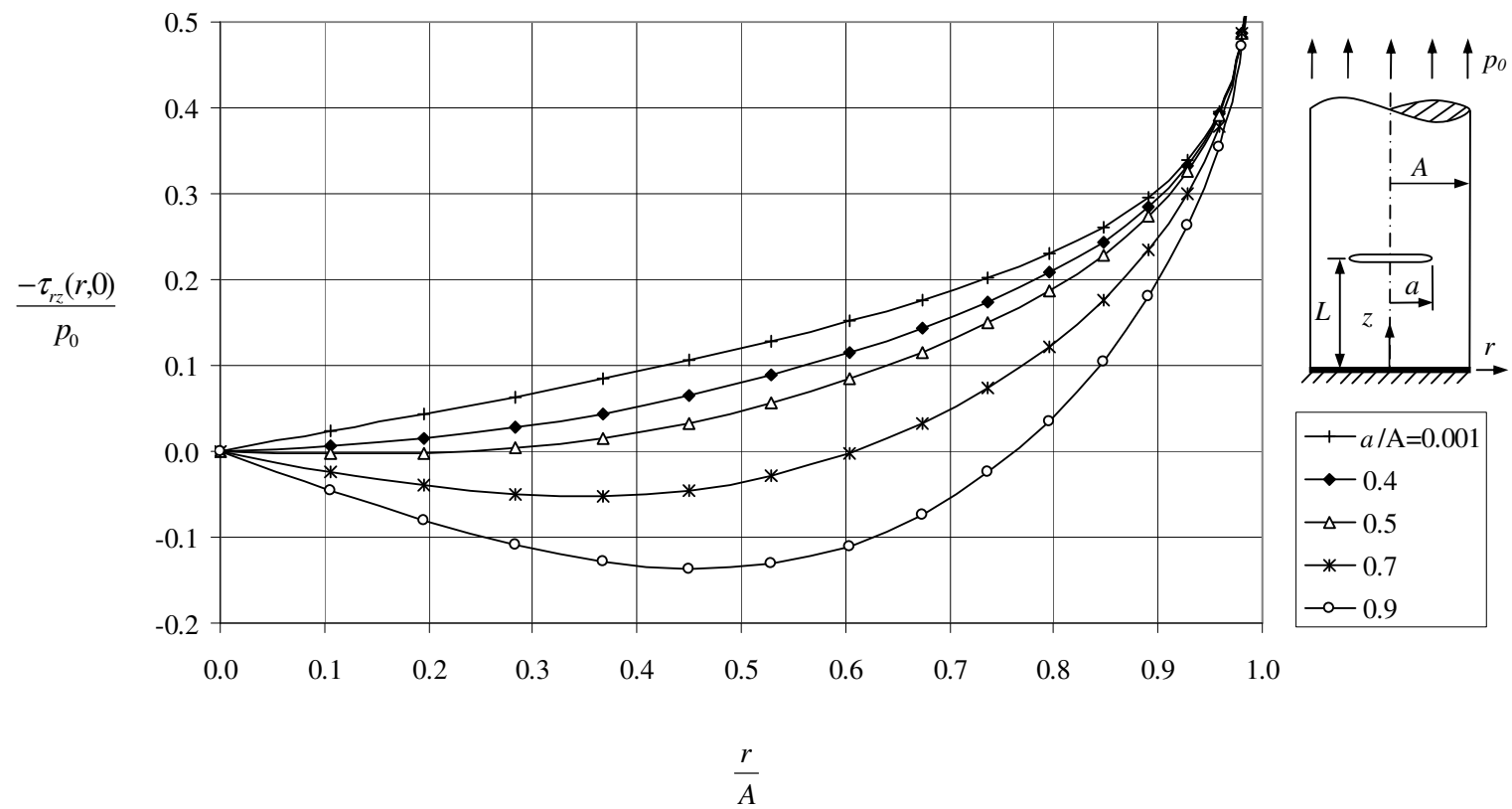
Figure 6.51 Shearing stress $\tau_{rz}(r,0)$ along the rigid support when $L = A$, $\nu = 0.3$.
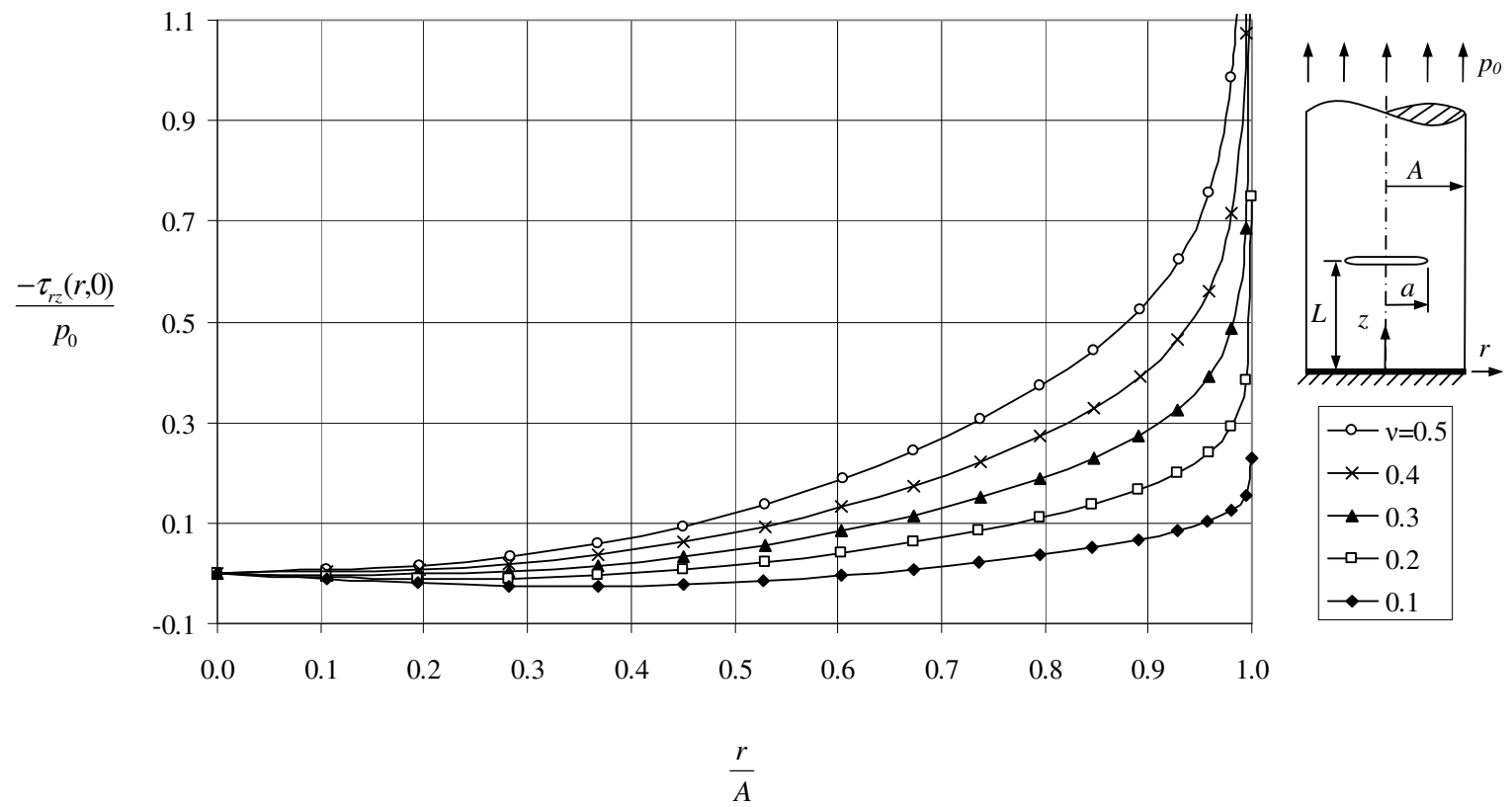
Figure 6.52 Shearing stress $\tau_{rz}(r,0)$ along the rigid support when $a = 0.5A$, $L = A$.
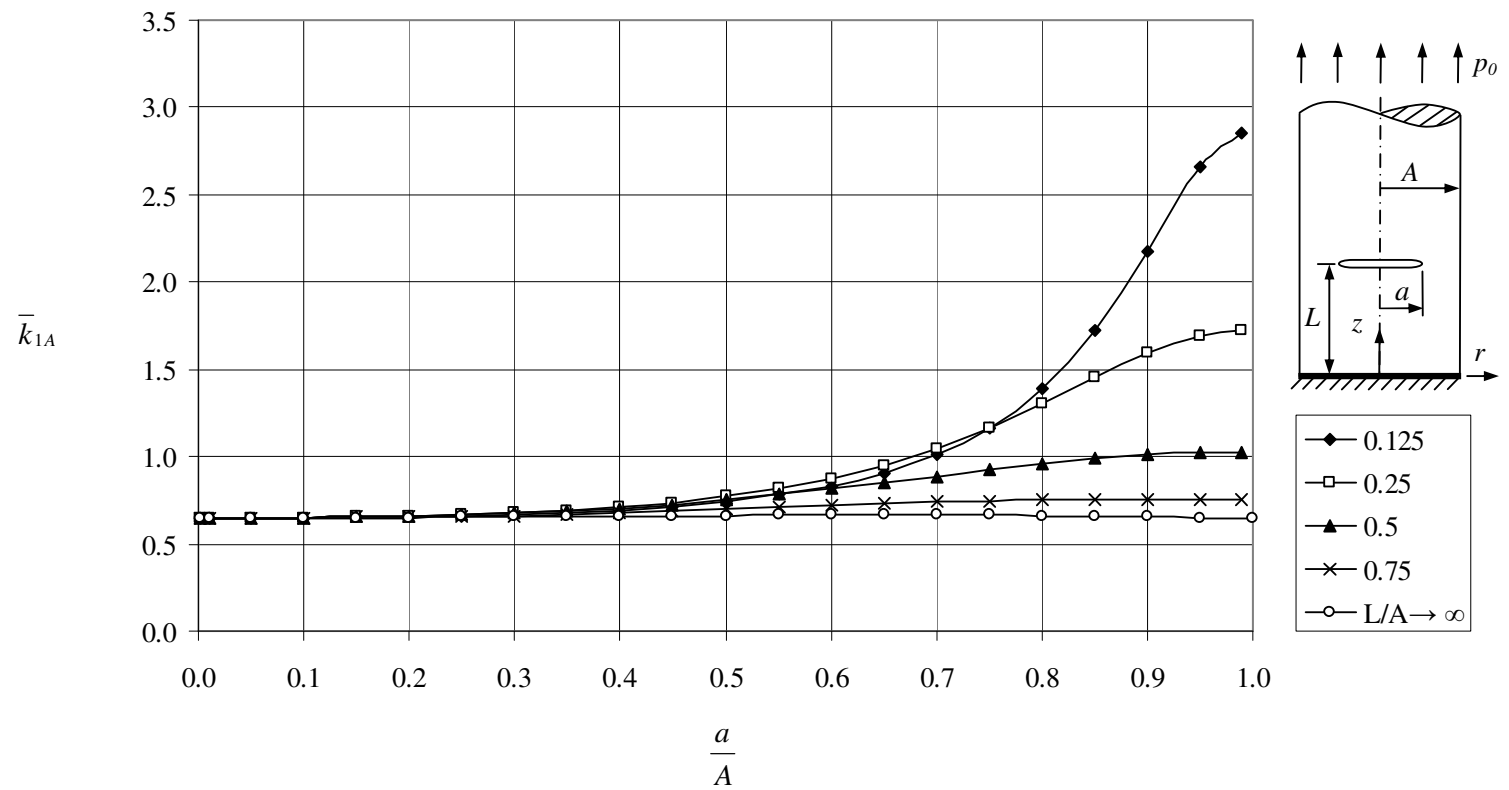
Figure 6.53 Normalized Mode I stress intensity factor $\overline{k}_{1A}$ at the edge of rigid support when $\nu = 0.3$.
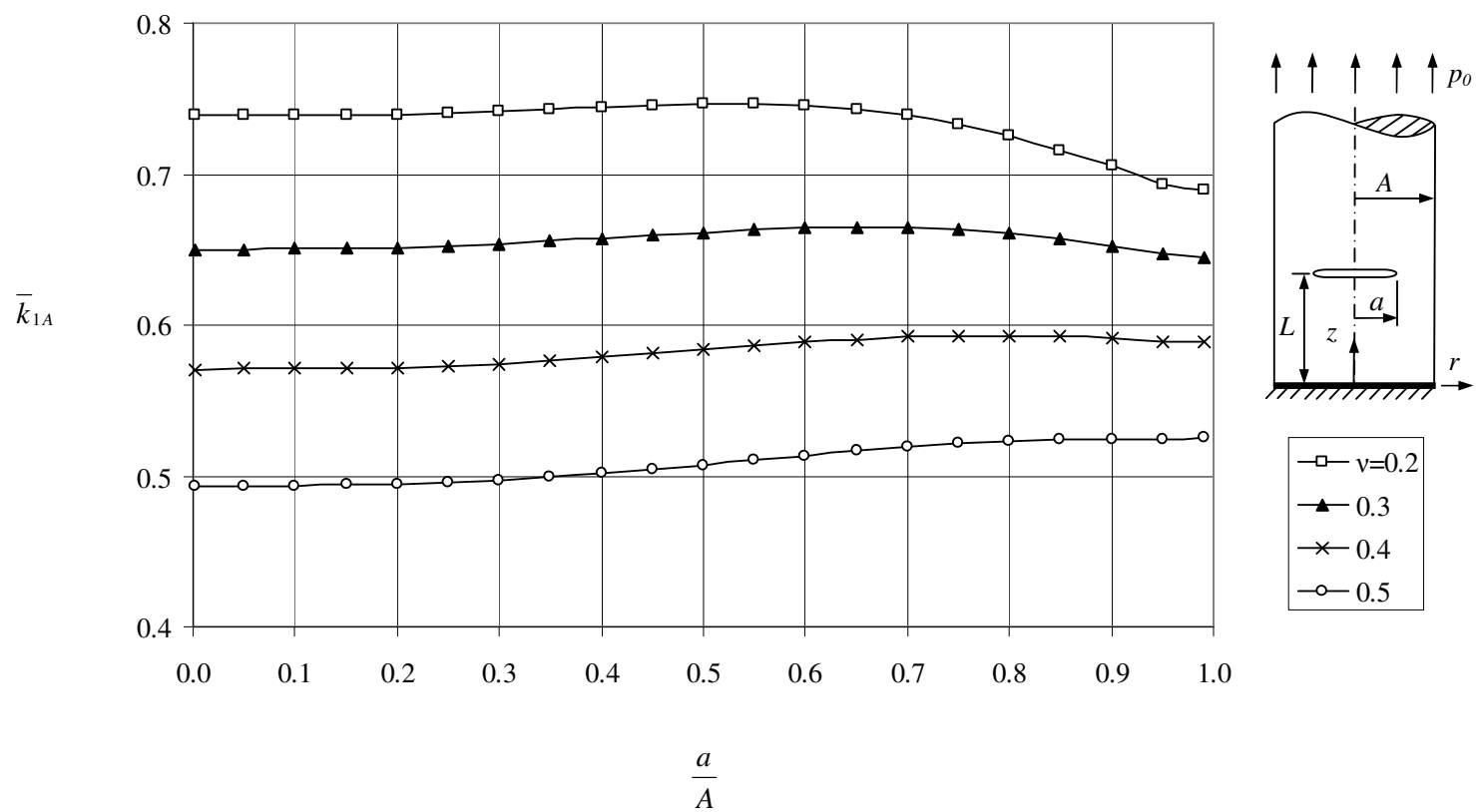
Figure 6.54 Normalized Mode I stress intensity factor $\bar{k}_{1A}$ at the edge of rigid support when $L = A$.
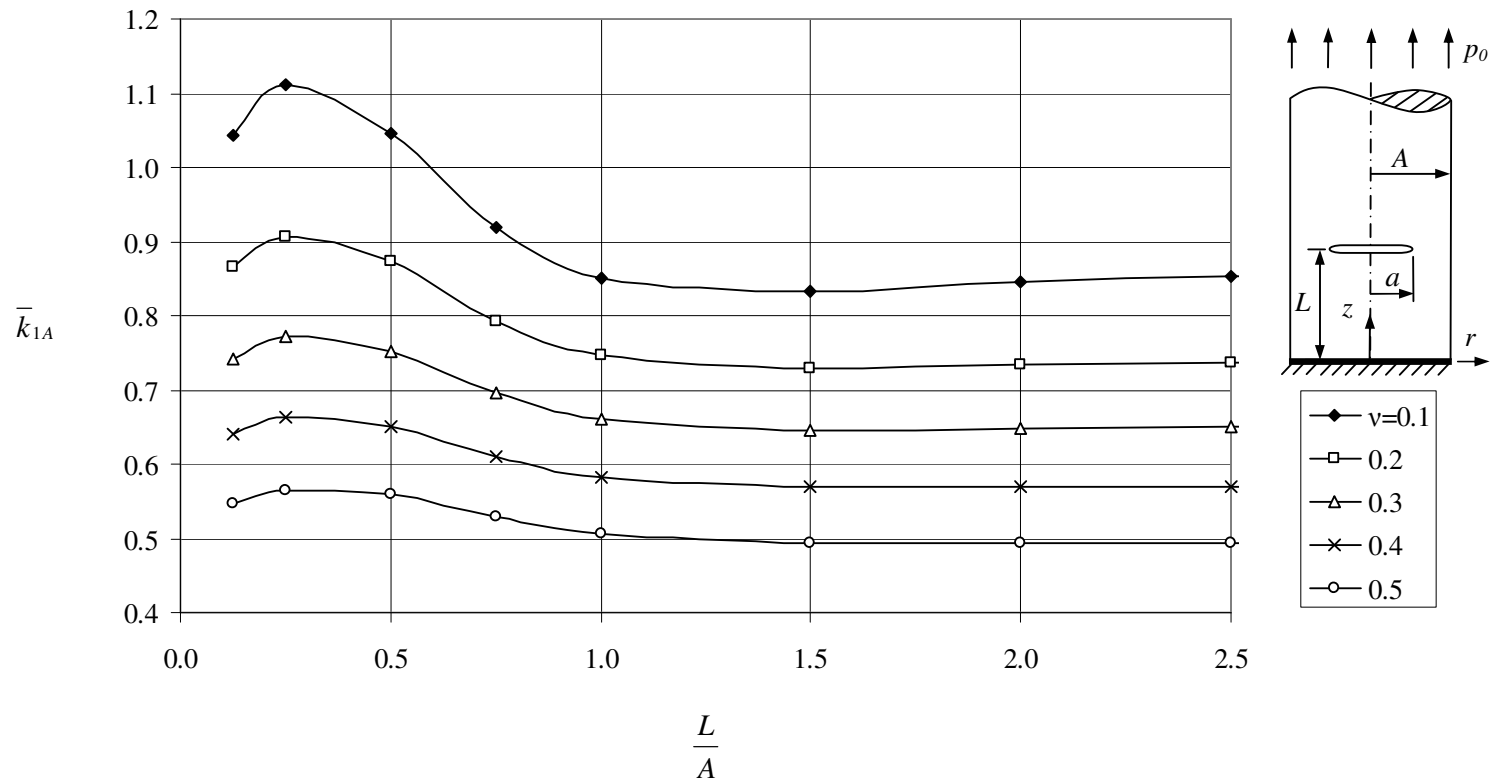
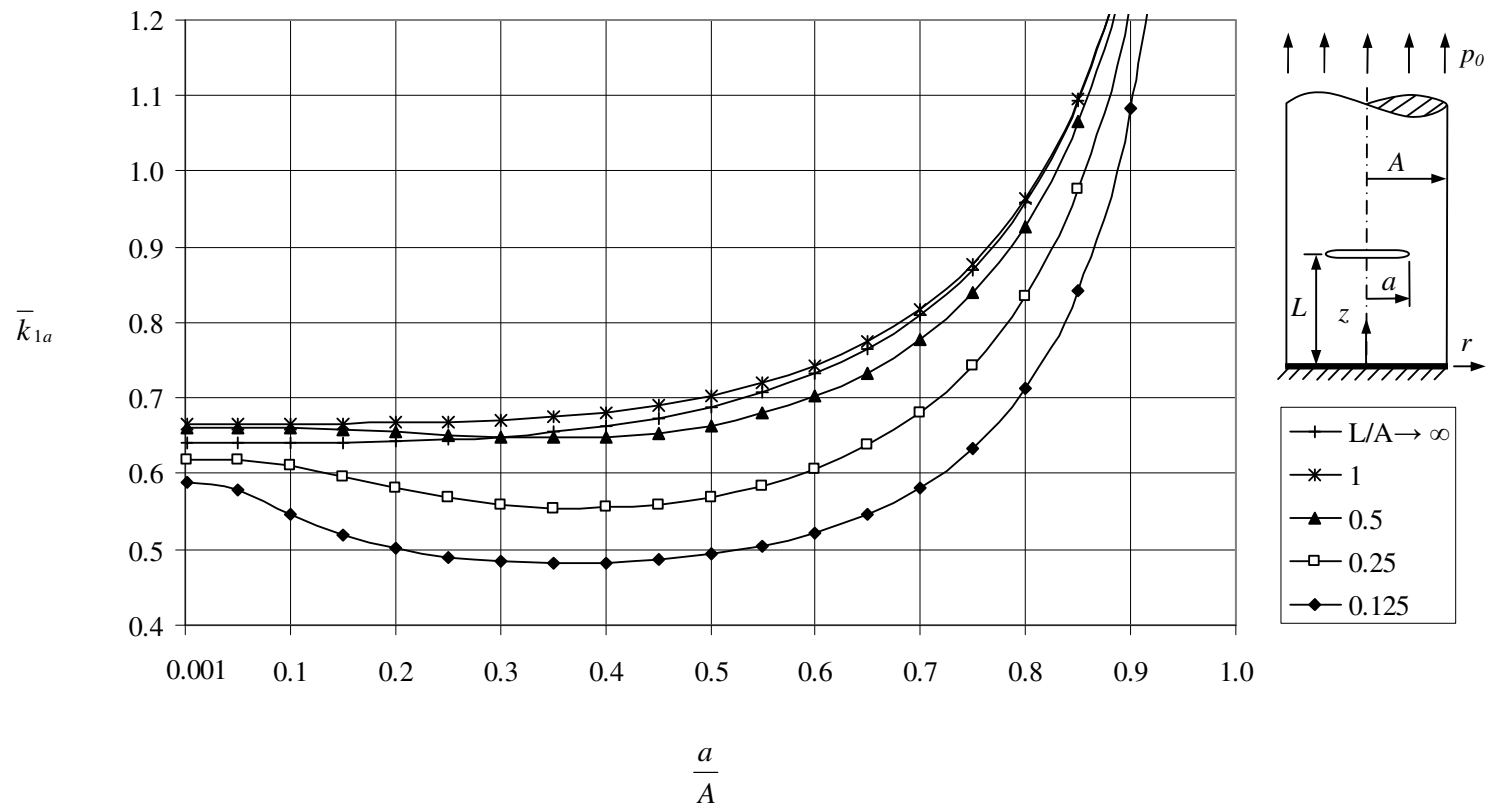Figure 6.55 Normalized Mode I stress intensity factor $\bar{k}_{1A}$ at the edge of rigid support when $a = 0.5A$.
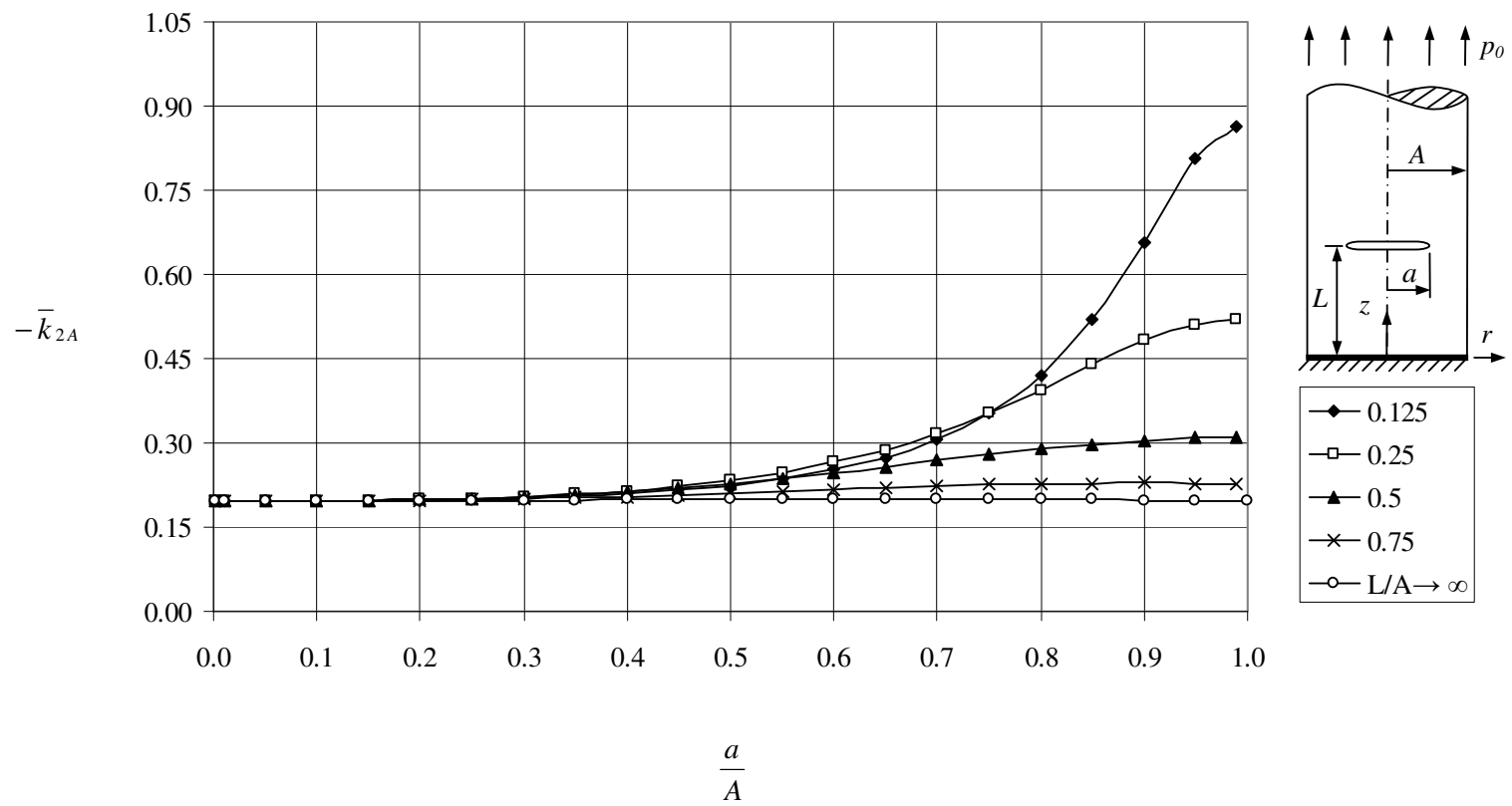
Figure 6.56 Normalized Mode II stress intensity factor $\bar{k}_{2A}$ at the edge of rigid support when $\nu = 0.3$.

Figure 6.57 Normalized Mode II stress intensity factor $\bar{k}_{2A}$ at the edge of rigid support when $L = A$.

Figure 6.58 Normalized Mode II stress intensity factor $\bar{k}_{2A}$ at the edge of rigid support when $a = 0.5A$.
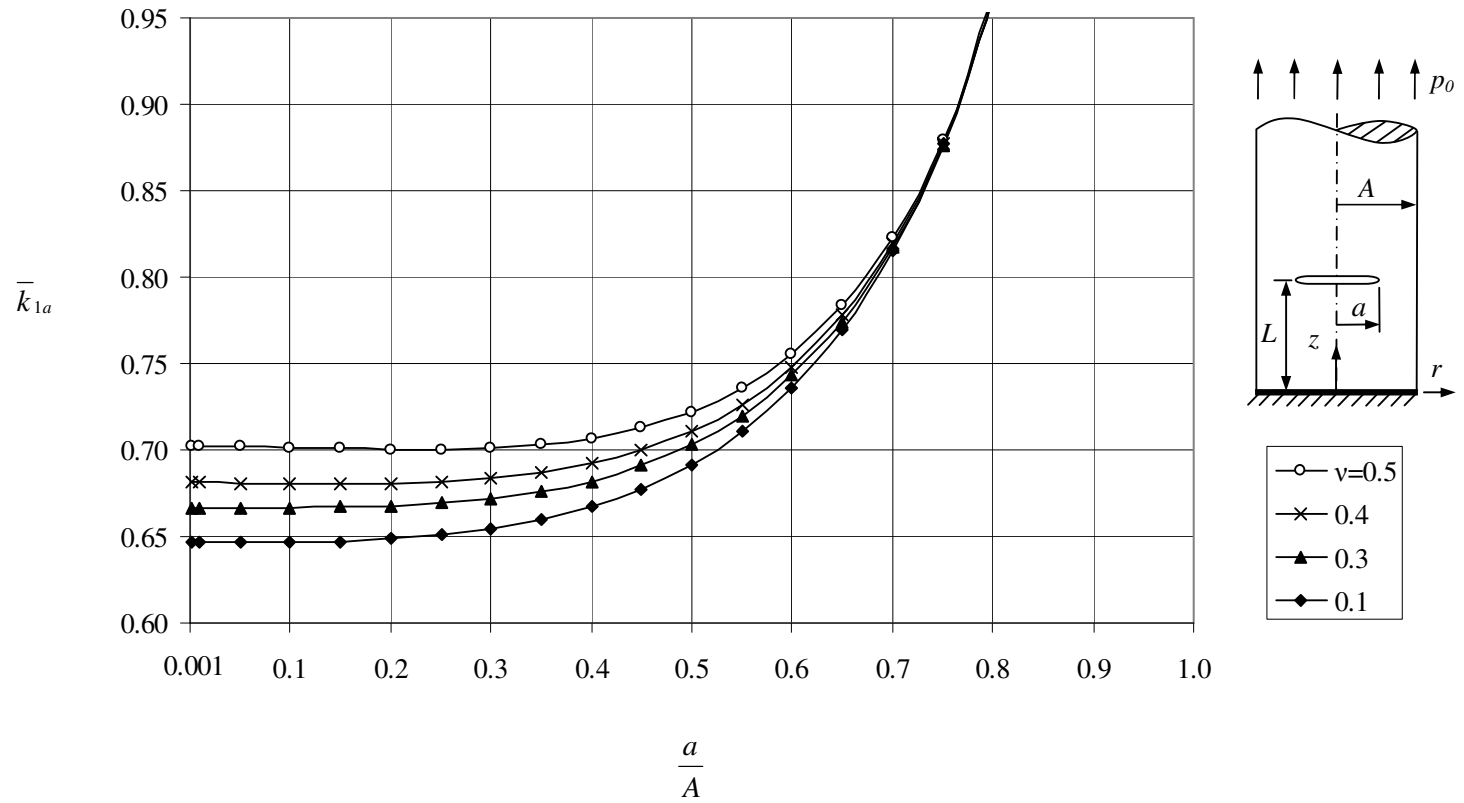
Figure 6.59 Normalized Mode I stress intensity factor $\bar{k}_{1a}$ when $L = A$.

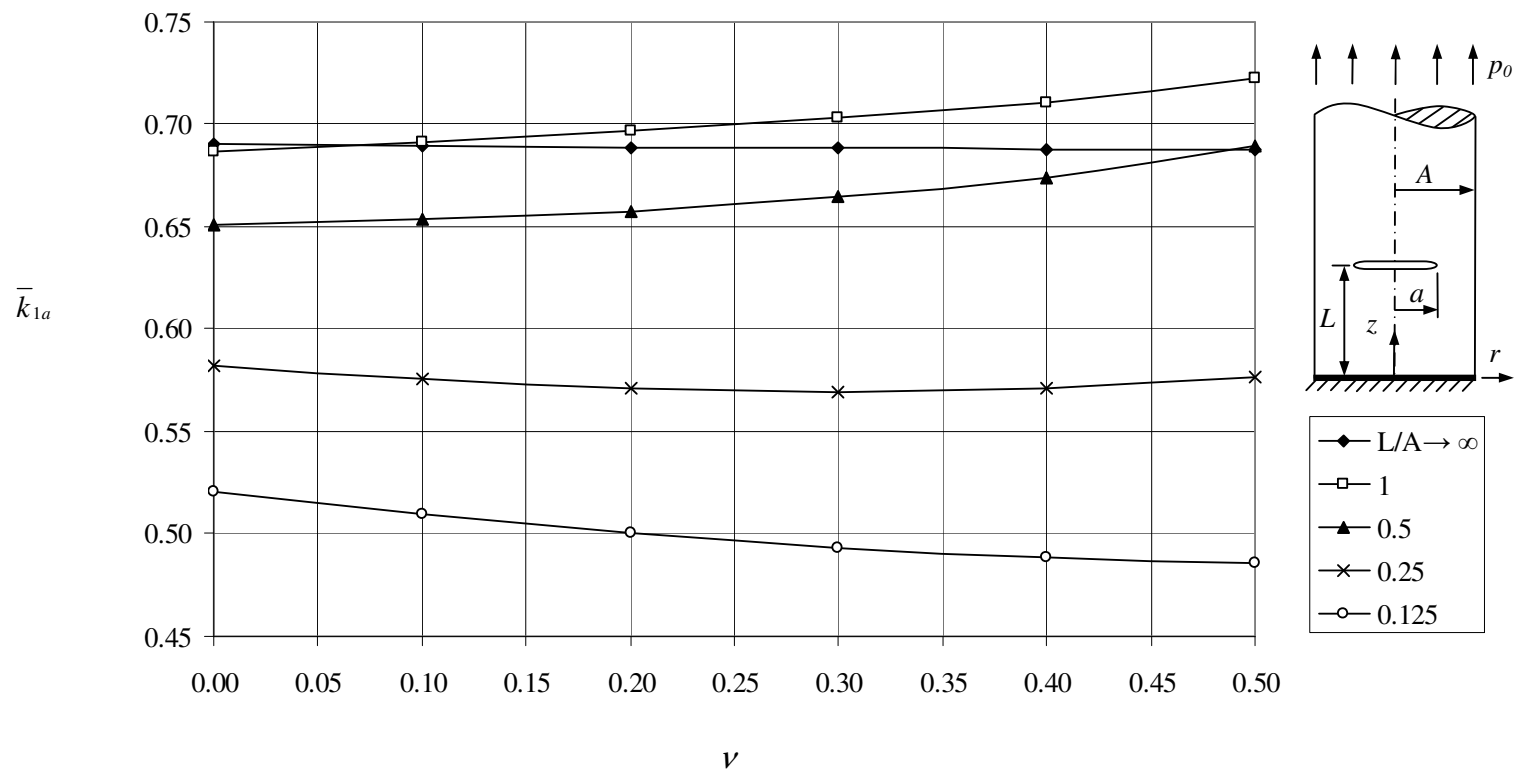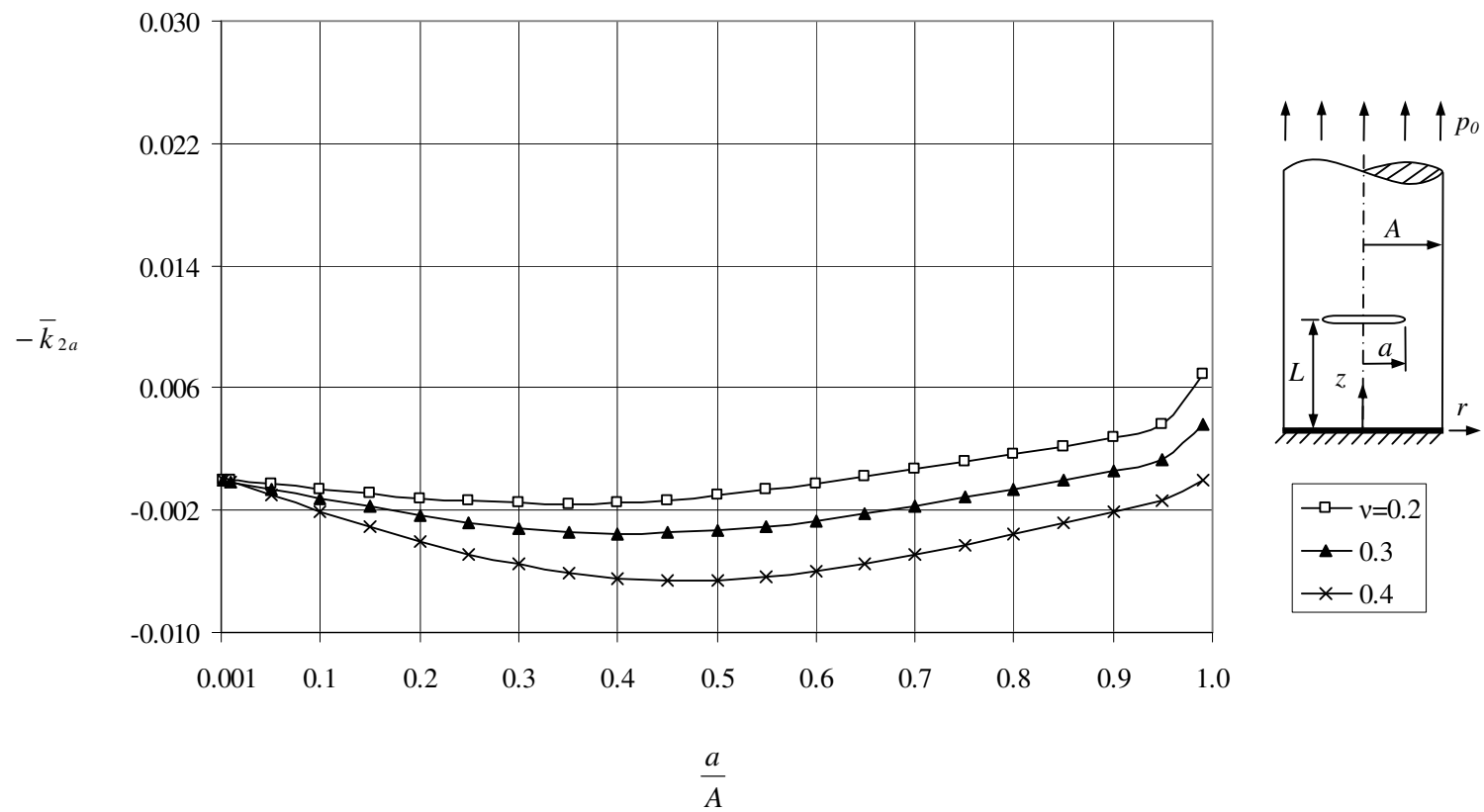Figure 6.60 Normalized Mode I stress intensity factor $\overline{k}_{1a}$ when $\nu = 0.3$.
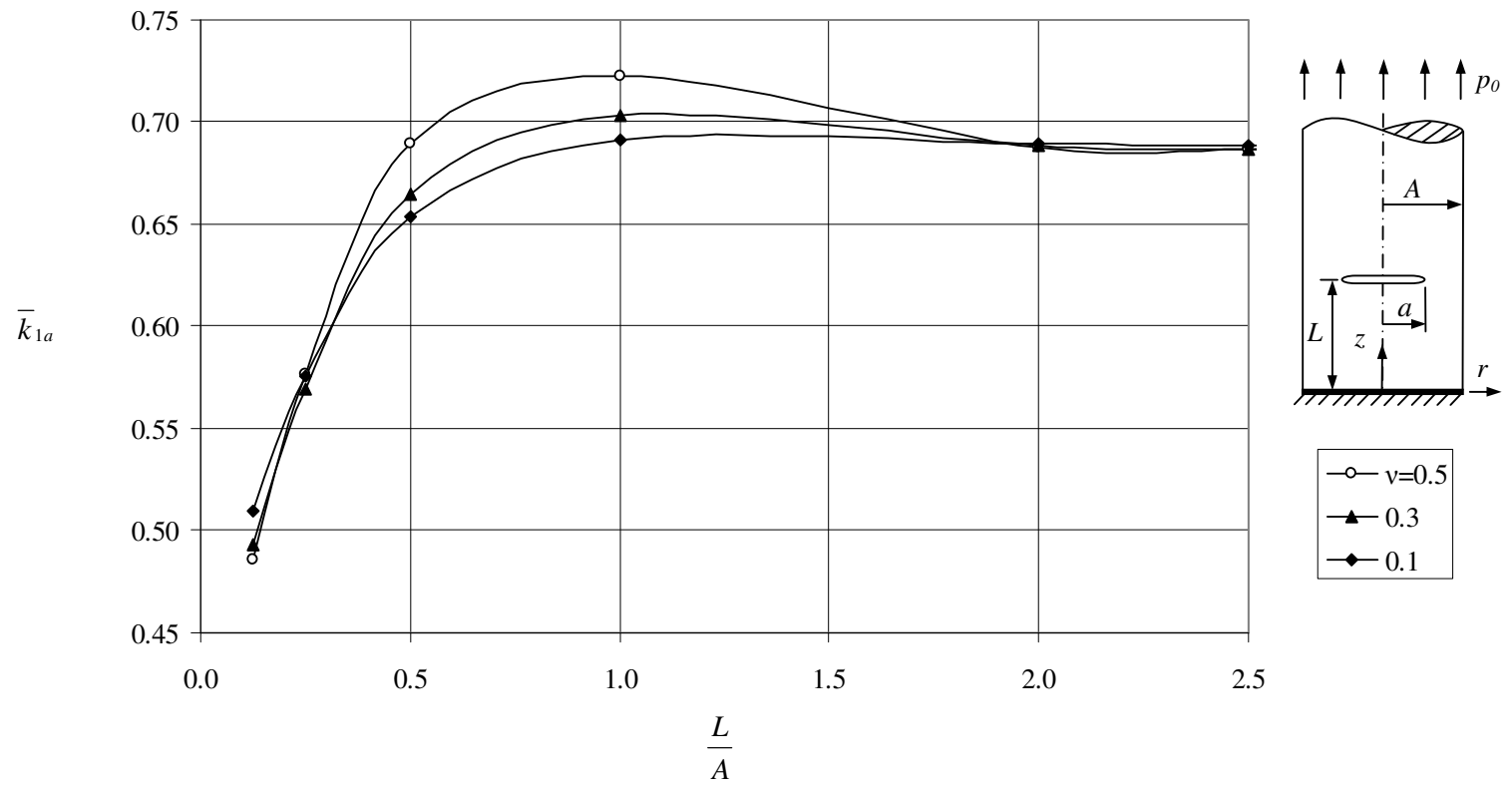
Figure 6.61 Normalized Mode I stress intensity factor $\overline{k}_{1a}$ when $a = 0.5A$.
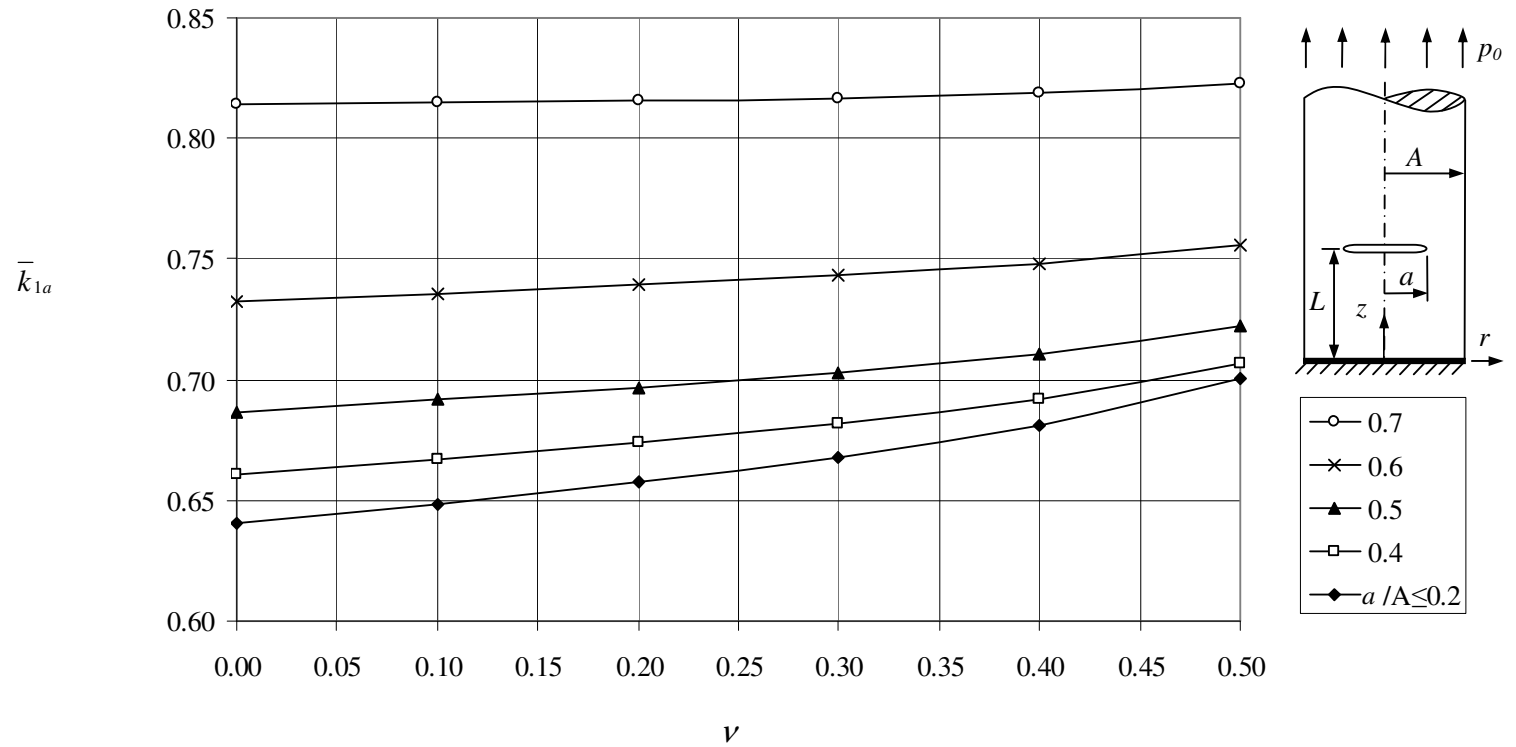
Figure 6.62 Normalized Mode I stress intensity factor $\bar{k}_{1a}$ when $L = A$.

Figure 6.63 Normalized Mode I stress intensity factor $\overline{k}_{1a}$ when $a = 0.5A$.

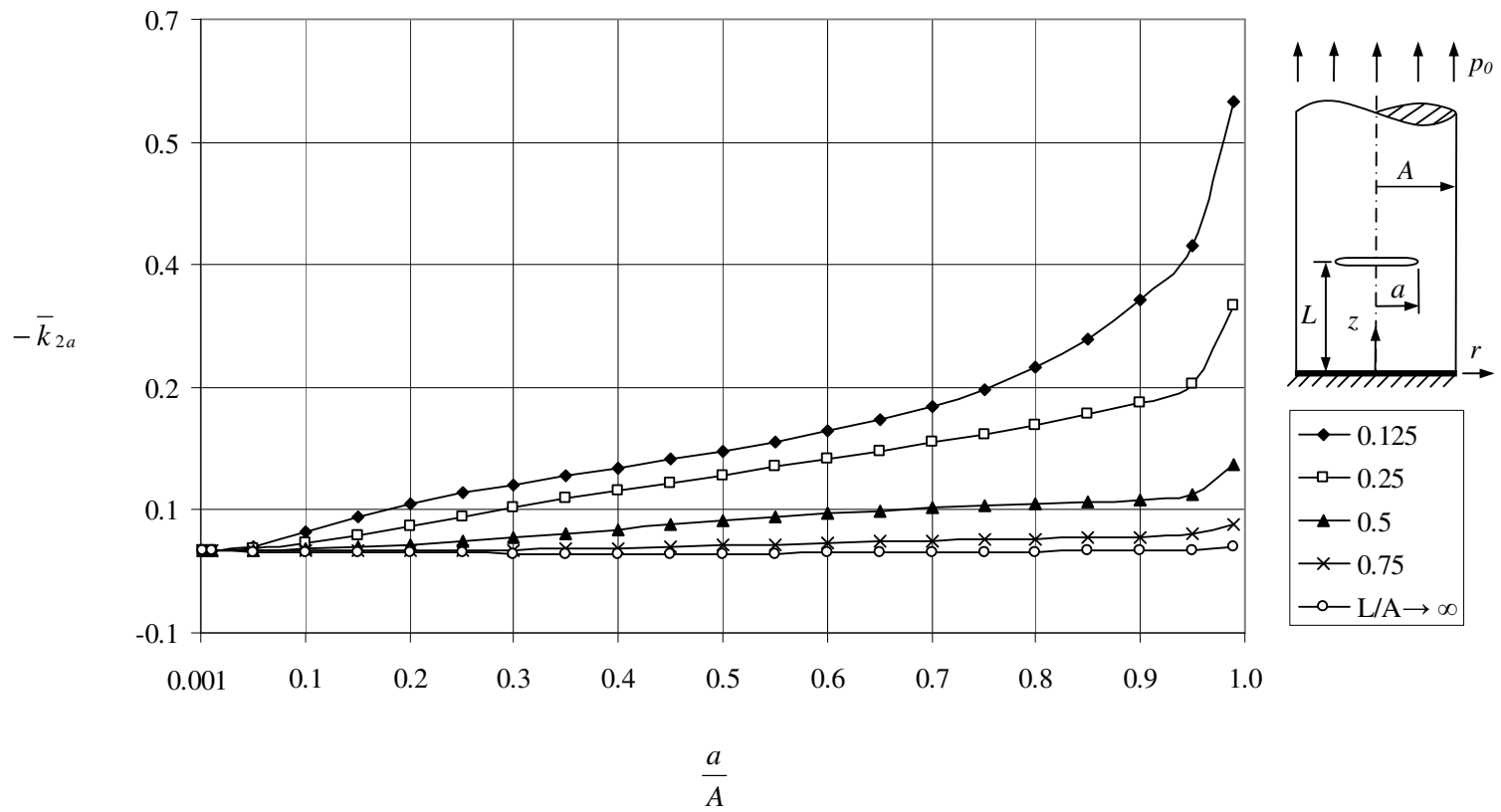Figure 6.64 Normalized Mode II stress intensity factor $\bar{k}_{2a}$ when $L = A$.

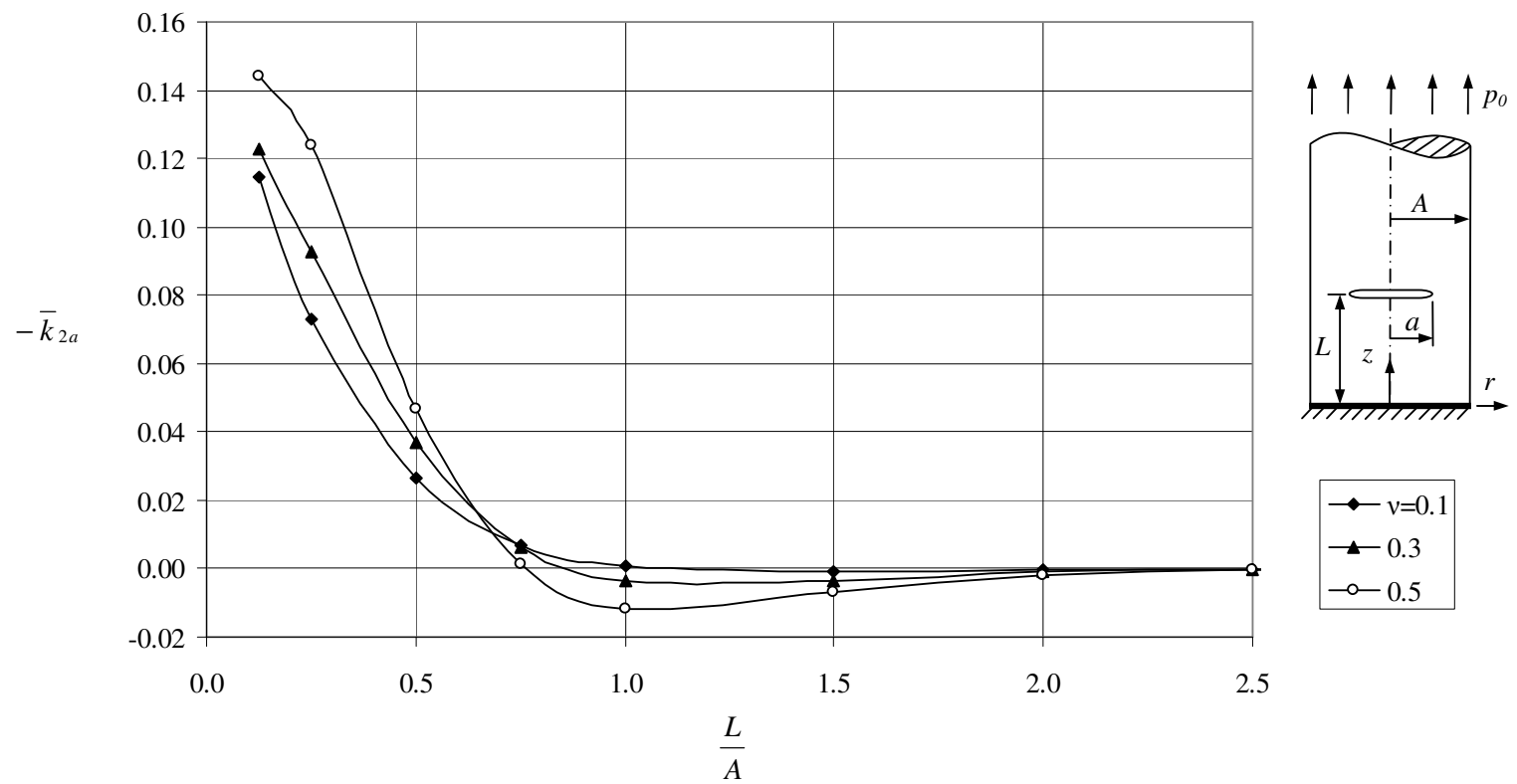Figure 6.65 Normalized Mode II stress intensity factor $\bar{k}_{2a}$ when $\nu = 0.3$.
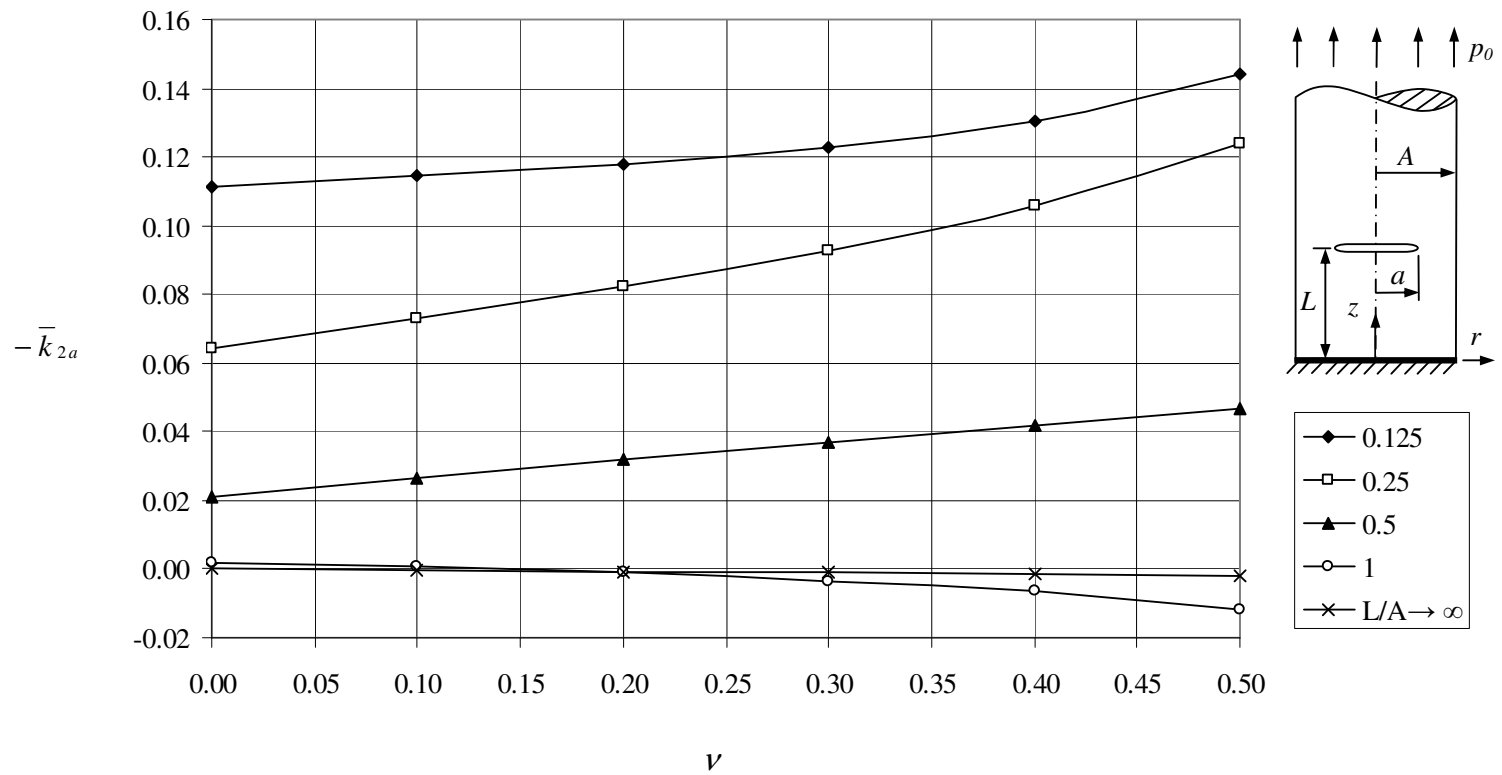
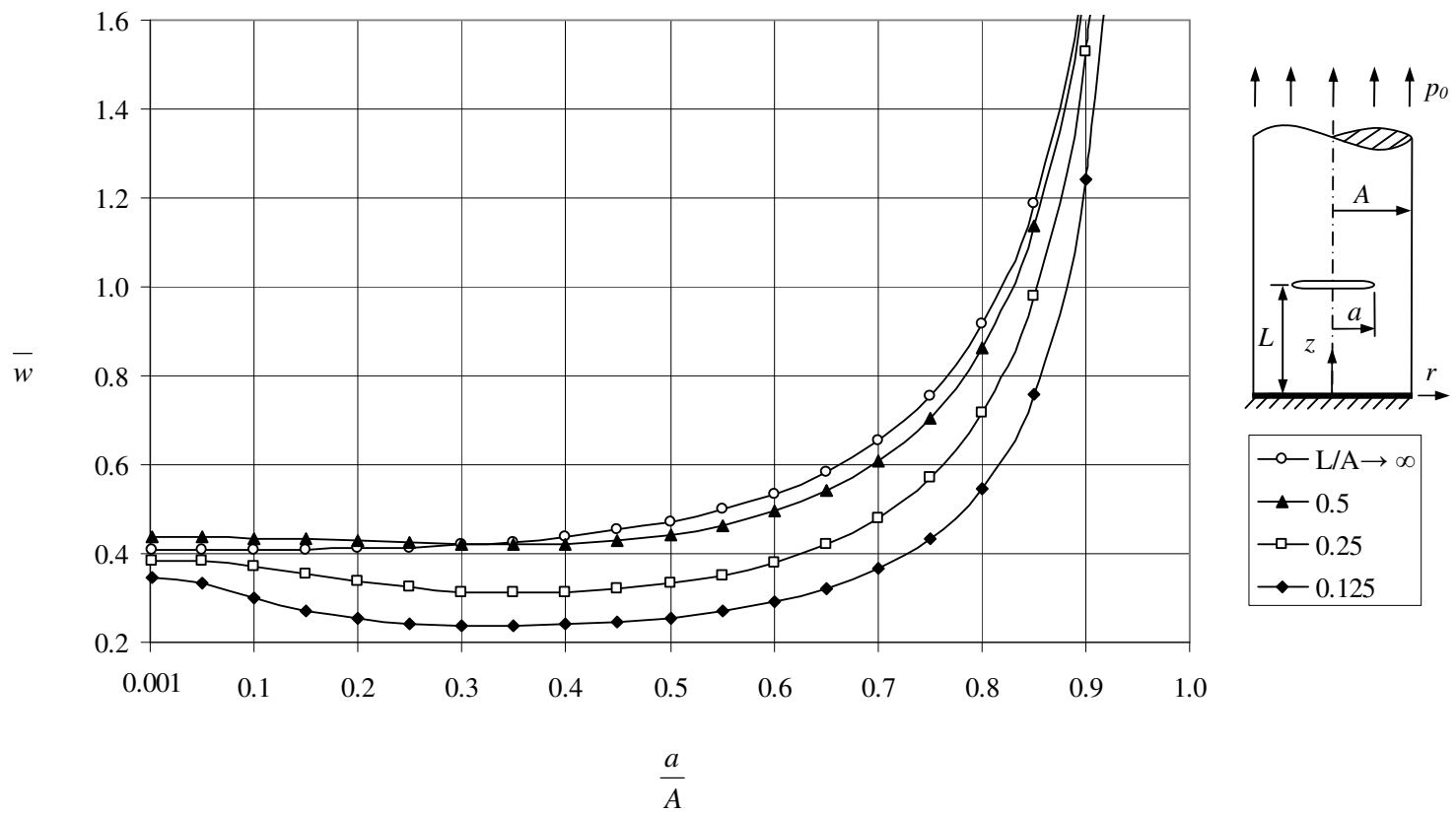Figure 6.66 Normalized Mode II stress intensity factor $\overline{k}_{2a}$ when $a = 0.5A$.

Figure 6.67 Normalized Mode II stress intensity factor $\overline{k}_{2a}$ when $a = 0.5A$.

Figure 6.68 Normalized energy release rate $\overline{w}$ when $\nu = 0.3$.
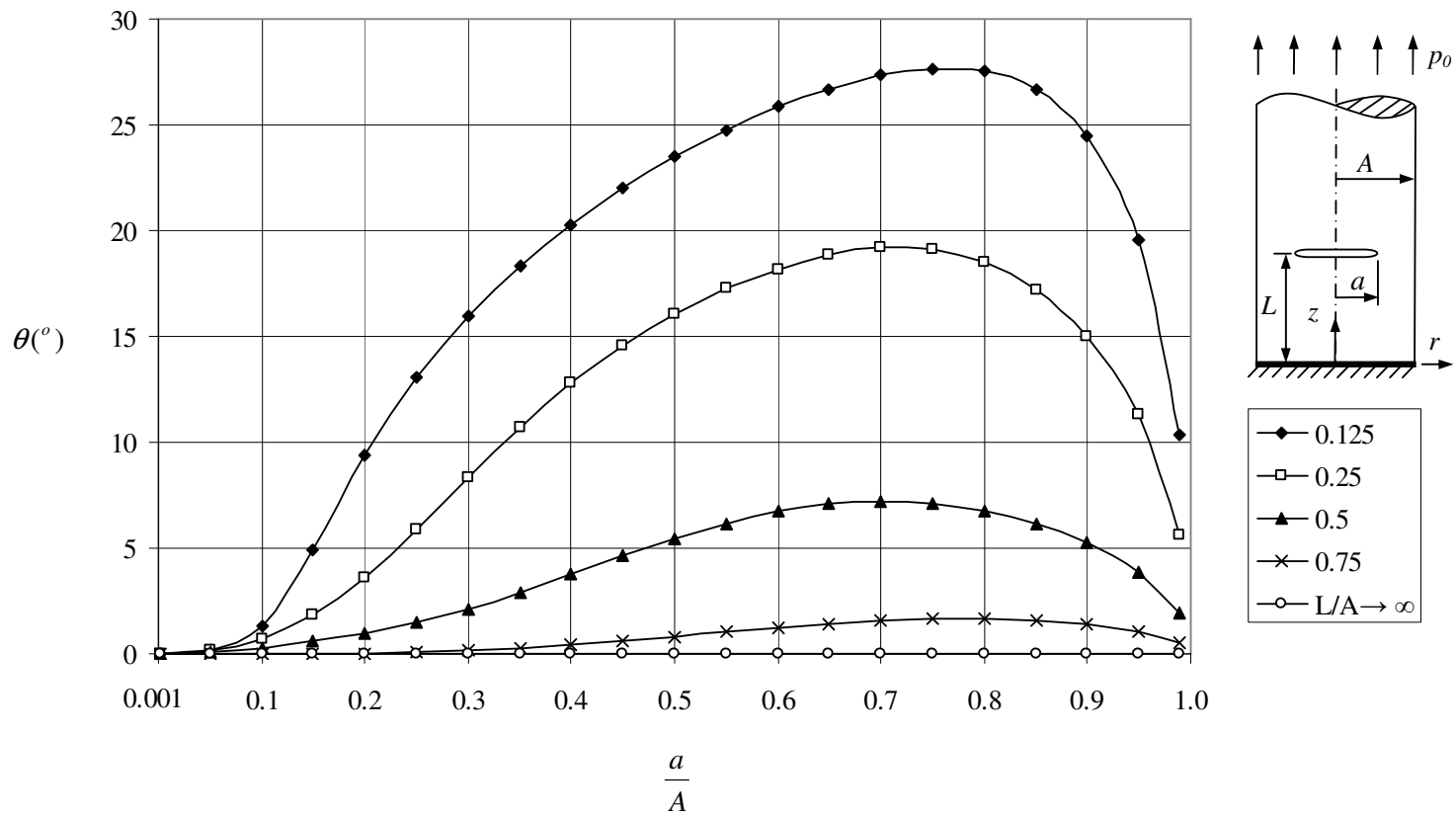
Figure 6.69 Probable crack propagation angle θ when $\nu = 0.3$.

Figure 6.70 Normal stress $\sigma_z(r,0)$ along the rigid support when $\nu = 0.1$.

Figure 6.71 Normal stress $\sigma_z(r,0)$ along the rigid support when $\nu = 0.3$.
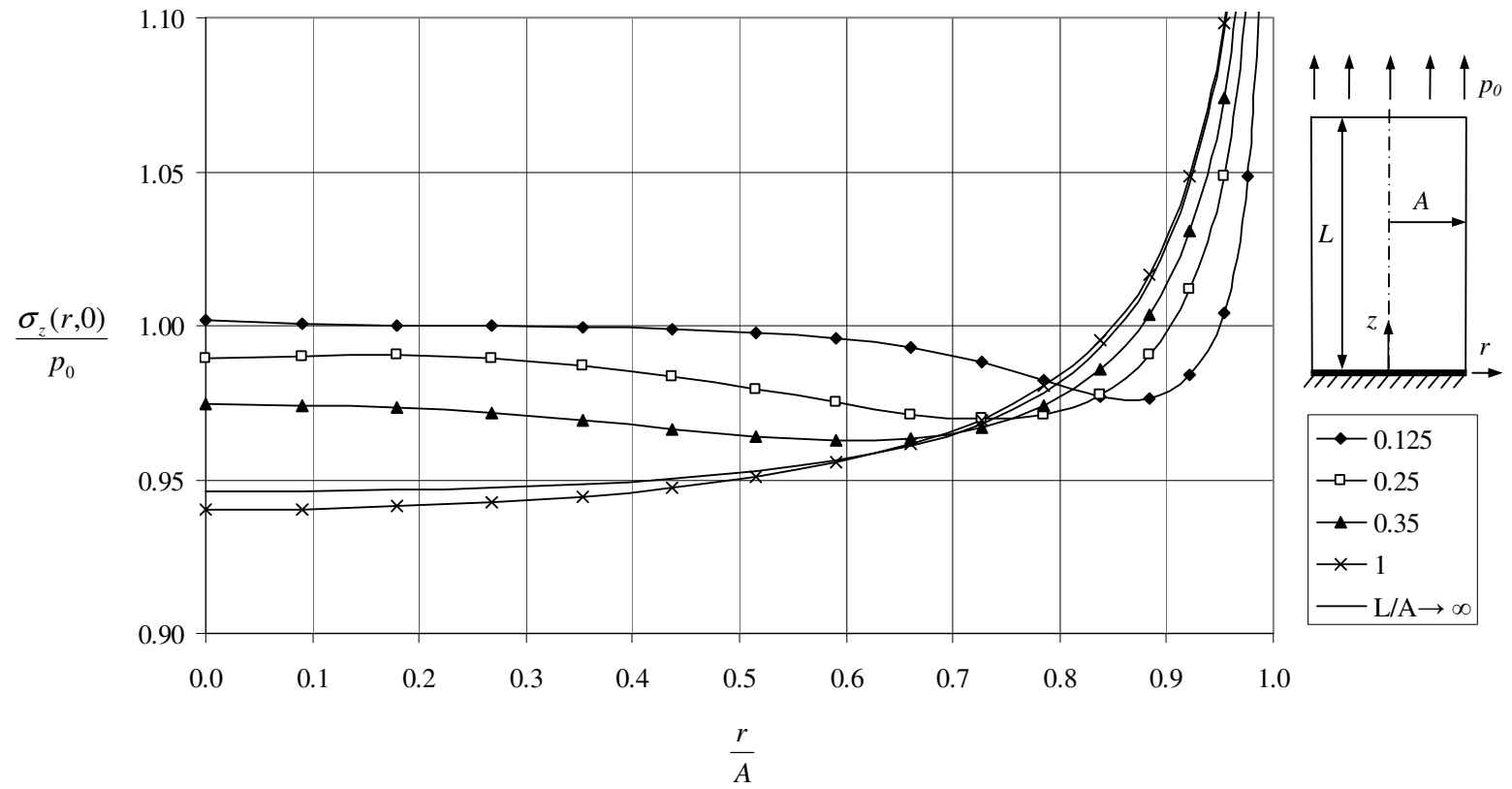
Figure 6.72 Normal stress $\sigma_z(r,0)$ along the rigid support when $\nu = 0.5$.

Figure 6.73 Normal stress $\sigma_z(r,0)$ along the rigid support when $L = 0.25A$.
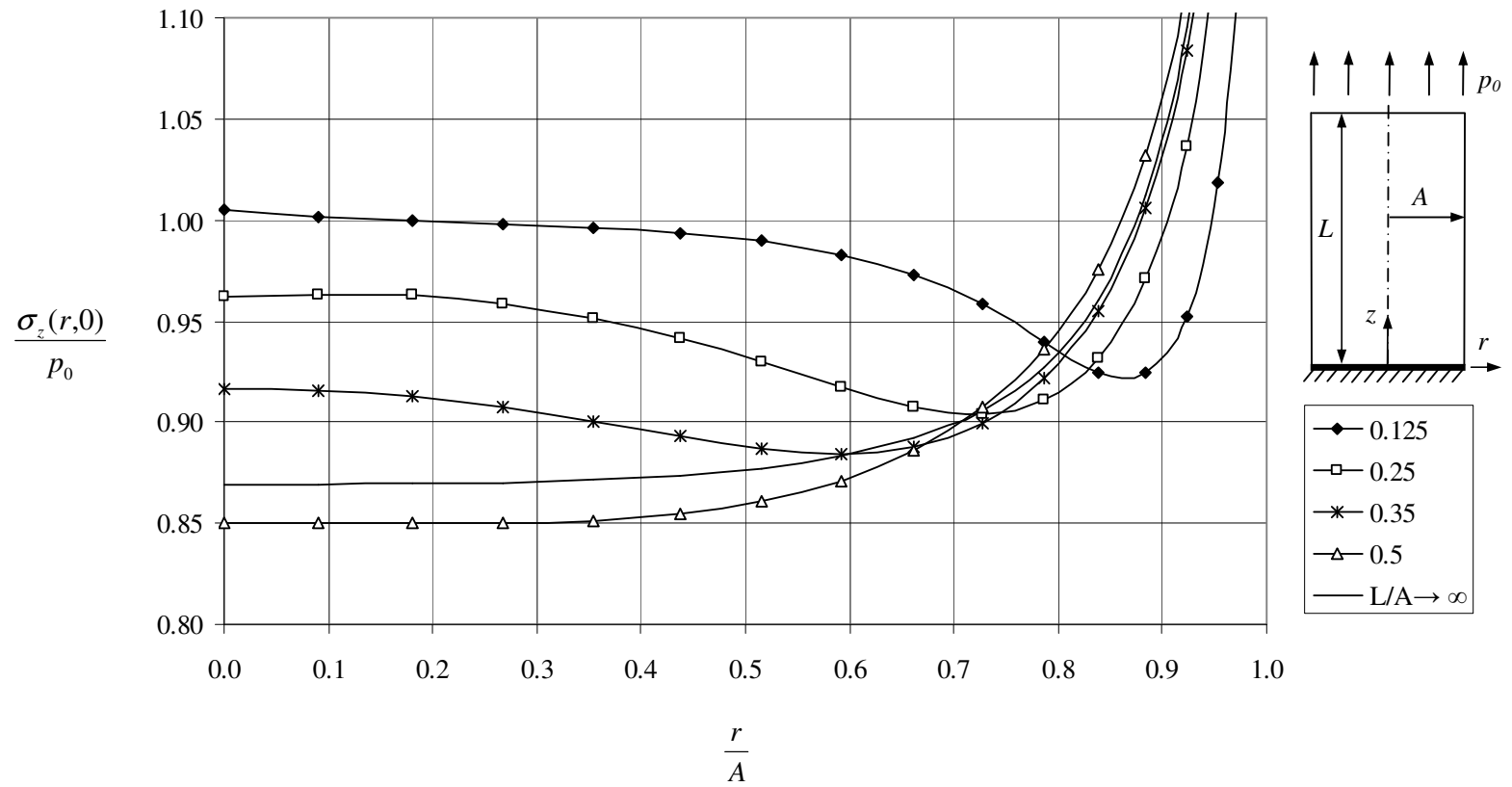
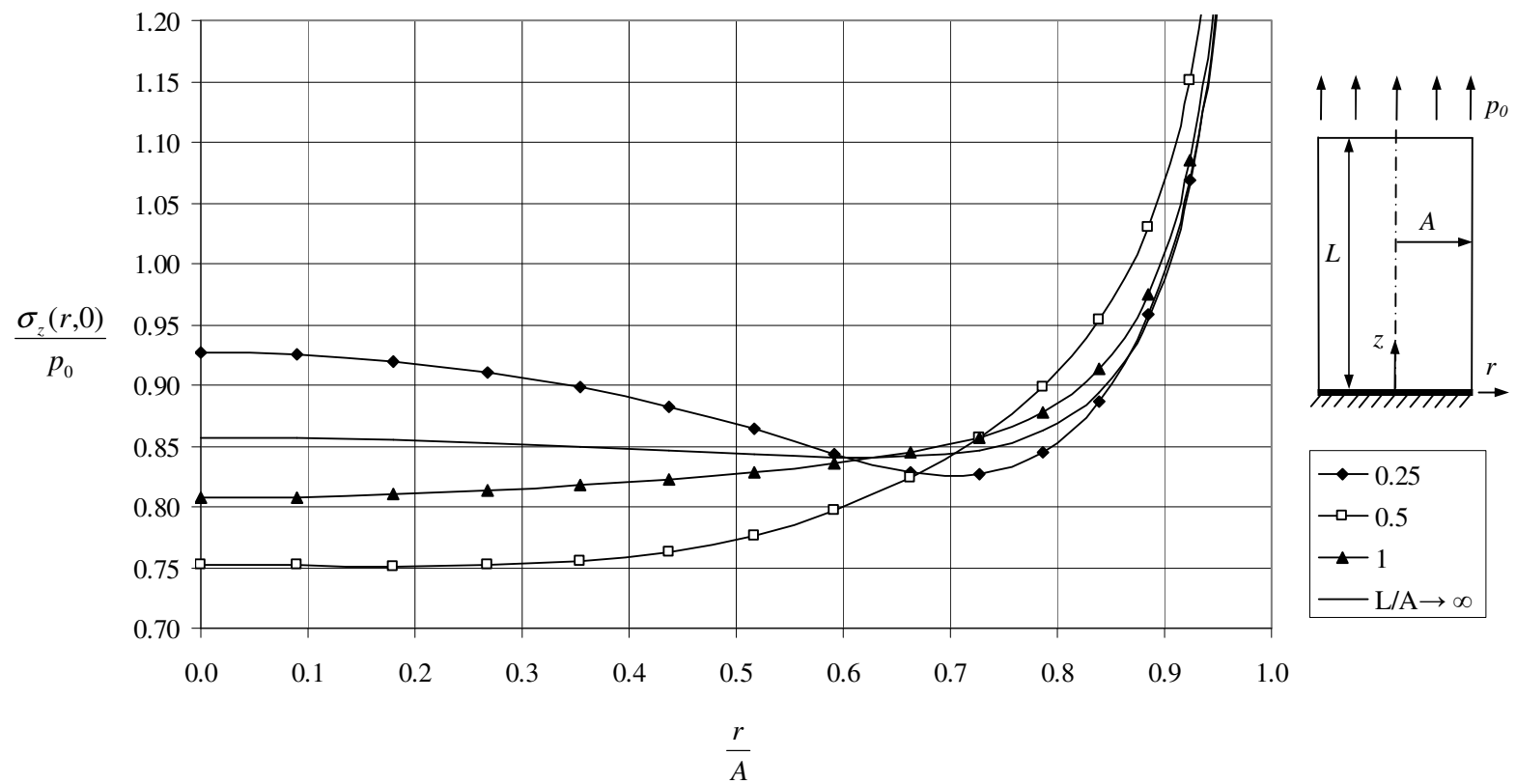Figure 6.74 Normal stress $\sigma_z(r,0)$ along the rigid support when $L = 0.5A$.
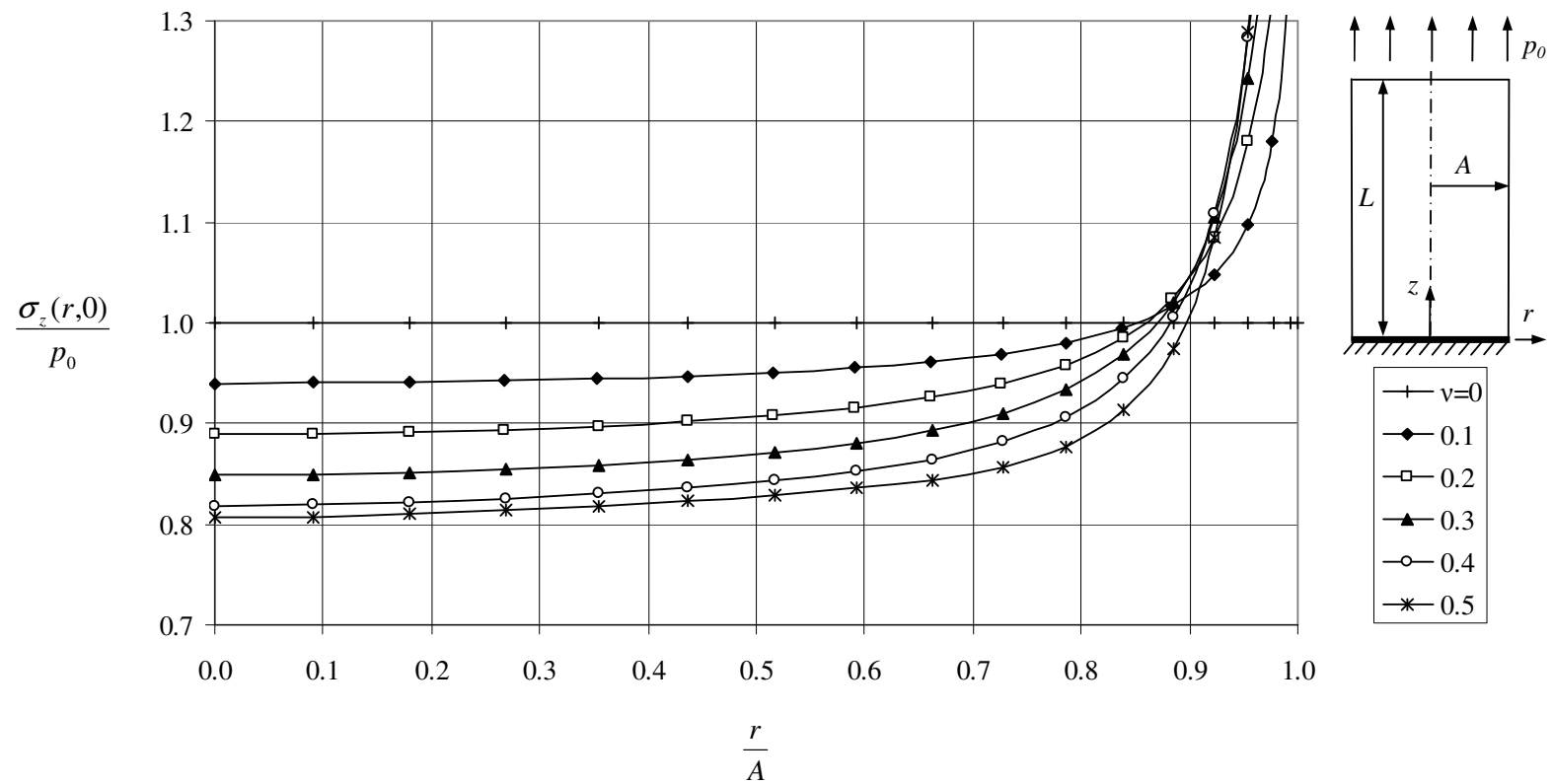
Figure 6.75 Normal stress $\sigma_z(r,0)$ along the rigid support when $L = A$.
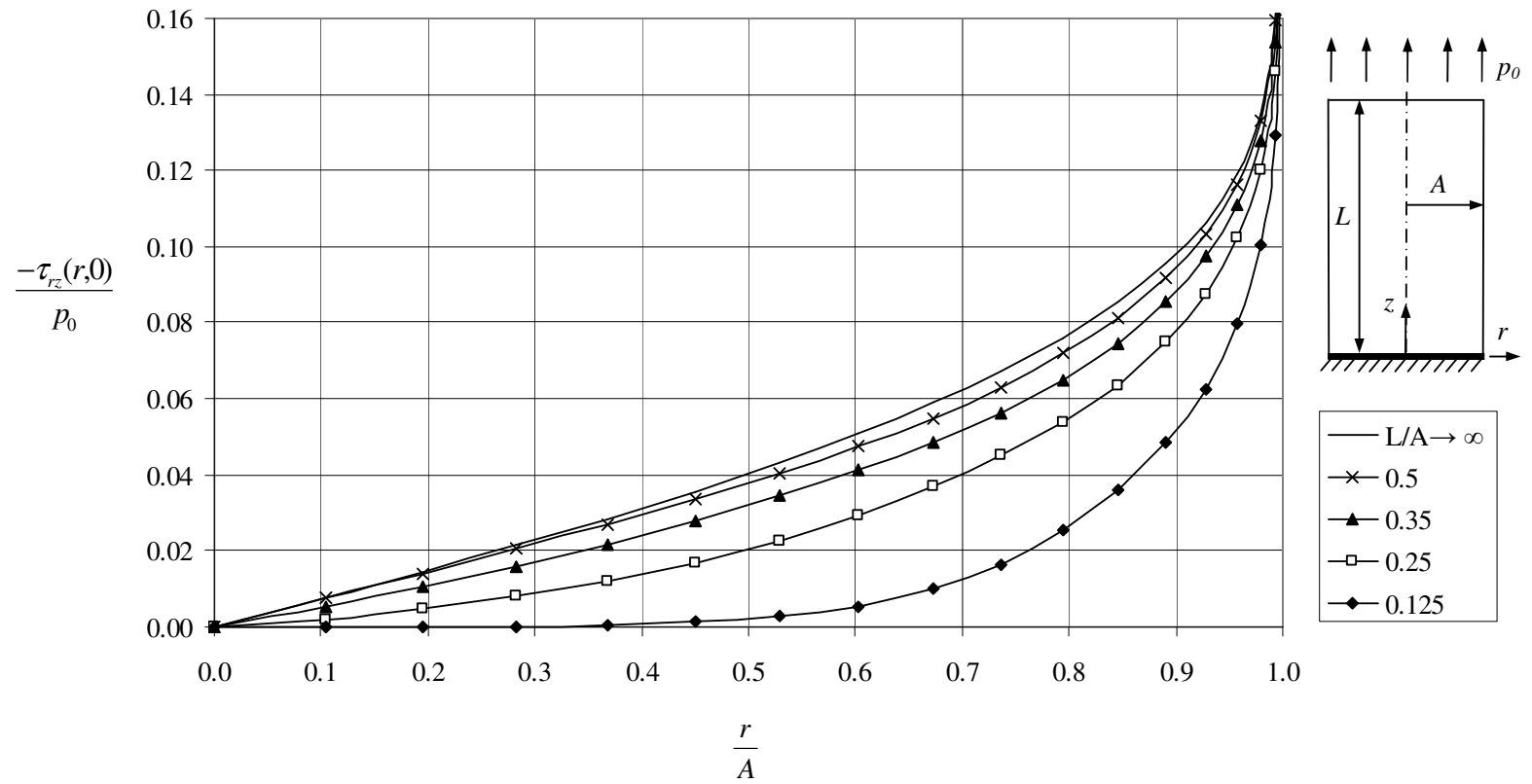
Figure 6.76 Shearing stress $\tau_{rz}(r,0)$ along the rigid support when $v = 0.1$.
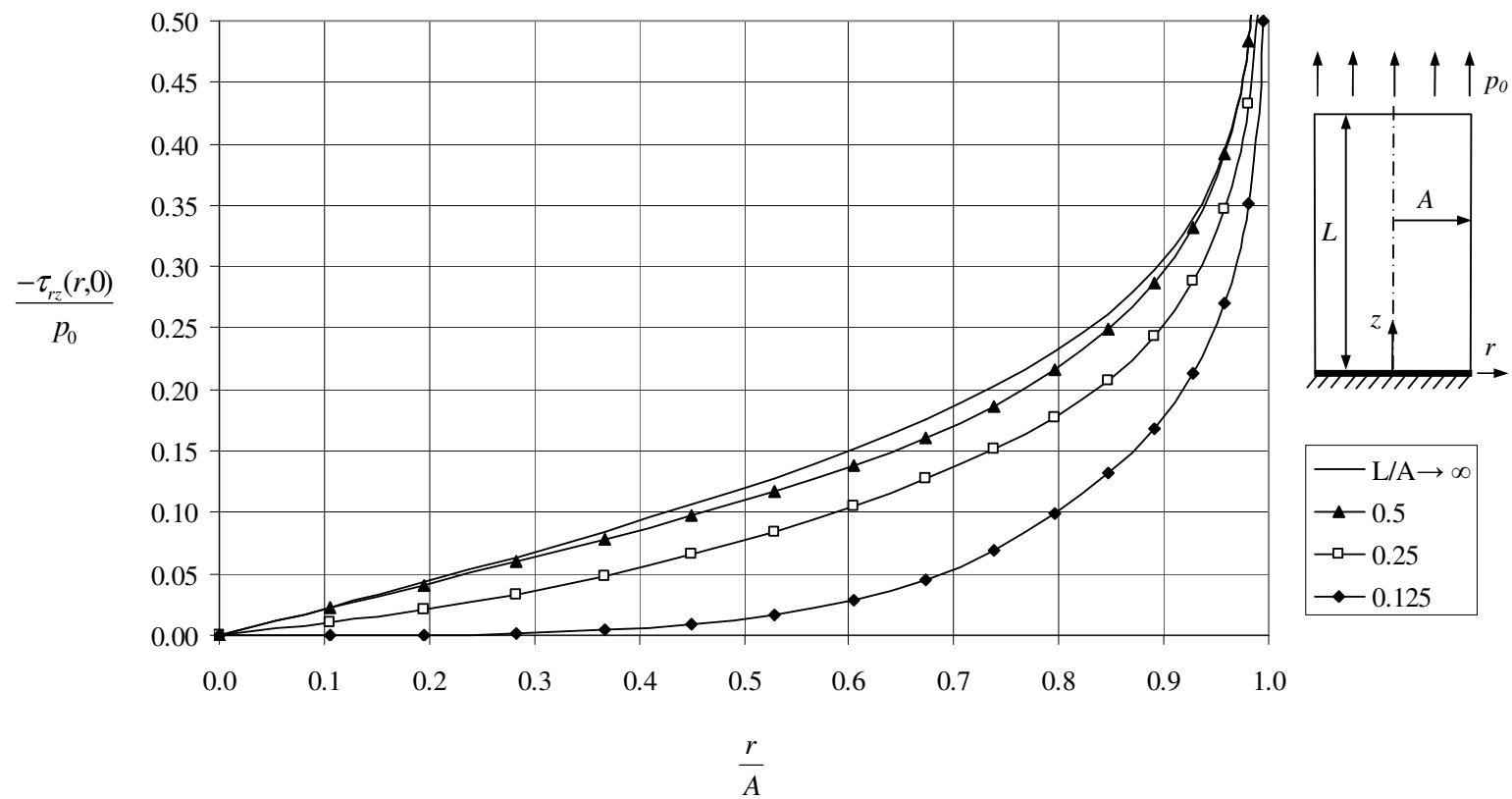
Figure 6.77 Shearing stress $\tau_{rz}(r,0)$ along the rigid support when $\nu = 0.3$.
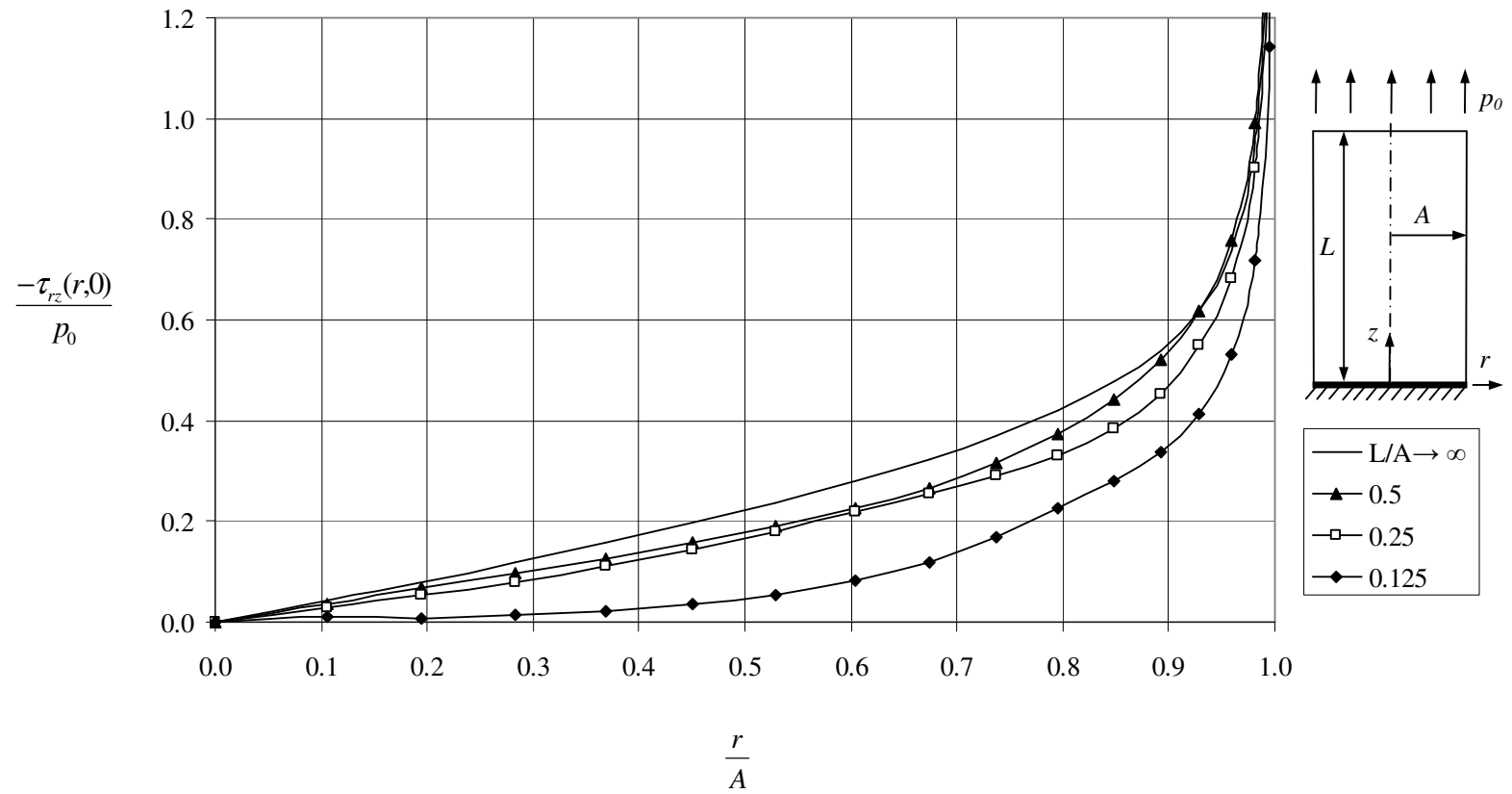
Figure 6.78 Shearing stress $\tau_{rz}(r,0)$ along the rigid support when $\nu = 0.5$.
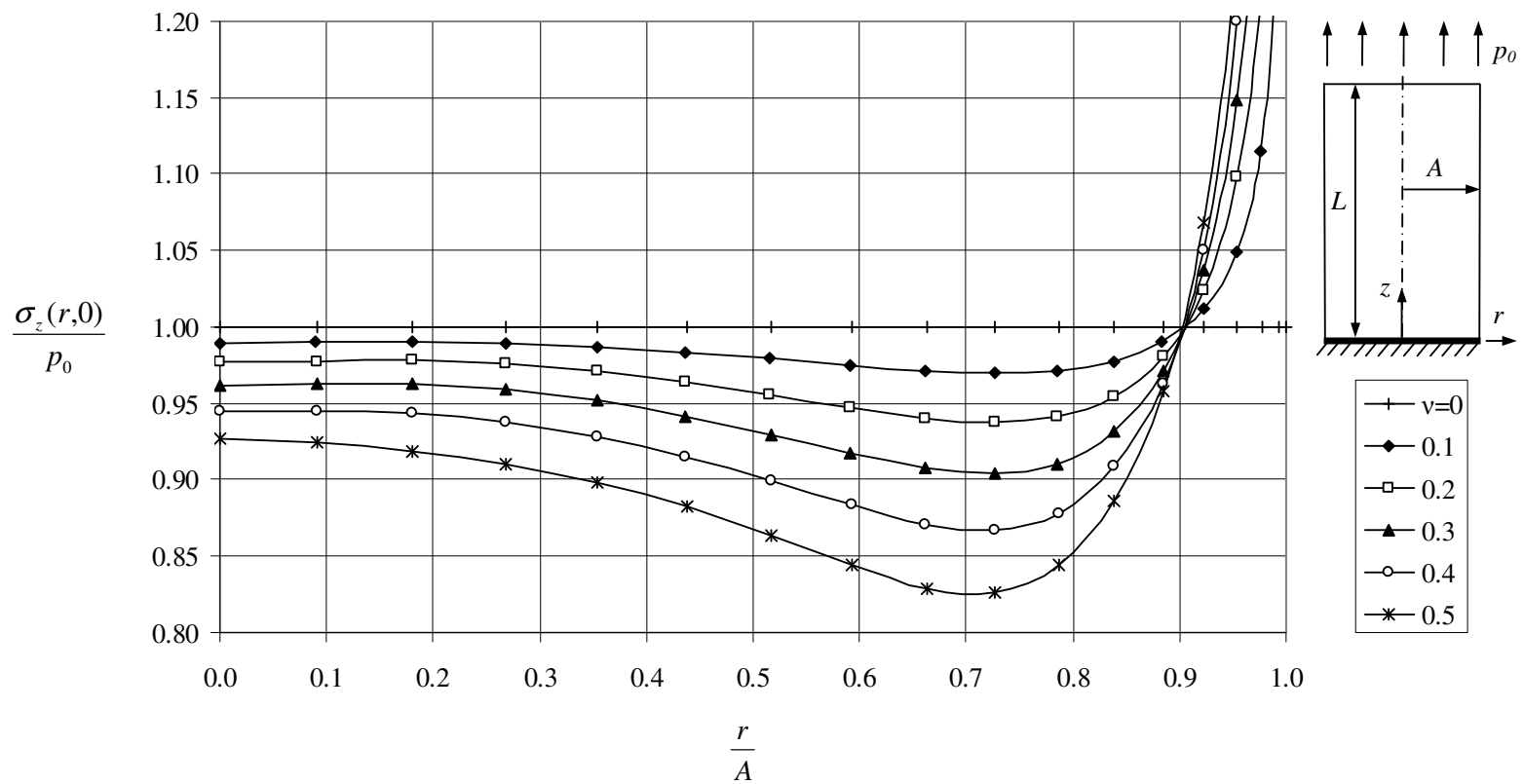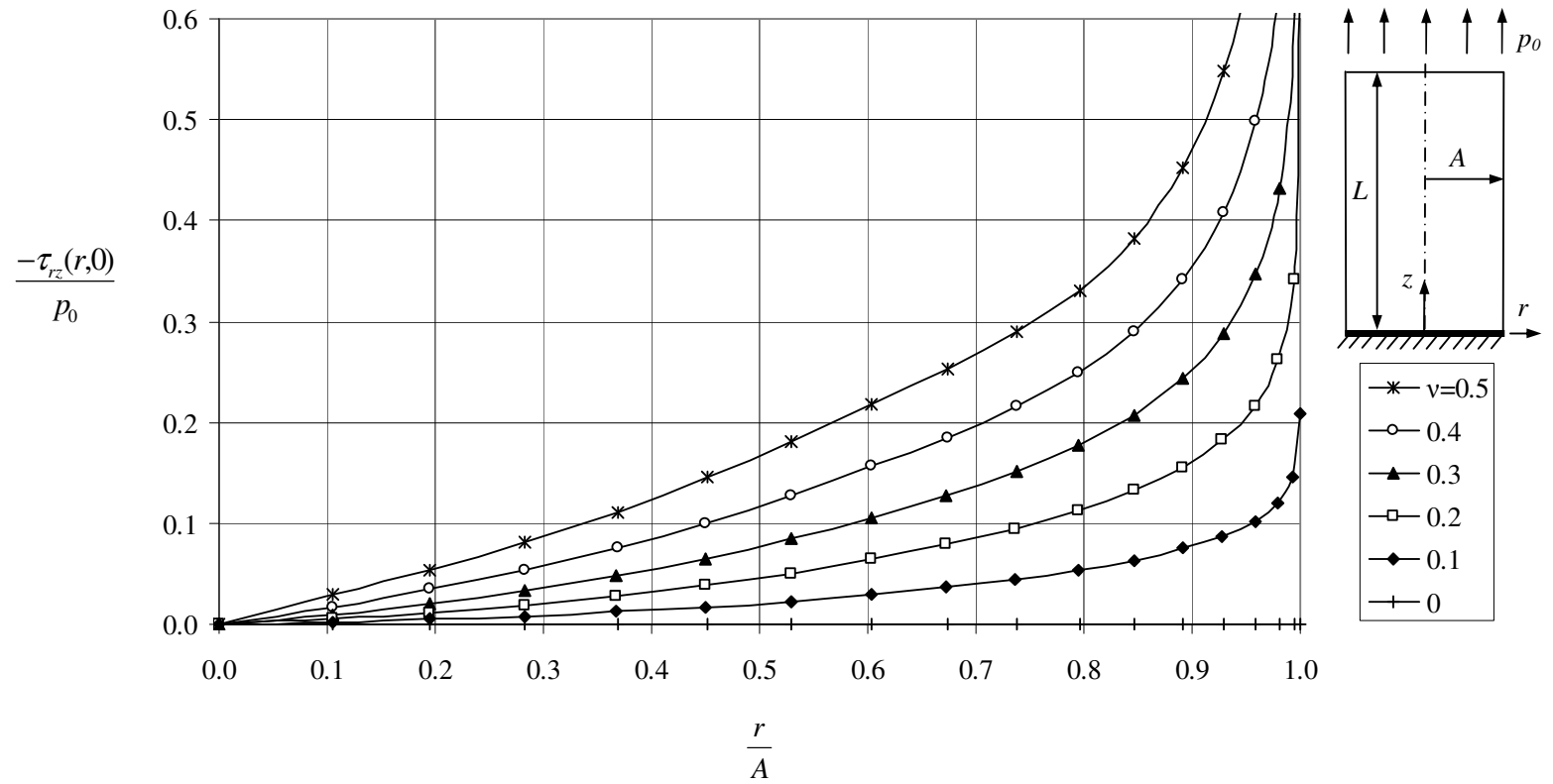
Figure 6.79 Shearing stress $\tau_{rz}(r,0)$ along the rigid support when $L = 0.25A$.
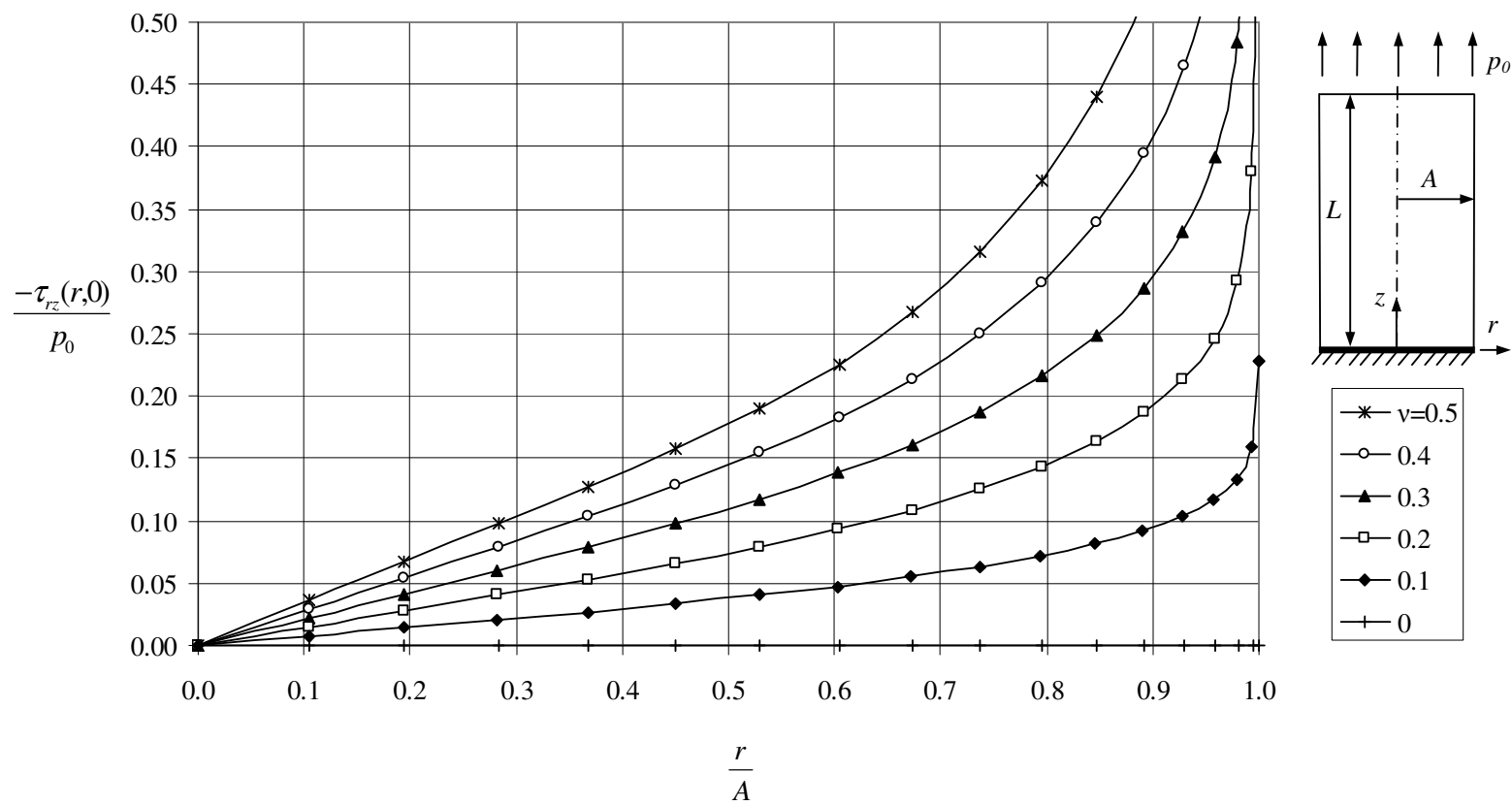
Figure 6.80 Shearing stress $\tau_{rz}(r,0)$ along the rigid support when $L = 0.5A$.
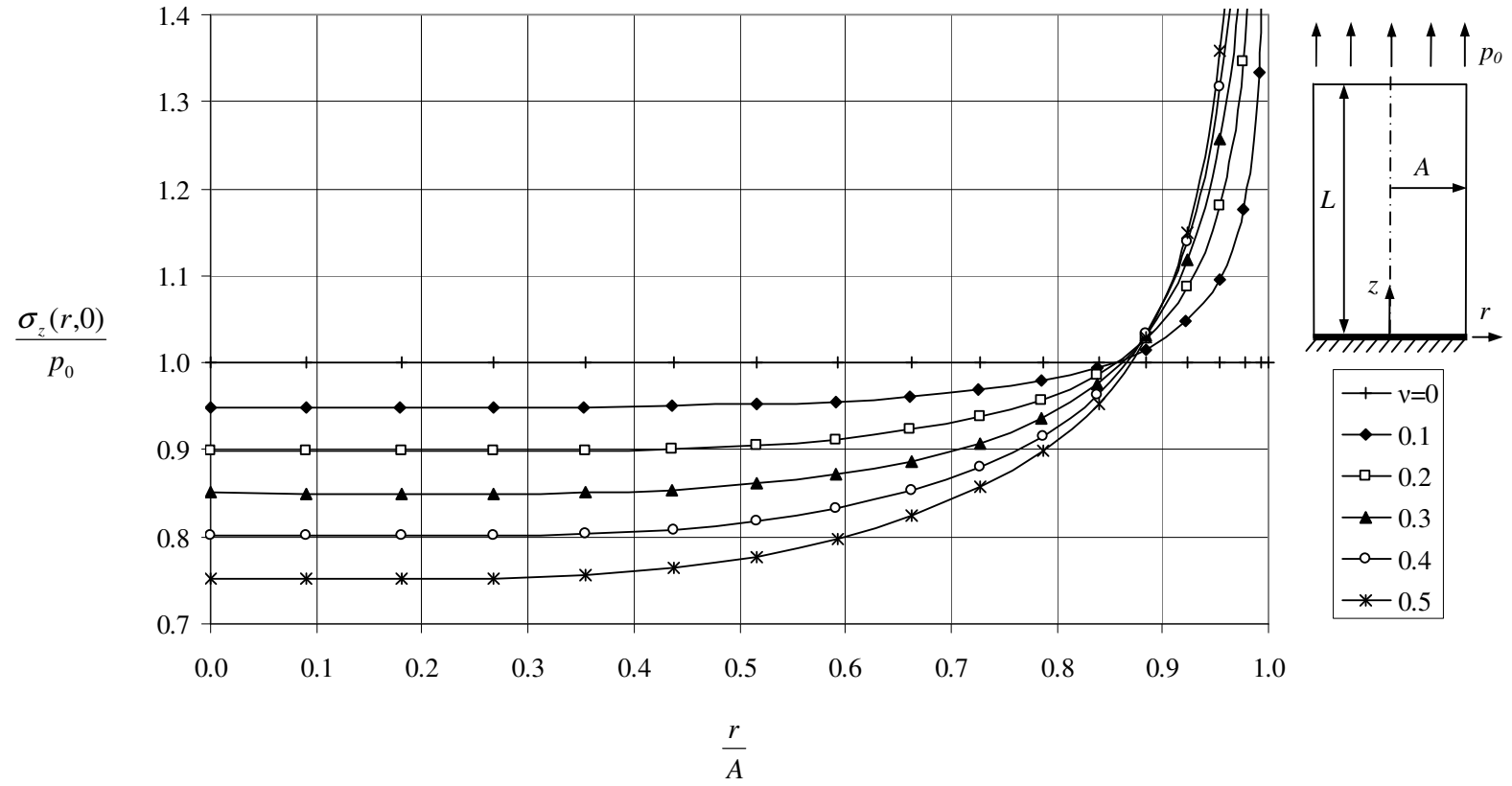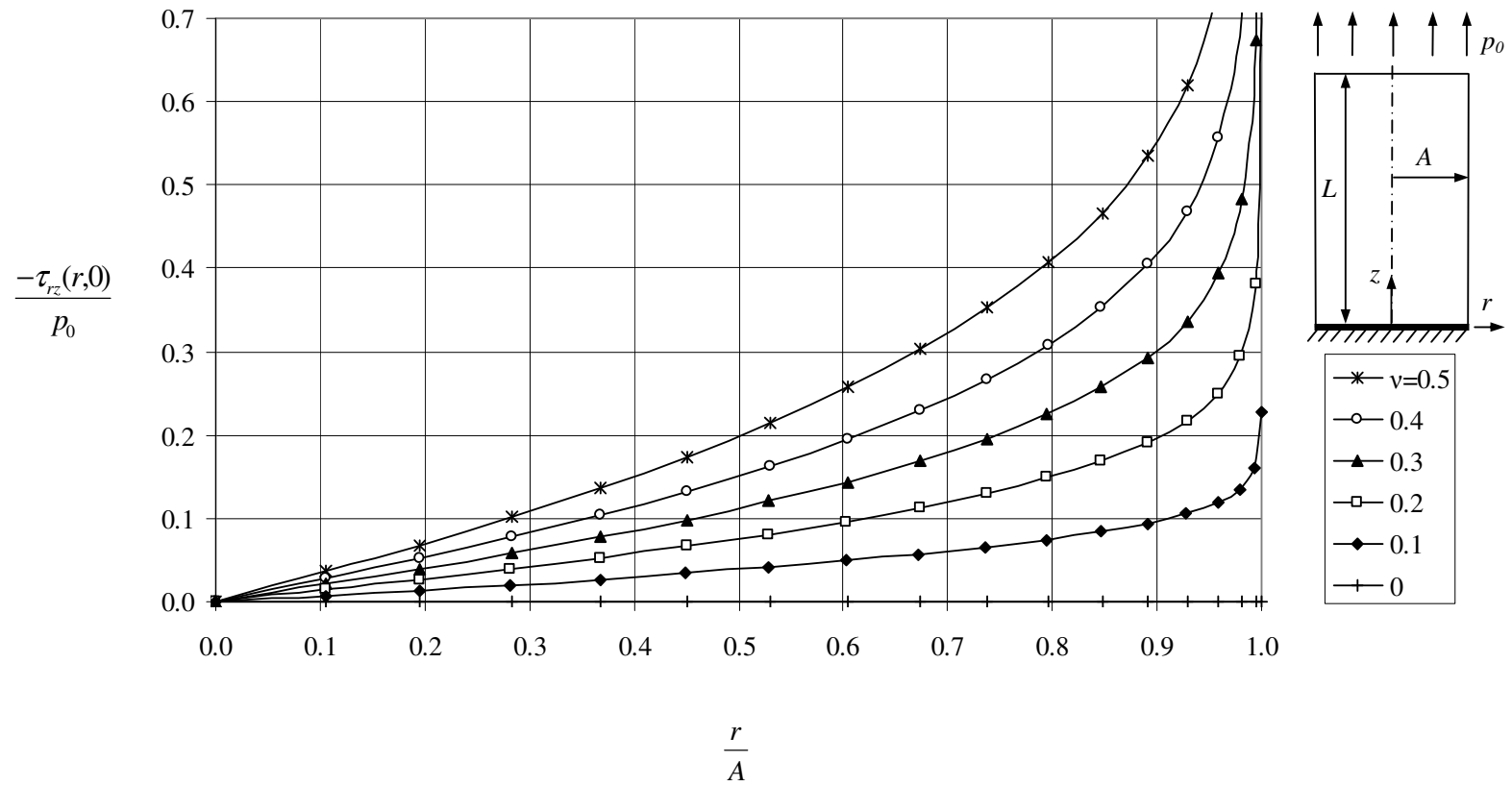
Figure 6.81 Shearing stress $\tau_{rz}(r,0)$ along the rigid support when $L = A$.
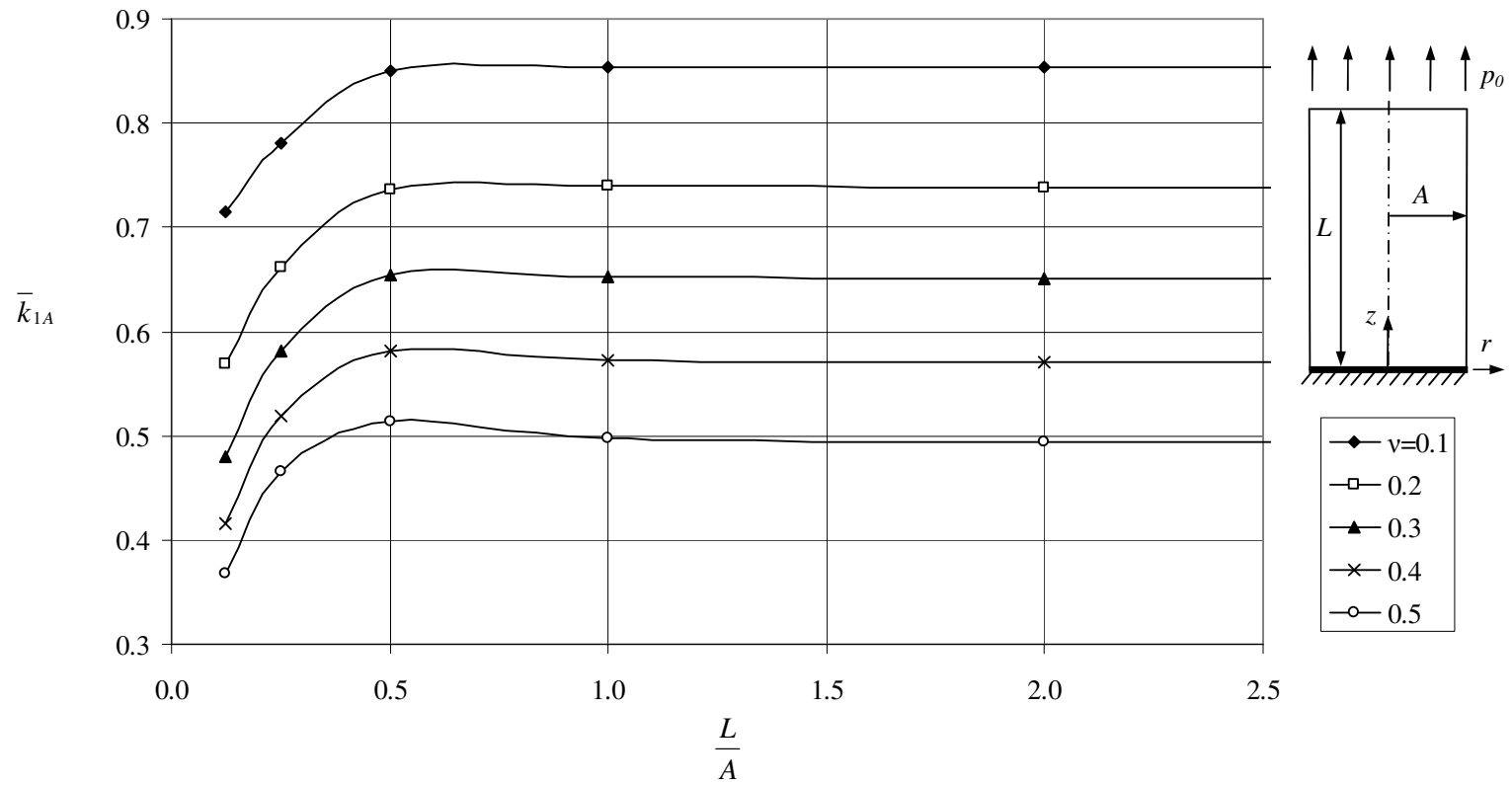
Figure 6.82 Normalized Mode I stress intensity factor $\bar{k}_{1A}$ at the edge of rigid support.
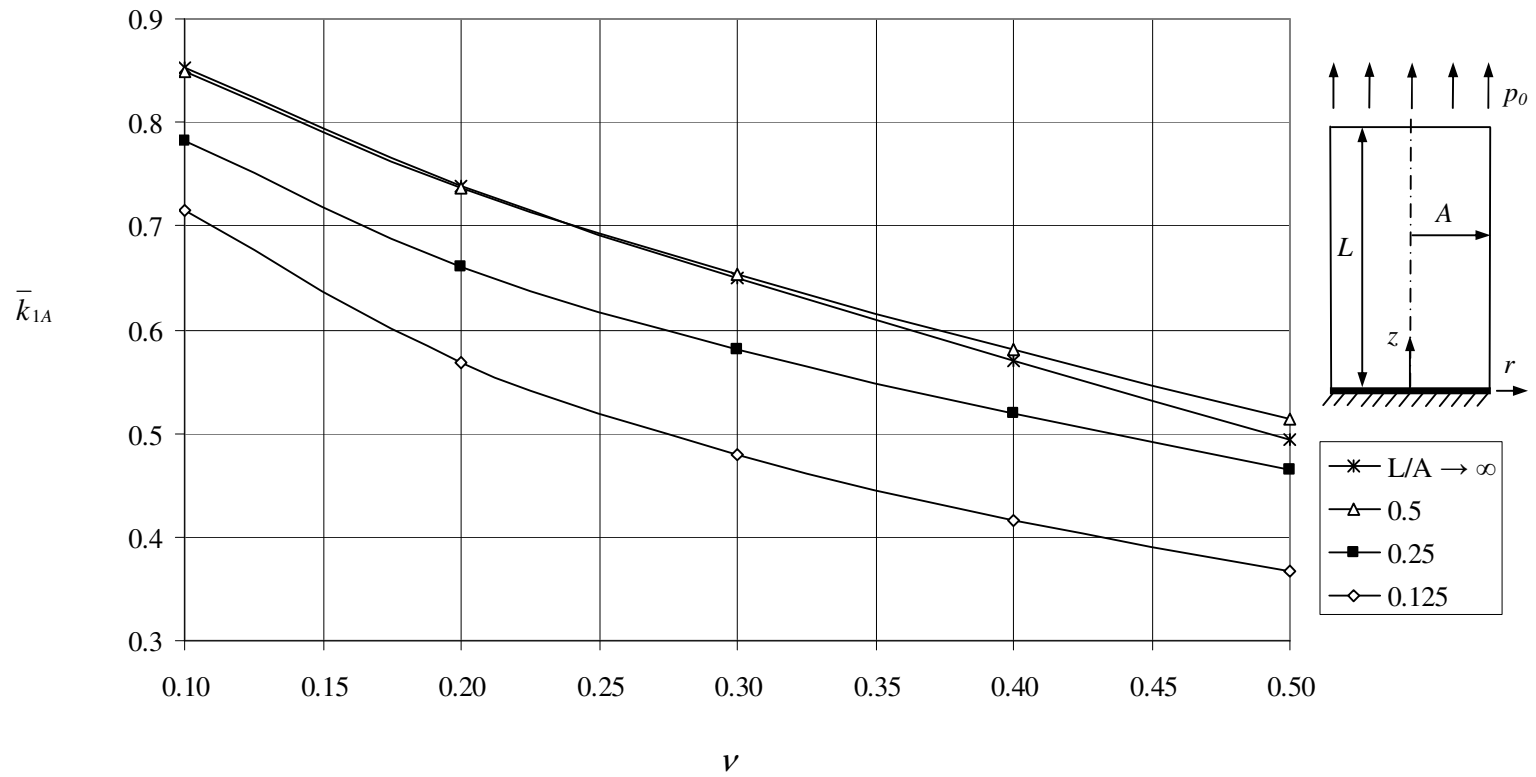
Figure 6.83 Normalized Mode I stress intensity factor $\overline{k}_{1A}$ at the edge of rigid support.
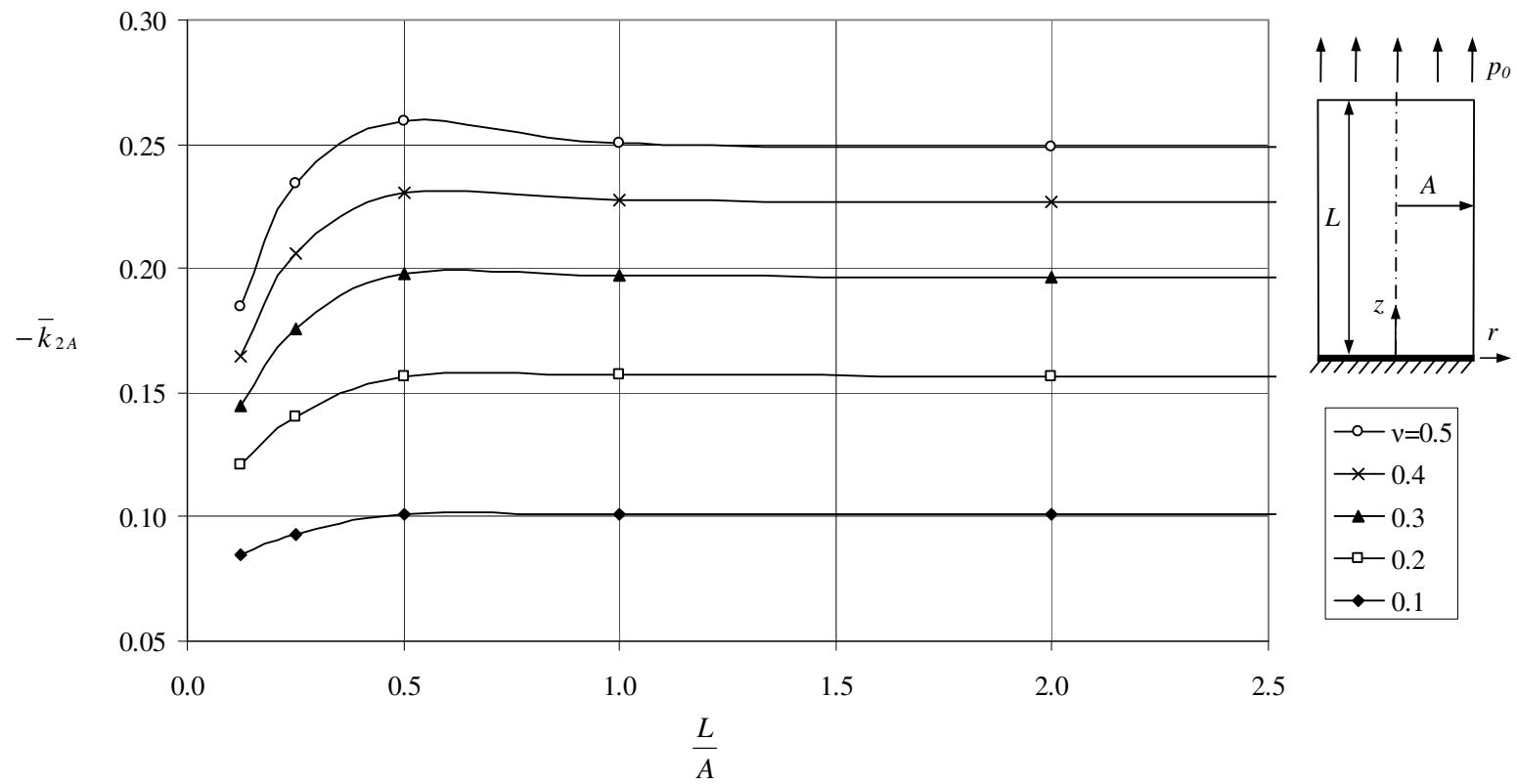
Figure 6.84 Normalized Mode II stress intensity factor $\bar{k}_{2A}$ at the edge of rigid support.
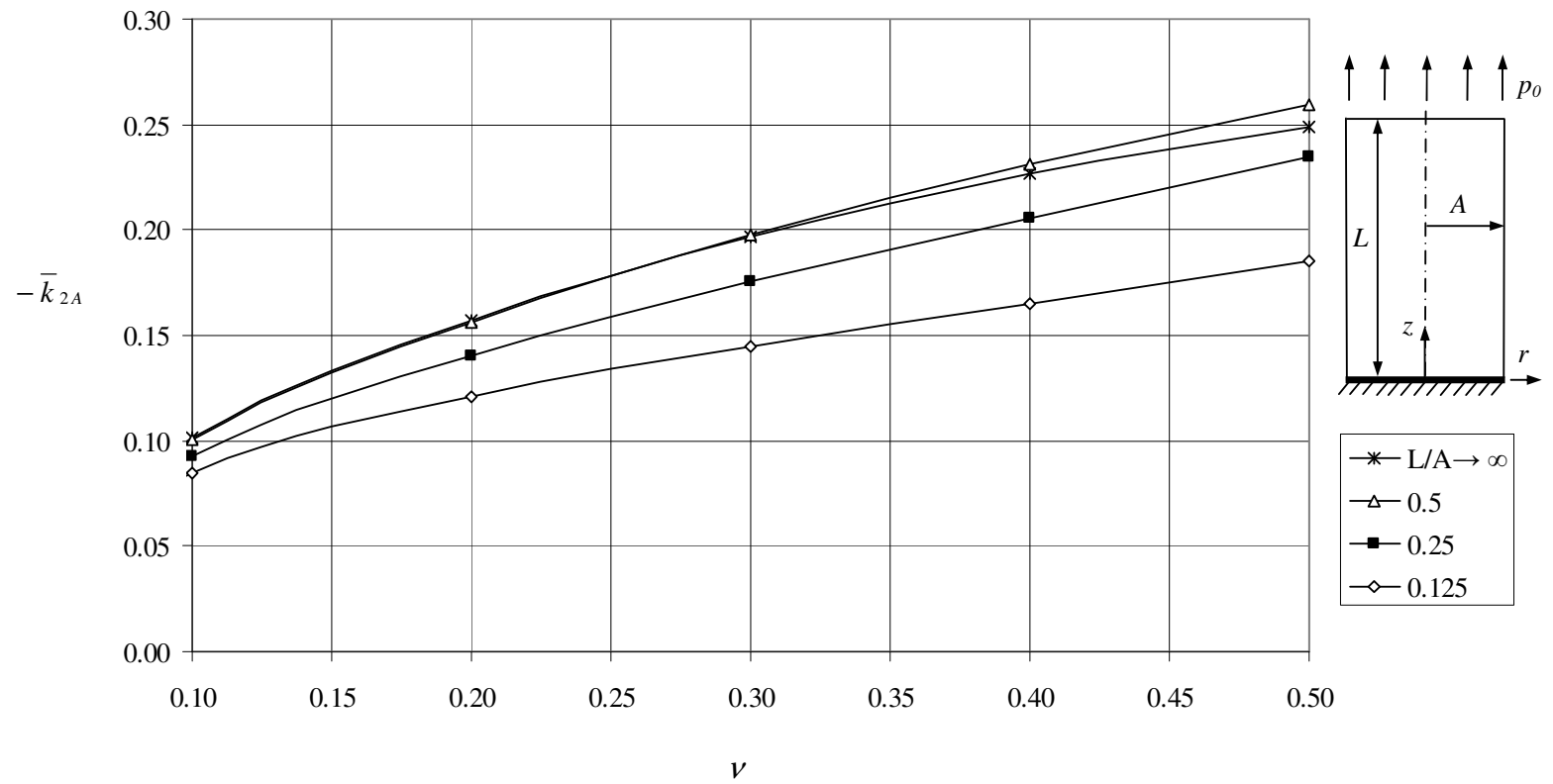
Figure 6.85 Normalized Mode II stress intensity factor $\overline{k}_{2A}$ at the edge of rigid support.

REFERENCES

Abramowitz, M. and Stegun, I.A., Handbook of Mathematical Functions, Dover, 1965.

Agarwal, Y.K., "Axisymmetric Solution of the End Problem for a Semi-Infinite Elastic Circular Cylinder and Its Application to Joined Dissimilar Cylinders under Uniform Tension", International Journal of Engineering Science, Vol.16, 1978, pp.985-998.

Arın, K. and Erdoğan F., "Penny-Shaped Crack in an Elastic Layer Bonded to Dissimilar Half Spaces", International Journal of Engineering Science, Vol.9, 1971, pp.213-232.

Artem, H.S.A. and Geçit, M.R., "An Elastic Hollow Cylinder under Axial Tension Containing a Crack and Two Rigid Inclusions of Ring Shape", Computers and Structures, Vol.80, 2002, pp.2277-2287.

Benthem, J.P. and Minderhoud, P., "The Problem of the Solid Cylinder Compressed between Rough Rigid Stamps", International Journal of Solids and Structures, Vol.8, 1972, pp.1027-1042.

Benthem, J.P. and Koiter, W.T., "Asymptotic Approximations to Crack Problems", Mechanics of Fracture 1, Methods of Analysis and Solutions of Crack Problems, Edited by Sih, G.C., Noordhoff International Publishing Leyden, 1973, pp.131-170.

Chaudhuri, R.A., "Three Dimensional Asymptotic Stress Field in the Vicinity of the Circumference of a Penny Shaped Discontinuity", International Journal of Solids and Structures, Vol.40, 2003, pp.3787-3805.

Chen, Y.Z., "Stress Intensity Factors in a Finite Length Cylinder with a Circumferential Crack", International Journal of Pressure Vessels and Piping, Vol.77, 2000, pp.439-444.

Collins, W.D., "Some Axially Symmetric Stress Distributions in Elastic Solids Containing Penny-Shaped Cracks. I. Cracks in an Infinite Solid and a Thick Plate", Proceedings of the Royal Society of London. Series A, Mathematical and Physical Sciences, Vol.266, 1962, pp.359-386.

Collins, W.D., "Some Coplanar Punch and Crack Problems in Three-Dimensional Elastostatics", Proceedings of the Royal Society of London. Series A, Vol.274, 1963, pp.507-528.

Cook, T.S. and Erdoğan, F., "Stresses in Bonded Materials with a Crack Perpendicular to the Interface", International Journal of Engineering Science, Vol.10, 1972, pp.677-697.

Delale, F. and Erdoğan, F., "Stress Intensity Factor in a Hollow Cylinder Containing a Radial Crack", International Journal of Fracture, Vol.20, 1982, pp.251-265.

Erdoğan, F. and Sih, G. C., "On the Crack Extension in Plates under Plane Loading and Transverse Shear", Journal of Basic Engineering-Transactions of the ASME, Vol. 85, 1963, pp. 519-527.

Erdoğan, F., Gupta, G.D. and Cook, T.S., "Numerical Solution of Singular Integral Equation", Mechanics of Fracture 1, Methods of Analysis and Solutions of Crack Problems, Edited by Sih, G.C., Noordhoff International Publishing Leyden, 1973, pp.368-425.

Erdöl, R. and Erdoğan, F., "Thick-Walled Cylinder with an Axisymmetric Internal or Edge Crack", Journal of Applied Mechanics-Transactions of the ASME, Vol.45, 1978, pp.281-286.

Fu, W.S., and Keer, L.M., "Coplanar Circular Cracks under Shearing Loading", International Journal of Engineering Sciences, Vol.7, 1969, pp.361-372.

Geçit, M.R., "Antiplane Shear in Adhesively Bonded Semi-infinite Media with Transverse Cracks", International Journal of Fracture, Vol.24, 1984, pp.163-178.

Geçit, M.R., "Axisymmetric Contact Problem for a Semi-Infinite Cylinder and a Half Space", International Journal of Engineering Science, Vol.24, 1986, pp.1245-1256.

Geçit, M.R., "Analysis of Tensile Test for a Cracked Adhesive Layer Pulled by Rigid Cylinders", International Journal of Fracture, Vol.32, 1987, pp.241-256.

Geçit, M.R., "Axisymmetric Pull-off Test for a Cracked Adhesive Layer", Journal of Adhesion Science and Technology, Vol.2, 1988, pp. 349-362.

Geçit, M.R. and Turgut A., "Extension of a Finite Strip Bonded to a Rigid Support", Computational Mechanics, Vol.3, 1988, pp.398-410.

Gradshteyn, I.S. and Ryzhik, I.M., Table of Integrals, Series and Products, Fifth Edition, Boston: Academic Press, 1994.

Graham, G.A.C. and Lan, Q., "Stress Intensity Factors for Two Offset Parallel Circular Cracks: Part I-Infinite Elastic Solid", Theoretical and Applied Fracture Mechanics, Vol.20, 1994a, pp.207-225.

Graham, G.A.C. and Lan, Q., "Stress Intensity Factors for Two Offset Parallel Circular Cracks: Part II-Semi-Infinite Solid", Theoretical and Applied Fracture Mechanics, Vol.20, 1994b, pp.227-237.

Gupta, G.D., "An Integral Approach to the Semi-Infinite Strip Problem", Journal of Applied Mechanics, Transactions of the ASME, Vol.40, 1973, pp.948-954.

Gupta, G.D., "The Analysis of Semi-Infinite Cylinder Problem", International Journal of Solids and Structures, Vol.10, 1974, pp.137-148.

Gupta, G.D., "The Problem of a Finite Strip Compressed between Rough Rigid Stamps", Journal of Applied Mechanics, Transactions of the ASME, Vol.42, 1975, pp.81-87.

Isida, M., Hirota, K., Noguchi, H. and Yoshida, T., "Two Parallel Elliptical Cracks in an Infinite Solid Subjected to Tension", International Journal of Fracture, Vol.27, 1985, pp.31-48.

Kassir, M.K., and Sih, G.C., Three-Dimensional Crack Problems, Mechanics of Fracture 2, Noordhoff International Publishing, Leyden, 1975.

Krenk, S., "Quadrature Formulae of Closed Type for Solution of Singular Integral Equations", Journal of the Institute of Mathematics and its Applications, Vol.22, 1978, pp.99-107.

Lee, D.S., "Penny-Shaped Crack in a Long Circular Cylinder Subjected to a Uniform Shearing Stress", European Journal of Mechanics A-Solids, Vol.20 2001, pp.227-239.

Lee, D.S., "A Long Circular Cylinder with a Circumferential Edge Crack Subjected to a Uniform Shearing Stress", International Journal of Solids and Structures, Vol.39, 2002, pp.2613-2628.

Leung, A.Y.T. and Su, R.K.L., "Two Level Finite Element Study of Axisymmetric Cracks", International Journal of Fracture, Vol.89, 1998, pp.193-203.

Meshii, T. and Watanabe, K., "Stress Intensity Factor for a Circumferential Crack in a Finite-Length Thin to Thick-Walled Cylinder under an Arbitrary Biquadratic Stress Distribution on the Crack Surface", Engineering Fracture Mechanics, Vol.68, 2001, pp.975-986.

McLachlan, N.W., Bessel Functions for Engineers, Oxford at the Clarendon Press, 1934.

Muki, R., "Asymmetric Problems of the Theory of Elasticity for a Semi-Infinite Solid and a Thick Plate", Progress in Solid Mechanics, Vol.1, Edited by Sneddon, I.N., and Hill, R., North-Holland, Amsterdam, 1961, pp.401-439.

Muskhelishvili, N.I., Singular Integral Equations, P.Noordhoff, Gröningen, Holland, 1953.

Nied, H.F. and Erdoğan, F., "The Elasticity Problem for a Thick-Walled Cylinder Containing a Circumferential Crack", International Journal of Fracture, Vol.22, 1983, pp.277-301.

Selvaduri, A.P.S., "The Penny-Shaped Crack at a Bonded Plane with Localized Elastic Non-Homogeneity", European Journal of Mechanics A-Solids, Vol. 19 2000, pp.525-534.

Selvadurai, A.P.S., "Mechanics of a Rigid Circular Disk Bonded to a Cracked Elastic Half-Space", International Journal of Solids and Structures, Vol.39, 2002, pp.6035-6053.

Sneddon, I.N., Fourier Transforms, McGraw-Hill Book Company, Inc., 1951.

Sneddon, I.N., The Use of Integral Transforms, McGraw-Hill Book Company, 1972.

Sneddon, I.N. and Welch, J.T., "A note on the Distribution of Stress in a Cylinder Containing a Penny-Shaped Crack", International Journal of Engineering Science, Vol.1, 1963, pp.411-419.

Tsang, D.K.L., Oyadiji, S.O. and Leung, A.Y.T., "Multiple Penny-Shaped Cracks Interaction in a Finite Body and their Effect on Stress Intensity Factor", Engineering Fracture Mechanics, Vol.70, 2003, pp.2199-2214.

Turgut, A. and Geçit, M.R., "A Semi-Infinite Elastic Strip Containing a Transverse Crack", The Arabian Journal for Science and Engineering, Vol.13, 1988, pp.71-80.

Vrbik, J., Singh, B.M., Rokne, J. and Dhaliwal, R.S., "On the Expansion of a Penny-Shaped Crack by a Rigid Circular Disc Inclusion in a Thick Plate", Zeitschrift fur Angewandte Mathematik und Meckanik, Vol.84, 2004, pp.538-550.

Xiao, Z.M., Lim, M.K. and Liew, K.M., "Determination of Stress Field in an Elastic Solid Weakened by Parallel Penny-Shaped Cracks", Acta Mechanica, Vol.114, 1996, pp.83-94.

Yetmez, M. and Geçit, M.R., "Finite Strip with a Central Crack under Tension", International Journal of Engineering Science, Vol.43, 2005, pp.472-493.

Williams, M.L., "Stress Singularities Resulting from Various Boundary Conditions in Angular Corners of Plates in Extension", Journal of Applied Mechanics, Vol.19, 1952, pp.526-528.

APPENDIX A

Integral formulas used in deriving the expressions in Eqs. (2.42a,b) are, Gradshteyn and Ryzhik (1994):

$$\int_0^\infty \frac{\xi}{\alpha^2 + \xi^2} J_1(\xi A) J_1(\xi t) d\xi = K_1(\alpha A) I_1(\alpha t), \qquad\qquad (t < A) \quad (A.1)$$

$$\int_0^\infty \frac{\xi}{(\alpha^2 + \xi^2)^2} J_1(\xi A) J_1(\xi t) d\xi = \frac{1}{2\alpha}\Big[A K_0(\alpha A) I_1(\alpha t)$$

$$+ \frac{2}{\alpha} K_1(\alpha A) I_1(\alpha t) - t K_1(\alpha A) I_0(\alpha t) \Big], \quad (t < A) \quad (A.2)$$

$$\int_0^\infty \frac{\xi^2}{\alpha^2 + \xi^2} J_1(\xi A) J_0(\xi t) d\xi = \alpha K_1(\alpha A) I_0(\alpha t), \qquad\qquad (t < A) \quad (A.3)$$

$$\int_0^\infty \frac{\xi^2}{(\alpha^2 + \xi^2)^2} J_1(\xi A) J_0(\xi t) d\xi = \frac{1}{2}\Big[A K_0(\alpha A) I_0(\alpha t) - t K_1(\alpha A) I_1(\alpha t) \Big], \quad (t < A) \quad (A.4)$$

$$\int_0^\infty \frac{\xi^3}{(\alpha^2 + \xi^2)^2} J_1(\xi A) J_1(\xi t) d\xi = \frac{\alpha}{2}\Big[t K_1(\alpha A) I_0(\alpha t) - A K_0(\alpha A) I_1(\alpha t) \Big], \quad (t < A) \quad (A.5)$$

$$\int_0^\infty \frac{\xi^2}{\alpha^2 + \xi^2} J_0(\xi A) J_1(\xi t) d\xi = -\alpha K_0(\alpha A) I_1(\alpha t), \qquad\qquad (t < A) \quad (A.6)$$

$$\int_0^\infty \frac{\xi}{\alpha^2 + \xi^2} J_0(\xi A) J_0(\xi t) d\xi = K_0(\alpha A) I_0(\alpha t), \qquad (t < A) \quad (A.7)$$

$$\int_0^\infty \frac{\xi}{(\alpha^2 + \xi^2)^2} J_0(\xi A) J_0(\xi t) d\xi = \frac{1}{2\alpha} \left[A K_1(\alpha A) I_0(\alpha t) - t K_0(\alpha A) I_1(\alpha t) \right], \ (t < A) \quad (A.8)$$

$$\int_0^\infty \frac{\xi^2}{(\alpha^2 + \xi^2)^2} J_0(\xi A) J_1(\xi t) d\xi = \frac{1}{2} \left[t K_0(\alpha A) I_0(\alpha t) - A K_1(\alpha A) I_1(\alpha t) \right], \qquad (t < A) \quad (A.9)$$

$$\int_0^\infty J_1(\xi A) J_0(\xi t) d\xi = \frac{1}{A}, \qquad (t < A) \quad (A.10)$$

$$\int_0^\infty \frac{J_1(\xi A) J_0(\xi t)}{\alpha^2 + \xi^2} d\xi = \frac{1}{A\alpha^2} - \frac{K_1(\alpha A) I_0(\alpha t)}{\alpha}, \qquad (t < A) \quad (A.11)$$

$$\int_0^\infty \frac{J_1(\xi A) J_0(\xi t)}{(\alpha^2 + \xi^2)^2} d\xi = \frac{1}{A\alpha^4} - \frac{K_1(\alpha A) I_0(\alpha t)}{\alpha^3}$$
$$- \frac{1}{2\alpha^2} \left[A K_0(\alpha A) I_0(\alpha t) - t K_1(\alpha A) I_1(\alpha t) \right], \qquad (t < A). \quad (A.12)$$

APPENDIX B

Integrals of products of Bessel functions of the first kind, exponential functions and power functions used in deriving the expressions in Eqs. (2.43), Gradshteyn and Ryzhik (1994):

$$\int_0^\infty e^{-z\xi} J_0(t\xi) J_0(r\xi) d\xi = \frac{2}{\pi\sqrt{q_1}} K(2\sqrt{\frac{tr}{q_1}}),$$ (B.1)

$$\int_0^\infty e^{-z\xi} \xi J_0(t\xi) J_0(r\xi) d\xi = \frac{2z}{\pi\sqrt{q_1 q_2}} E(2\sqrt{\frac{tr}{q_1}}),$$ (B.2)

$$\int_0^\infty e^{-z\xi} \xi^2 J_0(t\xi) J_0(r\xi) d\xi = \frac{2z^2}{\pi q_1^{3/2} q_2} \left[2E(2\sqrt{\frac{tr}{q_1}}) - K(2\sqrt{\frac{tr}{q_1}}) \right]$$

$$- \frac{2\left[(t-r)^2 - z^2\right]}{\pi\sqrt{q_1} q_2^2} E(2\sqrt{\frac{tr}{q_1}}),$$ (B.3)

$$\int_0^\infty e^{-z\xi} J_1(t\xi) J_1(r\xi) d\xi = \frac{(t^2 + r^2 + z^2)}{\pi tr\sqrt{q_1}} K(2\sqrt{\frac{tr}{q_1}}) - \frac{\sqrt{q_1}}{\pi tr} E(2\sqrt{\frac{tr}{q_1}}),$$ (B.4)

$$\int_0^\infty e^{-z\xi} \xi J_1(t\xi) J_1(r\xi) d\xi = \frac{z(t^2 + r^2 + z^2)}{\pi tr\sqrt{q_1 q_2}} E(2\sqrt{\frac{tr}{q_1}}) - \frac{z}{\pi tr\sqrt{q_1}} K(2\sqrt{\frac{tr}{q_1}}),$$ (B.5)

$$\int_0^\infty e^{-z\xi} \xi^2 J_1(t\xi) J_1(r\xi) d\xi = \frac{z^2(t^2 + r^2) + (t^2 - r^2)^2}{\pi tr q_1^{3/2} q_2} K(2\sqrt{\frac{tr}{q_1}})$$

$$+ \frac{4z^2(t^2 + r^2 + z^2)^2}{\pi tr q_1^{3/2} q_2^2} E(2\sqrt{\frac{tr}{q_1}}) - \frac{(t^2 + r^2 + 4z^2)}{\pi tr\sqrt{q_1 q_2}} E(2\sqrt{\frac{tr}{q_1}}),$$ (B.6)

$$\int_0^\infty e^{-z\xi}\xi J_0(t\xi)J_1(r\xi)d\xi = \frac{1}{\pi r\sqrt{q_1}}K(2\sqrt{\frac{tr}{q_1}}) + \frac{(r^2-t^2-z^2)}{\pi r\sqrt{q_1}q_2}E(2\sqrt{\frac{tr}{q_1}}),\qquad\text{(B.7)}$$

$$\int_0^\infty e^{-z\xi}\xi^2 J_0(t\xi)J_1(r\xi)d\xi = \frac{z(r^2-t^2-z^2)}{\pi r q_1^{3/2}q_2}\left[2E(2\sqrt{\frac{tr}{q_1}}) - K(2\sqrt{\frac{tr}{q_1}})\right]$$

$$+ \frac{z[(t-r)(t-5r)+z^2]}{\pi r\sqrt{q_1}q_2^2}E(2\sqrt{\frac{tr}{q_1}}),\qquad\text{(B.8)}$$

$$\int_0^\infty e^{-z\xi}\xi J_1(t\xi)J_0(r\xi)d\xi = \frac{1}{\pi t\sqrt{q_1}}K(2\sqrt{\frac{tr}{q_1}}) + \frac{(t^2-r^2-z^2)}{\pi r\sqrt{q_1}q_2}E(2\sqrt{\frac{tr}{q_1}}),\qquad\text{(B.9)}$$

$$\int_0^\infty e^{-z\xi}\xi^2 J_1(t\xi)J_0(r\xi)d\xi = \frac{z(t^2-r^2-z^2)}{\pi t q_1^{3/2}q_2}\left[2E(2\sqrt{\frac{tr}{q_1}}) - K(2\sqrt{\frac{tr}{q_1}})\right]$$

$$+ \frac{z[(t-r)(5t-r)+z^2]}{\pi t\sqrt{q_1}q_2^2}E(2\sqrt{\frac{tr}{q_1}}),\qquad\text{(B.10)}$$

where K and E are the complete elliptic integrals of the first and the second kinds and

$$q_1 = (t+r)^2 + z^2,$$

$$q_2 = (t-r)^2 + z^2.\qquad\text{(B.11a,b)}$$

APPENDIX C

The expressions for $S_i(r,t)$ $(i=1-8)$ appearing in Eqs.(3.3) are as follows

$$S_1(r,t) = \frac{(t^2 - r^2 - 4L^2)}{t\sqrt{y_3}\,y_4} E(2\sqrt{\frac{tr}{y_3}}) + \frac{1}{t\sqrt{y_3}} K(2\sqrt{\frac{tr}{y_3}})$$

$$+ \frac{4L^2[(t-r)(5t-r)+4L^2]}{t\sqrt{y_3}\,y_4^2} E(2\sqrt{\frac{tr}{y_3}})$$

$$+ \frac{4L^2(t^2 - r^2 - 4L^2)}{ty_3^{3/2}y_4}\left[2E(2\sqrt{\frac{tr}{y_3}}) - K(2\sqrt{\frac{tr}{y_3}})\right], \tag{C.1}$$

$$S_2(r,t) = -\frac{16L^3}{y_3^{3/2}y_4}\left[2E(2\sqrt{\frac{tr}{y_3}}) - K(2\sqrt{\frac{tr}{y_3}})\right] + \frac{4L[(t-r)^2 - 4L^2]}{\sqrt{y_3}\,y_4^2} E(2\sqrt{\frac{tr}{y_3}}), \tag{C.2}$$

$$S_3(r,t) = \frac{(\kappa-1)}{4}\left[\frac{y_5}{t\sqrt{y_1}\,y_2} E(2\sqrt{\frac{tr}{y_1}}) + \frac{1}{4t\sqrt{y_1}} K(2\sqrt{\frac{tr}{y_1}})\right]$$

$$- \frac{L^2(t-r)(5t-r)+L^2)}{2t\sqrt{y_1}\,y_2^2} E(2\sqrt{\frac{tr}{y_1}}) - \frac{L^2 y_5}{2ty_1^{3/2}y_2}\left[2E(2\sqrt{\frac{tr}{y_1}}) - K(2\sqrt{\frac{tr}{y_1}})\right], \tag{C.3}$$

$$S_4(r,t) = \frac{2L[4L^2(t^2 + r^2)+(t^2-r^2)^2]}{try_3^{3/2}y_4} K(2\sqrt{\frac{tr}{y_3}}) + \frac{32L^3(t^2 + r^2 + 4L^2)^2}{try_3^{3/2}y_4^2} E(2\sqrt{\frac{tr}{y_3}})$$

$$- \frac{2L(t^2 + r^2 + 16L^2)}{tr\sqrt{y_3}\,y_4} E(2\sqrt{\frac{tr}{y_3}}), \tag{C.4}$$

$$S_5(r,t) = \frac{1}{r\sqrt{y_3}} K(2\sqrt{\frac{tr}{y_3}}) + \frac{(r^2 - t^2 - 4L^2)}{r\sqrt{y_3}\,y_4} E(2\sqrt{\frac{tr}{y_3}})$$

$$-\frac{4L^2(r^2-t^2-4L^2)}{ry_3^{3/2}y_4}\left[2E(2\sqrt{\frac{tr}{y_3}})-K(2\sqrt{\frac{tr}{y_3}})\right]$$

$$-\frac{4L^2[(t-r)(t-5r)+4L^2]}{r\sqrt{y_3}\,y_4^2}E(2\sqrt{\frac{tr}{y_3}}),\tag{C.5}$$

$$S_6(r,t)=\frac{(\kappa+1)}{4}\left[\frac{L(t^2+r^2+L^2)}{tr\sqrt{y_1}\,y_2}E(2\sqrt{\frac{tr}{y_1}})-\frac{L}{tr\sqrt{y_1}}K(2\sqrt{\frac{tr}{y_1}})\right]$$

$$-\frac{L[L^2(t^2+r^2)+(t^2-r^2)^2]}{2try_1^{3/2}y_2}K(2\sqrt{\frac{tr}{y_1}})-\frac{2L^3(t^2+r^2+L^2)^2}{try_1^{3/2}y_2^2}E(2\sqrt{\frac{tr}{y_1}})$$

$$+\frac{L(t^2+r^2+4L^2)}{2tr\sqrt{y_1}\,y_2}E(2\sqrt{\frac{tr}{y_1}}),\tag{C.6}$$

$$S_7(r,t)=(\kappa-1)\left[\frac{y_5}{t\sqrt{y_1}\,y_2}E(2\sqrt{\frac{tr}{y_1}})+\frac{1}{t\sqrt{y_1}}K(2\sqrt{\frac{tr}{y_1}})\right]$$

$$-\frac{2L^2[(t-r)(5t-r)+L^2]}{t\sqrt{y_1}\,y_2^2}E(2\sqrt{\frac{tr}{y_1}})-\frac{2L^2y_5}{ty_1^{3/2}y_2}\left[2E(2\sqrt{\frac{tr}{y_1}})-K(2\sqrt{\frac{tr}{y_1}})\right],\tag{C.7}$$

$$S_8(r,t)=-\frac{2L(\kappa+1)}{\sqrt{y_1}\,y_2}E(2\sqrt{\frac{tr}{y_1}})+\frac{4L^3}{y_1^{3/2}y_2}\left[2E(2\sqrt{\frac{tr}{y_1}})-K(2\sqrt{\frac{tr}{y_1}})\right]$$

$$-\frac{4L[(t-r)^2-L^2]}{\sqrt{y_1}\,y_2^2}E(2\sqrt{\frac{tr}{y_1}}),\tag{C.8}$$

where

$$y_1=(t+r)^2+L^2,$$

$$y_2=(t-r)^2+L^2,$$

194

$$y_3 = (t + r)^2 + 4L^2 \, ,$$

$$y_4 = (t - r)^2 + 4L^2 \, ,$$

$$y_5 = t^2 - r^2 - L^2 \, . \qquad\qquad\qquad\qquad\qquad\qquad\qquad\qquad \text{(C.9a-e)}$$

APPENDIX D

The expressions for the integrands $K_{ij}(r,t,\alpha)$ $(i,j=1-3)$ appearing in Eq. (3.9) are as follows

$$K_{11}(r,t,\alpha) = \frac{4\alpha}{d_0}\{r\alpha I_1(r\alpha)[-2t\alpha I_0(t\alpha)+(g_3+g_1g_4)I_1(t\alpha)]+I_0(r\alpha)\{t\alpha I_0(t\alpha)(-4$$
$$+g_3+g_1g_4)+I_1(t\alpha)[2g_3+g_1(-1+2g_4)]\}\}\cos^2(\alpha L),\tag{D.1}$$

$$K_{12}(r,t,\alpha) = \frac{4}{Ad_0}\{A\alpha\{r\alpha g_3 I_0(t\alpha)I_1(r\alpha)+I_0(r\alpha)[1+\kappa+2g_3+t\alpha g_3 I_1(t\alpha)]\}$$
$$+r\alpha I_1(r\alpha)[-2At\alpha^2 I_1(t\alpha)-I_1(A\alpha)(\kappa+1)+A\alpha g_1 g_4 I_0(t\alpha)]$$
$$+I_0(r\alpha)[-4At\alpha^2 I_1(t\alpha)+A\alpha g_1\ I_0(t\alpha)(-1+2g_4)$$
$$-2(1+\kappa)I_1(A\alpha)+At\alpha^2 g_1 g_4 I_1(t\alpha)]\}\cos(\alpha L)\sin(\alpha L),\tag{D.2}$$

$$K_{13}(r,t,\alpha) = -\frac{\alpha}{2d_0}\{2r\alpha I_1(r\alpha)[-2t\alpha I_0(t\alpha)+I_1(t\alpha)(1+\kappa+g_3+g_1g_4)]$$
$$+I_0(r\alpha)\{2t\alpha I_0(t\alpha)(-4+g_3+g_1g_4)+I_1(t\alpha)[2g_1-(-3+\kappa)g_3$$
$$+(g_1-2\kappa g_1+\kappa^2)g_4]\}\}\cos(\alpha L),\tag{D.3}$$

$$K_{21}(r,t,\alpha) = \frac{4\alpha}{d_0}\{I_1(r\alpha)[-g_1 I_1(t\alpha)+t\alpha I_0(t\alpha)(g_3+g_1g_4)]$$
$$+r\alpha I_0(r\alpha)[-2t\alpha I_0(t\alpha)+I_1(t\alpha)(g_3+g_1g_4)]\}\cos(\alpha L)\sin(\alpha L),\tag{D.4}$$

$$K_{22}(r,t,\alpha) = \frac{4\alpha}{Ad_0}\{rI_0(r\alpha)\{A\alpha[-2\alpha t I_1(t\alpha)+g_3 I_0(t\alpha)]-I_1(A\alpha)(1+\kappa)$$
$$+A\alpha g_1 g_4 I_0(t\alpha)\}+AI_1(r\alpha)\{I_0(A\alpha)(1+\kappa)+t\alpha g_3 I_1(t\alpha)$$

$$+ g_1 \left[- I_0(t\alpha) + t\alpha g_4 I_1(t\alpha) \right] \} \} \sin^2(\alpha L), \tag{D.5}$$

$$K_{23}(r,t,\alpha) = \frac{\alpha}{2d_0} \{ - 2r\alpha I_0(r\alpha) \left[- 2t\alpha I_0(t\alpha) + I_1(t\alpha)(1 + \kappa + g_3 + g_1 g_4) \right]$$

$$+ I_1(r\alpha) \{ - 2t\alpha I_0(t\alpha)(g_3 + g_1 g_4) + I_1(t\alpha) \left[(1 + \kappa) g_3 \right.$$

$$\left. + 2g_1 + g_1 g_4 (1 + \kappa) \right] \} \} \sin(\alpha L), \tag{D.6}$$

$$K_{31}(r,t,\alpha) = \frac{2}{d_0} \{ - g_2 \left[- 2t\alpha I_0(t\alpha) + I_1(t\alpha)(g_3 + g_1 g_4) \right]$$

$$+ \alpha I_0(r\alpha) \{ - 2t\alpha I_0(t\alpha)(1 + \kappa + g_3 + g_1 g_4) + I_1(t\alpha) \left[(1 + \kappa) g_3 \right.$$

$$\left. + 2g_1 + g_1 g_4 (1 + \kappa) \right] \} \} \cos(\alpha L), \tag{D.7}$$

$$K_{32}(r,t,\alpha) = - \frac{2}{A\alpha d_0} \{ g_2 \{ A\alpha \left[- 2\alpha t I_1(t\alpha) + g_3 I_0(t\alpha) \right] - I_1(A\alpha)(1 + \kappa)$$

$$+ A\alpha g_1 g_4 I_0(t\alpha) \} + \alpha I_0(r\alpha) \{ (1 + 2\kappa + \kappa^2) I_1(A\alpha) + 2At\alpha^2 (1 + \kappa) I_1(t\alpha)$$

$$+ A\alpha I_0(A\alpha)(2 + 2\kappa - g_3) + 2At\alpha^2 g_3 I_1(t\alpha) + g_4 I_1(t\alpha)(2At\alpha^2$$

$$+ 2A\kappa t\alpha^2 + 4A^3 t\alpha^4) - A\alpha g_1 I_0(t\alpha) \left[2 + (1 + \kappa) g_4 \right] \} \} \sin(\alpha L), \tag{D.8}$$

$$K_{33}(r,t,\alpha) = \frac{1}{2d_0} \{ g_2 \left[- 2t\alpha I_0(t\alpha) + I_1(t\alpha)(1 + \kappa + g_3 + g_1 g_4) \right]$$

$$+ \alpha I_0(r\alpha) \{ 2t\alpha I_0(t\alpha)(1 + \kappa + g_3 + g_1 g_4)$$

$$- I_1(t\alpha) \left[g_1 + 2(1 + \kappa)(\kappa + 2g_3), + 2g_1 g_4(\kappa + 1) \right] \} \}, \tag{D.9}$$

where

$$g_1 = 1 + \kappa + 2A^2 \alpha^2,$$

$$g_2 = 4\alpha I_0(r\alpha) + 2r\alpha^2 I_1(r\alpha),$$

197

$$g_3 = 2A^2\alpha^2 I_0(A\alpha)K_0(A\alpha),$$

$$g_4 = I_1(A\alpha)K_1(A\alpha). \hspace{3cm} \text{(D.10a-e)}$$

APPENDIX E

The expressions for $K_{ij\infty 0}(t,\alpha) = \lim_{\alpha\to\infty} K_{ij}(0,t,\alpha)$, $(i=1,3; j=1-3)$ appearing in Eq. (4.18) are defined as follows:

$$K_{11\infty 0}(t,\alpha) = \cos^2(\alpha L)\, e^{-\alpha(2A-t)}\sqrt{\frac{\pi\alpha}{2t}}\left[8A(-A+t)\alpha^2 + (20A-16t)\alpha - (\frac{19}{2}+2\kappa)\right], \quad \text{(E.1)}$$

$$K_{12\infty 0}(t,\alpha) = \cos(\alpha L)\sin(\alpha L) e^{-\alpha(2A-t)}\sqrt{\frac{\pi\alpha}{2t}}\left[-8A(A-t)\alpha^2 + (12A-6t)\alpha + (\frac{7}{2}-2\kappa)\right]$$
$$- \cos(\alpha L)\sin(\alpha L) e^{-\alpha A}\sqrt{\frac{\pi\alpha}{2t}}\left[-\frac{4(1+\kappa)\sqrt{t}}{\sqrt{A}}\right], \quad \text{(E.2)}$$

$$K_{13\infty 0}(t,\alpha) = \cos(\alpha L)\, e^{-\alpha(2A-t)}\sqrt{\frac{\pi\alpha}{2t}}\left[4A(A-t)\alpha^2 + (-8A+2A\kappa+8t)\alpha - \frac{15\kappa}{4}\right], \quad \text{(E.3)}$$

$$K_{31\infty 0}(t,\alpha) = \cos(\alpha L)\, e^{-\alpha(2A-t)}\sqrt{\frac{\pi\alpha}{2t}}\left[4A(A-t)\alpha^2 - (8A-2A\kappa-6t+2\kappa t)\alpha + \frac{15}{4}\right], \quad \text{(E.4)}$$

$$K_{32\infty 0}(t,\alpha) = \sin(\alpha L)\, e^{-\alpha(2A-t)}\sqrt{\frac{\pi\alpha}{2t}}\left[4A(A-t)\alpha^2 - (4A-2A\kappa-6t+2\kappa t)\alpha + (-\frac{3}{4}+2\kappa)\right]$$
$$+ \sin(\alpha L)\, e^{-\alpha A}\sqrt{\frac{\pi\alpha}{2t}}\left[-\frac{2(1+\kappa)\sqrt{t}}{\sqrt{A}}\right], \quad \text{(E.5)}$$

$$K_{33\infty 0}(t,\alpha) = e^{-\alpha(2A-t)}\sqrt{\frac{\pi\alpha}{2t}}\left[2A(-A+t)\alpha^2 + (3A-2A\kappa-3t+\kappa t)\alpha + \frac{\kappa}{8}(11-4\kappa)\right]. \quad \text{(E.6)}$$

APPENDIX F

The expressions for $N_{ij\,s0}(t)$ $(i=1,3;\ j=1-3)$ appearing in Eq. (4.18) are in the form

$$N_{11s0}(t) = \frac{\pi}{\sqrt{2t}} \left\{ \frac{15A(-A+t)}{2s_1^{7/2}} \left[1 + \frac{\cos(\frac{7}{2}s_3)}{s_5^{7/4}} \right] + \frac{3(20A-16t)}{8s_1^{5/2}} \left[1 + \frac{\cos(\frac{5}{2}s_3)}{s_5^{5/4}} \right] \right.$$

$$\left. - \frac{(\frac{19}{2}+2\kappa)}{4s_1^{3/2}} \left[1 + \frac{\cos(\frac{3}{2}s_3)}{s_5^{3/4}} \right] \right\}, \tag{F.1}$$

$$N_{12s0}(t) = \frac{\pi}{\sqrt{2t}} \left[\frac{15A(-A+t)}{2} \frac{\sin(\frac{7}{2}s_3)}{s_1^{7/2}s_5^{7/4}} + \frac{3(12A-6t)}{8} \frac{\sin(\frac{5}{2}s_3)}{s_1^{5/2}s_5^{5/4}} \right.$$

$$\left. + (\frac{7}{2}-2\kappa)\frac{\sin(\frac{3}{2}s_3)}{4s_1^{3/2}s_5^{3/4}} + (1+\kappa)\sqrt{t}\,\frac{\sin(\frac{3}{2}s_8)}{A^2 s_9^{3/4}} \right], \tag{F.2}$$

$$N_{13s0}(t) = \frac{\pi}{\sqrt{2t}} \left[\frac{15A(A-t)}{2} \frac{\cos(\frac{7}{2}s_2)}{s_1^{7/2}s_4^{7/4}} + \frac{3(-8A+2A\kappa+8t)}{4} \frac{\cos(\frac{5}{2}s_2)}{s_1^{5/2}s_4^{5/4}} \right.$$

$$\left. - \frac{15\kappa}{8} \frac{\cos(\frac{3}{2}s_2)}{s_1^{3/2}s_4^{3/4}} \right], \tag{F.3}$$

$$N_{31s0}(t) = \frac{\pi}{\sqrt{2t}} \left[\frac{15A(A-t)}{2} \frac{\cos(\frac{7}{2}s_2)}{s_1^{7/2} s_4^{7/4}} + \frac{3(-8A + 2A\kappa + 6t - 2\kappa t)}{4} \frac{\cos(\frac{5}{2}s_2)}{s_1^{5/2} s_4^{5/4}} \right.$$

$$\left. + \frac{15}{8} \frac{\cos(\frac{3}{2}s_2)}{s_1^{3/2} s_4^{3/4}} \right],$$ (F.4)

$$N_{32s0}(t) = \frac{\pi}{\sqrt{2t}} \left[\frac{15A(A-t)}{2} \frac{\sin(\frac{7}{2}s_2)}{s_1^{7/2} s_4^{7/4}} + \frac{3(-4A + 2A\kappa + 6t - 2\kappa t)}{4} \frac{\sin(\frac{5}{2}s_2)}{s_1^{5/2} s_4^{5/4}} \right.$$

$$\left. - (\frac{3}{4} - 2\kappa) \frac{\sin(\frac{3}{2}s_2)}{s_1^{3/2} s_4^{3/4}} - (1 + \kappa)\sqrt{t} \frac{\sin(\frac{3}{2}s_6)}{A^2 s_7^{3/4}} \right],$$ (F.5)

$$N_{33s0}(t) = \frac{\pi}{\sqrt{2t}} \left[\frac{30A(-A+t)}{8s_1^{7/2}} + \frac{3(3A - 2A\kappa - 3t + \kappa t)}{4s_1^{5/2}} + \frac{\kappa(11 - 4\kappa)}{16s_1^{3/2}} \right],$$ (F.6)

where

$$s_1 = 2A - t,$$

$$s_2 = Arc\tan(\frac{L}{s_1}),$$

$$s_3 = Arc\tan(\frac{2L}{s_1}),$$

$$s_4 = 1 + (\frac{L}{s_1})^2,$$

$$s_5 = 1 + (\frac{2L}{s_1})^2,$$

$$s_6 = Arc\tan(\frac{L}{A}),$$

$$s_7 = 1 + (\frac{L}{A})^2,$$

$$s_8 = Arc\tan(\frac{2L}{A}),$$

$$s_9 = 1 + (\frac{2L}{A})^2. \tag{F.7a-i}$$

APPENDIX G

The expressions for $K_{4j}(r,t,\alpha)$ ($j=1-3$) appearing in Eq.(5.4) are as follows

$$K_{41}(r,t,\alpha) = \frac{4\alpha}{d_0}\{r\alpha I_1(\alpha r)[-2t\alpha I_0(t\alpha) + I_1(\alpha t)(h_2 + h_1 h_3)] + I_0(r\alpha)\{t\alpha I_0(t\alpha)(-4$$

$$+ h_2 + h_1 h_3) + I_1(t\alpha)[2h_2 + h_1(-1 + 2h_3)]\}\}\cos(\alpha L) , \qquad (G.1)$$

$$K_{42}(r,t,\alpha) = \frac{4}{Ad_0}\{A\alpha\{r\alpha h_2 I_0(t\alpha)I_1(r\alpha) + I_0(r\alpha)[1 + \kappa + 2h_2 I_0(t\alpha) + t\alpha h_2 I_1(t\alpha)]\}$$

$$+ r\alpha I_1(r\alpha)[-2At\alpha^2 I_1(t\alpha) - (1 + \kappa)I_1(A\alpha) + A\alpha h_1 h_3 I_0(t\alpha)]$$

$$+ I_0(r\alpha)[-4At\alpha^2 I_1(t\alpha) + A\alpha h_1\ I_0(t\alpha)(-1 + 2h_3)$$

$$- 2(1 + \kappa)I_1(A\alpha) + At\alpha^2 h_1 h_3 I_1(t\alpha)]\}\sin(\alpha L) , \qquad (G.2)$$

$$K_{43}(r,t,\alpha) = -\frac{\alpha}{d_0}\{2r\alpha I_1(\alpha r)[-2t\alpha I_1(t\alpha) + I_1(\alpha t)(1 + \kappa + h_2 + h_1 h_3)]$$

$$+ I_0(r\alpha)\{2t\alpha I_0(t\alpha)(-4 + h_2 + h_1 h_3)$$

$$+ I_1(t\alpha)[2(1 + \kappa - 2A^2\alpha^2) + (3 - \kappa)(h_2 + h_1 h_3)]\}\} , \qquad (G.3)$$

where

$$h_1 = 1 + \kappa + 2A^2\alpha^2 ,$$

$$h_2 = 2A^2\alpha^2 I_0(A\alpha)K_0(A\alpha) ,$$

$$h_3 = I_1(A\alpha)K_1(A\alpha) . \qquad (G.4a\text{-}d)$$

The expressions for $K_{4j\infty}(r,t,\alpha) = \lim_{\alpha\to\infty} K_{4j}(r,t,\alpha)$, $(j=1-3)$ are in the form

$$K_{41\infty}(r,t,\alpha) = \frac{\cos\alpha L e^{-\alpha(2A-t-r)}}{\sqrt{tr}}\left[4(-A+r)(A-t)\alpha^2 + (8A-2r-6t)\alpha - 4\right], \quad (G.5)$$

$$K_{42\infty}(r,t,\alpha) = \frac{\sin\alpha L e^{-\alpha(2A-t-r)}}{\sqrt{tr}}\left[4(-A+r)(A-t)\alpha^2 + (4A+2r-6t)\alpha + 2\right]$$

$$+ \frac{\sin\alpha L e^{-\alpha(A-r)}}{\sqrt{tr}}\left[\frac{2(1+\kappa)(A-r)\sqrt{At}}{A^2}\right], \quad (G.6)$$

$$K_{43\infty}(r,t,\alpha) = -\frac{e^{-\alpha(2A-t-r)}}{\sqrt{tr}}\left\{2(-A+r)(A-t)\alpha^2 + \left[3(A-t)+\kappa(-A+r)\right]\alpha + \frac{3\kappa-1}{2}\right\}. (G.7)$$

The singular parts of kernels, $N_{4j_s}(r,t) = \int_0^\infty K_{4j\infty}(r,t,\alpha)d\alpha$ $(j=1-3)$ are

calculated to be

$$N_{41_s}(r,t) = \frac{1}{\sqrt{tr}}\left\{\frac{8(-A+r)(A-t)(2A-r-t)\left[-3L^2 + (-2A+r+t)^2\right]}{\left[L^2 + (-2A+r+t)^2\right]^3}\right.$$

$$\left. + \frac{(8A-2r-6t)(2A-L-r-t)(2A+L-r-t)}{\left[L^2 + (-2A+r+t)^2\right]^2} + \frac{4(-2A+r+t)}{\left[L^2 + (-2A+r+t)^2\right]}\right\},$$

$$(G.8)$$

$$N_{42_s}(r,t) = \frac{1}{\sqrt{tr}}\left\{-\frac{8L(-A+r)(A-t)\left[L^2 - 3(-2A+r+t)^2\right]}{\left[L^2 + (-2A+r+t)^2\right]^3}\right.$$

$$+ \frac{2L(4A+2r-6t)(2A-r-t)}{\left[L^2 + (-2A+r+t)^2\right]^2} + \frac{2L}{\left[L^2 + (-2A+r+t)^2\right]}$$

$$\left. + \frac{2L(1+\kappa)(A-r)\sqrt{At}}{A^2\left[L^2 + (A-r)^2\right]}\right\}, \quad (G.9)$$

$$N_{43_s}(r,t) = -\frac{1}{\sqrt{tr}} \left\{ -\frac{4(-A+r)(A-t)}{(-2A+r+t)^3} + \frac{\left[3(A-t)+\kappa(-A+r)\right]}{(-2A+r+t)^2} - \frac{3\kappa-1}{2(-2A+r+t)} \right\}.$$

(G.10)

APPENDIX H

The expressions for the kernels in Eq. (5.6) are in the form

$$\overline{N}_{41s}(0,\phi) = \frac{z_2{}^2\pi}{\sqrt{2z_2\phi}}\left\{15(1-z_2\phi)\frac{\cos(\frac{7}{2}z_5)}{z_4{}^{7/2}z_6{}^{7/4}} + \frac{3(-20+16z_2\phi)}{4}\frac{\cos(\frac{5}{2}z_5)}{z_4{}^{5/2}z_6{}^{5/4}}\right.$$

$$\left. + (\frac{19}{2}+2\kappa)\frac{\cos(\frac{3}{2}z_5)}{z_4{}^{3/2}z_6{}^{3/4}}\right\}, \tag{H.1}$$

$$\overline{N}_{42s}(0,\phi) = \frac{z_2{}^2\pi}{\sqrt{2z_2\phi}}\left\{15(1-z_2\phi)\frac{\sin(\frac{7}{2}z_5)}{z_4{}^{7/2}z_6{}^{7/4}} - \frac{3(-12+6z_2\phi)}{4}\frac{\sin(\frac{5}{2}z_5)}{z_4{}^{5/2}z_6{}^{5/4}}\right.$$

$$\left. - (\frac{7}{2}+2\kappa)\frac{\sin(\frac{3}{2}z_5)}{z_4{}^{3/2}z_6{}^{3/4}} + 2(1+\kappa)\sqrt{z_2\phi}\frac{\sin(\frac{3}{2}z_7)}{A^2z_8{}^{3/4}}\right\}, \tag{H.2}$$

$$\overline{N}_{43s}(0,\eta) = \frac{z_3{}^2\pi}{\sqrt{2z_3\eta}}\left\{\frac{60(1-z_3\eta)}{8z_9{}^{7/2}} + \frac{3(-8+2\kappa+8z_3\eta)}{4z_9{}^{5/2}} - \frac{15\kappa}{8z_9{}^{3/2}}\right\}, \tag{H.3}$$

where

$$z_1 = \frac{L}{A},$$

$$z_2 = \frac{a}{A},$$

$$z_3 = \frac{b}{A},$$

$$z_4 = 2 - z_2\tau,$$

$$z_5 = Arc\tan(\frac{z_1}{z_4}),$$

$$z_6 = 1 + (\frac{z_1}{z_4})^2,$$

$$z_7 = Arc\tan(z_1),$$

$$z_8 = 1 + z_1^2,$$

$$z_9 = 2 - z_3\eta.$$
(H.4a-i)

VITA

Mete Onur Kaman was born in Elazığ on July 27, 1975. He attended Atatürk Primary School and Mehmet Akif Ersoy High School in Elazığ. He received the degrees of Bachelor of Science and Master of Science from the Department of Mechanical Engineering in Fırat University in 1997 and in 2000. He worked as a Research Assistant in the same department from 1999 to 2002. He has been in the Department of Engineering Sciences since 2002.